Nuevas funciones biológicas de MXD1 y MNT, proteínas de la red MYC-MAX-MXD

New biological functions of MXD1 and MNT, proteins of the MYC-MAX-MXD network

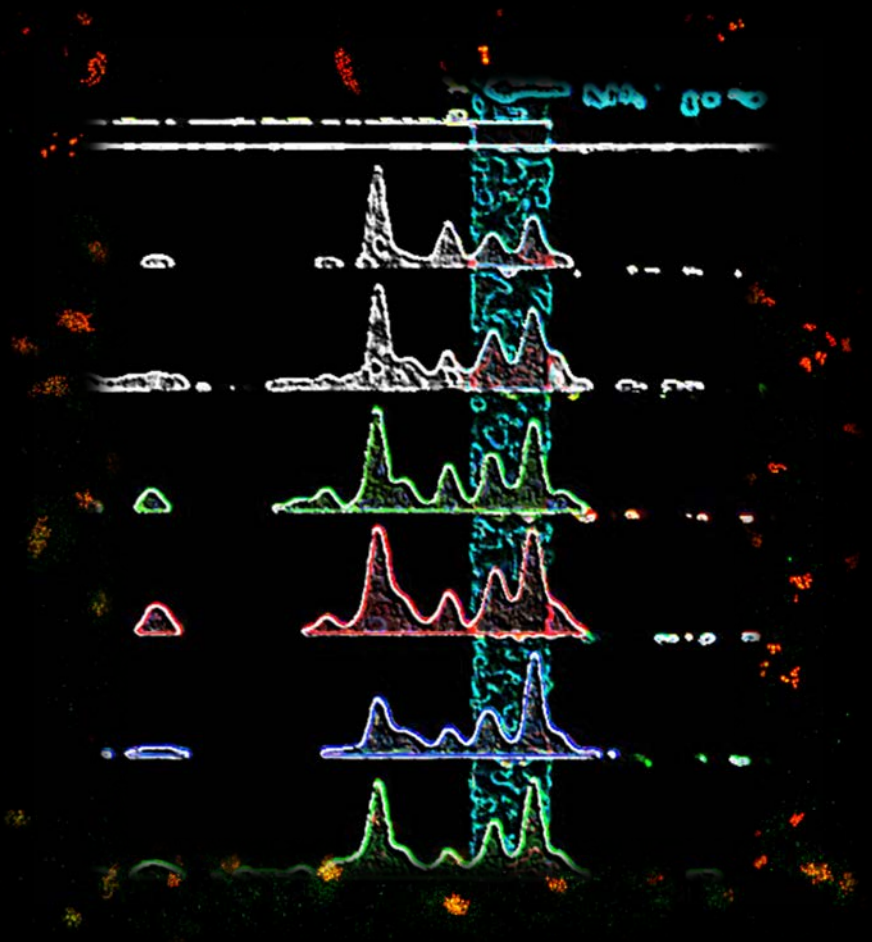

UNIVERSIDAD DE CANTABRIA

INSTITUTO DE BIOMEDICINA Y BIOTECNOLOGÍA DE CANTABRIA (IBBTEC)

MªCarmen Lafita Navarro

Santander 2015

UNIVERSIDAD DE CANTABRIA

FACULTAD DE MEDICINA

DEPARTAMENTO DE BIOLOGÍA MOLECULAR

INSTITUTO DE BIOMEDICINA Y BIOTECNOLOGÍA DE CANTABRIA (IBBTEC)

Nuevas funciones biológicas de MXD1 y MNT, proteínas de la red MYC-MAX-MXD

Tesis Doctoral presentada por

Mª Carmen Lafita Navarro para optar

al Grado de Doctor por la Universidad de Cantabria

Febrero 2015

El **Dr. Javier León Serrano**, Catedrático de Bioquímica y Biología Molecular de la Facultad de Medicina de la Universidad de Cantabria

CERTIFICA: que la Lda. Dña. Mª Carmen Lafita Navarro ha realizado bajo su dirección el presente trabajo titulado **"Nuevas funciones biológicas de MXD1 y MNT, proteínas de la red MYC-MAX-MXD**" **(New biological functions of MXD1 and MNT, proteins of the MYC-MAX-MXD network)** en el Departamento de Biología Molecular de la Universidad de Cantabria.

Considero que este trabajo reúne los requisitos de originalidad y calidad científica necesarios para su presentación como Memoria de Doctroado por la interesad, al objeto de poder optar al grado de Doctor por la Universidad de Cantabria.

Y para que conste y surta los efectos oportunos, firmo el presente certificado.

Santander, a 24 de Febrero de 2015

.

Fdo. Javier León Serrano

Esta Tesis ha sido realizada en el Instituto de Biomedicina y Biotecnología de Cantabria (IBBTEC) y el Departamento de Biología Molecular de la Facultad de Medicina de la Universidad de Cantabria (Santander).

La financiación necesaria para la realización de esta Tesis doctoral ha sido aportada por el Miniterio de Educación y Ciencia (SAF2008-01581 y SAF2011-23796) por el Instituto Carlos III (RD06/0020/0017).

El autor de esta Tesis ha disfrutado de una beca predoctoral de Formación de Profesorado Universitario (FPU) (Orden EDU/3083/2009) concedida por el Ministerio de Educación y de un contrato de 7 meses por la Universidad de Cantabria.

AGRADECIMIENTOS GENERALES

Difícil esto de agradecer cuando se trata de hacerlo a tanta gente. Tanta gente porque para mí este trabajo empezó cuando en el instituto me asaltó la idea de querer curar el cáncer. Lo único que sabía era que tendría que hacer el doctorado, así que es por eso que he de agradecer a todas aquellas personas que me han acompañado ya sea directa o indirectamente en este largo camino.

Comenzaré por agradecer enormemente a mi director de Tesis el Dr. Javier León por haberme dado la oportunidad de hacer este trabajo. Primero de todo, gracias por ser mi primer y mejor referee, enseñarme a dudar de todos los resultados hasta el último momento (y volver a dudar por si acaso…) y que todo tiene explicación, sólo que hay que encontrarla. Gracias por tu paciencia y por "reñirnos" si faltamos a los seminarios, no nos hemos registrado al NCBI o bien no hemos completado la colección de plásmidos. Gracias también por fomentar el trabajo en equipo y por entre llamada, e-mail, reunión, clases, asamblea y bolo, encontrar siempre un hueco para nosotros. Y gracias por el cineforum en blanco y negro, por llevarnos a ver el Carrillón de Marienplatz, por mostrarnos cuán sabio era J. Elliot o enseñarnos las Goldberg variations. En definitiva, muchas gracias Javier por ser un gran jefe, un gran investigador además de una gran persona.

Muchas gracias también a la Dra. Dolores Delgado. Gracias Dolo por estar siempre dispuesta a ayudar a tu grupo hermano, por transmitirnos que el orden es importante, y enseñarme a venderme mejor. Gracias también por esa espontaneidad, y por tratarnos junto a Javier como a una pequeña familia.

Gracias al resto de jefes y demás cargos del departamento de Biología Molecular y Celular de la Facultad de Medicina y del IBBTEC que han contribuido de una forma u otra a la realización este trabajo. Especialmente, gracias al Dr. José Carlos Rodríguez Rey por animarnos en el labo con todas sus historietas además de sus cursos básicos de Tai Chi. También, gracias Nacho por toda la ayuda y paciencia con el tema de la bioinformática de la de verdad, ayudarnos a solventar problemas en los *labmeetings* y estar siempre dispuesto para cualquier cosa.

Gracias al Dr. Don Ayer por haberme permitido hacer la estancia en su laboratorio y a John O'shea y Mohan Kaadige por enseñarme cómo es la ciencia americana.

SANTANDER:

Ahora ya toca agradecer a esos grandes compañeros y amigos de poyata, tarea difícil cuando se tiene tanto que decir en pocas palabras. Puea nada, comenzaré por mis dos grandes: gracias María por sacarme de la onda MNT (chica, ¡que he silenciao!), hacerme reír tanto, interesarte por mis historias sin (y con) historia y por hacerme ver que existe algo más que esto; y gracias Lucía por esas conversaciones en las que arreglamos (o no) todos nuestros problemas científicos, donde nosotras pasamos a ser las ratas de laboratorio de quién sabe quién, por hacerme disfrutar de esos días interminables y por ser otra motivada como yo. Y madre mía, madre mía! gracias Silvia por intentar venderme a tipos inteligentes, por tenerme siempre en cuenta, por congeniar tan bien conmigo y por confiar en mí. Gracias Rosa por hacernos experimentar el efecto Bach cada mañana, por poner orden en el labo y por estar siempre dispuesta a ayudarnos y cuidarnos. También, gracias Lore por arreglar mis frecuentes problemas de informática, Marina por contagiarnos esa felicidad que llevas dentro, Iago por esos ricos e ingeniosos pasteles, Magda por recordarme mis vacaciones y a las nuevas generaciones Judit (¡ánimo con ello!), Esther, Julia y Javi por transmitirnos vuestras ganas de aprender e intentar seguir nuestro "humor". No puedo olvidarme de mis comienzos. Gracias Pilar por ser nuestra

madre del laboratorio, Eva por ser mi compañera MXD, Ana por resolver mis dudas médicas, y Cris por ponernos patas arriba. Gracias Andrea por presentarme a las URHebo y URMAX con las cuales hemos podido hacer este trabajo. También esa cabecita que asomaba, gracias Alfonso por apreciarme y gracias Juan por mostrarme cada tres por cuatro que los monos también comen carne. Y sí hombre sí, lógicamente, gracias Gabi por enseñarme que hay que controlar todas las técnicas y saber para qué sirve cada cosa y escuuuuucha, muchas gracias también por ayudarme en mi etapa final de la tesis aunque haya sido sin GFPfusión. Cómo no, gracias Javi prrrr ser tan atento, escuchar mis historias de MOCK y POCK y hacerme reír con esa facilidad. Y por supuesto, gracias por enseñarme la paleta de colores huesico, lo magnífico de la simetría, eso de la cultura sin hacerme sentir pequeña ni dejar de sorprenderme, por saber mandarme a recoger habas con elegancia y por demostrarme una y otra vez que no todos los robores están hechos de metal, mil gracias MAJ.

También tengo que agradecer a todos compañeros de pasillo o entre-poyatas:

En primer lugar, muchísimas gracias Marcos por permitirme conocer a una de las mejores personas que he conocido nunca, por entenderme y mostrarme que no sólo es cosa mía, y por saber sacarme carcajadas a diario, gracias. También, gracias Paula por dejarme ver esa personita encantadora que llevas dentro, Lore por enseñarme a "duolinkear" y ser mi cómplice reveladora, Javi por ayudarnos con todo el tema de la proteómica, Iñaki "pues" por alegrarme cada mañana, Emilio por subirme o bajarme (ya no sé) la serotonina y a todos aquellos que han formado parte de mi etapa pre-tésica: Maigüi, Ana P., Rocío B., María R.S., Juantxo, Alejandro, Nacho, Jorge P., Pilar, Juanje, María A., Lolo, Jorge, Rocío, Fuen, Patri… y muchos otros que seguro me dejo.

EL OTRO SANTANDER:

No puedo olvidarme de Fendisc. Gracias a todo el equipo por permitirme conocer esa otra parte de Santander y a esos grandes amigos con los que he podido disfrutar de una de las cosas que más me gustan. Especialmente gracias Maryrose, María y Adri por levantarme el ánimo una y otra vez y hacerme pasar esos grandes momentos tanto dentro como fuera del campo. También, gracias Nef por ser mi fiel acompañante en esas carreras en cuesta y escaleras, Andrea por tu ayuda con el inglés y la escalada y Jota, Manu y Amador por enseñarme este deporte.

Muchas gracias a mis compañeras de piso. Gracias Alba por esas conversaciones infinitas y abrirme los ojos ante esos otros mundos de este planeta; y gracias Katie Revuelta por todos esos momentos de risas y por haber hecho que vivir en Cazoña se haya convertido en una experiencia inolvidable.

BARCELONA:

Gracias Encarna y Tere por hacer que me decantase por estudiar Biología en Barcelona, Emilio por ayudarnos en los comienzos y Lourdes por esa peculiar y envidiable forma de ser.

Gracias a mi equipo Maravilla por hacer que las clases, entre-clases y prácticas fuesen más divertidas. Gracias Migüel por tener siempre algo con qué alegrarnos el día y transmitirnos esa positividad. Y gracias Ari por sacarme de esa burbuja, desbarajustarme los esquemas, por confiar en mí, por todas las risas que nos hemos echado y por compartir conmigo toda mi etapa en Barcelona.

Gracias a los "hippies" del Penyafort-Monserrat. Especialmente gracias Francesc por recibirme siempre con una sonrisa, contarme siempre esas cosas tan interesantes y avisarme de los riesgos de comer chocolate. Gracias Alfred por apreciar a las aragonesas, Oskar por ayudarnos con el impala y Sergio por tu autenticidad.

Gracias también a la Dra. Lluïsa Vilageliu por haberme permitido hacer prácticas en su grupo y enseñarme lo que es un laboratorio de verdad.

Y gracias a todo el grupo de Señalización Celular del IRB. Especialmente gracias Carme Caelles y Joan Roig por permitirme estar en vuestro laboratorio y hacerme sentir parte de vuestro grupo, por introducirme en este mundo de la investigación y también, por haberme ayudado a encontrar al Dr. Javier León. Por supuesto, gracias Laura por ser la primera en enseñarme a clonar, cultivar y emparejar levaduras siempre con una sonrisa.

MI ENTORNO:

Gracias a todos Los Okupas y la gente de Rivas por esa característica forma de ser. Gracias Angela por compartir conmigo tantos momentos, estar siempre allí y creer en mí (algún día saldré en la tele ¡lo prometo!). Gracias Miguel por intentar que vuelva a sentirme como en casa una y otra vez, Jorge por ser tan especial y por saber y hacerme saber sin saberlo que siempre seremos amigos, Iñaki por intentar animarme siempre y permanecer como siempre por mucho que pasen los años, Marcos por ser como eres y ser la chispa de mi vocación y Marta por ser tan buena amiga y entender a esta petarda que escribe. También, gracias Esther por ser mi mejor compañera y amiga de pupitre en el instituto. Y por supuesto, gracias Diego por tragarte las lecciones sobre cualquier cosa que aprendiera esa semana, aguantar mis síntomas pre-exámenes, por mostrarme el poder que tiene la mente y por saber hacerme reír en cualquier momento, gracias.

MI FAMILIA:

Los mejores, lo primero de todo gracias por haber permitido que hoy pueda estar escribiendo estas palabras.

Gracias YAYA y YAYO por tener esa confianza ciega en mí. Gracias también a todos mis primos, tíos y tías (en especial mi tía Merche, mi tío Ignacio y mi tía Tere) por tener siempre guardada una sonrisa.

Y los más importantes: gracias MAMÁ por entenderme siempre tanto, por enseñarme y demostrarme que ante todo hay que ser buena persona, por estar siempre dispuesta a todo y a todos de la mejor de las maneras y por aceptar y querer la manera de ser de cada uno de nosotros. Gracias PAPÁ por tener esa capacidad de trabajo, por enseñarme que hay que ser cuidadoso (aunque no hayas tenido mucho éxito), por procurar que siempre estemos en las mejores condiciones, por fomentar el deporte en mí y por enseñarme que siempre se puede hacer mejor. Gracias a los dos por encargaros de que nunca nos haya faltado de nada. Por supuesto, mis hermanos: gracias Isabel por cuidarme y protegerme (aunque a veces demasiado…), Ana por apoyarme siempre y entender todo con esa facilidad y gracias, gracias y más gracias Hermano por llevarme siempre de la mano. No me olvido de los enanos, Javier, Fernando y Gloria que me alegran cada fin de semana que paso por casa (aunque sean pocos) ni tampoco de los apegados Chus, Seb y Pilar.

En definitiva, gracias a todos por quererme incondicionalmente a pesar de lo desastre que es esta pequeña.

Probablemente me haya dejado mucha gente en el tintero, así que sólo puedo decir que muchas gracias a todos los que formáis parte de mi vida ☺.

AGRADECIMIENTOS A COLABORADORES

También me gustaría agradecer a todos aquellos que por su colaboración han hecho posible que este trabajo haya salido adelante.

Gracias al Dr. Miguel Ángel Lafarga y Dra. María Teresa Berciano (grupo de Biología Celular del Núcleo, Facultad de Medicina e IDIVAL, Santander) por su enorme ayuda con la biología celular, consejos de experimentos, microscopía confocal y por proporcionarnos el plásmido CFP-Fibrilarina y la línea celular C6.

Gracias al Dr. Víctor M. Campa (Servicio de Microscopía, IBBTEC, Santander) por su paciencia y ayuda con la microscopía de fluorescencia, microscopía confocal y el análisis de imágenes.

Gracias al Dr. René Rodríguez González (Banco Andaluz de Células Madre, Centro de Investigaciones Biomédicas, Granada) por proporcionarnos la línea celular MSC-3H.

Gracias al Dr. Alex von Kriegsheim y al Dr. Javier Rodríguez (Systems Biology Ireland, Conway Institute, Dublín) por su colaboración y análisis de la proteómica.

Gracias al Dr. José Luis Fernández Luna (grupo de Señalización Celular y Dianas Terapéuticas en Cáncer, IDIVAL, Santander) por proporcionarnos el anticuerpo anti-p65 y la línea celular T98G.

Gracias al Dr. Jose Pedro Vaqué (Molecular mechanisms promoting human cancer, IBBTEC, Santander) por proporcionarnos el plásmido pNF-κB.

Gracias a la Dra. Angela Celetti (IEOS, CNR, Nápoles) por proporcionarnos los plásmidos de CCDC6.

Gracias a la Dra. Montserrat Céspedes (Grupo de Genes y Cáncer, IDIBELL, Barcelona) por proporcionarnos la línea celular H1417.

Gracias al Dr. Don Ayer (Hustman Cancer Institute, University of Utah, Salt Lake City) por permitirme hacer la estancia en su laboratorio y proporcionarnos el anticuerpo anti-MLX.

Gracias al Dr. Ignacio Varela (grupo de Análisis Genómico del Desarrollo Tumoral, IBBTEC, Santander) por su enorme ayuda y paciencia con el análisis bioinformático del RNA-seq y ChIP-seq.

Y gracias a todos aquellos que nos han ayudado y prestado todo lo que necesitábamos de una forma desinteresada.

UNIVERSIDAD DE CANTABRIA

FACULTAD DE MEDICINA

DEPARTAMENTO DE BIOLOGÍA MOLECULAR

INSTITUTO DE BIOMEDICINA Y BIOTECNOLOGÍA DE CANTABRIA (IBBTEC)

New biological functions of MXD1 and MNT, proteins of the MYC-MAX-MXD network

Mª Carmen Lafita Navarro

Abbreviations

ABBREVIATIONS

A_{260nm}	Absorbance at 260 nm
A_{595nm}	Absorbance at 595 nm
aa	Amino acid
ATP	Adenosine triphosphate
BSA	Bovine serum albumin
bp	Base pairs
CDK	Cyclin-dependent kinase
cDNA	Complementary DNA
ChIP	Chromatin Immunoprecipitation
ChIP-seq	Chromatin Immunoprecipitation sequencing
CML	Chronic Myeloid Leukemia
CMV	Cytomegalovirus
Ct	Cycle threshold
CTD	Carboxy-terminal domain of RNA Polymerase II
DAPI	4, 6´-diamino-2 phenylindole dihydrochloride
Dex	Dexamethasone
DMEM	Dulbecco's Modified Eagle Medium
DMSO	Dimethyl sulphoxide
DNA	Deoxyribonucleic acid
DNMT	DNA-methyltransferase
dNTP	Deoxyribonucleoside Triphosphate
DTT	Dithiothreitol
EDTA	Ethylenediaminetetracetic acid
EGTA	Ethyleneglycoltetraacetic acid
ER	Estrogen receptor
FBS	Foetal bovine serum
FITC	Fluorescein isothiocyanate
GFP	Green Fluorescent Protein
h	Hour/s
HAT	Histone Acetyltransferase
HDAC	Histone deacetylase
HLH	Helix-loop-helix
IF	Immunofluorescence
IgG	Immunoglobulin G
Inr	Initiator element

IP	Immunoprecipitation
kb	Kilobase
kDa	Kilodalton
KO	Knockout
LB	Luria Broth
LiCl	Lithium chloride
LZ	Leucine zipper
M	Molar
MB	MYC box
MEFs	Mouse embryonic fibroblasts
min	minutes
miRNA	Micro-RNA
MW	Molecular weight
NES	Nuclear export signal
NGF	Nerve growth factor
NLS	Nuclear Localization Signal
NP40	Nonidet-P40 or octyl phenoxylpolyethoxylethanol
o/n	over night
PAGE	Polyacrylamide Gel Electrophoresis
PBS	Phosphate Buffer Saline
PCR	Polymerase Chain Reaction
PLA	proximity ligation assay
pLKO	short hairpin RNA control
Pol	Polymerase
qPCR	Quantitative polymerase chain reaction
rDNA	Ribosomal DNA
R.L.U.	Relative light units
RNA	Ribonucleic Acid
RNA-seq	Ribonucleic Acid sequencing
rpm	Revolutions per minute
RPMI	Roswell Park Memorial Institute medium
RPKM	Reads per kilobase per million reads
RT	room temperature
RT-qPCR	Reverse transcription and quantitative polymerase chain reaction
rRNA	Ribosomal RNA
s	seconds
SAGE	Serial analysis of gene expression
SCF	SKP1-Cullin-F-box protein complex
SDS	Sodium Dodecyl Sulfate
seq	Sequencing
shRNA	Short hairpin RNA
siRNA	small interference RNA
sh-MNT	short hairpin RNA against MNT gene

TAE	Tris-acetate-EDTA buffer
TBS-T	Tris buffer saline –Tween 20
TE	Tris-EDTA buffer
TSS	Transcription Start Sites
UV	ultra violet
UTR	(3´and 5´) Untranslated regions
V	Volt/s
Vo	empty vector
wt	Wild type

Index

Introduction

1. INTRODUCTION

1.1. MYC family of proteins

The c-MYC protein (MYC herein after) is a transcription factor belonging to the MYC family of proteins, also composed by N-MYC and L-MYC. It was the first transcription factor with oncogenic capacity discovered in the mid-seventies. The discovery of such activity came out when some avian acute transforming retroviruses (MC29, CMII, MH2 and OK10) that caused a type of leukaemia in chickens, "MYeloCytomatosis", were studied. All of these retroviruses had incorporated the same transforming gene called *v-MYC* that in fact was a MYC-GAG fusion gene responsible for their transforming activity (Duesberg and Vogt, 1979; Hu et al., 1979; Sheiness and Bishop, 1979).

The MYC gene was later identified in the chicken host genome by homology with the v-MYC oncogene (Vennstrom et al., 1982) and following homology studies allowed the identification and characterization of the *MYC* gene in human, mouse and rat genomes (Crews et al., 1982; Dalla-Favera et al., 1982b; Hayashi et al., 1987). Further studies in MYC made clear that it was involved in many human and other animal neoplasms including avian bursal lymphomas, murine and feline T-cell lymphomas, small cell lung carcinomas, neuroblastomas, Burkitt's lymphomas, murine plasmacytomas, rat immunocytomas and others (Alitalo and Schwab, 1986; Cory, 1986; Eisenman and Hann, 1985; Magrath, 1990). Nowadays, deregulated MYC by different mechanisms like genomic alterations, deregulation of its promoter and protein stabilization is considered to be one of the most common oncogenic alteration in human cancers (Eilers and Eisenman, 2008; Vervoorts et al., 2006).

Studies on neuroblastomas and small cell lung carcinomas allowed the identification of two homologous proteins: the N-MYC and L-MYC respectively. The N-MYC protein is encoded by the *MYCN* gene (Kohl et al., 1983; Schwab et al., 1983) and L-MYC by the MYCL1 gene (Nau et al., 1985).

The MYC proteins have been shown to have nuclear localization (Abrams et al., 1982; Hann et al., 1983), a short half-life and an expression pattern generally correlated with cell proliferation and cell cycle progression (Grandori et al., 2000; Hann et al., 1985; Thompson et al., 1985). On the contrary, it has been shown to be downregulated in differentiation statements or cell cycle arrest (Grandori et al., 2000; Pietenpol et al., 1990)

Both MYC and N-MYC are crucial for proper functioning of Hematopoietic Stem Cell (HSCs) (Laurenti et al., 2008) and knock-out mice mutant for the MYC family members showed that the MYC and N-MYC proteins are essential for embryo development since these knock-out mice died before birth (Charron et al., 1992; Dubois et al., 2008). On the contrary, *MYCL* knock-out mice survived making it non-essential for embryo development (Murphy et al., 2005).

1.1.1. Structure of MYC gene and protein

In humans, the MYC gene maps in the locus 8q24.21. *MYC* has 3 exons and its expression is regulated by four potential promoters as there are four transcription initiation sites (TSS): P0, P1, P2 and P3 (Figure 1.1). The mRNAs starting in the TSS of P1 and especially of P2 are the most prevalent *MYC* mRNAs (Liu and Levens, 2006; Wierstra and Alves, 2008). Depending on the translation start codon used, the MYC protein can be translated into three different isoforms, which differ at the N-terminal region of the protein. The predominant isoform (MYC-2) is translated from the canonical AUG located at the beginning of the second exon and contains 439 amino acids with a molecular weight in a denaturing SDS-PAGE of 64 kDa (Persson et al., 1984). A minor MYC (MYC-1) protein variant of 454 amino acids and 67 kDa in SDS-PAGE, is synthesized from the CUG-leucine codon at the 3´-end of the first exon (Hann et al., 1988). In addition, the *MYC* gene also produces a third isoform, smaller protein called MYC-S (MYC-Short), translated from an internal AUG codon and lacking most of the N-terminal region of the protein, in which resides the transcriptional regulatory region. That is the reason why MYC-S has been suggested to act as a dominant negative of the MYC protein (Spotts et al., 1997; Xiao et al., 1998).

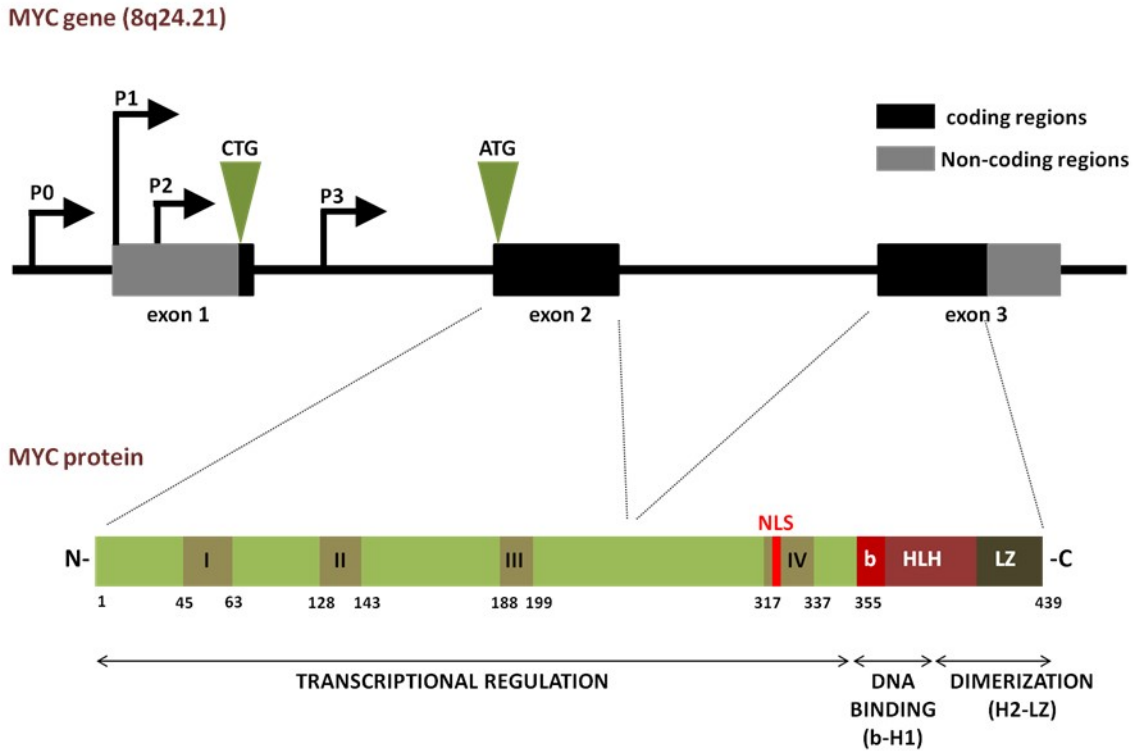

Figure 1.1.- MYC human gene and protein structure. Scheme of the human MYC gene located in chromosome 8q24.21. The different elements refers as follows: P: Promoter; AUG: main translation start codon and CUG: alternative translation start codon. In the protein representation, I, II, III and IV refers to MYC boxes (MB); b-HLH-LZ to basic Helix Loop Helix Leucine Zipper domain and NLS to nuclear localization signal.

MYC belongs to the b-HLH-LZ super-family of transcription factors. All of them contain the common basic (b), helix-loop-helix (HLH) and leucine zipper (LZ) domains (Dang et al., 1989; Landschulz et al., 1988; Murre et al., 1989; Prendergast and Ziff, 1989) that allows specific DNA-protein (b-H1) and protein-protein (H2-LZ) interactions. The MYC proteins present these domains in the C-terminal region and heterodimerize with MAX throughout its b-HLH-LZ also present in this protein. This heterodimer recognize and bind to specific sequences in the DNA called E-boxes (Amati et al., 1992; Blackwood et al., 1992a; Kato et al., 1992; Kretzner et al., 1992b).

The MYC protein also contains several highly conserved regions termed MYC Boxes (MB). These regions are responsible for the transcriptional regulatory function of MYC as well as for MYC protein stability. Four different MYC boxes have been identified: MBI, MBII, MBIII and MBIV (Figure 1.1). MBI and MBII are located in the Transcriptional Activation Domain (TAD) region (Kato et al., 1990). MBI contains two major phosphorylation sites, Thr58 and Ser62, associated with MYC stability and transforming capacity (Sears et al., 2000; Stone et al., 1987). MBII is the most important region regarding the transcriptional regulation function of MYC. Mutations in this region inhibit the binding of transcription coactivators needed for MYC transactivation function (Freytag et al., 1990; McMahon et al., 1998; Oster et al., 2003). Both MBI and MBII are needed for MYC-induced transformation, differentiation blockade and apoptosis induction (Evan et al., 1992; Freytag et al., 1990; Stone et al., 1987). On the other hand, MBIII is involved in the repression of transcription (Herbst et al., 2005; Kurland and Tansey, 2008) and the MBIV contains a Nuclear Localization Signal (NLS) to direct MYC to the nucleus. MBIV has been shown to be needed for DNA binding despite being located outside of the basic domain (Cowling et al., 2006; Dang and Lee, 1988).

A cytoplasmic form of MYC generated by calpain-dependent proteolysis at Lys298 of MYC has been described that lacks the nuclear localization signal and the b-HLH-LZ domain so that, proposed to abrogate MYC function (Conacci-Sorrell et al., 2010)

1.1.2. Regulation of MYC expression

MYC expression is tightly regulated by transcriptional, posttranscriptional and posttranslational mechanisms that make possible a control of the MYC levels in the cell (Liu and Levens, 2006; Thomas and Tansey, 2011; Vervoorts et al., 2006).

First, MYC expression is controlled by many transcriptional regulatory motives found within its proximal promoter region in which converge multiple signaling pathways that are triggered from diverse extracellular signals (Dang, 2012; Levens, 2010; Wierstra and Alves, 2008). In this context, MYC expression remains almost undetectable when cells are at differentiation and quiescent states and increases rapidly upon mitogenic stimuli. When cells are proliferating, MYC is constantly expressed at moderate levels (Hann et al., 1985; Rabbitts et al., 1985; Thompson et al., 1985) due to a sequence 1.5 kb upstream the P1 promoter called FUSE (Far Up-Stream Element) where the FUSE binding protein (FBP) constitutively binds activating MYC transcription (He et al., 2000). However,

MYC regulates its own expression negatively allowing a controlled MYC expression in the cells (Facchini et al., 1997; Luo et al., 2004). Contrarily, when cells are not proliferating or in a differentiated state, complexes formed by the E2F (1, 2 and 4) members; pocket family members (Rb, p107,p130) and histone deacetylases (HDACs) bind to the *MYC* promoter repressing its transcription (Albert et al., 2001). MYC repression during differentiation is also controlled by specific transcription factors depending on the cell type such as GATA-1 (Acosta et al., 2008), CTCF (Delgado et al., 1999; Torrano et al., 2005), C/EBPα (Freytag and Geddes, 1992) or KLF4 and OVOL1 (Nascimento et al., 2011). Furthermore, MYC expression is also altered due to indirect oncogenic stimuli. For instance, the constitutive nuclear localization of the β-catenin cofactor TCF4 promotes a constitutive MYC expression (Pomerantz et al., 2009; Sotelo et al., 2010; Tuupanen et al., 2009) or the BRD4 (Bromodomain-containing protein 4) mutated in leukaemia and lymphoma cell lines binds to *MYC* promoter activating its expression (Delmore et al., 2011; Mertz et al., 2011).

Second, MYC expression is controlled by posttranscriptional mechanisms affecting MYC mRNA stability. MYC mRNA has a short half-life of about 30 minutes. This feature is due to A-U rich sequences located in the 3'-UTR (Brewer and Ross, 1988; Jones and Cole, 1987). In addition, MYC mRNA has also been shown to be targeted by several miRNAs such as let-7, miR-34 or miR-145 (Cannell et al., 2010; Kim et al., 2009; Sachdeva et al., 2009).

Finally, posttranslational modifications also affect the stability of MYC protein (Hann, 2006; Vervoorts et al., 2006). MYC protein has a half-life of 20-30 min (Gregory and Hann, 2000) and its protein stability is mainly controlled by phosphorylation at two residues, Thr58 and Ser62. Phosphorylation at Ser62 leads to MYC stabilization meanwhile phosphorylation at Thr58 targets MYC for ubiquitination by the SCF^{FBW7} complex and proteasome degradation (Arnold et al., 2009; Sears, 2004). It has been also reported that acetylation of MYC by acetyltransferases such as GCN5, PCAF, TIP60 or p300/CBP increase MYC protein stability (Faiola et al., 2005; Patel et al., 2004; Vervoorts et al., 2003) and that its deacetylation by HDAC-Sin3B complexes decrease it (Garcia-Sanz et al., 2014). However, it has been also described that deacetylation by SIRT1 (a NAD^+-dependent deacetylase) promotes MYC ubiquitination in Lys63 increasing MYC stability (Menssen et al., 2012).

1.1.3. Transcriptional activation by MYC

Since *MYC* discovery as an oncogenic gene and transcription factor, MYC interactors responsible for such function were highly searched. The use of the b-HLH-LZ region of MYC responsible for protein-protein interaction as a bait for searching new interacting proteins led to the identification of a new b-HLH-LZ protein called MAX. MAX was found to bind to all the MYC family members (Blackwood and Eisenman, 1991) allowing them to bind to the DNA in the b-HLH-LZ specific sequences (CANNTG) called E-boxes (Blackwood and Eisenman, 1991; Prendergast et al., 1991).

Further studies transfecting reporter plasmid regulated by E-box sequences together with MYC and MAX genes showed that MYC-MAX presence mediated the activation of transcription of the reporter

genes indicating that MYC-MAX heterodimers regulate positively genes with E-box sequences in their promoters (Amati et al., 1993; Amati et al., 1992; Amin et al., 1993; Gu et al., 1993; Kretzner et al., 1992b). Besides, it was discovered that this transactivation of genes was dependent on the TAD domain of MYC protein (Kretzner et al., 1992a). Moreover, in vivo analysis by chromatin immunoprecipitation (ChIP) on CpG island arrays defined that MYC and MAX bind to identical promoters (Mao et al., 2003). So that, since the MYC-MAX interaction discovery, this mechanism was considered the key for the transcriptional regulation mediated by MYC. However, thereafter, several reports described MYC-MAX-independent mechanism of action. For instance, it was described a rat pheochromocytoma cell line (PC12) that did not express the MAX protein (Greene and Tischler, 1976; Hopewell and Ziff, 1995) and still being able to proliferate and having MYC activity such as inhibition of differentiation (Ribon et al., 1994; Vaque et al., 2008). Moreover, genetic studies in *Drosophila* also describe dMYC (MYC orthologue) functions that were dMAX (MAX orthologue) independent (Steiger et al., 2008). Furthermore, recent studies of human pheochromocytomas and small cell lung cancer samples described MAX inactivating mutations that enforce this MAX-independent mechanism of action of MYC (Comino-Mendez et al., 2011; Romero et al., 2014). Nonetheless, some of the mechanisms used by MYC-MAX heterodimers to activate gene transcription are described in the next lines (figure 1.2).

Chromatin remodelling SWI/SNF complexes regulate gene expression by inducing a nucleosome conformation that enhances the accessibility of the transcriptional machinery. The energy for SWI/SNF-mediated chromatin remodelling is obtained by the catalytic subunit BRM or BRG1, that have DNA-dependent ATPase activity (Muchardt and Yaniv, 1999). These complexes are highly conserved in evolution and are involved in the transcriptional regulation mediated by many diverse transcription factors making it a very important complex in gene regulation (Reisman et al., 2009). MYC was described as one of these transcription factors that depended on SWI/SNF complexes to induce gene expression of its target genes since MYC interacts with the INI1/hSNF5 subunit of SWI/SNF to induce gene expression (figure 1.2) (Cheng et al., 1999).

On the other hand, MYC proteins were found to be associated to DNA in acetylated histone regions (Bouchard et al., 2001; Eberhardy et al., 2000; Frank et al., 2001; Xu et al., 2001). These findings suggested that MYC might regulate transcription by inducing the acetylation of such proteins in order to allow the RNA polymerase I, II and III (RNApol I, II, III) complexes to act. To mediate histone acetylation MYC would require to interact with proteins with histone acetytransferase activity. TRRAP (transformation-transactivation domain-associated protein) protein was found to interact with the MBI and MBII of the MYC protein (figure 1.2) (McMahon et al., 1998). This protein has the capacity to interact with other proteins with histone acetyltransferases (HAT) activity such as GCN5 and TIP60 (Frank et al., 2003; Nagy and Tora, 2007). TRRAP complexes for MYC-dependent gene transcription relate not only to RNApol II but also to RNApol I and RNApol III transcription. TRRAP complexes are recruited by MYC to RNApol II-transcribed genes but also to the RNApol III-transcribed genes tRNA and 5S RNA to enhance H3 core histone acetylation (Kenneth et al., 2007). Other proteins with histone acetyltransferase activity have been also shown to interact directly with MYC protein such as

CBP and p300 although throughout the C-terminal domain of MYC protein (figure 1.2) (Vervoorts et al., 2003).

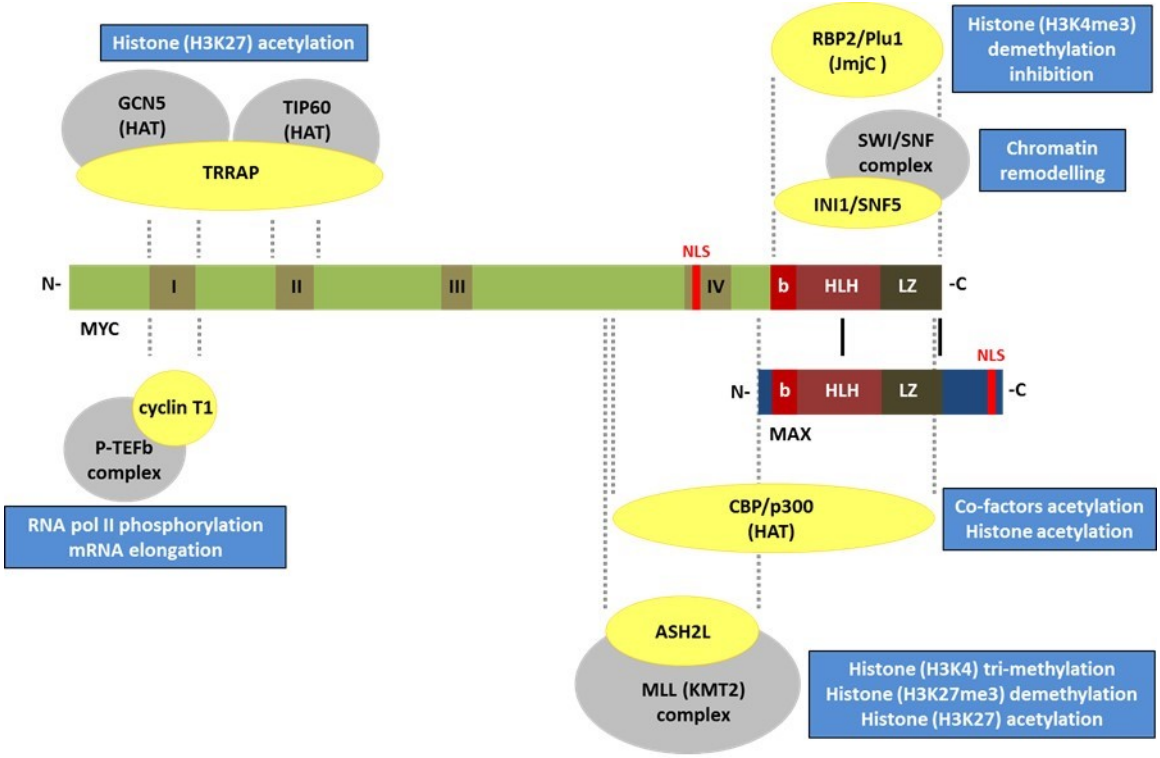

Figure 1.2.- Transcriptional activation by MYC protein. Different mechanisms throughout MYC-MAX is able to regulate positively gene transcription are described (blue boxes). Proteins that interact directly with MYC are represented in yellow and the interacting regions in MYC are indicated by dotted lines. The complex where MYC interacting proteins belong to are represented in grey.

MYC DNA binding is associated with accessible chromatin. Apart from lysine acetylation, methylation of lysine 4 of histone H3 (H3K4) is also associated with accessible chromatin (Voigt and Reinberg, 2013). This residue can be mono-, di- or trimethylated by different enzymes, including the mixed lineage leukaemia (MLL) and the SET1A/B methyltransferases. Both the MLL and SET1A/B proteins are part of larger complexes related to the yeast methyltransferase complex COMPASS (Shilatifard, 2012). It has been described that MYC interacts with ASH2L, a component of the MLL methyltransferase complex (figure 1.2) (Ullius et al.). However, MYC does not affect H3K4me3 levels despite the direct interaction with ASH2L. Instead, ASH2L-MYC interaction promotes H3K27 demethylation and H3K27 acetylation mediated by p300/CBP allowing gene transcription. RBP2/JARID1A and Plu1/JARID1B H3K4me3 demethylases have been also shown to bind to MYC similarly as described in *Droshophila.*, indicating a conserved MYC function in regulating chromatin methylation environment (figure 1.2) (Secombe and Eisenman, 2007; Secombe et al., 2007).

Apart from modifying chromatin structure allowing RNA polymerases accession to transcribe DNA, MYC proteins have also been shown to regulate transcription elongation directly. P-TEFb is a transcription elongation factor with CTD (C-terminal domain) kinase activity of the RNApol II large subunit. P-TEFb is composed of two subunits: CDK9 with CTD kinase activity and cyclin T1/T2/K (subunits needed for such function, being cyclin T1 the most frequent). It mediates RNA polymerase II phosphorylation increasing mRNA transcription (Fu et al., 1999). It has been reported that MYC interacts with cyclin T1 recruiting P-TEFb factor and thus promoting RNA polymerase II transcription elongation and mRNA production (figure 1.2) (Eberhardy and Farnham, 2001; Kanazawa et al., 2003).

These are some examples of the positive gene transcriptional regulation mediated by MYC. As a broad range transcription factor, MYC either interacts with cofactors to recruit active remodelers that lead a change in chromatin structure or directly with proteins whose activity enhance the activity of RNA polymerases and RNA transcription. This allows a regulation of transcription of different genes in many diverse contexts.

1.1.4. Transcriptional repression by MYC

MYC protein not only mediates transcriptional activation of its target genes, it also drives gene repression. Although the mechanisms underlying such function remain unclear, raising evidences support this mechanism of gene regulation.

Some of the mechanism by which MYC leads to gene repression is through the interaction with other transcription factors. For instance, MIZ1 and SP1 transcription factors act as transactivators of their target genes. MYC is known to bind either to MIZ1 or SP1 converting gene transactivation in gene repression (figure 1.3) (Gartel et al., 2001; Staller et al., 2001; Vaque et al., 2005). Whether MYC binding to these transcription factors is MAX-dependent or independent is not clear yet. However, several reports suggested that MYC-MAX heterodimers and E-box DNA sequences were necessary to bind to these factors and drive gene repression (Herkert and Eilers, 2010; Mao et al., 2003).

Apart from impairing a transactivation complex formation with MIZ1, SP1 and other transcription factors, MYC is able to interact with histone deacetylases, what creates a close chromatin environment typical of gene repression (figure 1.3). For example, MYC and SP1 recruit HDAC1 to and repress the human immunodeficiency virus type 1 long terminal repeat promoter (Jiang et al., 2007). Also, MYC-MAX recruits HDAC3 to E-box-containing promoters through the MBIII (figure 1.3) (Kurland and Tansey, 2008). Furthermore, MYC recruits the DNA methyltransferase DNMT3A and by interacting with MIZ1 form a ternary complex that repress the transcription of MIZ1 target genes (figure 1.3) such as *CDKN1A*, encoding $p21^{CIP1}$ (Acosta et al., 2008; Brenner et al., 2005; Mao et al., 2003; Wu et al., 2003).

In summary, these examples show that MYC protein can mediate transcriptional regulation in both directions, either activating or repressing gene expression. This, again, makes MYC a broad spectrum transcription factor able to regulate multiple genes and thus, cellular functions.

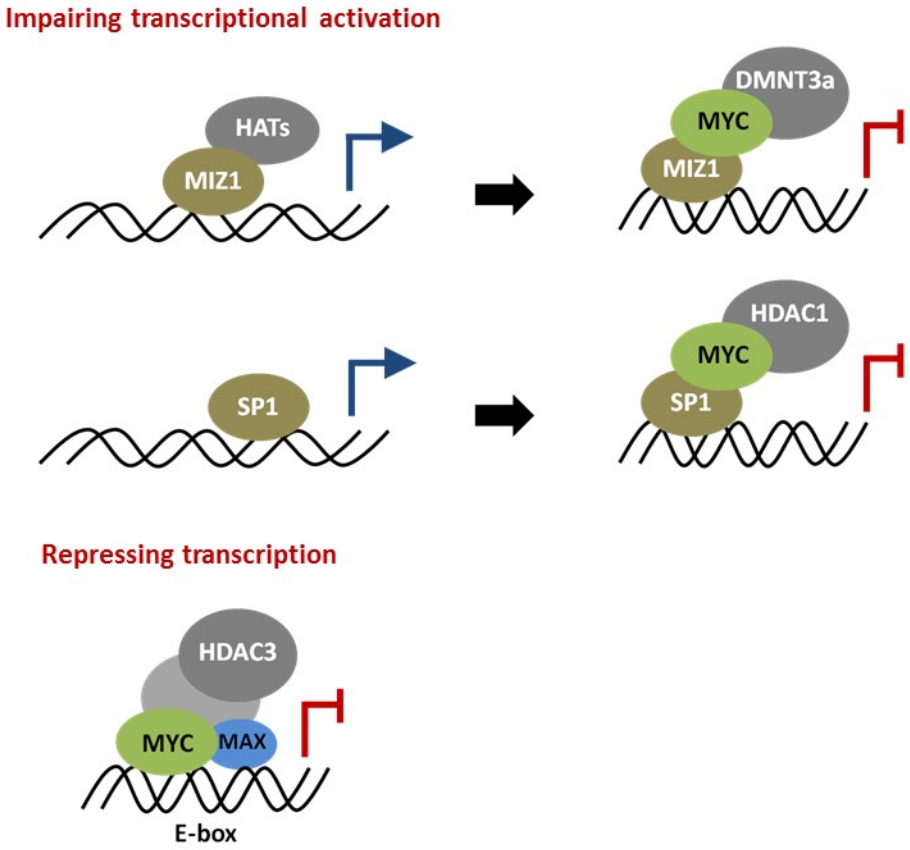

Figure 1.3.- Transcriptional repression by MYC protein. Different mechanisms by which MYC is able to regulate negatively gene transcription. MYC represses gene transcription by impairing other transcriptional activator complexes like MIZ1 and SP1 (upper pannels) or directly on E-box promoters by forming repressor complexes (lower pannel).

1.1.5. MYC target genes

The identification of MYC target genes it is a difficult task due to the high number of genomic sites where MYC is bound. It is mainly bound to regions containing E-boxes in the promoters and first exons of its target genes but it is also bound to other regions (i.e. Inr regions) direct or indirectly within the genome and not always involving gene regulation. Moreover, MYC transactivation capacity it is modulated by other factors what makes more difficult the identification of genes regulated by MYC when comparing expression profiles in modified cell lines (Grandori et al., 2000). However, different strategies have been developed in order to follow MYC activity.

For instance, the identification of the first target gene of MYC was throughout the utilization of a MYC-ER fusion protein. MYC-ER protein it is composed of the MYC gene and the hormone-binding domain of the human oestrogen receptor gene (ER) (Eilers et al., 1989). This chimeric protein it is expressed constitutively but in a inactivated form until oestrogens ligands are added to the medium, when that happens, the ligands bind to the MYC-ER and it becomes activated, translocating to the nucleus and so acting as a MYC activated protein regulating gene expression. Experiments where protein synthesis was abrogated by the addition of cycloheximide led to the confirmation of the direct regulation of gene transcription mediated by MYC and the identification of many additional target genes. With these strategies *PTMA* (encoding α-Prothymosin*)*, *CAD*, *GADD45* and *CDK4* were identified as MYC target genes (Bush et al., 1998; Eilers et al., 1991; Hermeking et al., 2000; Mateyak et al., 1997).

The development of genome wide studies techniques such as SAGE (Serial Analysis of Gene Expression), expression arrays, ChIP (Chromatin ImmunoPrecipitation) on chip, ChIP-sequencing, RNA-sequencing... have made possible the identification of thousands of putative MYC binding sites and target genes. (Chen et al., 2007; Cotterman and Knoepfler, 2009; Fernandez et al., 2003; Kim et al., 2008; Li et al., 2003; Liu et al., 2008; Martinato et al., 2008; O'Connell et al., 2003; Perna et al., 2012; Zeller et al., 2006). Some of the putative targets genes have been confirmed by conventional techniques such as gene reporter assays and ChIP. All these studies suggest that MYC binds (and likely regulates) to 10 - 15 % of all mammalian genes (Dang et al., 2006; Luscher and Vervoorts, 2012).

Taking into account all the studies that have been made and that MYC regulates all three mammalian polymerases, and so all forms of RNA (mRNA, rRNA, tRNA, miRNA and other non-coding RNAs), it is worth to consider that MYC regulates many different physiological processes such as protein biosynthesis, energy metabolism, nucleotide and amino acid metabolism, cell cycle progression, cell survival, and cell adhesion, processes that when deregulated contribute to cancer development (Luscher and Vervoorts, 2012).

1.1.6. MYC biological functions

As mentioned above MYC is a transcription factor that regulates DNA transcription of many different genes. This fact makes MYC a protein involved in many biological processes that will be resumed in the following lines.

a) MYC in cell cycle

There is a strong correlation between MYC expression and proliferation. MYC expression is induced in many cell types by a wide range of growth factors, cytokines, and mitogens (reviewed in (Bretones et al., 2014) and its expression responds immediately to most mitogenic factors (Bretones et al., 2014; West et al., 1998).

MYC stimulates the G1-S phase transition of cell cycle and the inactivation of the G1-S checkpoint that is needed to overcome S phase transition (Adams, 2001; Ekholm and Reed, 2000; Sherr and Roberts, 1999). It reduces the requirements for growth factors; blocks exit from the cell cycle; accelerates cell division and increases cell size (Bretones et al., 2014).

MYC exerts this effect by regulating genes involved direct or indirectly in cell cycle progression such as *CCND2* (encoding cyclin D2) and *CDK4* (Bouchard et al., 2001; Bouchard et al., 1999; Bretones et al., 2014; Coller et al., 2000; Hermeking et al., 2000; Perez-Roger et al., 1999) among others contributing to cell proliferation.

b) MYC in differentiation

Another important biological function of MYC has to do with the differentiation blockade. MYC levels rapidly diminish during terminal differentiation (Gonda and Metcalf, 1984; Grosso and Pitot, 1985; Lachman and Skoultchi, 1984). Accordingly, ectopic MYC expression inhibits terminal differentiation of myoblasts (Miner and Wold, 1991), leukaemia cells (Birrer et al., 1989; Coppola and Cole, 1986), adipocytes (Freytag, 1988), B lymphoid cells (Thompson et al., 1987), and myeloid cells (Larsson et al., 1988) among others (Henriksson and Luscher, 1996). Meanwhile the inhibition of MYC expression induces myeloid differentiation in HL-60 cells (Holt et al., 1988). Furthermore, the discovery that MYC was one of the four transcription factors (together with OCT4, KLF4 and SOX2) responsible for the generation of induced pluripotent stem cells (iPSC), enforces the role of MYC in maintaining the undifferentiated state (Takahashi and Yamanaka, 2006).

MYC capacity to block cell differentiation it is not only due to the inhibition of cell cycle exit that is required for terminal differentiation (La Rocca et al., 1989; Miner and Wold, 1991) but also to the capacity of repressing genes involved in specific differentiation programs such as the *CEBPA* (encoding C/EBP-α) involved in adipocyte differentiation (Freytag and Geddes, 1992; Tao and Umek, 1999) or *GATA1* in erythroid differentiation (Acosta et al., 2008).

c) MYC in cell growth

One of the first evidence that related MYC functions with cell growth was found *in Drosophila melanogaster.* dMYC mutants flies were smaller with no change in the number of cells but in the mass and size (Johnston et al., 1999). In mammals, MYC also contributes to cell growth. Murin B cell derived from Eμ-MYC mice with ectopic MYC expression were bigger in size than the control littermates with an overall increase in protein synthesis (Iritani and Eisenman, 1999; Schuhmacher et al., 2001) and murine hepatocytes over-expressing MYC protein led to a hypertrophic liver without an increase in proliferation (Kim et al., 2000).

Again, MYC role in cell growth has to do with the regulation of genes related to cell growth, metabolism, protein synthesis and different types of RNA production. For instance, MYC regulates the expression of: rRNAs genes (by RNApol I); proteins involved in rRNA processing and maturation (van

Riggelen et al., 2010); the 5S ribosomal RNA and transfer RNAs (tRNAs) by RNApol III (Gomez-Roman et al., 2003; Kenneth et al., 2007) and genes involved in mitochondrial biogenesis (Li et al., 2005), nucleotide and glucose metabolism (Kim et al., 2004; Liu et al., 2008; Shim et al., 1997; Wang et al., 2011).

d) MYC in apoptosis

In the absence of survival factors, *MYC* overexpression elicits a proliferative response but leads to apoptosis (Askew et al., 1991; Evan et al., 1992; Harrington et al., 1994; Hermeking and Eick, 1994; Wagner et al., 1994; Zindy et al., 1998). It sensitizes cells to undergo apoptosis by both p53-dependent and independent mechanisms (Sakamuro et al., 1995).

MYC can also mediate apoptosis by regulating pro- and anti-apoptotic factors. For instance, in the Eμ–MYC mouse model, MYC indirectly suppresses the expression of the anti-apoptotic proteins BCL-2 and BCL-XL and triggers apoptosis by inducing the expression of the pro-apoptotic proteins BAX or BIM (Adhikary and Eilers, 2005; Dansen et al., 2006).

e) MYC in tumorigenesis and cancer

The MYC protein is involved in tumorigenesis of many different types such as melanoma, lymphoma, multiple myeloma, myeloid leukaemia, breast, prostate, lung and gastrointestinal cancers (Nesbit et al., 1999). When MYC expression is altered, so does this gene regulation and consequently all biological processes that it regulates leading to cancer development.

The mechanisms that mainly provoke *MYC* deregulation are genome rearrangements including *v-MYC* retroviral transductions (the first evidence of MYC as an oncogenic agent), gene amplification, chromosomal translocation and viral insertions that disrupt normal gene regulation leading to an increase in MYC mRNA and protein levels (Cole, 1986; Cory, 1986; DePinho et al., 1991; Magrath, 1990; Neel et al., 1982; Nesbit et al., 1999). The first evidence of these chromosome alterations were found in human Burkitt lymphoma (B-cell lymphoma). Translocations between chromosome 8 and 14, 2 or 22 were found making MYC gene being regulated by the promoters of the heavy and light immunoglobulin chains that are constitutively expressed in these cell types (Dalla-Favera et al., 1982a; Taub et al., 1982). Other examples of this are found in multiple myeloma and in diffuse large B-cell lymphoma (DLBCL) (Boxer and Dang, 2001). Mutations in the MYC protein are rare but they do occur sometimes affecting MYC activity and stability (Gavine et al., 1999; Gupta et al., 1993; Salghetti et al., 1999). Also, post-transcriptional and post-translational mechanisms alter MYC expression contributing to tumorigenesis.

In addition, MYC contributes to the establishment of a tumor microenvironment that enhances tumor development and it also overcomes the negative signals elicited by primary transformed cells to die in such conditions. Altogether, MYC is intimately linked to tumorigenesis by being implicated in the hallmarks of cancer described by Hanahan and Weinberg (Hanahan and Weinberg, 2011).

1.2. MAX proteins

The MAX gene maps to human chromosome 14q22-24. The MAX protein was first identified in an attempt to find MYC partners interactors. To do so the b-HLH-LZ domain of the MYC protein responsible for protein-protein interaction was used as a probe to screen a B cell cDNA library in a phage vector. This led to the identification of two mRNA splice variants that encodes the majority of the MAX protein species within the cell, a 151 and 160 amino acids proteins with a molecular weight of 21 ($p21^{MAX}$) and 22 ($p22^{MAX}$) kDa respectively (figure 1.4). The latter has 9 additional amino acids in the amino-terminal region of the protein due to the usage of an alternative exon. Both mRNA species contain the b-HLH-LZ domain, thus the MAX protein belongs to the b-HLH-LZ family of proteins (Blackwood and Eisenman, 1991).

MAX is able to interact with the c-, N- and L-MYC proteins and mediates specific DNA binding throughout the b-HLH-LZ domain acting as a transcriptional co-factor (Blackwood and Eisenman, 1991; Blackwood et al., 1992a; Blackwood et al., 1992b; Prendergast et al., 1991). It also homodimerises and binds to E-boxes in the DNA although with lower affinity than the MYC-MAX heterodimers (Berberich and Cole, 1992; Kato et al., 1992; Littlewood et al., 1992; Reddy et al., 1992; Solomon et al., 1993). However, while the MYC-MAX heterodimers transactivate transcription (Amati et al., 1993; Amati et al., 1992; Gu et al., 1993; Kretzner et al., 1992a, b), reporter experiments showed that the MAX homodimers are unable to transactivate gene expression but that they antagonize the MYC transcriptional effect by DNA competition (Kato et al., 1992).

MAX like MYC is a nuclear protein (Blackwood et al., 1992a) that has an efficient NLS (figure 1.4) (Kato et al., 1992). However, conversely to MYC that has a very short half-life, MAX is a constitutively expressed and stable protein that is in excess amounts over the MYC protein (Blackwood et al., 1992b). This fact, make possible that when MYC is expressed under certain conditions, it heterodimerizes rapidly with MAX and becomes active as a transctiption factor activating gene transcription (Eisenman, 2000).

1.2.1. MAX isoforms

Several other mRNA splice variants have been reported (Blackwood and Eisenman, 1991; King et al., 1993; Makela et al., 1992; Tonissen and Krieg, 1994; Vastrik et al., 1993). For instance, it was described an alternative spliced MAX mRNA variant that resulted in a truncated MAX protein called ΔMAX lacking the carboxy-terminal region of the p21-$p22^{MAX}$ protein with a molecular weight of 16-17 kDa (p16-$17^{\Delta MAX}$) (figure 1.4). ΔMAX homodimerizes, heterodimerizes with the p21-22^{MAX} and associates with MYC to bound DNA in vitro. However, it has cytoplasmic localization when homodimerizes and unlike the p21-22^{MAX}, the overexpression of ΔMAX does not reduce the MYC transformation activity in a RAS cotransformation assay (Koskinen et al., 1994; Makela et al., 1992).

Furthermore, a variant form of the MAX protein as a result of alternative splicing, termed dMAX, was identified (different from *Drosphila sp.* dMAX). dMAX has a molecular weight of 16-17 kDa (p16-17^{dMAX}) and it lacks amino acids between 22 and 58 that is the basic, helix 1 and loop regions of the b-HLH-LZ domain (figure 1.4). Its localization is still nuclear and it maintains the capability of interacting with MYC. However, it is unable to bind to E-boxes in the DNA. Thus, the dMAX protein could act as a natural dominant negative regulator of the MYC function by producing transcriptional incompetent MYC-MAX dimers (Arsura et al., 1995).

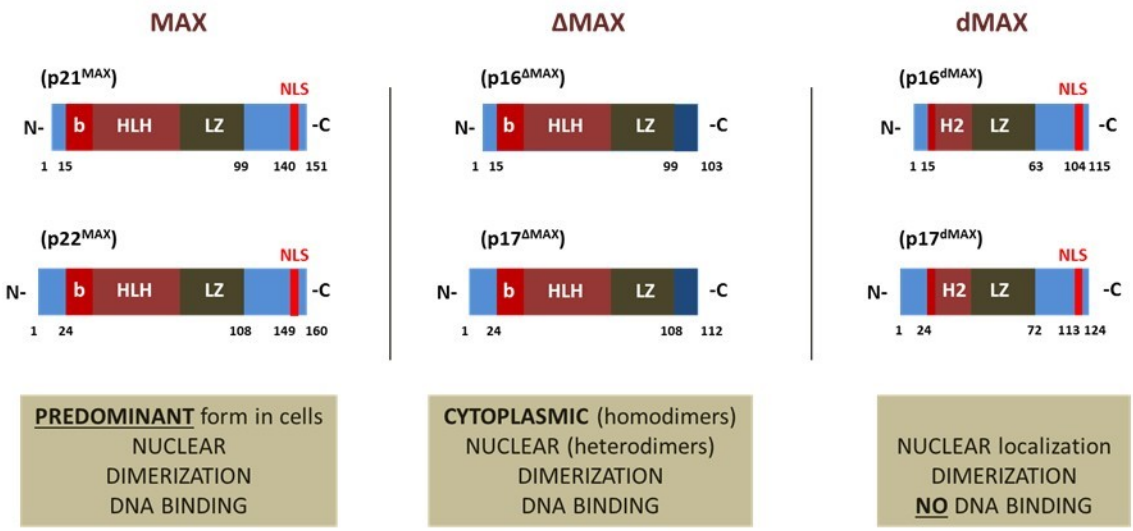

Figure 1.4.- MAX splice variants. The different splice variants of MAX protein and their characteristics are represented. The p22 and p17 MAX variants have the 9 additional amino acids in the N-terminal region.

1.2.2. MAX in tumorigenesis

Despite of its well-known role as MYC dimerization partner, a tumor cell line was described that lack the MAX protein, the rat pheochromocytoma cell line PC12. This lack of expression seemed to be a consequence of aberrant processing of the MAX transcripts. The synthesis of these transcripts appeared to be due to a homozygous chromosomal rearrangement or translocation within the MAX gene. These mutant transcripts of PC12 cells do not encode the helix2 and LZ regions of the b-HLH-LZ domain that are responsible for dimerization. Furthermore, this MAX mutant was unable to repress E-box dependent transcription in reporter assays what confirms that it is unfunctional as a transcription co-factor. Moreover, the MAX wild type in PC12 cells repressed this E-box mediated transcription and had a mild growth-inhibitory effect suggesting that loss of MAX expression may have conferred a selective growth advantage on the cells (Hopewell and Ziff, 1995).

More recently, several reports described mutations in human tumors (Burnichon et al., 2012; Comino-Mendez et al., 2011; Romero et al., 2014). For instance, exome sequencing allowed the

identification of *MAX* mutations in human hereditary pheochromocytomas. The patients analysed presented just one mutated allele of the *MAX* gene since the other allele of the *MAX* gene was deleted. Initially, three mutations were found in the *MAX* allele leading to a lack of full-length MAX protein. These observations suggested that germline mutations in *MAX* were associated with pheochromocytomas susceptibility (Comino-Mendez et al., 2011). Thereafter, mutations in *MAX* were further studied in other patients with pheochromocytomas or paraganglyomas that did not present other mutations in known genes, describing that germline mutations in *MAX* are responsible for 1.12 % of the pheochromocytomas and paraganglyomas (Burnichon et al., 2012). Furthermore, *MAX* intragenic homozygous deletions causing a complete loss of the MAX protein were also found in 6 % of Small Cell Lung Cancer tumors studied (53 cell lines and 45 primary tumors) (Romero et al., 2014). Altogether, these observations point MAX as a key component of cancer development that behaves as a classic tumor suppressor gene.

1.3. MXD family

The feature that MAX conversely to MYC it is constitutively expressed drove a search for other possible MAX interactors that could be acting in MYC absence. First, it was identified MAD1 (now termed MXD1 in HUGO nomenclature), a novel b-HLH-LZ protein (Ayer et al., 1993) and another related MXD1 protein called MXI1 (Zervos et al., 1993). Two years later, two other relatives MAD3 and MAD4 (now MXD3 and MXD4) were also identified (Hurlin et al., 1995b) and in 1997 two different groups identified also MNT that was slightly different in structure but with similarities in behaviour (Hurlin et al., 1997b; Meroni et al., 1997). All these five members (MXD1, MXI1, MXD3, MXD4 and MNT) conforms the MXD family of proteins.

Each of the MXD genes has different chromosomal locations (Hurlin et al., 1997b; Hurlin et al., 1995b; Zervos et al., 1993). They all share two common domains, the b-HLH-LZ and the SID domains (figure 1.5) that will be described later. Besides, the sequences of MXD1-MXD4 are highly related to each other both within and outside their conserved domains with an overall similarity ranging from 56–72 % (Hurlin et al., 1995b). The MXD family members act as transcription factors, regulating gene transcription.

1.3.1. MXD family expression

The MXD proteins expression has been linked to quiescence and terminal differentiation statements in a wide range of cell types, including chondrocytes, colonic epithelia, epidermal keratinocytes, adipocytes and motor neurons, as well as erythroid and myeloid hematopoietic cells (Luscher, 2012).

Studies in embryonic tissues during mouse development point MXDs expression to differentiating tissues like the skin, bone, colon, neural tube, brain, retina, and thymus (Hurlin et al., 1995a; Hurlin et al., 1995b; Luscher, 2012; Queva et al., 1998). MXD1 expression was restricted to late differentiation

statements meanwhile MXI1 and MXD4 were also detected at low levels in precursor layers. Moreover, MXD3 expression has been also detected in the S phase of proliferating cells (Hurlin et al., 1995b; Pulverer et al., 2000; Queva et al., 1998).

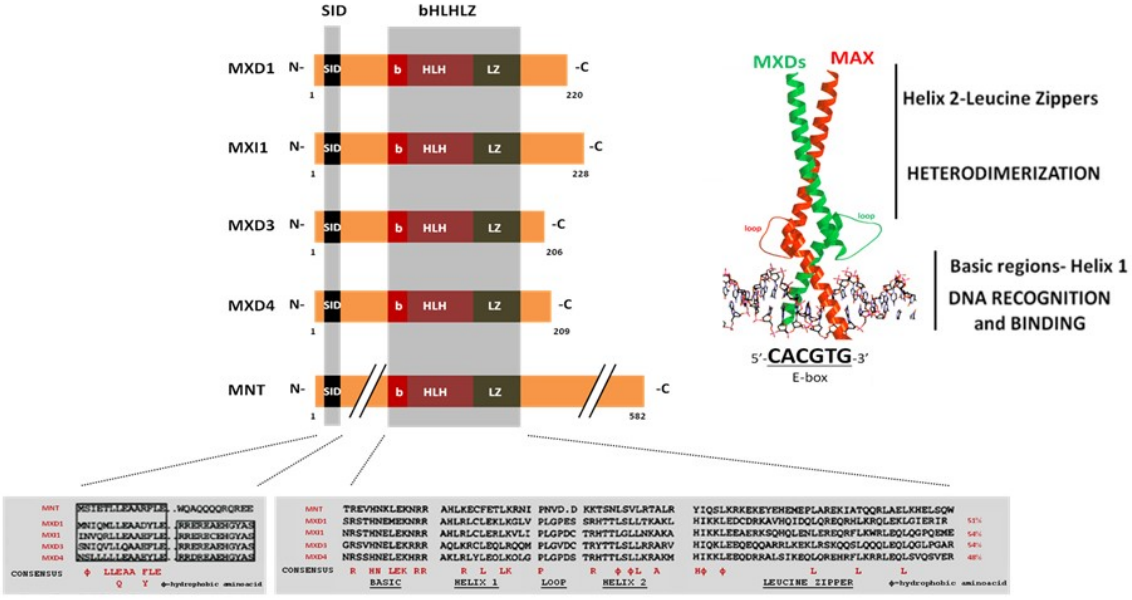

Figure 1.5.- MXD proteins. MXD family members representation. The SID and b-HLH-LZ common domains are highlighted in grey and their sequence similarity compared with MNT domains sequences. On the right, a structure representation of the b-HLH-LZ of MXD-MAX heterodimers obtained after crystallography and X ray diffraction is shown (modified from Nair and Burley, 2003).

Furthermore, MXD correlation with cell cycle exit and differentiation has been confirmed by several studies where the induction of hematopoietic differentiation led to an increase in MXD1 and MXI1 mRNA levels (Ayer and Eisenman, 1993; Delgado et al., 1995; Larsson et al., 1994; Zervos et al., 1993) and where MXD1 overexpression inhibits cell proliferation capacity of 3T3 cells after CSF-1 (colony-stimulating factor 1) stimulation (Roussel et al., 1996). Moreover, the MYC-RAS co-transformation potential was reduced in assays were the MXD members were overexpressed suggesting a role of these proteins in cell cycle progression inhibition (Grandori et al., 2000; Hurlin et al., 1995b; Koskinen et al., 1995; Lahoz et al., 1994; Vastrik et al., 1995).

There is an exception in one member of the MXD family that is the MNT protein. MNT, conversely to the rest of MXD members, is expressed constitutively and also ubiquitously with independence of cell cycle progression, quiescence or differentiation (Hurlin et al., 1997b; Hurlin et al., 2003, 2004; Meroni et al., 1997; Popov et al., 2005). Thus, MNT is co-expressed with either MYC or other MXD proteins in the cells.

1.3.2. Gene expression regulation by MXD proteins

All MXDs members shared biochemical properties characteristic of the MYC family (Eisenman, 2000). First, they are proteins with a very short half-life similar to that of MYC of about 20 min, however, they have an opposite pattern of expression. All of them but MNT are highly expressed in non-proliferating and in a wide range of terminal differentiating cells and at almost no detectable levels in proliferating and undifferentiated cells (Ayer and Eisenman, 1993; Hurlin et al., 1995a; Hurlin et al., 1995b; Larsson et al., 1994; Queva et al., 1998; Vastrik et al., 1995). MNT on the contrary, it is constitutively expressed in the different cell statements (Hurlin et al., 1997b).

Secondly, they all have the b-HLH-LZ domain (figure 1.5) that, like MYC, allows them to heterodimerize with MAX and bind to E-box sequences. It has been shown that the affinity of MXD1 for MAX heterodimerization and DNA binding is similar to that of MYC (Eisenman, 2000; Sommer et al., 1998). Moreover, similarly to MYC proteins, the MXDs cannot homodimerize in vivo (Ayer et al., 1993; Hurlin et al., 1995a; Hurlin et al., 1997b; Hurlin et al., 1995b; Meroni et al., 1997). Only homodimerization capacity has been attributed to the MNT protein but to a limited extent (Meroni et al., 1997).

On the other hand, they all have another domain highly conserved between all the family members and across species in the N-terminal region of the protein. This region conforms a putative amphipathic α-helix structure that allows them to interact with the mSIN3A or mSIN3B corepressors (Hurlin et al., 1995b; Kiermaier and Eilers, 1997; Knoepfler and Eisenman, 1999; Schreiber-Agus and DePinho, 1998). mSIN3A/B are the mammalian orthologues of the *Saccharomyces cerevisiae* transcriptional corepressor SIN3 which is 30 % identical (Halleck et al., 1995; Wang et al., 1990). This domain of MXDs is called SIN3 Interactor Domain (SID) (figure 1.5) (Ayer et al., 1996). The interaction between the MXD proteins and mSIN3 proteins requires this SID domain of MXDs and one of the four paired amphipathic helix regions (PAH) in mSIN3 that mediate protein interactions, the PAH2 (figure 1.6) (Ayer et al., 1995; Halleck et al., 1995; Schreiber-Agus et al., 1995).

mSIN3A/B are two proteins that are 60 % identical and act as scaffold proteins contributing to the formation of a gene repressor complex. mSIN3A/B have the ability to interact with other proteins with histone deacetylase activity such as HDAC1/2 through the HID (Histone deacetylase Interaction Domain) or co-factors such as N-CoR corepressors through the PAH1 and PAH3/HID domains (figure 1.6) (Halleck et al., 1995; Heinzel et al., 1997; Laherty et al., 1997). Interaction between MXD and mSIN3 is strongly correlated with repression what is supported by SID point mutations studies (Ayer et al., 1995; Laherty et al., 1997). In addition, the abolishment of the mSIN3-MXD1 interaction makes MXD1 incapable of inhibiting MYC-RAS co-transformation or cell cycle progression (Koskinen et al., 1995; Roussel et al., 1996). In support of the latter is that MNTΔSID mutants (lacking SID domain) gains transforming activity in cooperation with an activated RAS oncoprotein, whereas MNT and MXD1 proteins with functional SIDs interfere with this transformation (Grandori et al., 2000).

Furthermore, naturally occurring splice variants of the MXI1 protein (MXI1-WR) which lack the SID also fail to block co-transformation by MYC-RAS (Schreiber-Agus et al., 1995).

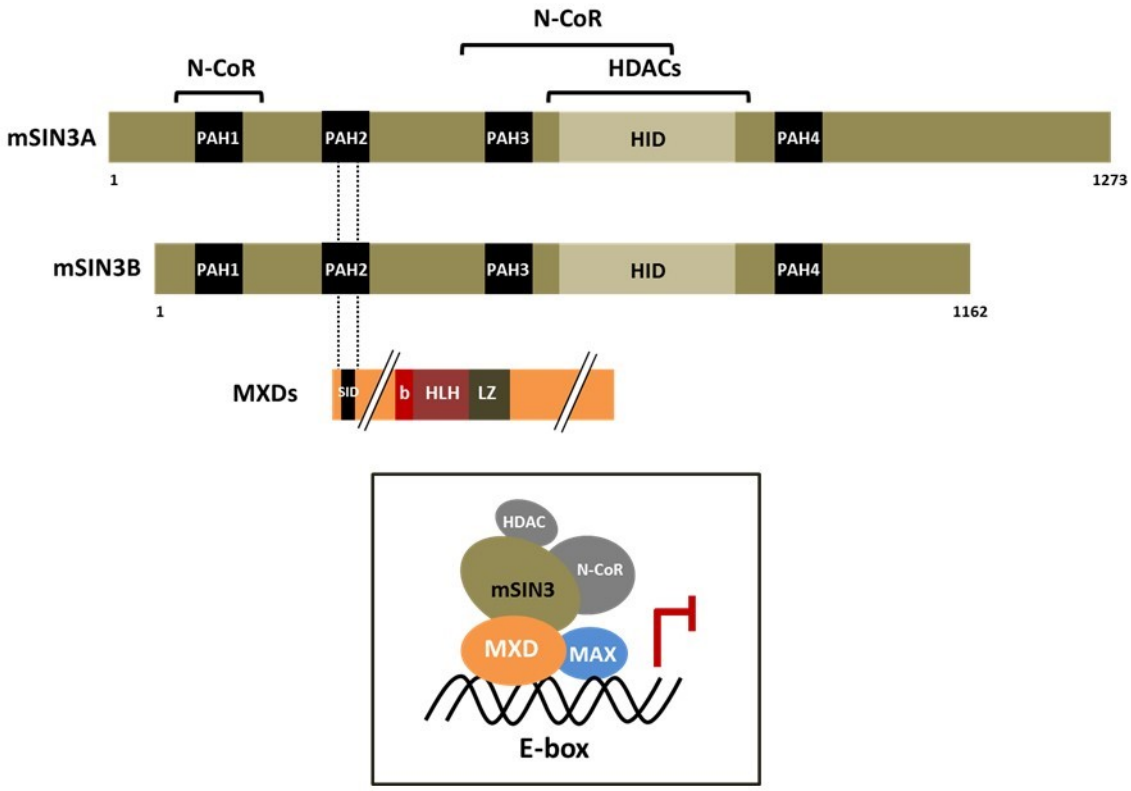

Figure 1.6.- MXD-SIN3-HDAC/N-CoR complexes. Scheme of mSIN3A/B protein structures. PAH refers to Pair Amphipathic Helix and HID to Histone deacethylases Interaction Domains. The interaction region of mSIN3A/B with MXD proteins is represented by dotted lines and the interacting regions with N-CoR and HDACs indicated (upper pannel). A representation of the repressor complex formed with MXD-MAX heterodimers on E-Box promoters is shown (lower pannel).

In summary, MXD-MAX heterodimers bind to E-boxes, what suggests that they might have common target genes with MYC, and regulate gene transcription in a negative direction through the formation of an mSIN3-repressor complex in the promoter of their target genes, opposite to MYC-MAX gene regulation (figure 1.6).

1.4. MYC/MAX/MXD network

The MYC, MAX and MXD proteins are three families of transcription factors that regulate multiples functions of cell biology like cell metabolism, proliferation, differentiation, apoptosis and development by regulating gene expression. They compose an important network that must be highly regulated and balanced.

The network output depends on MYC and MXD expression since MAX is constitutively expressed. These two families have opposite functions regarding gene regulation and they share many target genes. Generally, when cells are proliferating or in undifferentiated states the high MYC levels displace the equilibrium of the network towards MYC-MAX heterodimers. MYC-MAX species then will regulate positively gene regulation of genes involved in cell cycle progression or undifferentiated state. On the other hand, when cells are quiescent or when they undergo differentiation, an upregulation of MXD1-4 occurs displacing the equilibrium towards MXD-MAX dimers that will regulate negatively genes involve in cell cycle progression or undifferentiated states. MNT is an exception as it is always expressed and thus ready to form heterodimers with MAX. This allows a control of gene expression in situations where there are no high levels of MYC neither of MXD, contributing to maintain the homeostasis of cell biology (figure 1.7).

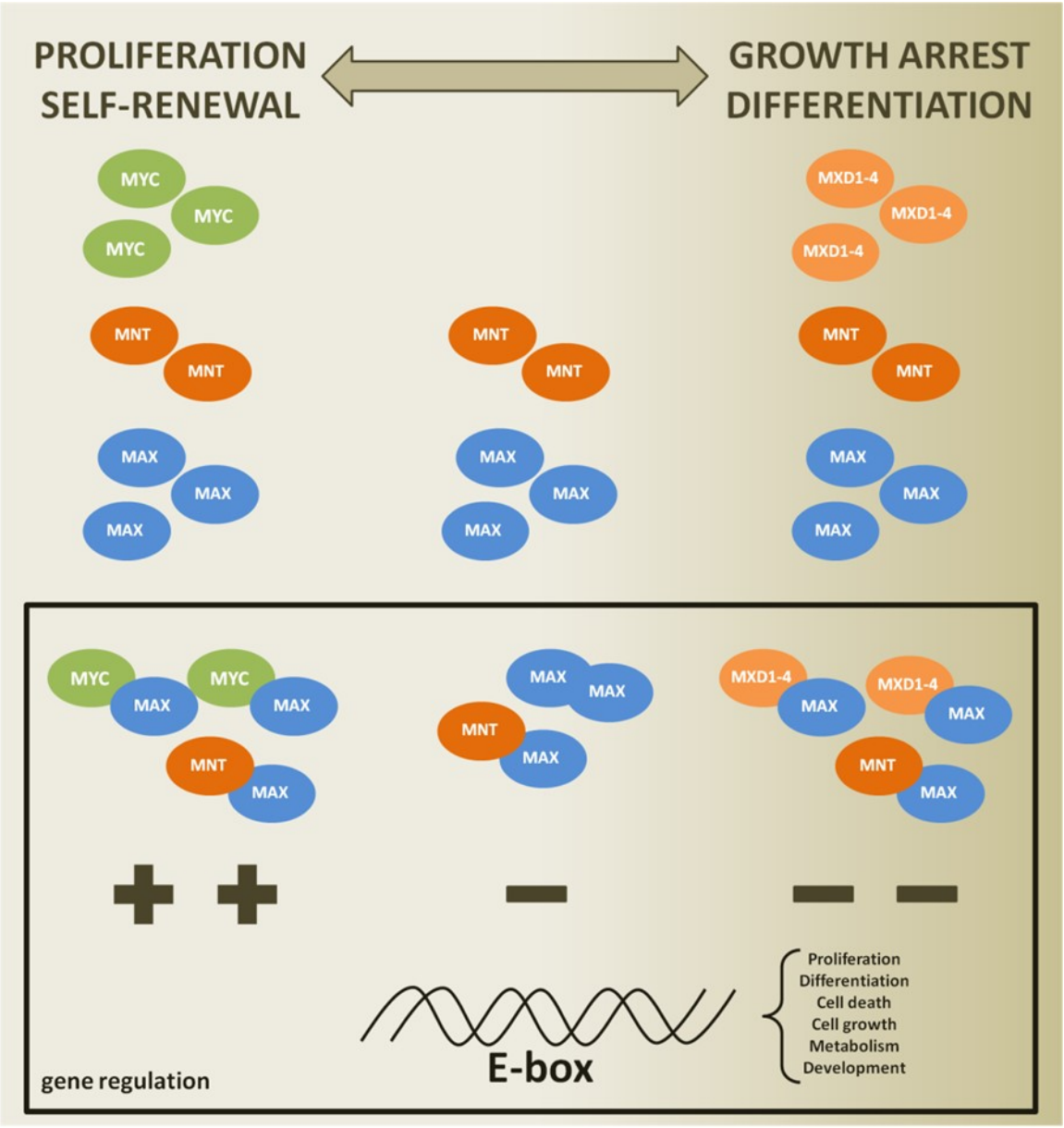

Figure 1.7.- MYC/MAX/MXD network. Representation of MYC, MAX, MXD1-4 and MNT relative expression and the predominant dimers formed in the different cell states. MYC proteins are highly expressed in proliferation and self-renewal statements but almost not detectable at differentiation or growth arrest statements. On the contrary MXD1-4 are highly expressed in differentiation and growth arrest statements and poorly expressend in proliferation or self-renewal. MNT and MAX are expressed at constant levels in every cell state. The overall response to MYC, MXD1-4 and MNT expression levels is translated in different gene regulation directions. Highly expressed MYC heterodimerizes with MAX and activate gene transcription (+ +) meanwhile highly expressed MXD1-4 heterodimerizes with MAX and represses gene transcription (- -). MNT-MAX heterodimers actively and MAX homodimers pasively repress gene transcription (-) constitutively acting as buffers on MYC activity.

1.5. MXD1

MXD1 was together with MXI1, the first MXD member identified in an attempt to find other MAX interacting proteins (Ayer et al., 1993). It is one of the best characterized members of the family and its function known so far regarding cell behaviour will be resumed in the next lines since the biology of this gene has been studied in the present Thesis.

1.5.1. MXD1 in proliferation

The MXD proteins inhibit proliferation by switching MYC-MAX to MXD-MAX heterodimers. The first evidence of MXDs as cell cycle inhibitors came in MYC-RAS co-transformation assays where the MXD presence reduced the transformation capacity of the cells (Grandori et al., 2000; Hurlin et al., 1995b; Koskinen et al., 1995; Lahoz et al., 1994).

Then, it was suggested that this proliferation inhibition mediated by MXD1 was due to an accumulation of cells in G1 phase that correlated with a reduce number of cells in the S and G2/M phases (Roussel et al., 1996). In addition, MXD1 inhibited serum-induced entry into S phase of 3T3-L1 cells (Rottmann et al., 2005). This indicates that MXD1 influences negatively the transition to S/G2 phases thus inhibiting cell cycle progression.

Also, experiments with the MXD1-ER fusion protein, a chimeric protein of MXD1 and the oestrogen receptor (ER) that becomes active upon tamoxifen addition, also confirm the negative effect of MXD1 in proliferation. Cells transfected with MYC, RAS and MXD1-ER were injected to syngenic rats and an inhibition of tumor cell outgrowth was achieved in tamoxifen treated rats (Cerni et al., 2002). On the other hand, UTA osteosarcoma cells transfected with a MXD1 tetracycline regulatable plasmid that induce its expression after tetracycline withdrawal (tet-off system) showed a decrease in the number of colonies and a slower growth rate (Gehring et al., 2000) and NIH3T3 cells with tetracycline regulatable MXD1 in a tet-on system, present the same effect upon the tetracycline homologue doxycycline treatment (Bejarano et al., 2000).

Furthermore, the phenotypes of genetically modified mice overexpressing the MXD1 protein support the idea that MXD1 regulates cell cycle exit. For instance, MXD1 transgenic mice with MXD1 regulated by the β-actin promoter (i.e., expressed in most tissues) presented postnatal lethality and defects in proliferation in multiple cell types (Queva et al., 1999). In addition, MXD1 expression directed to B and T cells in mice showed proliferative defects and a reduced cellularity in the lymphoid compartment (Iritani et al., 2002; Rudolph et al., 2001).

1.5.2. MXD1 in differentiation

There is a correlation between differentiation and MXD1 expression that has been shown in different systems. For instance, in myeloid leukaemia cells lines induced to differentiate with chemical inducers, the MXD1 mRNA levels were increased immediately after treatment meanwhile the MYC mRNA levels decreased rapidly and the MAX mRNA remained invariant (Ayer and Eisenman, 1993; Larsson et al., 1994). Also, the MXD1 overexpression in myeloid leukaemia cells was found to induce an erythroid differentiation program (Acosta et al., 2008). Moreover, the HL60 cells that were induced to differentiate to a granulocytic linage with DMSO, showed an increase in the MXD1 levels. A switch of MYC to MXD1 binding to DNA was detectable at late differentiation stages indicating a role of MXD1 in late differentiation. Surprisingly, MXD1 was not forming complexes with MAX in this system (Ryan and Birnie, 1997). Furthermore, it was shown that granulocytic differentiation upon cytokine granulocyte-colony stimulating factor (G-CSF) treatment, activates the JAK/STAT and the RAS/RAF/ERK pathways leading to an upregulation of MXD1 through the C/EBPβ factor (Jiang et al., 2008; Werner et al., 2001). Also, MXD1 can block the ability of MYC to inhibit terminal differentiation of murine erythroleukemia cells (Cultraro et al., 1997a, b) and an inhibition of cell cycle exit during granulocyte differentiation was shown in $MXD1^{-/-}$ mice (Foley et al., 1998). Altogether these examples show that MXD1 is able to promote cell cycle exit and intimately involved in the haematological differentiation program.

The MXD1 expression has been also linked to keratinocyte differentiation. In general, the MXD family members are predominantly expressed in the suprabasal, differentiated layers of embryonic and adult skin (Hurlin et al., 1995a; Hurlin et al., 1995b; Lymboussaki et al., 1996; Vastrik et al., 1995). Furthermore, the induction of keratinocyte differentiation in vitro is accompanied by an increase in MXD1 and MXI1 expression (Gandarillas and Watt, 1995). In addition, the TGF-β superfamily members Activin and TGF-β1 that are involved in the regulation of keratinocyte proliferation and differentiation (Munz et al., 1999; Seishima et al., 1999; Shimizu et al., 1998), induce MXD1 expression (Werner et al., 2001) what results in an inhibitory effect on keratinocyte proliferation needed for the differentiation of the cells. However, overexpression of MXD1 in keratinocytes is not sufficient to induce the differentiation program (Grandori et al., 2000). Moreover, MXD1 was expressed in squamous cells in the skin, in hypertrophied chondrocytes and in many other terminally differentiated cells (Chin et al., 1995; Hurlin et al., 1995a; Vastrik et al., 1995).

On the other hand, contrarily to what was expected, the MXD1 overexpression in 3T3-L1 cells led to less adipogenic differentiation (Cornelius et al., 1994; Fajas et al., 1998; Hwang et al., 1997). This is likely to be a consequence of inhibiting the proliferative burst that is necessary for 3T3-L1 adipogenic differentiation (Pulverer et al., 2000).

These examples show clearly that MXD1 is involved in the differentiation program of cells and that MXD1 does that mainly through the inhibition of cell cycle progression and the attenuation of the MYC activity.

1.5.3. MXD1 in apoptosis

The MXD1 involvement in apoptosis has been also reported. Haematopoietic cells isolated from MXD1$^{-/-}$ mice that were treated with limiting prosurvival cytokines to induce apoptosis were more sensitive, resulting in a decrease ability to survive under limiting conditions (Foley et al., 1998). On the other hand, myeloid precursor cells from MXD1 transgenic mice were less sensitive to limiting prosurvival cytokines levels (Queva et al., 1999) indicating an antiapoptotic role of MXD1.

Another example of the MXD1 involvement in antiapoptotic processes is the identification of *PTEN* as a direct MXD1 target gene. PTEN is a phosphatase that controls the PI3K/AKT pathway. It is known as a tumor suppressor gene that is mutated or silenced in a broad range of human tumors (Di Cristofano and Pandolfi, 2000). MXD1 represses *PTEN* expression which leads to an activation of AKT and then promotes survival. Therefore, PTEN is a critical target gene for the antiapoptotic function of MXD1 (Rottmann et al., 2008). On the other hand, it has been also described that in other cell contexts, the PI3K/AKT pathway upon TRAIL stimulation activates apoptosis by downregulating MXD1 expression (Reuss et al., 2013).

Furthermore, in the UTA cells (derived from the U2OS human osteosarcoma cells) overexpressed MXD1 confers an antiapoptotic effect when the cells are exposed to ultraviolet light or treated to induce the FAS and TRAIL pathways. This antiapoptotic effect was abrogated when using MXD1 mutants lacking the SID domain, suggesting that the SID domain is important for the MXD1 antiapoptotic function (Gehring et al., 2000).

Together, these examples show that MXD1 again presents biological functions that are opposite to MYC since MYC is known and described earlier to induce apoptosis programs.

1.5.4. MXD1 in cancer

MXD1 has been described to be deregulated in some tumor samples. For instance, MXD1 appeared downregulated in samples of invasive breast cancers whereas it is expressed in benign lesions (Han et al., 2000). Also, MXD1 was identified as one of six genes downregulated at the transcriptional level in Barrett's metaplasia and oesophageal adenocarcinoma (Hourihan et al., 2003). However, regarding the latter, other work found that MXD1 together with MYC and MXI1 was upregulated in oesophageal adenocarcinomas (Boult et al., 2008). They suggest that this might be a mechanism to counteract aberrant MYC signaling in these tumors.

Another example of the MXD1 implication in tumorigenesis is the identification of MXD1 as a substrate of c-IAP1 (Xu et al., 2007). c-IAP1 is a member of the inhibitor of apoptosis protein (IAP) family with ubiquitin ligase (E3) activity proposed to be an oncogene (Imoto et al., 2001; Wright and Duckett, 2005). c-IAP expression leads to MXD1 ubiquitination and subsequent proteasome degradation, enhancing MYC-mediated tumorigenesis (Xu et al., 2007).

In addition, it has been recently described a direct contribution of MXD1 to drug resistance. It has been shown that HIF-1α regulates positively and directly MXD1 expression. This confers doxorubicin resistance to hypoxic colon cancer cells by attenuating the MYC activity in mitochondria biogenesis (Cho et al., 2013).

Furthermore, a search for MXDs mutations led to the identification of point mutations in haematological tumor samples. Among 10 cell lines and 26 samples, nine mutations were revealed: two in MXD1, four in MXI1 and three in MNT. Some of them were found in conserved residues among the MXD members. For instance, a point mutation at position Lys78 in MXD1 that might have significant implication for MAX heterodimerization; a point mutation within the helix I of MXI1, with a His82Tyr substitution and a point mutation within the helix I of MNT, with a Pro248Leu substitution. In addition, two patients had other MXI1 mutations (Ser52Glu and His82Tyr) and two others showed MNT mutations (Pro248Leu and Lys300Asn). However, the implication in cancer development and how these mutations affect the functionality of these proteins is unknown (Guo et al., 2007).

These examples show that although it may not be a prevalent alteration in cancer, deregulated MXD1 expression might contribute to cancer development.

1.5.5. MXD1 target genes

Due to the similarities in DNA binding and MAX heterodimerization, it is suggested that MXD1 may have MYC common target genes and that they regulate them in opposite direction. However, the MXD1-mediated regulation of the MYC target genes has not been confirmed for all known MYC target genes. In addition, some studies show that MXD1 and MYC have common (Nikiforov et al., 2003) and different transcriptional programs (Gehring et al., 2000; James and Eisenman, 2002) making unclear this suggestion. Nonetheless, some of the relevant MXD1 target genes described so far will be summarized in this section.

The hTERT is the catalytic subunit of telomerase enzymatic complex, known to be positively regulated by MYC (Greenberg et al., 1999; Wang et al., 1998; Wu et al., 1999). When cells undergo differentiation, hTERT is downregulated and this effect is at least in part mediated by MXD1 (Gunes et al., 2000). Moreover, MXD1 recruits the histone demethylase RBP2 to the hTERT gene promoter to demethylate histone H3-K4 and repress gene transcription (Ge et al., 2010).

In several cases it has been described a shift from MYC-MAX to MXD1-MAX as both dimers bound to some common genes. One example is the shift from MYC-MAX to MXD1-MAX that occurs in the E-box-containing promoter of the *CCND2* (endocing cyclin D2) target gene during hematopoietic differentiation, correlating with histone deacetylation and repression of the gene (Bouchard et al., 2001; Xu et al., 2001). Another example of the MYC-MAX to MXD1-MAX shift occurs in the ornithine decarboxylase (*ODC*) gene promoter after retinoic acid (RA) and interferon ɣ (IFN-ɣ) treatment to

induce differentiation of neuroblastoma cells what results in a more condensed chromatin structure linked to gene repression (Cetinkaya et al., 2007). Also, a dynamic shift from MYC-MAX to MXD1-MAX and MNT-MAX occurs at the proximal promoters of the *MLH1* and *MSH2* genes (two mismatch repair genes) in hypoxic conditions leading to a downregulation of these genes and an increase in genetic instability in tumor cells (Bindra and Glazer, 2007) indicating a direct gene regulation by MYC, MXD1 and MNT.

In addition the role of MXD1 in apoptosis is in part mediated by a direct downregulation of the PTEN gene what enhances a prosurvival PI3K/AKT pathway (Rottmann et al., 2008), as commented above.

Some of these genes are also MYC target genes. However, MYC regulates them in a positive direction meanwhile MXD1 does it in a negative direction. This correlates with the antagonizing function of MXD1 over MYC corresponding to an opposite regulation of cell metabolism, proliferation, apoptosis and differentiation.

1.6. MNT

MNT was identified in 1997 by two different groups. Hurlin et al. (1997b) described the murine *MNT* in a yeast two-hybrid screen using MAX as the bait and cDNA libraries from day 9.5 and 10.5 mouse embryos while Meroni et al. (1997) identified the human homologue of *MNT* (there termed ROX) in a search for transcribed sequences from the human chromosome 17p13.3 locus. The human MNT gene expands a sequence less than 40 kb long and it has 6 exons (figure 1.8) (Lo Nigro et al., 1998) that produces a protein of 582 amino acids with a molecular weight of 72 and 74 kDa. These variations in the molecular weight are due to MNT phosphorylation (74 kDa) and it is shown as a double band in SDS-PAGE. Also, MNT was described to have nuclear localization (Hurlin et al., 1997b; Meroni et al., 1997; Popov et al., 2005).

1.6.1. MNT, unique among MXD members

MNT as an MXD member has features in common with the rest of MXD (Fig 1.5). For instance, it heterodimerises with MAX throughout the b-HLH-LZ to bind to DNA in E-box sequences although with higher affinity for CACGCG sites compared to CACGTG sequences and it also functions as a transcriptional repressor since it presents the SID domain in the amino terminal region of the protein (Hurlin et al., 1997b; Meroni et al., 1997).

However, MNT presents some differences that make it unique among the other MXDs. First, it is the largest one with a molecular weight of 72-74 kDa contrarily to the rest of MXD that have a molecular weight around 30-34 kDa. Second, contrarily to the rest of MXD members MNT protein is expressed constitutively and also ubiquitously with independence of cell cycle progression, quiescence or differentiation (Hurlin et al., 1997b; Hurlin et al., 2003, 2004; Meroni et al., 1997; Popov et al., 2005).

Third, it has been shown that deletion of the SID domain not only abrogates MNT function as a repressor but it converts it into a transcriptional activator. This is thought to be because of the presence of a proline-rich sequence at its N-terminal region (figure 1.8) which resembles the activation domain of several transcription factors including Myc Box I (Hurlin et al., 1997b). This proline-rich region presents also SH3-binding motives (protein interaction domains) (figure 1.8). In addition, MNT has a proline/histidine rich sequence at its C-terminal region (figure 1.8) with a yet uncharacterized function (Hurlin et al., 1997b). Fourth, $MNT^{-/-}$ mice are not viable (Hurlin et al., 2003; Toyo-oka et al., 2004) meanwhile $MXD1^{-/-}$, $MXI1^{-/-}$ and $MXD3^{-/-}$ mice survive possibly as a redundancy in the MXD1-4 activities (Foley et al., 1998; Queva et al., 1999; Schreiber-Agus and DePinho, 1998). Fifth, only dMNT protein has been identified in *Droshophila* but no other dMXD (Orian et al., 2003) and even more interesting, in the worm *Caenorhabditis elegans* functional MAX and MNT but no MYC orthologues have been found, indicating that these genes are more evolutionary conserved than the well-known *MYC* (Yuan et al., 1998). Finally, MNT has been found to be the most abundant MAX-binding partner in several human tumor cell lines (Popov et al., 2005; Smith et al., 2004; Sommer et al., 1998; Sommer et al., 1999).

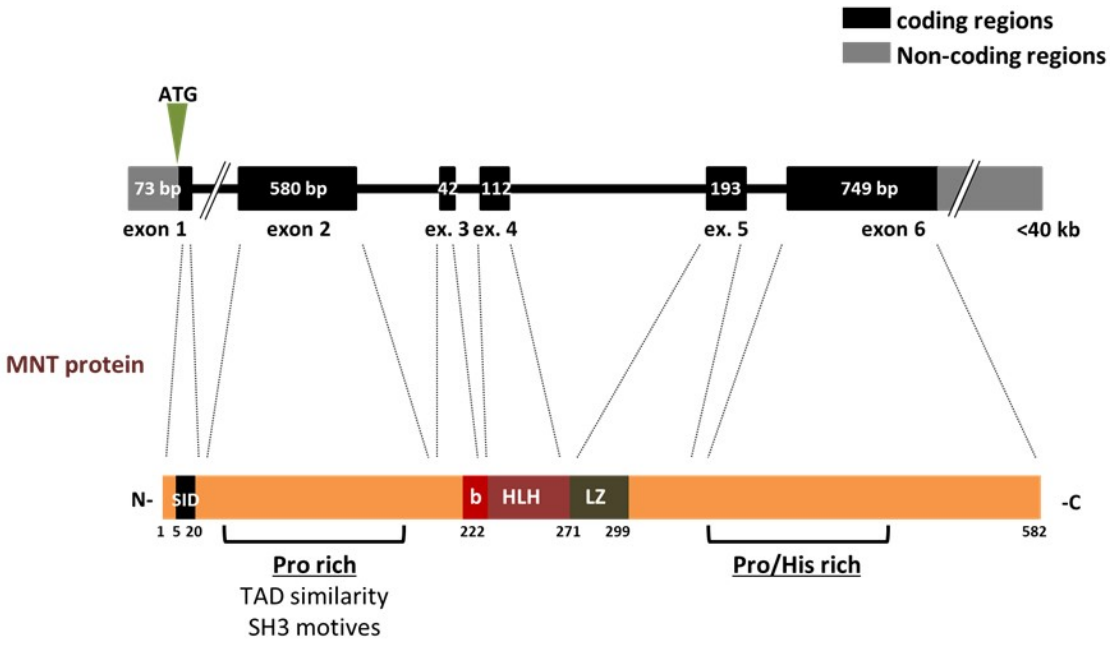

Figure 1.8.- MNT human gene and protein structure. MNT gene located in human chromosome 17p13.3 is represented. AUG refers to the translation start codon. In the protein representation, SID refers to Sin3 Interaction Domain, and b-HLH-LZ to basic Helix Loop Helix Leucine Zipper domain. Other characteristics of MNT protein structure are indicated.

1.6.2. MNT in proliferation and cell growth

MNT is expressed throughout the cell cycle and the MYC-MAX and MNT-MAX dimers coexist in proliferating cell types (Hurlin et al., 1997b; Popov et al., 2005; Pulverer et al., 2000; Sommer et al., 1998; Sommer et al., 1999) suggesting a role of MNT as a modulator of the MYC-MAX activity.

The first evidence of MNT as an antagonist of MYC in proliferation came with the discovery that MNT overexpression was able to override the transformation effect of MYC and RAS in cells (Hurlin et al., 1997b). Another example are MNT transgenic mouse embryos. These embryos present a delay in development and die in mid gestation when MYC function in proliferation is critical (Hurlin et al., 1997b). It has been suggested that MNT has an important role in the regulation of cell cycle progression because it suppresses cell cycle entry and proliferation when overexpressed but accelerates the G0 to S transition in mouse embryo fibroblasts (MEFs) lacking MNT. This seems to be linked to an upregulation of *CDK4* and *CCNE* (encoding cyclin E) (Hurlin et al., 2003). In addition, down-regulation of MNT by siRNA (small interfering RNA) has been shown to be sufficient to provoke typical MYC responses, such as increased cell proliferation and transformation by RAS even in MYC null cells (Hurlin et al., 2003). Furthermore, in *Drosophila melanogaster*, MNT (dMNT) is important for cell cycle progression, proliferation, and cell growth in the fly since overexpression of dMNT resulted in small flies whereas dMNT null flies have larger cells, increased weight, and decreased life span compared to wild-type flies (Loo et al., 2005).

Popov et al. described that MNT was phosphorylated at cell cycle entry resulting in a disruption of the MNT-mSIN3-HDAC1 interaction. They showed that non-phosphorylated MNT was the responsible for mSIN3B interaction and that the MNT-mediated transcriptional repression of CCND2 (cyclin D2) gene was reduced upon phosphorylation of MNT at cell cycle entry resulting in augmented levels of cyclin D2. Besides, since MYC is upregulated when cells proliferate, they suggest that MYC-MAX heterodimers augment even more the cyclin D2 levels leading to cell cycle progression (Popov et al., 2005).

These examples together with the constitutive expression of MNT highlight the importance of this MXD member in the restriction of MYC activities associated with cell proliferation.

1.6.3. MNT in apoptosis

Another characteristic of MNT function is its capability of regulating apoptosis. It has been shown in several models that MNT deficiency leads to an increase in apoptosis, a feature that also occurs in conditions of MYC overexpression.

For instance, MNT null MEFs and mouse and rat fibroblasts where MNT was silenced with RNA interference, showed an increase in apoptosis in response to serum withdrawal. The effect is reproduced even in MYC null fibroblast, and linked to an increase in p53 levels and a downregulation of the antiapoptotic protein BCL-XL (Hurlin et al., 2003; Nilsson et al., 2004; Walker et al., 2005). In

addition, conditional deletion of MNT in T cells has been shown to cause increased apoptosis of thymic T cells leading to smaller thymus (Dezfouli et al., 2006).

Furthermore, MNT deficiency was associated with high levels of mitochondria-generated ROS (reactive oxygen species) in both T cells and MEFs with or without MYC overexpression. ROS can be toxic and induce apoptosis when accumulated beyond thresholds dictated by cellular anti-oxidant capacity (Fruehauf and Meyskens, 2007; Mates et al., 2008). In addition, along with high ROS, MNT null cells were extremely sensitive to apoptosis induced by small molecule inhibitors of different anti-oxidant systems, and this hypersensitivity was completely reversed by enhancing antioxidant mechanism (Link et al., 2012). Thus, apoptosis in MNT null cells seem to be caused by increased ROS levels.

1.6.4. MNT in development

MNT is one of 20 genes deleted in a heterozygous fashion in Miller-Dieker syndrome (MDS), a contiguous gene syndrome that consists of severe neuronal migration defects and craniofacial dysmorphic features. All MDS cases are associated with deletions of chromosome 17p13.3. In mice, loss of *MNT* results in perinatal lethality and growth retardation. Furthermore, $MNT^{-/-}$ mice also display cleft palate and retardation of skull development, suggesting that MNT may play a role in the craniofacial defects displayed by MDS patients (Toyo-oka et al., 2004). Interestingly MNT of *Xenopus laevis* is expressed in migrating cranial neuronal crest cells in the frog (Juergens et al., 2005) suggesting that MNT is involved in neural development.

In addition, conditional deletion of MNT in T cells has been shown to interfere with T cell development contributing to a decrease in thymus size (Dezfouli et al., 2006). Also, loss of *MNT* in mammary gland epithelium causes defects in mammary gland development (Toyo-oka et al., 2004).

Mice with *MNT* loss in heterozygosis are viable, healthy and have a normal lifespan. However, male *MNT* heterozygotes become infertile prematurely, a defect that seems to be associated with degeneration of their testes (Hurlin and Huang, 2006).

1.6.5. MNT in tumorigenesis

MNT is also involved in tumorigenesis. For instance, mice injected with MEFs expressing MNT siRNA and RAS developed fibrosarcomas. Also, RAS alone can transform $MYC^{-/-}$ MEFs when *MNT* is downregulated by siRNA (Hurlin et al., 2003; Nilsson and Cleveland, 2004). These data suggest that removal of MNT is sufficient to provoke tumorigenesis in cells that have undergone immortalization.

Moreover, spontaneous adenocarcinomas are developed in mice when *MNT* is conditionally deleted in breast epithelium (Hurlin et al., 2003, 2004) and characterization of the mammary gland tissue after *MNT* deletion showed that loss of *MNT* leads to hyperplastic duct formation (Toyo-oka et al., 2006).

Another example is the deficiency of *MNT* in T cells. *MNT* deficiency causes increased apoptosis and a decrease in T-cell development leading to smaller thymus. However, this *MNT* loss it is followed later by splenomegaly and inflammatory lesions due to a higher release of prosurvival cytokines by *MNT* null CD4+ cells (Th1 T-cells). This leads primarily to lymphocyte infiltration in young mice associated with inflammation and tissue damage but finally to malignant T-cell lymphoma in old mice. These results demonstrate that MNT might functions as a tumor suppressor in T cells and that it plays an essential role in T-cell development and immune homeostasis (Dezfouli et al., 2006).

In addition, MNT has been proposed as a potential tumor suppressor since the gene is located in a region frequently undergoing loss of heterozygosity (LOH) in several malignancies including breast cancer (Devilee et al., 1989; Lindblom et al., 1993; Mackay et al., 1988a; Mackay et al., 1988b; Stack et al., 1995), ovarian cancer (Phillips et al., 1993), astrocytoma (Saxena et al., 1992), bladder cancer (Williamson et al., 1994), medulloblastoma (McDonald et al., 1994), neuroectodermal cancer (Biegel et al., 1992), and ostesarcoma (Andreassen et al., 1993). This would suggest that MNT could be a potential tumor suppressor. However, some discrepancies rise among distinct studies. For instance, several tumor types in which *MNT* mutations or deletions were searched such as breast cancer (Lo Nigro et al., 1998), lung cancer (Takahashi et al., 1998), or medulloblastoma (Sommer et al., 1999), did not present indeed such abnormalities questioning MNT role as a tumor suppressor. On the other hand, MNT expression was reported to be reduced in 6 out of 14 medulloblastoma tumors analysed (Cvekl et al., 2004), and some mutations in MNT gene were found in acute myeloid and lymphoblastic leukaemias(Guo et al., 2007). Also, deletions of MNT gene locus were found in a minor fraction of chronic lymphocytic leukaemia (CLL) (Edelmann et al., 2012) and in the cutaneous T cell lymphoma/leukaemia Sezary syndrome (Vermeer et al., 2008) indicating a possible role of *MNT* as a tumor suppressor gene in this malignancy.

The fact that the MNT loss triggers an apoptosis program similar to what happens in MYC overexpressed conditions, might explain the absence of MNT inactivating mutations or deletions in tumors. MYC-driven tumors need alternative mutations that allow bypass the checkpoint of the apoptosis cell death. Similarly, *MNT* loss might need suppression of key apoptotic pathways to develop tumor growth (Hurlin and Huang, 2006).

1.6.6. MNT target genes

Genes such as *CDK4* and *CCND2* (cyclin D2) (also described as MYC target genes) have been described to be direct targets of MNT protein, being upregulated in MNT deficiency conditions (Dezfouli et al., 2006; Hourihan et al., 2003; Nilsson et al., 2004; Popov et al., 2005; Walker et al., 2005). Also *ODC*, another well-known MYC target gene, was found to be regulated by MNT as shown by a shift of MNT-MAX heterodimers in quiescent cells to MYC-MAX after serum-stimulation on the *ODC* promoter in BALB/c-3T3 fibroblasts (Nilsson et al., 2004). Also, a shift from MYC-MAX to MXD1-MAX and MNT-MAX occurs at the promoters of the *MLH1* and *MSH2* mismatch repair genes in hypoxic conditions

leading to a downregulation of these genes (Bindra and Glazer, 2007) indicating a direct gene regulation by MNT. In addition, MNT-MAX heterodimers were bound to the *hTERT* promoter in the *Xenopus laevis* experimental system, regulating the *hTERT* gene negatively (Wahlstrom et al., 2013). Moreover, MNT and MYC were shown to have a significant overlap in promoter binding in mammary tumor tissues of MYC transgenic mice and similar mRNA expression patterns in mammary tumors from *MNT*$^{-/-}$ and *MYC* transgenic mice (Toyo-oka et al., 2006).

However, analysis of some MYC target genes in *MNT* $^{-/-}$ T-lymphocytes revealed that MNT and MYC may and may not regulate the same genes and molecular pathways and that they may possess distinct and perhaps cell type-specific biological activities (Dezfouli et al., 2006). One example of this was observed in the T98G glioblastoma cells. In these cells the PI3K pathway promotes proliferation by inhibiting a set of genes involved in apoptosis (*ATROGIN-1/FBXO32*), cell cycle progression inhibition (*CCNG2*), or both (*TXNIP* and others,). It was described that MNT-MAX, but not MYC-MAX complexes, were bound to the promoters of the ATROGIN-1/FBXO32 and TXNIP genes when the PI3K pathway is activated in proliferating cells leading to a repression of the genes (Terragni et al., 2011).

1.6.7. MNT-MYC antagonism

The ability of MNT to antagonize MYC has been suggested to be due, first, to a competition for MAX heterodimerization and later for E-box binding capacity at the shared target genes (Hurlin and Dezfouli, 2004).

The MYC and MNT proteins have short half-lives of about 25-30 min (Gregory and Hann, 2000; Hurlin et al., 1997b), whereas MAX is highly stable (Blackwood et al., 1992b). Then, the formation of novel MNT-MAX and MYC-MAX complexes is mainly dependent on the amounts and newly synthesized MNT or MYC that is present in the cell. For instance, even though the total levels of the MNT protein remained unchanged, an upregulation of MYC occurs when quiescent cells renter cell cycle corresponding to a switch from the MNT-MAX to the MYC-MAX complexes at E-boxes on the shared target genes (Hooker and Hurlin, 2006; Walker et al., 2005).

Furthermore, MEFs *MNT*$^{-/-}$ present hallmark features of MYC overexpression, such as sensitivity to apoptosis, escape from senescence, and cell transformation ability with activated RAS (Hurlin et al., 2003, 2004). Similarly, cells in which *MNT* was down-regulated by siRNA also showed MYC-overexpressing characteristics such as increase proliferation rate, apoptosis and transformation capacity (Nilsson et al., 2004).

In conclusion, the fact that MNT is ubiquitously expressed, in contrast to the more restricted expression of the other MXD proteins support the notion that MNT is the key MYC antagonist, modulating MYC activity when it is both absent or highly expressed.

1.7. MGA and MLX

MGA (MAX's giant associated protein) is another MAX interacting protein that also has the b-HLH-LZ domain and also a second DNA binding domain called T-domain. However, apart from the b-HLH-LZ domain, its sequence is divergent form the other MXD proteins and actually it is not included in the MXD family by many authors. The T-domain is typical of the TBX family of proteins and allows them to bind to Brachyury binding sites to regulate embryonic development (Hurlin et al., 1999). MGA can function as transcriptional activator or repressor. The transcriptional repression function of MGA seems to be dependent on the presence of Brachyury-binding sites and the transcriptional activation function of MGA seems to be dependent on the formation of MGA-MAX heterodimers in both Brachyury binding sites and E-boxes (Hurlin et al., 1999). However, MGA presence inhibits MYC transcriptional activation on E-box sequences or MYC transformation capacity as reported by Hurlin et al. (Hurlin et al., 1999). Also, the MGA-MAX complexes have been described to be part of the E2F6 repression complex (Ogawa et al., 2002). Moreover, mutations in *MGA* have been described in human tumors such as chronic lymphocytic leukemia, (De Paoli et al., 2013; Edelmann et al., 2012) and lung cancers (Romero et al., 2014) highlighting its role as tumor suppressor.

Furthermore, there is another important network of transcription factors that is mainly involved in metabolism regulation, which is the MLX network. Two research groups independently identified MLX (another b-HLH-LZ protein) as the binding partner of MXD1 (Billin et al., 1999) and MNT (Meroni et al., 2000). They showed that the MXD-MLX complexes mediated transcriptional repression of E-box containing promoters (Billin et al., 1999; Meroni et al., 2000). Subsequently, two larger b-HLH-LZ proteins were found to heterodimerize with MLX and regulate transcription by binding to E-box containing promoters, MONDOA and CHREBP (also known as MONDOB) proteins (also known as MONDOB) (Billin et al., 2000; Cairo et al., 2001).

Interestingly, MLX and MAX present biochemical similarities: they are b-HLH-LZ small proteins that are constitutively expressed and that are transcriptionally inert since they do not present transactivation nor repression domains. However, the MLX and MONDO proteins contain dimerization and cytoplasmic localization domains (DCD domain) in their C-terminus region (Billin and Ayer, 2006). MLX and MONDO localize mainly in the cytoplasm (specifically in the outer membrane of mitochondria) and can shuttle between the two compartments in response to glucose and other metabolic stimuli. These MLX-MONDO heterodimers compound the MLX network that is involved in regulating the metabolism of the cell and found to be important in cancer development.

The fact that MGA heterodimerizes with MAX and that some of the MXD members like MXD1 and MNT were found to interact with MLX, suggest that the MYC/MAX/MXD network might present crosstalks with MLX and MGA transcription factors. In fact, a very recent work by Carrol et al., 2015 described that MYC needs MONDOA and MLX to transcriptionally reprogram cell metabolism in

neoplasia, since MONDOA or MLX depletion blocks this MYC mechanism resulting in apoptosis (Carroll et al., 2015). These facts show that another grade of complexity is added to the processes regulated by the MYC/MAX/MXD transcription factors that should be further studied.

1.8. NF-κB and REL

The NF-κB (Nuclear Factor-κB) proteins belongs to a family of transcription factors that control a wide range of genes regulating multiple processes such us apoptosis, proliferation and immune response. Sometimes they enhance apoptotic processes meanwhile sometimes they activate survival pathways. This phenomenon that is mainly dependent on the cell type and environment make this transcription factors very important in the control of cell and organism behaviour (Fullard et al., 2012; Smale, 2012).

There are five NF-κB members, RELA (p65), RELB, REL, p50 and p52. They all share a common domain in the N-terminal region of the protein of about 300 amino acids that is the responsible for the dimer formation and DNA binding, the Rel Homology Domain (RHD) (Hayden and Ghosh, 2004). RELA, RELB and REL have a transactivation domain (TAD) in the C-terminal region of the protein that allows them to activate the transcription of genes (Perkins, 1997; Verma et al., 1995). On the other hand, p50 and p52 proteins, encoded by the genes *NFκB1* and *NFκB2*, are first synthesized as precursor proteins p105 and p100 respectively. These p105 and p100 precursors contain a C-terminal region with ankyrin repeats responsible for their inactivated state. To be activated they suffer a proteolysis step becoming p50 and p52 respectively. These members conversely to RELA (p65), RELB and REL do not have a transactivation domain.

The mechanism throughout NF-κB transcription factors regulate gene expression is by homo or heterodimerization of the different members, making a high range of possible combinations. The NF-κB dimers then bind to specific regions in the DNA of nine nucleotides with the consensus sequence GGRNNYYCC, known as κB sites in the promoter of their target genes (Wietek and O'Neill, 2007). These κB sites are recognized specifically by the different dimers formed (with the exception of RELB homodimers) (Ishikawa et al., 1998; Leung et al., 2004) allowing unique transcriptional programs that are basically dependent on cell type and activation stimulus (Dejardin et al., 2002; Fullard et al., 2012; Hoffmann et al., 2006; Saccani et al., 2003; Udalova et al., 2002).

These NF-κB dimers are constitutively expressed in the cells. However, they remain inactive in the cytoplasm in normal conditions. This cytoplasm localization is due to the interaction with the Inhibitor of κB (IκB) proteins that seems to mask nuclear localization signals present in the -κB members. The IκB family of proteins is composed of IκBα, IκBβ, IκBɣ, IκBƐ and BCL-3. These proteins (like p105 and p100 precursors) have ankyrin repeats within the C-terminal region throughout they interact with NF-κB proteins. They also have a leucine-rich nuclear export sequence (NES) that shuttles them to the

cytoplasm. So that, the IκB - NF-κB complexes localize inactive in the cytoplasm (Yamamoto and Gaynor, 2004).

There are two main pathways (canonical and non-canonical) that activate NF-κB dimers (figure 1.9). They are both based in the phosphorylation of IκB proteins, which is followed by poly-ubiquitination and proteasome-mediated degradation (Karin and Ben-Neriah, 2000). This leads to a release of the NF-κB dimers that translocate to the nucleus, ready to regulate gene transcription. The canonical pathway that is stimulated by cytokines such as IL-1 and TNFα through TLRs (Toll-like receptors), drives the activation of the IκB kinase complex (IKK) formed by the IKKα and IKKβ kinases and the NEMO/IKKγ structural subunit, that will phosphorylate IκB proteins targeting them for proteasome degradation (figure 1.9). The non-canonical or alternative pathway that is stimulated by CD40 ligand (CD40L) and lymphotoxin-β (LT-β) among others, will activate another kinase, the NF-κB Inducing Kinase (NIK) that will phosphorylate and activate IKKα kinase that in turn will phosphorylate and target p100 precursor polyubiquitination to be processed into p52 by the proteasome (figure 1.9) (Adhikari et al., 2007; Hayden and Ghosh, 2004; Perkins, 2007)

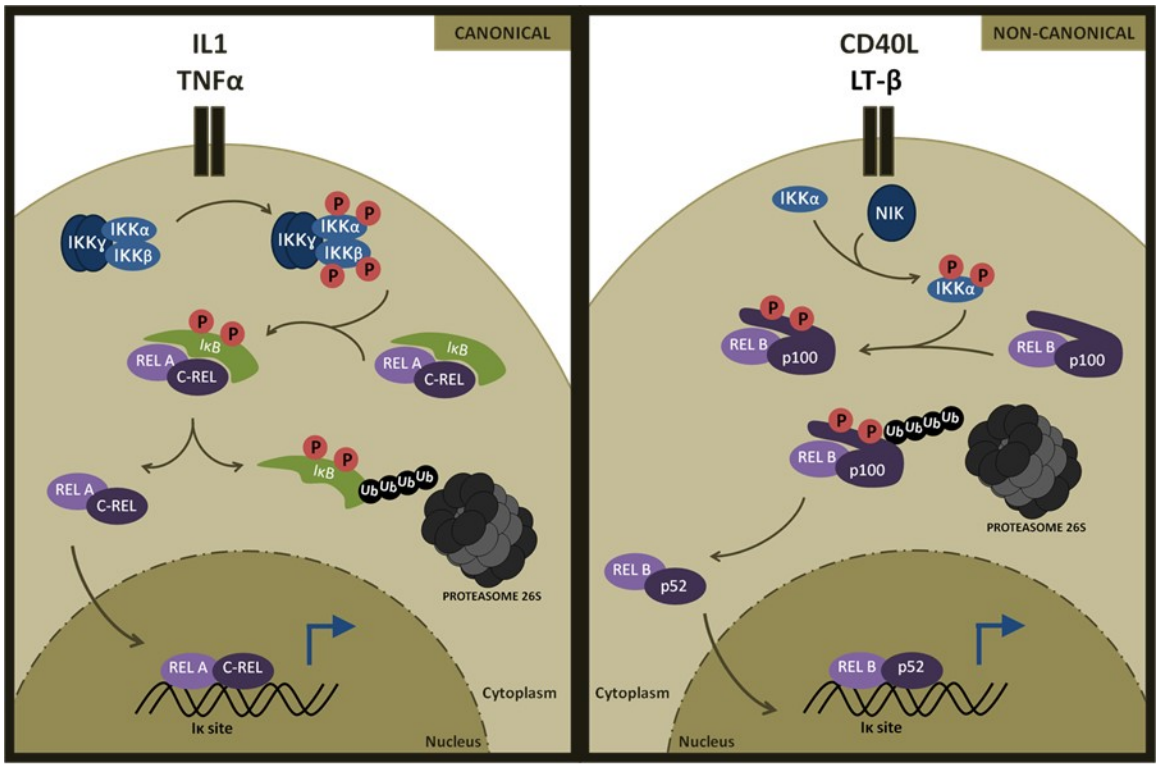

Figure 1.9.- NF-κB canonical and non-canonical pathways. On the left a representation of the canonical NF-κB pathway: Ικκγ/Ικκα/Ικκβ kinase complex activated by IL1 or TNFα, phosphorylates the IκB inhibitor to target it for proteasome degradation. RELA/REL heterodimers are liberated and translocate to the nucleous to activate gene transcription. On the right a representation of the non-canonical NF-κB pathway: NIK kinase activated by CD40L or LT-β, phosphorylates and activates the Ικκα kinase that will phosphorylate p100 precursor to target it for proteasome degradation and p52 processing. RELB/ p52 heterodimers translocate to the nucleous to activate gene transcription (modified from Hayden and Ghosh, 2004).

This mechanism of action allows an accurate gene regulation remaining inactive in normal conditions and being triggered rapidly when cells receive the appropriate stimulus.

In the next lines I will describe further the REL member since some of the work described in this Thesis is focused on this protein. The REL gene, encoding the REL protein (also known as c-REL), was firstly identified as the oncogene v-REL in an avian oncogenic retrovirus (Wilhelmsen et al., 1984). Further studies revealed that the central and C-terminal regions of REL and v-REL were necessary for their malignant transformation properties (Sylla and Temin, 1986).

The human REL protein has 587 amino acids. The human *REL* promoter contains transcription factor binding sites for SP1, Oct and also NF-κB. The SP1 and one κB sites are sufficient for basal transcription of *REL*. Loss of two or more NF-κB sites reduces the promoter activity what suggests that they are require for maintaining high constitutive expression. It has been shown that RELA/p50 heterodimers, p50 homodimers and also REL homodimers bind to the κB sites suggesting an autoregulation of REL gene (Grumont et al., 1993). However, mutations altering the TAD domain of REL did not affect the *REL* promoter regulation suggesting the possibility of an indirect mechanism (Grumont et al., 1993).

The RHD of REL is located in the N-terminal region (figure 1.10) and is essential for DNA binding, protein dimerization and interaction with IκBs. Phosphorylation of REL in S266 is a post-translational modification that regulates its ability to dimerize and bind to DNA (Gilmore, 1999; Mosialos and Gilmore, 1993; Mosialos et al., 1991). The TAD domain of REL spans amino acids 424–587 and is required for REL to drive gene transcription. Martin et al., 2001 identified two sub domains within the TAD, sub domain I (amino acids 424–490) and sub domain II (amino acids 518–587) (Martin et al., 2001). Both regions have basal activity but sub domain I also increase its activity in response to TNFα (Leeman et al., 2008; Martin et al., 2001; Starczynowski et al., 2003, 2005). Moreover, the TAD of REL is highly negatively charged containing multiple serine residues susceptible of phosphorylation that positively regulate REL activity. Indeed several point mutations of serine residues to unphophorylable alanines within the TAD domain of REL have been shown to reduce its transactivation potential. Also, S471 residue has been identified as a key phosphorylation site in REL since S471D mutations increase considerably its transactivation activity (Martin et al., 2001; Starczynowski et al., 2003, 2005).

Furthermore, it has been described a REL inhibitory domain (RID) spanning amino acids 323–424 (figure 1.10), with deletions of this region resulting in increased transactivation by REL. Two splice variants were described, a 32 amino acid Alu insertion and an exon 9 deletion (RELΔ9), that alter the RID domain and increase the transactivation activity (Leeman et al., 2008). However, the presence of this RID domain does not interfere with IκB interaction. Thus, apart from IκB regulation of the REL dimers, a hinge between the RHD and TAD domains would facilitate their interaction and reduce its DNA binding affinity and transactivation capacity (Leeman et al., 2008). Moreover, Leeman et al. also described that the RELΔ9 splice variant is preferentially expressed in lymphoma (Leeman et al., 2008).

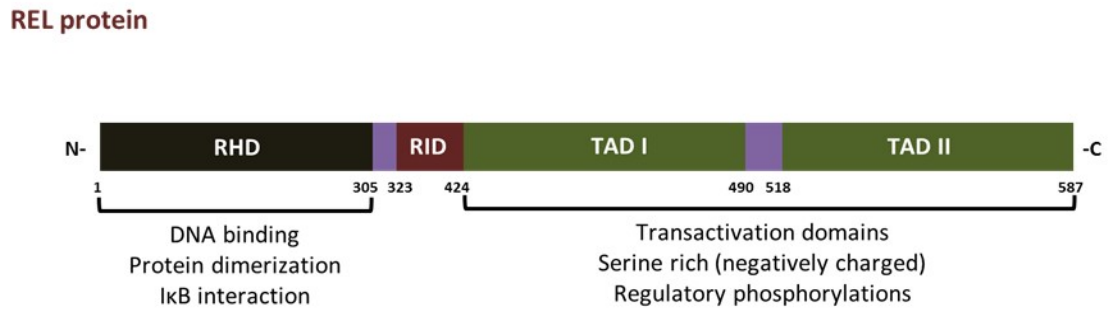

Figure 1.10.- REL human protein structure. REL protein structure, RHD refers to the REL Homology Domain that is common to all NF-κB family members; RID refers to Rel Inhibitory Domain and TAD I and TAD II to transactivation domains.

1.8.1. REL and gene regulation

There are more than 400 NF-κB target genes (http://www.bu.edu/nf-kb/gene-resources/target-genes/; http://bioinfo.lifl.fr/NF-KB/). REL as an NF-κB member regulates direct or indirectly the expression of numerous cytokines. Mice lacking the REL protein for instance present alterations in the expression of IL-2, IL-3, IL-6, IL-10 IL-13, IL-15, IL-21, IFNɣ, MIP1α and GM-CSF (Gerondakis et al., 1996; Liou et al., 1999; Tumang et al., 2002). IL-2 is of particular interest since it has been shown that IL-2 is needed for T cells activation and differentiation, with decrease levels leading to immunocompromisation (Liou et al., 1999; Tumang et al., 2002). Another example is the regulation of interferon (IFN) molecules. For instance, the REL/RELA heterodimers activate IFN-λ1 expression by replacing p50 homodimers in the promoter upon stimulation (Siegel et al., 2011).

1.8.2. REL, apoptosis and survival role

The roles of NF-κB in cell survival and apoptosis are conflicting (Fullard et al., 2012; Hayden and Ghosh, 2004; Wietek and O'Neill, 2007). In certain situations, NF-κB acts as an antiapoptotic, whereas in others it functions as proapoptotic transcription factor. For instance, it has been shown that REL directly controls the expression of the anti-apoptotic protein A1, a BCL-2 homologue, and the pro-proliferative IRF-4 gene. Both genes contain κB sites where the REL/p50 heterodimers bind (Grumont et al., 1999; Gugasyan et al., 2000). REL mediates IRF-4 and A1 upregulation in activated lymphocytes and is required for cell cycle progression and B cell proliferation since $REL^{-/-}$ B cells present a decrease in proliferation linked to an increase in apoptosis (Grumont et al., 1998). Furthermore, $REL^{-/-}$ B cells were more susceptible to apoptosis due to reduce expression of BCL-XL (Owyang et al., 2001). On the other side of the coin, it has been also shown that activation of REL results in induction of apoptosis-related genes such as DR4, DR5, and BCL-Xs, and in inhibition of survival genes such as c-IAP1, c-IAP2, and survivin/BIRC5 (Chen et al., 2003).

1.8.3. REL in cancer

In relation with its function in immune cells as a proliferative and antiapopotic agent, human lymphomas have been associated with gains in chromosome 2 in the region of 2p13 (which encodes the REL gene) and other alterations that result in an overactivation of *REL*. Many B cell lymphomas, including Hodgkin's lymphoma, diffuse large B cell lymphoma and follicular lymphoma cells have elevated levels of nuclear REL (Barth et al., 2001; Barth et al., 2003; Houldsworth et al., 1996; Martin-Subero et al., 2002). In addition, silencing of *REL* using RNA interference in B cell lymphoma cell lines lead to growth arrest and apoptosis (Tian and Liou, 2009). Together, this indicates a role of REL in lymphomas. Overactivated REL is a highly significant risk factor for malignancies development and becomes an indicator of worse outcome in lymphoma patients (Curry et al., 2009).

In addition, REL is also involved in the development of other types of malignancies including breast, head and neck cancers (Lorenz et al., 2014; Sovak et al., 1997). One example came with the description of the REL interaction with the tumour suppressor TP53 family member ΔNp63α in head and squamous cell carcinomas. This interaction leads to the dissociation of the ΔNp63α-TAp73 dimer. Then, the REL-ΔNp63α complex inhibit the expression of growth arrest and apoptotic genes leading to the development of malignancies (Lu et al., 2011). In many breast cancer cases REL is activated and localize in the nucleus, promoting the expression of cell cycle genes like *CCND1* (cyclin D1) (Belguise and Sonenshein, 2007).

1.9. CCDC6

H4/PTC1 gene, now called CCDC6, was identify and isolated because of its frequent rearrangement with the RET proto-oncogene in cancer cells. This rearrangement generates the RET-PTC1 oncogene responsible for human thyroid papillary carcinomas. The 5' region of this fusion gene corresponds to the H4/PTC1 gene. *CCDC6* encodes a 474 amino acids protein(65 kDa) that has an SH3 protein interaction domain in the C-terminal region and a long coiled-coil region (figure 1.11) with alpha helical conformation that are 30 % homologous to several proteins including tropomyosin, vimentin, keratin and the tail region of myosin heavy chain (Grieco et al., 1994; Pierotti et al., 1992). CCDC6 is ubiquitously expressed and it is nuclear or cytosolic dependent on its phosphorylation status. The CCDC6 phosphorylation is mediated by the ERK1/2 kinases following serum stimulation. Phosphorylated CCDC6 remains in the cytoplasm meanwhile in its unphosphorylated form localizes in the nucleus (Celetti et al., 2004).

1.9.1. CCDC6 in cancer

RET-PTC1 gene product includes the 101 first amino acids of the CCDC6 gene and the tyrosine kinase domain of the RET protein allowing a constitutive active kinase function (figure 1.11). This CCDC6 coiled-coil domain included in RET-PTC1 fusion protein is necessary for homodimerization,

constitutive activation and transforming ability of the oncoprotein (Jhiang, 2000; Tong et al., 1997). Also, an intrachromosomal rearrangement in chromosome 10 involving the *CCDC6* and *PTEN* was detected in cell lines derived from benign and malignant human thyroid tumors and in human papillary thyroid cancer specimens. The *CCDC6-PTEN* chimeric gene is predicted to encode for a truncated PTEN protein that lacks its tumor suppressor function (figure 1.11) (Puxeddu et al., 2005). Other rearrangements involving *CCDC6* have been also reported. For example, in two cases of atypical chronic myelogeneous leukaemia (CML), the first 368 amino acids of CCDC6 are fused to the PDGFβR tyrosine kinase domain as a consequence of t(5;10) (q33;q22) chromosomal translocation. The resulting fusion gene encodes a 948 amino acids protein with most of the coiled-coil of CCDC6 and the transmembrane and tyrosine kinase domains of the PDGFβR (figure 1.11). Again, the oncoprotein oligomerization and constitutive activity is dependent on the coiled-coil domain of the CCDC6 gene (Kulkarni et al., 2000; Schwaller et al., 2001). All these examples suggest a possible role of CCDC6 in these malignancies.

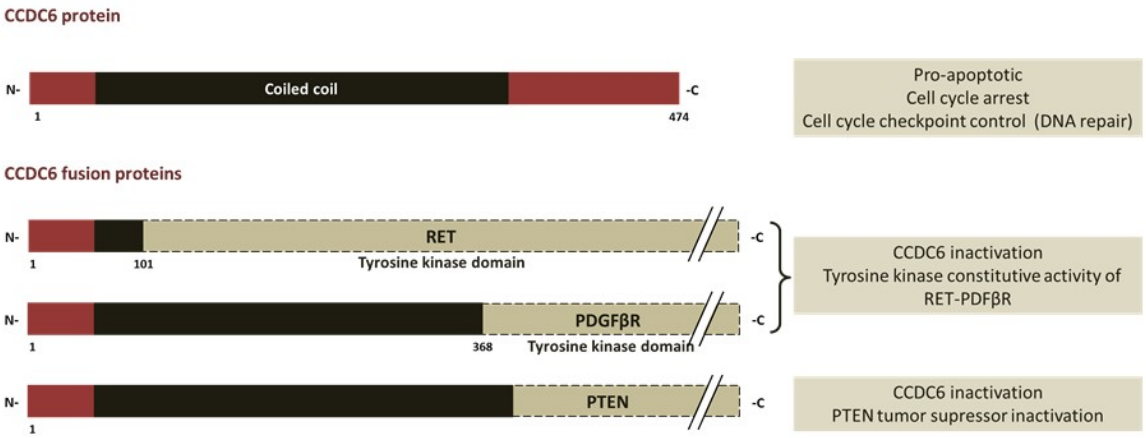

Figure 1.11.- CCDC6 human protein structure and its contribution to fusion proteins. CCDC6 protein scheme with a brief description of its functions (right box). In the lower pannel it is shown the CCDC6 protein regions taking part in several oncogene fusion proteins (CCDC6-RET = RET-PTC1 ; CCDC6-PDGFβR and CCDC6-PTEN) contributing to their oncogenic activity.

1.9.2. CCDC6 biological functions

The CCDC6 function it is not totally clear. However, several studies have been carried so far that describe possible roles of this protein and that will be summarized in this section.

CCDC6 has been shown to be involved in apoptosis since restoration of wild type CCDC6 protein in a human papillary thyroid cell line (TPC-1) that has the *RET-CCDC6* rearrangement and loss of normal *CCDC6* allele function, die by an activation of an apoptotic cell death program. Conversely, the expression of the truncated CCDC6 mutant [CCDC6(1–101)] that corresponds to the portion included in RET-CCDC6 oncoprotein in thyroid carcinomas, acted as dominant negative on wild type CCDC6

protein retaining it in the cytoplasm and enhancing cell survival. Moreover, this CCDC6 mutant was able to protect cells from several stress agents that normally induce cell death (Celetti et al., 2004). Therefore, wild type *CCDC6* would act as a tumor suppressor gene that gets inactivated upon translocation.

It has been also described that CCDC6 inhibits CREB1-dependent transcription. CCDC6 interacts with CREB1 and represses its transcriptional activity by recruiting at the CRE site of the CREB1 target genes the histone deacetylase 1 (HDAC1) and also the protein phosphatase 1 (PP1) that dephosphorylate CREB1 and diminish its activity. Moreover, papillary tumors carcinomas carrying the RET-CCDC6 oncogene present increased levels of two known CREB1 target genes, *AREG* and *CCNA* (cyclin A), adding another example of CCDC6 involvement in the cell cycle control (Leone et al., 2010).

On the other hand, several studies have revealed CCDC6 functions in the cell cycle checkpoint control. It has been described that CCDC6 is an ATM kinase substrate, being phosphorylated at Thr434 upon DNA damage like ionizing radiation. P-Thr434 CCDC6 localizes in the nucleus upon DNA damage response presenting negative actions on cell proliferation. By contrast, the T434A CCDC6 or the CCDC6(1-101) mutants are unable to induce cell death upon DNA damage, instead they increase cell survival (Merolla et al., 2007). CCDC6 has been also suggested to function as a stress response protein that protects genome integrity. Phosphorylation of H2AX is one of the earliest responses to DNA damage, and controls the accumulation of checkpoint response proteins to chromatin regions surrounding the break sites (Rogakou et al., 1998). Dephosphorylation of pH2AX on Ser 139 and its exclusion from chromatin regions is crucial for cell cycle re-entry (Fernandez-Capetillo et al., 2004). One of the phosphatases responsible for dephosphorylation of pH2AX Ser 139 is the Protein Phosphatase 4c (PP4C). CCDC6 interacts with the catalytic subunit of PP4C and negatively modulates its activity. *CCDC6* loss is suggested to increase PP4C activity resulting in limited amounts of pH2AX Ser 139 and thus contributing to DNA instability and cancer (Merolla et al., 2012; Merolla et al., 2007). Also, *CCDC6* loss has been linked to a downregulation of 14-3-3 proteins leading to an altered nuclear localization of the phosphatases CDC25 promoting mitosis by activation of the CDK1/cyclin B complexes (Thanasopoulou et al., 2012). Loss of *CCDC6* results in S phase deregulation, cells do not arrest in G1 or S phase upon DNA damage impairing the ability of the cells to maintain genomic integrity thus, contributing to genomic instability what finally results in cell death (Thanasopoulou et al., 2012).

1.10. Nucleolus

The nucleolus it is a non-membrane structure present in the nucleus of cells. There can be more than one nucleolus within the same cell at a time and they vary in form and size from one cell type to another, and even within a single cell. They are dynamic structures that assembly and disassembly during each cell cycle. These structures are formed around clusters of repeated rRNA genes (rDNA) that encode the ribosomal RNAs, the scaffold structures of eukaryotic ribosome. The first and best

known functions attributed to these compartments were related to ribosome biogenesis (figure 1.12) that are: 1) rDNA transcription in situ by RNA polymerase I (RNApol I) that gives rise to the 47S pre-ribosomal RNA (pre-rRNA); 2) pre- rRNA processing into the mature rRNAs (28S, 18S and 5.8S) and 3) generation of the 40S and 60S subunits of ribosomes by the assembly of the 28S, 18S, 5.8S and the 5S rRNAs (this latter transcribed by RNA polymerase III) with ribosomal proteins (RPs) (transcribed by RNA polymerase II) before the exportation to the cytoplasm (Scheer and Hock, 1999; Shaw et al., 1995; Shaw and Jordan, 1995).

1.10.1. Structure of nucleolus

These non-membrane and variable structures have different compartments that can be differentially seen by electron microscopy (EM). These are the fibrillar centers (FCs) that appear as clear areas surrounded by the dense fibrillar component (DFC) that appears as a highly contrasted region, and the granular component (GC) that surrounds the FC and DFC and that is seen as a region containing granules of 15-20 nm in diameter (Schwarzacher and Wachtler, 1991).

These three morphologically distinct compartments reflect the sequential steps of ribosome biogenesis (figure 1.12) (Scheer and Hock, 1999). In this manner, firstly, in the FC where the RNA polymerase I transcription machinery concentrates, the ribosomal genes (rDNA) are transcribed giving rise to the precursor 47S rRNA. Secondly, in the DFC, the nucleolar proteins involved in rRNA processing like fibrillarin, nucleolin and the U3 snoRNA (small nucleolar RNAs) among others localize, processing the pre-rRNA to the mature 18S, 28S and 5.8S rRNAs (Boisvert et al., 2007; Moss et al., 2007). Finally, in the GC, the assembly of the 40S and 60S ribosome subunits take place since there localizes proteins involved in intermediate or later stages of rRNA processing like B23 (or nucleophosmin) and Nop52 (Biggiogera et al., 1989; Gautier et al., 1994) together with other ribonucleoproteins (RP), the 5S rRNA and the already mature rRNA 18S, 28S and 5.8S.

1.10.2. rDNA and its regulation

The mammalian rRNA genes (rDNA) are disposed in clusters or repeated large units of about 43 kb in humans (Gonzalez and Sylvester, 1995; Grozdanov et al., 2003) termed nucleolar organizer regions (NORs) (figure 1.13). There are about 200 NORs that localize among the short arms of the five human acrocentric chromosomes 13, 14, 15, 21, and 22 (Henderson et al., 1972). Firstly, it was thought that NORs were located in ordered tandem repeats; however, nowadays it is believed that NORs disposition is not ordered being some of them forming palindromic structures with an uncharacterized function (Caburet et al., 2005).

As mention above, one unit of the human rDNA is about 43 kb where the sequences encoding the pre-rRNA comprise about 13 kb long separated by long intergenic spacers (IGSs) of approximately 30 kb (figure 1.13). Regulatory elements, including gene promoters, spacer promoters, repetitive enhancer elements, and transcription terminators, are located in the IGS. The rDNA promoter has two main domains, a core promoter element (CORE) adjacent to the transcription start site and an

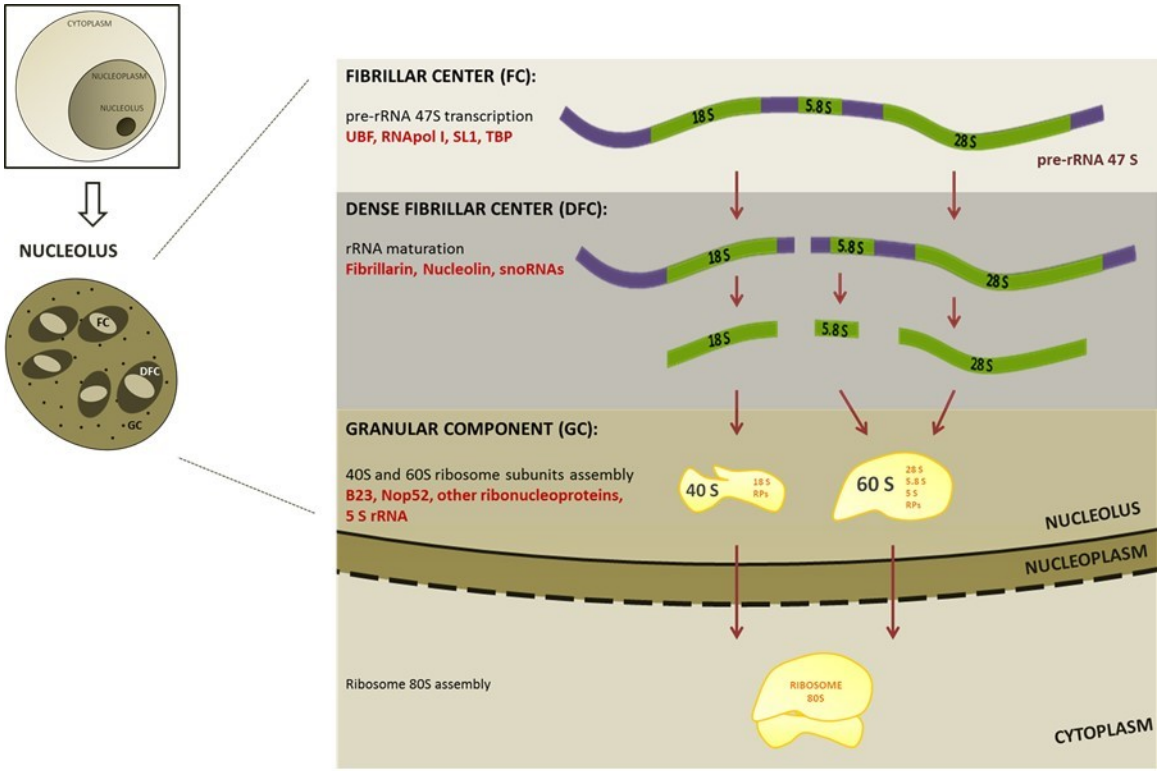

Figure 1.12.- Nucleolus and ribosome biogenesis. A representation of the different regions of nucleolus and their functions. There is a vectorial distribution of the machineries involved in ribosome biogenesis throughout the different compartments that correlates with the different steps of the process: in the fibrilar centers (FC) the rRNA genes are transcribed producing the pre-rRNA 47S. This pre-rRNA is processed to produce mature rRNAs 18 S, 5.8 S and 28 S in the dense fibrillar center (DFC). In the granular component (GC) the mature rRNAs together with other ribonucleoproteins and the 5 S rRNA (synthesized by RNApol III) form the 40S and 60S ribosome subunits. Finally, the 40S and 60S subunits translocate to the cytoplams to assemble the 80S ribosome.

upstream control element (UCE) approximately 100 bp upstream (Haltiner et al., 1986; Learned et al., 1986; McStay and Grummt, 2008). In addition, these rDNA units are flanked by several terminator elements that are recognized by the transcription termination factor (TTF-I), a specific DNA binding protein that stops elongation by RNApol I (figure 1.13) (Grummt et al., 1986a; Grummt et al., 1985; Grummt et al., 1986b; Henderson and Sollner-Webb, 1986; McStay and Reeder, 1986).

The rDNA transcription is carried out by RNA polymerase I (RNApol I) and it requires firstly the formation of a preinitiation complex (PIC) on the promoter, including binding of UBF (upstream binding factor) and the promoter selectivity factor SL1 that forms a complex responsible for promoter specificity (figure 1.13) (Friedrich et al., 2005). This PIC complex contains TBP (TATA box binding protein) and RNApol I specific TBP-associated factors (TAFIs) (Comai et al., 1992; Comai et al., 1994; Gorski et al., 2007; Heix et al., 1997; Zomerdijk et al., 1994). These factors and UBF bind to TIFIA, a basal regulatory factor that is associated with the initial RNApol I complex (figure 1.13) to recruit

RNApol I to rDNA. Then, a productive transcription initiation complex is assembled in the promoter of the rDNA (Grummt, 2003).

Ribosomes are particularly important when cells receive proliferation or differentiation stimulus, conditions where protein synthesis is highly required (Haaf et al., 1991). That is the reason why the rDNA expression has to be highly regulated to respond accurately to cell demands. In this manner, the regulation of rDNA expression is achieved by several mechanisms at different levels from direct rRNA polymerase machinery activity to epigenetic modifications of rDNA. Both mechanisms are used to that purpose but it is thought that short-term regulation that responds to multiple signaling pathways affects directly to rDNA transcription machinery such as the assembly of the preinitiation complex, the RNA polymerase I activity, and the transcription elongation or termination (Russell and Zomerdijk, 2005). On the other hand, long-term regulation is mainly due to chromatin modifications allowing an activation or inactivation of new NORs increasing or decreasing the potential of rRNA synthesis. It is important to note that not all NORs are active at the same time, only 40-50 % of them are implicated in the rRNA synthesis at a given moment (Grummt, 2007; Lawrence and Pikaard, 2004; McStay and Grummt, 2008; Russell and Zomerdijk, 2005).

An important component of rDNA regulation is NoRC (nucleolar remodelling complex). NoRC is a chromatin remodelling complex that silences rDNA by establishing a closed chromatin structure (Li et al., 2006). In the silent promoters, nucleosomes disposition provokes a separation of the CORE and UCE sequences prohibiting the cooperative binding of UBF and SL1 so that blocking the initiation complex assembly. On the contrary, in active genes the DNA conformation juxtaposes the CORE and UCE sequences allowing the assembly of the RNA polymerase I machinery (Li et al., 2006).

Furthermore, non-coding RNAs also control the rDNA expression. It has been described in mice the existence of IGS transcripts synthesized at ~2 kb upstream of the transcription start site that control rDNA gene expression. These transcripts called pRNA (promoter-associated RNA) are processed into 150-300 bp transcripts and they acquire a secondary conformation that allows their interaction with the NoRC subunit TIP5. This interaction is required for both NoRC localization to the nucleolus and its role in rDNA silencing (Mayer et al., 2006).

The UBFT gene encodes two major rDNA transcriptional factors: the UBF1 (here referred as UBF) and UBF2 proteins. UBF1 protein have a dimerization domain at the N-terminal region followed by six HMG-boxes (sequences similar to the DNA binding domains of High Mobility Group (HMG) proteins 1 and 2) and a highly acidic tail at the C-terminal region. Nonspecific DNA binding domains have been described in UBF and consequently it does not present any DNA binding consensus sequence (Copenhaver et al., 1994; Putnam et al., 1994). UBF2 is formed by alternative splicing and it lacks 37 amino acids from the second HMG box. UBF2 seems to be 5-fold less active than UBF1 and has poor transcriptional activity (Kuhn et al., 1994; O'Mahony and Rothblum, 1991).

UBF has the ability to bend and loop DNA. It binds DNA as dimers and bend the rDNA throughout their HMG-boxes, generating a single 360º loop of DNA of about 140 bp in length and 17 nm of diameter that is required for SL1 recruitment at the pre-initiation complex (Bazett-Jones et al., 1994; Putnam et al., 1994). This structure dubbed rDNA enhanceosome (figure 1.13) resembles the histone nucleosome in both its size and protein-DNA composition (Stefanovsky et al., 2001).

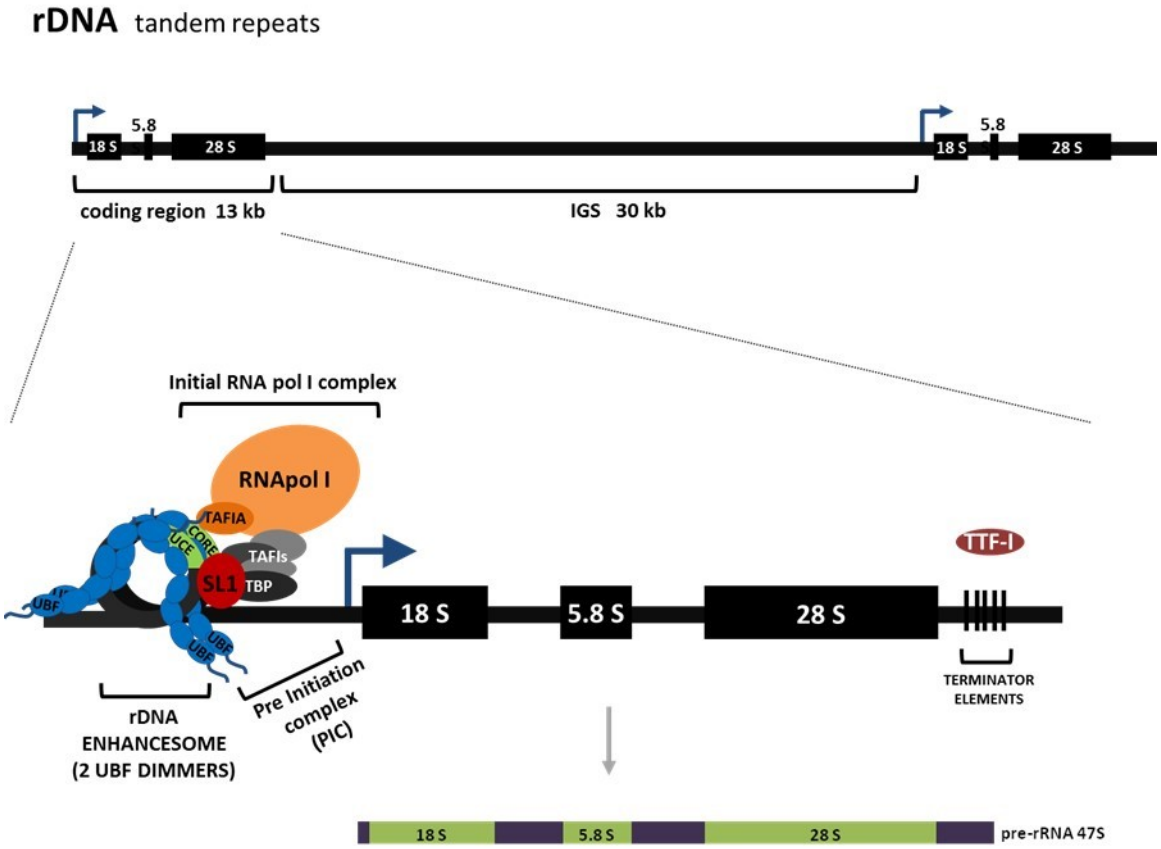

Figure 1.13.- rDNA structure and transcription. A representation of one rDNA tamdem repeat that contains the rRNA 18 S, 5.8 S and 28 S genes in about 13 kb long region (coding region) followed by an intergenic spacer (IGS) region of about 30 kb long. In the lower figure, a representation of the enhancesome (juxtapossed UCE and CORE promoters sequences and 2 UBF dimers), the pre-initiation complex (PIC) (containing the SL1, TBP and TAFIs: TBP associated factors) and the initial RNA pol I complex (RNA pol I and the TAFIA initial factor) needed for rRNA genes trancription by RNA polymerase I. The TTF-I (transcription terminator factor I) participates in the finalization of rRNA gene transcription by binding to the terminator elements. The resulting pre-rRNA 47 S transcript is represented.

UBF binds DNA throughout the entire rDNA repeat (transcribed sequences and IGS) contrarily to RNApol I and SL1 that bind exclusively to transcribed sequences and promoter regions respectively (O'Sullivan et al., 2002). This, together with the above characteristic described, suggest that UBF apart from its role in the pre-initiation complex assembly at the rDNA promoter as described before, it plays

an epigenetic role in the formation and maintenance of active rRNA gene chromatin (r-chromatin) (O'Sullivan et al., 2002; Sanij et al., 2008). Furthermore, UBF binding is maintained during metaphase at active NORs assuring that these NORs will be ready to be transcribed in the subsequent cells rapidly after mitosis (Gebrane-Younes et al., 1997).

Moreover, post-translational modifications such as phosphorylations and acetylations in UBF lead to modulations of its activity and so of rDNA transcription. Phosphorylated UBF promotes DNA binding; enhances the stability of the SL1 pre-initiation complex; interacts with RNApol I and remodels r-chromatin contributing to an activation of rDNA transcription (Hannan et al., 2003; Lin et al., 2006; Stefanovsky et al., 2006; Tuan et al., 1999). On the other hand, acetylated UBF interacts with the RNApol I promoting its association with the rDNA leading to an increase in pre-rRNA synthesis (Meraner et al., 2006).

As it has been described in this section, rDNA expression is a highly regulated process with high interdependence of biochemical together with chromatin conformation mechanisms that in the end affect the transcriptional output from rDNA.

1.11. UR61 cell line model

The UR61 cells derive originally from the PC12 cell line that was established from a rat pheochromocytoma, a neuroendocrine tumor. PC12 cells after NGF treatment present several differentiation properties of sympathetic neurons, including neurite outgrowth, electrical excitability, and the presence of synaptic vesicles (Greene and Tischler, 1976; Tischler and Greene, 1978). NGF treatment triggers the activation of the RAS-MAPK pathway leading to this differentiation process (Cowley et al., 1994). In addition, PC12 cells do not express a functional MAX protein because of aberrant processing of *MAX* transcripts due to a homozygous chromosomal rearrangement or translocation within the MAX gene. These mutant transcripts (MAX^{PC12}) do not encode the C-terminal sequence including the helix2 (H2) and leucine zipper (LZ) regions of b-HLH-LZ domain that are the regions responsible for dimerization in the wild type MAX protein. Therefore, this MAX mutant product cannot dimerize with MYC, MXDs or with MAX itself. On the other hand, reintroduction of MAX wild type into PC12 cells represses transcription dependent on the E-box sequences and has a mild growth-inhibitory effect (Hopewell and Ziff, 1995).

U7 is a PC12 cell line variant that responds less to NGF (Greene and Rukenstein, 1981). UR61 were derived directly from U7 cells by stable transfection of the mouse *N-RAS* (N-RasQ61K) oncogene under the control of the long terminal repeat from mouse mammary tumor virus (LTR-MMTV). This promoter is activated by the synthetic glucocorticoid dexamethasone. Thus, UR61 in the presence of nanomolar concentrations (50-200 nM) of dexamethasone express the constitutively active N-RAS protein that activates the MAPK pathway leading to a neuronal-like differentiation process (Guerrero et al., 1988). Previous work of our lab showed that enforced MYC expression impaired RAS-induced

differentiation of UR61 cells (Vaque et al., 2008). Also, our laboratory generated two UR61 derivative cell lines called UR61-MT-MAX that express a MAX wild type protein in response to Zn_2SO_4 since the MAX gene is under the control of the metallothionein (MT) promoter and UR61-MT-Hebo with an empty construction as a control that do not express the MAX protein upon Zn_2SO_4 treatment (Andrea Quintanilla, PhD Dissertation).

Aims

2. AIMS

The MXD proteins are part in the MYC/MAX/MXD network of transcription factors. MYC and MXDs form heterodimers with MAX. It has been assumed since their discovery that MYC and MXD proteins regulate transcription of many genes involved in different processes of cell biology, binding to the same or very similar E boxes but eliciting opposite effects. *MYC* is a well-known oncogene and the MXD proteins are considered their antagonists in cell biology and gene regulation. We have focused in this Thesis on two MXD proteins: MXD1 and MNT. MXD1, the first member of the family discovered, is highly involved in cell differentiation and cell cycle arrest processes. MNT is the most divergent member of the family, it has constitutive expression and its depletion leads to effects similar to that of MYC overexpression (Walker et al., 2004). Previous work in our lab showed that MYC maintains its oncogenic effects as differentiation block even in the absence of MAX protein, in the UR61 cells (Vaque et al., 2008). However, the possibility of MXDs proteins having MAX-independent effects have not been explored.

In this study we aim:

1. To study MXD1 and MNT subcellular localization in cells with and without MAX.
2. To explore MXD1 and MNT functions independent of MAX in proliferation and differentiation.
3. To study MNT roles in transcriptional regulation in cells with and without MAX.
4. To identify new relevant proteins interacting with MNT.

Materials and Methods

3. MATERIALS AND METHODS

3.1. CELL CULTURE

3.1.1. Cell lines and maintenance

Generally cell lines were grown in either RPMI-1640 or DMEM (LONZA) supplemented with 10 % fetal bovine serum (FBS) (LONZA), 150 µg/ml of gentamicin (Lab. Normon) and 2 µg/ml of ciprofloxacin. UR61 cells were maintained with 250 µg/ml G418. UR61-derived cell lines UR61-MT-Hebo and UR61-MT-MAX were cultured with 100 µg/ml GIBCO® Hygromycin B (Life technologies) in addition to the G418.

Human mesenchymal stem cells MSC-3H, were grown on Mesencult medium (StemCell Technologies) containing 10 % human serum (STEMCELL Technologies) and 1 ng/ml basic fibroblast growth factor (R&D Systems).
Human embryonic stem cells (hESC) HS181.1 and VAL3, were grown on synthetic matrix Geltrex™ (GIBCO®, Life technologies) in the TeSR™-E8™ Kit for hESC Maintenance (STEMCELL Technologies).

All cell lines were grown at 37 ^{o}C in a humidified 5 % CO_2 atmosphere. Table 3.1 provides a list of the cell lines used in this study.

Table 3.1.-Cell lines used in this Thesis

CELL LINES	ORIGIN	CULTURE MEDIUM	ORIGIN/REFERENCE
UR61	PC12 derviative cell line with an inducible N-RAS oncogene	DMEM 10%FBS	Laboratory collection (Guerrero et al., 1988)
UR61-MT-Hebo	UR61 derivative cell line with the inducible empty construction	DMEM 10%FBS	Laboratory collection (A. Quintanilla)
UR61-MT-MAX	UR61 derivative cell line with an inducible MAX gene	DMEM 10%FBS	Laboratory collection (A. Quintanilla)
TGR1	Rat-1 fibroblasts Hprt-	DMEM 10%FBS	Laboratory collection (Prouty et al., 1993)
C6	Rat glioma	DMEM 10%FBS	Miguel Lafarga
Neuro-2a	Mouse neuroblastoma	DMEM 10%FBS	Ana Perez Castillo
MEF	Mouse embryonic fibroblast	DMEM 10%FBS	Laboratory collection (Prouty et al., 1993)
HEK293T	Human embryonic kidney with SV40 T antigen constitutive expression	DMEM 10%FBS	Laboratory collection (Graham et al., 1977)
K562	Human chronic myeloid leukemia	RPMI 10%FBS	Laboratory collection (Lozzio et al., 1975)
HeLa	Human cervical cancer	DMEM 10%FBS	Laboratory collection (Gey et al., 1952)

Ramos	B-cell lymphoma	RPMI 10%FBS	Laboratory collection (Bassat et al., 1997)
SH-SY-5Y	Human neuroblastoma	DMEM 10%FBS	Laboratory collection (Biedler JL, et al. 1978)
T98G	Human glioblastoma	DMEM 10%FBS	José Luis Fernández Luna
MSC-3H	human mesenchymal stem cells with 3 mutations: HPV-E6, HPV-E7 and hTERT+	Mesencult medium 10% human serum	René Rodríguez González, Banco Andaluz de Células Madre (BACM) (Funes et al., 2007)
H181.1	human embryonic stem cells	TeSR™-E8™ Kit	Dr. Outi Hovatta, Karolinska Institute, Stockholm
Val3	human embryonic stem cells	TeSR™-E8™ Kit	Banco Nacional de Lineas Celulares, Nodo de Valencia

3.1.2. Assessment of cell proliferation and viability

a) Cell proliferation rate analysis

5 x 10^5 cells/ml were seeded in a 12 or 6-well plate and cell proliferation was monitored the following days post-seeding, after transfection or drug treatment (depending on the experiment) with either the hemocytometer chamber, the cell counter NucleoCounter® NC-100™ system (Chemometec) or the cytometer Guava PCA (Merck Millipore). Values were represented as relative growth rate after normalising with the control condition.

b) Clonogenic assays

1-2 x 10^6 cells/ml were seeded in a 6-well or 60 mm plate after transfection by electroporation. Between 24-48 h post-transfection, cells were treated with antibiotic selection, normally puromycin at 0.5-1 µg/ml final concentration. Cell culture media supplemented with the antibiotic was refreshed every 2-3 days to select positive cell clones that had been acquired the DNA plasmid. After 6-17 days post-selection cells were fixed with pure methanol for 10 min at RT and dyed with Crystal Violet solution (1 % acetic acid, 1 % methanol, 1 % (w:v) crystal violet dye) other 10 min following several washes with water until colonies were seen clearly and stained plates were scanned. Alternatively, plates were destained with 10 % acetic acid for 10 min at RT and absorbance was measured at 590 nm in a spectrophotometer to quantify the results.

c) GFP positive cells quantification by FACS

2.5 x 10^6 cells were transfected with a mix of 5 µg of a short hairpin expression or empty vector along with 1 µg of a GFP gene construct. We assumed that most of GFP positive cells had incorporated not only the GFP gene construct but also the other DNA construct since there were 5 times more amounts of the latter. GFP positive cells were analysed by flow cytometry in the FACScan cytometer (BD Biosciences) 2 days post-transfection to check the transfection efficiency and after 7 days to study the effect of the short hairpin construct on cell proliferation. If the ratio of GFP positive cells between day 7 and 2 was less in the experimental condition than in the control (empty vector), these cells were

unable to proliferate due to the counterpart plasmid (short hairpin plasmid). On the contrary, if the ratio of GFP positive cells was higher in the experimental sample than in the control, these cells proliferated more quickly again due to the counterpart plasmid.

d) SubG0-G1 cell cycle phase analysis

Propidium iodide is a nucleic acid intercalating agent and fluorescent molecule used to stain DNA. We used this dye to quantify by flow cytometry the number of cells in each cell cycle phase including subGo-G1 phase corresponding to apoptotic cells.

2.5 x 10^6 cells were transfected with 5 µg of the short hairpin expression vector or the empty vector. 7 days post-transfection, cells were harvested and counted. 1 x 10^6 cells were washed with cold PBS, centrifuged 3 min at 1500 rpm and resuspended in 1.5 ml PBS. To fix the cells, 3.5 ml of pure cold ethanol was added to 70 % final concentration in a drop wise manner to the PBS cells suspension on top of a vortex device at low velocity. Cells were fixed for 20-30 min in ice. After that, cells were centrifuged 3 min at 1500 rpm and washed two times with cold PBS. In the last step cells were centrifuged again and resuspended in 5 ml of PBS 1 % BSA and 50 mM sodium-citrate. 200 µg/ml RNAse A DNAse-free and 10 µg/ml propidium iodide was added and incubated 30 min at 37 ^oC in dark conditions. After incubation, cells were analysed by flow cytometry in the FACScan cytometer (BD Biosciences) and subG0-G1 cells proportion was acquired.

3.1.3. Drug treatments

Dexamethasone was used at 100 nM during 24-48 h to induce N-RAS gene expression in UR61 cells.

Zn_2SO_4 was used at 100 µM during 24-48 h to induce MAX gene expression in UR61-MT-MAX and in the control UR61-MT-Hebo cells.

TNFα chemokine was used at 100 ng/ml during 15 min to 6 days (depending on the experiment) to activate the NF-κB pathway in UR61 and HeLa cells.

Actinomycin D was used at 0.05 µg/ml during 1 h to inactivate RNA transcription mediated by RNApol I in HEK293T, MSC-3H and HS181.1 cells.

Stock preparation:

Dexamethasone was dissolved in DMSO to a final concentration of 10 mM (Sigma-Aldrich). Zn_2SO_4 was dissolved in distilled water to a final concentration of 75 mM. TNFα (Peprotech) was dissolved in distilled water to a final concentration of 100 µg/ml. Actinomycin D (Sigma-Aldrich) was dissolved in DMSO to a final concentration of 5 mg/ml. All stock solutions were aliquoted and stored at -20 ^oC except Zn_2SO_4 that was stored at 4 ^oC.

3.1.4. Transfection

Different transfection reagents and methods were used depending on the cell line and aim of the study. The expression vectors and siRNA used for transfection are shown in Table 3.2.

Table 3.2.- Plasmid and siRNA used in this Thesis

NAME	CONSTRUCT	ORIGIN/REFERENCE
pmaxGFP	GFP gene	Commercial (Amaxa)
pCEFL	empty vector	Laboratory collection
pCMV-Sport6	empty vector	This thesis
pCEFL-MXD1	MXD1 gene	Laboratory collection
pCEFL-MAX	MAX gene	Laboratory collection
pCMV-Sport6-MNT	MNT gene	Commercial (Origene)
pcDNA4-CCDC6-myc	CCDC6 gene myc tagged	A. Celetti (Merolla F. et al, 2012)
pcDNA4-CCDC6 1-223-myc	1-223 amino acids of CCDC6 gene fragment myc-tagged	A. Celetti (Merolla F. et al, 2012)
pcDNA4-CCDC6 1-101-myc	1-101 amino acids of CCDC6 gene fragment myc-tagged	A. Celetti (Merolla F. et al, 2012)
pECFP-Fibrillarin	CFP-Fibrillarin fusion gene	M. Lafarga
pcDNA-UBF-Flag	mouse UBF gene Flag-tagged	Laboratory collection
pGL3basic	*Firefly* sp. luciferase reporter gene with no promoter region	Commercial (Promega)
pGL3-Ebox mut	*Firefly* sp. luciferase reporter gene regulated by 4 mutated E-box sequences	T.Berg (Kiessling, et al., 2006)
pGL3-Ebox	*Firefly* sp. Luciferase reporter gene regulated by 4 E-box sequences	T.Berg (Kiessling, et al., 2006)
pNF-κB	*Firefly* sp. luciferase reporter gene regulated by 5 putative NF-κB regulatory elements	José Pedro Vaqué (Martin D. et al., 2008)
pBV-luc	*Firefly* sp. luciferase reporter gene with no promoter region	Commercial (Addgene) (He et al., 1999)
pBV-800 MNT-luc	*Firefly* sp. luciferase reporter gene regulated by 800 bp upstream the TSS of human MNT gene	This thesis
pRL-null	*Renilla* sp. luciferase reporter gene regulated by the T7 promoter	Commercial (Promega)
pCMV-VSV-G	VSV-G gene encoding enveloped lentiviral protein	Didier Trono (Commercial Addgene)
psPAX2	GAG and POL genes enconding packaging lentiviral proteins	Robert A. Weinberg (Commercial Addgene)
pLKO.1 control	Empty vector	Commercial (Sigma- MISSION)
pLKO.1-sh-MNT mouse / rat	short hairpin RNA TRCN0000085733 against mouse/rat MNT mRNA	Commercial (Sigma- MISSION)
pLKO.5-sh-MNT human	short hairpin RNA TCR0000234788 against human MNT mRNA	Commercial (Sigma- MISSION)
siRNA Universal Negative Controls	scramble RNA sequence with no homology to known gene sequences	Commercial (Sigma- MISSION)
MXD1 siRNA ID: SASI_Hs01_00179640	siRNA sequence against human MXD1 mRNA	Commercial (Sigma- MISSION)
MXD1 siRNA ID: SASI_Hs01_00179641	siRNA sequence against human MXD1 mRNA	Commercial (Sigma- MISSION)

MAX siRNA ID: SASI_Hs01_00011941	siRNA sequence against human MAX mRNA	Commercial (Sigma- MISSION)
MAX siRNA ID: SASI_Hs01_00011942	siRNA sequence against human MAX mRNA	Commercial (Sigma- MISSION)

a) Transfection with jetPEI reagent

JetPEI® (Polyplus transfection) was used for HEK293T and HeLa cells. The day before transfection, cells were seeded at 40-60 % of confluence. The day of transfection DNA or siRNA were diluted in 100-200 µl 150 mM NaCl. 2 µl of jetPEI® per µg of DNA/siRNA used were diluted separately in other 100-200 µl 150 mM NaCl. Both dilutions were vortexed and incubated for 5 min at RT. After the 5 min, the jetPEI® dilution was added to the DNA dilution, mixed by vortexing again and incubated for at least 30 min at RT. Meanwhile new media was added to the cells. Then, the mixture was added in a drop wise manner to the plate. Cells were recollected for analysis between 24-72 h after transfection.

b) Transfection with Polyethylenimine (PEI)

PEI reagent (1 µg/µl pH: 7, Polysciences, Inc.) was used for HEK293T and HeLa cells transfection. The day before transfection, cells were seeded at 40-60 % of confluence. The day of transfection DNA was diluted in 200 µl 150 mM NaCl. Three times more of PEI reagent was diluted separately in other 200 µl 150 mM NaCl. Both dilutions were vortexed and incubated for 5 min at RT. After 5 min the PEI dilution was added to the DNA dilution, mixed by vortexing again and incubated for at least 30 min at RT. Meanwhile new media was added to the cells. Then, the mixture was added in a drop wise manner to the plate. Cells were recollected for analysis between 24-72 h after transfection.

c) Transfection by electroporation

Amaxa™ Nucleofector™ Device (LONZA) was used for HeLa, K562 and UR61 cells. Cells were harvested and different transfection protocols were followed for each cell line according to Amaxa™ Nucleofector™ Technology. Briefly, 2.5 x 10^6 cells were resuspended in Ingenio® Electroporation solution (MIRUS bio) and 2 to 5 µg of DNA plasmid or 30 µl siRNA (10 µM) were added. Cells were put into the cuvettes and HeLa, K562 or PC12 electroporation protocol was selected in the nucleofector device. After electroshock, cells were resuspended in the corresponding media and seeded in plates. Cells were collected for analysis between 24 to 72 h after transfection according to the experiment.

3.1.5. Lentivirus production and infection

Lentivirus particles were produced to transduce different cell lines. Short hairpin (sh) sequences constructs were used to produce siRNA against human or rat MNT mRNA.

To produce these lentiviral particles, HEK293T cells were transfected according to the PEI reagent method with a set of three different construct (pCMV-VSV-G, psPAX2, and the short hairpin sequence lentiviral plasmid of interest) to make virus production possible. VSV-G and PAX2 genes are necessary for virion packaging; they provide *in trans* the structural and replication proteins required (GAG, POL

and VSV-G). The gene or short hairpin sequence lentiviral plasmid provides the packaging signal (Ψ) and the LTRs (Long Terminal Repeats) needed to integrate the construct in the genome of the infected cell. The ratio amount for pCMV-VSV-G: psPAX2: construct of interest is 1:3:4 respectively. For a 150 mm plate, a total of 24 µg of DNA was transfected.

Two days after transfection, supernatants containing lentivirus were collected, centrifuged for 3 min at 1500 rpm and filtered through 0.22 µm pore size sterile syringe filters (Merck Millipore). Next, 40 % PEG8000 PBS (Sigma-Aldrich) stock solution was added to a final concentration of 15 % and let stay at 4 ^{o}C for at least 6 h. After that, the medium was centrifuged for 30 min at 1500 rpm and 4 ^{o}C to precipitate lentivirus particles. Supernatant was discarded and the pellet containing lentivirus was resuspended in 250 to 500 µl DMEM buffer to concentrate lentivirus particles.

HeLa or Rat1a cells were used to titer lentivirus particles. About 2.5 x 10^4 cells were seeded in a 6-well plate. The following day, different volumes of the lentiviral preparation (e.g. 1, 5 and 10 µl) was added in half amount volume of cell culture medium usually used containing 5 µg/ml hexadimethrine bromide (Polybrene®, Sigma-Aldrich). Polybrene® neutralizes charge repulsion between virions and sialic acid on cell surface and improves lentiviral infection. 12 h later new medium was added to the cells to complete the volume normally used for 6-well plates. 48 h post-transduction medium was removed and new medium was added with the corresponding selection antibiotics. In our titrations puromycin (Sigma-Aldrich) was used at 1 µg/ml final concentration. Puromycin selection was controlled by using a control well with cells without lentiviral particles addition. After several days, cell colonies were stained with Crystal Violet solution (1 % acetic acid, 1 % methanol, 1 % (w:v) crystal violet) and the number of cell colonies that survived puromycin selection were counted.

Different titration determinations used for the same lentiviral particles preparation were averaged.

For cell transduction, 5 x 10^5 cells were seeded in a 6-well plate with 1.5 ml of cell culture medium. Polybrene® was added to a final concentration of 5 µg/ml and 5 µl of medium containing lentiviral particles were added. In the next 12 h up to 3 ml of cell culture medium was added. 48 h post-transduction, medium was removed and new medium was added with 0.3-1 µg/ml puromycin to select stably cell lines. After several days post-selection, cells were harvested and checked for short hairpin sequence construct acquisition and functionality by western blot.

3.2. DNA AND RNA ANALYSIS

3.2.1. Bacterial transformation and plasmid DNA purification

Plasmid DNA was transformed into *E. coli* DH5α competent cells (Life technologies) for DNA amplification using the heat-shock method. 30 µl *E. coli* DH5α cells were mixed with 100-200 ng of plasmid DNA. The mixture was incubated in ice for 30 min. After that, a heat shock of 20 seconds at 37 °C was done followed by 2 others min incubation in ice. 1 ml LB growth media was added to the

transformed cells without antibiotics and incubated in an orbital shaking incubator at 37 ºC 160 rpm for 1 h. After this, *E.coli* cells were seeded on LB-agar growth media plates containing the corresponding antibiotic selection (100 µg/ml ampicillin or 50 µg/ml kanamycin) and incubated overnight at 37 ºC.
The following day, some single colonies were both seeded on LB-agar growth media plates containing the corresponding antibiotic selection and inoculated to let them grow separately overnight in 5 ml LB growth media containing the corresponding antibiotic selection in an orbital shaking incubator at 37 ºC 160 rpm. LB media grown cells were centrifuged at 3000 rpm for 10 min and plasmid DNA was purified with the NucleoSpin Plasmid Miniprep Kit (Macherey-Nagel) following manufacturer's instructions.
Purified DNA plasmids were checked by enzymatic restriction digestion using specific restriction endonucleases (Fermentas) for each plasmid following manufacturer's instructions. DNA fragments after enzymatic digestion were analysed by agarose gel electrophoresis to check DNA size fragments.
Agarose gel electrophoresis was carried out first by melting low melting point agarose (Pronadisa) in 0.5 X TAE buffer (Bio-Rad) to make a 0.8-1 % (w:v) agarose gel and nucleic acid stain "Real safe reagent" (Durvitz s.l.) was diluted 1:20,000 before gel solidification. DNA samples were mixed with 5 X DNA loading buffer to a 1 X final concentration (30 % glycerol (v/v)) and loaded in the gel. DNA fragments sizes were determined by using DNA size standards "1 Kb DNA ladder" or "100 bp DNA ladder" (Fermentas).
Electrophoresis was carried out in an iMupid Mini gel Electrophoresis system at 50-100 V for 30-40 min in 0.5 X TAE buffer. Finally, gels were visualized and recorded using a Gel Doc™ EZ System (Bio-Rad).
Once plasmids DNA were checked, positive single colonies that were seeded on LB-agar growth media plates were inoculated and let them grow overnight in 5 ml LB growth media containing the corresponding antibiotic selection in an orbital shaking incubator at 37 ºC 160 rpm. LB media grown cells were centrifuged at 3000 rpm for 10 min and transformed cells stocks were done by resuspending cell pellets in LB-glycerol 1:1 to conserve them at -80 ºC. To prepare higher amounts of plasmid DNA, a little amount of glycerol stock was inoculated into 5 ml LB growth medium containing the appropriate antibiotic and incubated in an orbital shaking incubator at 37 °C 160 rpm. After 6-8 h cell culture was added to 200 ml LB growth medium containing the corresponding antibiotic and let it grow overnight in the same culture conditions. The following day, bacterial culture was centrifuged at 6000 rpm for 10 min and plasmid DNA was purified using the Plasmid Midi Kit (Qiagen) following manufacturer's instructions. Plasmid DNA concentration was determined by measuring $A_{260\ nm}$ using a microvolume spectrophotometer (Thermo Scientific™ NanoDrop 2000).

3.2.2. DNA cloning

To generate the pBV -800 MNT-luc vector, two pair of primers were designed targeting a sequence of human genome corresponding to 800 bp upstream transcription start site (TSS) of MNT gene promoter to amplify this region by polymerase chain reaction (PCR). The MNT promoter sequence for this was obtained from the UCSC genome browser (http://genome.ucsc.edu/), created by the Genome Bioinformatics Group of UC Santa Cruz. Restriction endonuclease target sequences (EcoRI and HindIII target sequences) were added to the 5' region of the specific primers:

-800bp TSS MNT **EcoRV** Forward (5'→3'): TC**GATATC**ATGTGACCTGCAGACACTGG

-800bp TSS MNT **HindIII** Reverse (5'→3'): TG**AAGCTT**GGCACTGCCTCCCTTCTT

PCR was carried out with the Phusion High-Fidelity DNA Polymerase (ThermoScientific) following manufacturer's instructions. Briefly 130 ng genomic DNA was mixed with 10 µl of 5 X HF buffer; 1 µl of 10 mM dNTPs mix; 1.6 µl of 15 µM forward and reverse primer mix; 0.5 µl DNApoly HF (2 U/µl) and up to 50 µl of DNAse-free water. The mix was loaded into a thermocycler and the following protocol was set to amplify DNA: 98 ^{o}C 30 s / [98 ^{o}C 15 s ; 65 ^{o}C 15 s ; 72 ^{o}C 30 s] 35 cycles / 72 ^{o}C 7 min

After reaction DNA from PCR was purified with QIAquick PCR Purification Kit (Qiagen) following manufacturer's instructions. After DNA elution with DNAse-free water samples were ran in a 0.8 % (w:v) agarose gel to check PCR amplicons by DNA size using "1 kb DNA ladder" and "100 bp DNA ladder" (Fermentas) DNA standards.

Once the amplicon was checked for an approximately 800 bp DNA fragment, endonuclease restriction digestions were carried out with EcoRI and HindIII enzymes (Thermo Scientific) for DNA amplicon from PCR and the plasmid DNA pBV-luc vector following manufacturer's instructions: 300 ng DNA; 1 µl EcoRI (10 U/µl); 1 µl HindIII (10 U/µl); 2 µl 10 X Buffer R and up to 20 µl DNAse-free water. The mix was incubated overnight at 37 ^{o}C.

After DNA enzymatic digestion, samples were electrophoresed in a 0.8 % (w:v) agarose gel to check pBV-luc linearization and restriction fragments by DNA size. Once checked, DNA fragments were purified using the JETQUICK Gel Extraction Spin Kit (Genomed) following manufacturer's instructions.

Purified digested vector and PCR product fragments (insert) were ligated to create the pBV- 800bp TSS MNT-luc plasmid. For DNA ligation, T4 DNA ligase (Thermo Scientific) was used according to manufacturer's instructions as follows:

3 µl pBV-luc vector and 9 µl insert (ratio Vector: Insert = 1:3 in mass); 2 µl 10X T4 DNA ligase buffer; 0.2 µl T4 DNA ligase (5 U/µl) and up to 20 µl DNAse-free water. The mix was incubated 1 h at 22^{o}C following an enzyme inactivation step of 10 min at 65^{o}C.

After ligation, 5 µl of the reaction was transformed to *E.coli* DH5α by the heat-shock method, seeded on LB-agar growth media plates containing 100 µg/ml ampicillin and incubated overnight at 37 ^{o}C. The following day, some single colonies were both seeded on LB-agar growth media plates containing 100 µg/ml ampicillin and inoculated to let them grow separately overnight in 5 ml LB growth media containing 100 µg/ml ampicillin in an orbital shaking incubator at 37 ^{o}C 160 rpm. LB media grown cells were centrifuged at 3000 rpm for 10 min and plasmid DNA was purified with the NucleoSpin Plasmid Miniprep Kit (Macherey-Nagel) following manufacturer's instructions.

DNA plasmid purified from bacteria was checked for the presence of the insert (800 bp TSS upstream human MNT gene) by PCR with the primers used in the first step and by endonuclease restriction digestion with EcoRI and HindIII. The correct sequence of the reporter so generated was confirmed by

Sanger sequencing (Macrogen) also confirming the referred sequence of human MNT gene promoter present in the reporter.

3.2.3. RNA extraction and purification

Total RNA purification from cell cultures was performed using Trizol reagent (Invitrogen). 3 million cells were collected and lysed with 0.5 ml Trizol reagent. After 5-10 min at RT, 0.1 ml of chloroform was added, gently mixed for 15 s and centrifuged at 12,000 rpm for 15 min at 4 ^{o}C. The upper aqueous phase was recollected and transferred to new 1.5 ml tube. 0.250 ml of isopropanol was added, mixed and incubated for 10 min at RT. After incubation, the mixture was centrifuged at maximum speed for 20 min at 4 ^{o}C. Supernatant was discarded and the RNA pellet was washed with 75 % ethanol and centrifuged at 7500 rpm for 5 min at 4 ^{o}C. Ethanol supernatant was discarded and the RNA pellet was allowed to dry at RT for 5 min. After drying, RNA precipitated was resuspended in 30 µl of RNAse-free water. Finally RNA concentration was determined by measuring A_{260nm} using a microvolume spectrophotometer (Thermo Scientific^{TM} NanoDrop 2000).

Samples were subjected to electrophoresis in denaturing agarose gels with formaldehyde to evaluate RNA integrity. Gels were prepared with 1 % (w:v) agarose in MOPS buffer (20mM MOPS, 5 mM sodium acetate and 1 mM EDTA pH 7.0) and 2.2 M formaldehyde. RNA samples were mixed with 2 volumes of loading buffer (MOPS, 50 % formamide, 2.2 M formaldehyde, 6 % glycerol and 1:20,000 Real safe reagent dilution). Finally samples were heated for 10 min at 65 ^{o}C and loaded into the gel. The electrophoresis was ran in MOPS buffer for 30-40 min at 40 V.

Alternatively RNA for RNA-seq analysis from cell cultures was purified using RNeasy kit (Qiagen) following manufacturer's instructions. Briefly, samples (< 5 X 10^6 cells) were directly lysed and homogenized by pipetting in the presence of a highly denaturing guanidinethiocyanate containing buffer (RLT). Lysates in mixed with ethanol where applied to the RNeasy mini spin columns and the RNA was selectively bound to the silica membrane contained. After several washes with RWI and RPE washing buffers to eliminate contaminants, RNA was eluted in 50 µl RNase-free water. RNA concentration was determined by measuring A_{260} using a microvolume spectrophotometer (Thermo Scientific^{TM} NanoDrop 2000). RNA integrity was evaluated with the 2100 Agilent Bioanalyzer (Agilent technologies).

3.2.4. Reverse transcription and quantitative polymerase chain reaction (RT-qPCR)

In order to analyse the expression of genes at mRNA level, quantitative real time PCR (RT-qPCR) was assayed.

First, reverse transcription (RT) was performed of total extracted RNA from mammalian cell lines. 1 µg of RNA was used for reverse transcription to create complementary DNA (cDNA) of total RNA with the iScript cDNA Synthesis Kit (Bio-Rad) according to manufacturer's instructions in a total volume of 20 µl. The following protocol was set for the reaction:

5 min 25 ^{o}C / 30 min 42 ^{o}C / 5 min 85 ^{o}C.

The cDNA samples were stored at -20^{o}C until used.

To analyse the expression of a specific mRNA in an experimental condition, cDNA was amplified by quantitative PCR using specific primers for the gene of interest (Table 3.3).

The primers were designed using the online Primer 3 software tool (http: \\frodo.wi.mit.edu/primer3/) according to PCR standard guidelines: length 18 to 25 bp; GC content 40 to 65 %; no G at the 5' end; no secondary structures; Tm: 50 to 65 ^{o}C. PCR conditions were determined depending on the nature and complexity of primers. A PCR mix was prepared with the iQ SYBR® Green supermix (Bio-Rad) as follows:

[10 µl 2 X iQ SYBR® Green supermix; 0.2 µl of 15 µM forward and reverse primer mix and up to 20 µl of DNAse-free water (used for two 10 µl duplicate reactions)] * nº of samples.

20 µl of the PCR mix was added to 1 µl cDNA. Of this, 10 µl were loaded on a 96 well plate for duplicate reactions. PCRs were performed in the CFX Connect™ Real-Time PCR Detection System (Bio-Rad). The qPCR protocol normally used was the following:

For DNA amplification:

95 ^{o}C 5 min / [95 ^{o}C 5 min; 57 ^{o}C 15 s; 72 ^{o}C 15 s] 40 cycles / 95 ^{o}C 1 min

For real time melting curve:

[55 ^{o}C 10 s decreasing by half a degree each cycle] 80 cycles.

Quantitative PCRs were analysed with the CFX Manager™ software. Threshold cycles (Ct) were determined by default at the beginning of DNA amplification in the exponential phase. The mRNA expression of genes of interest was normalized to mRNA expression of housekeeping genes (β-actin and RPS14) using the comparative Delta Ct (ΔCt) method:

$$\Delta Ct = 2^{(Ct\ \text{normalizing gene} - Ct\ \text{gene of interest})}$$

Reactions with water instead of cDNA were used as negative controls to detect possible amplification signals from contaminant DNA or primer dimers.

Table 3.3- Primers for RT-qPCR used in this Thesis

GENE	SPECIES	PRIMERS SEQUENCE (5'→3')	Tm (^{O}C)	ORIGIN
β-Actin	*Homo sapiens*	AAAATCTGGCACCACACCTTC TAGCACAGCCTGGATAGCAA	57	Laboratory collection
RPS14	*Homo sapiens*	TCACCGCCCTACACATCAAACT CTGCGAGTGCTGTCAGAGG	57	Laboratory collection
MAX	*Homo sapiens*	TGTTGTTGTCGGTGACTTCC CATTATGATGAGCCCGTTTG	57	This thesis
MNT	*Homo sapiens*	AGCCAGTGGATGGACGTACT GACGATGGCTCAGCTTAGGT	57	This thesis
β-Actin	*Rattus norvegicus*	CTAAGGCCAACCGTGAAAAG ACCCTCATAGATGGGCACAG	57	Laboratory collection
RPS14	*Rattus norvegicus*	CAAGGGGAAGGAAAAGAAGG GAGGACTCATCTCGGTCAGC	57	Laboratory collection
MAX	*Rattus norvegicus*	CACCATAATGCACTGGAACG CTGGTGCGTATGGTTTTTCC	57	This thesis
MNT	*Rattus norvegicus*	GAGAAGATTGCCACACAGCA GGACGATGGTTCAGCTTAGG	57	This thesis
ENDOGLIN	*Rattus norvegicus*	AACCCAGACACCAGTCCAAG GGTATCGATGAGCCAGGAGA	57	This thesis
CDKN1C	*Rattus norvegicus*	CTCTCCTAACGTGGCTCCTG GATGCCCAGCAAGTTCTCTC	57	This thesis
NDRG4	*Rattus norvegicus*	GGATACCAGTTCCCCTCCAT CTCCACCAAATCAGGGAAGA	57	This thesis
TXNRD3	*Rattus norvegicus*	TCATAGCAACAGGGGAAAGG AAGCCACGAAGAAGGACAGA	57	This thesis
RET	*Rattus norvegicus*	TTGGTCCAGTCCAACAACAA GCACAGACACGTTGAAATGG	57	Laboratory collection
BRCA2	*Rattus norvegicus*	GGCCATGAACCACAGCTATT GGTCCTTTCTGGCCTTCTTT	57	This thesis
CDC6	*Rattus norvegicus*	CCCTGAGCAAGACAAACTCC GGCGGAGAACATGGAGATAA	57	This thesis
TRIP13	*Rattus norvegicus*	AGGGTGGATCTTCGTACAGC GCCTGTAAACGCTCTGCTTT	57	This thesis
POLE2	*Rattus norvegicus*	CGCTTTCCTAGCAGCAGTTT CGGATCGTACTTGTCTGCAA	57	This thesis
NEIL3	*Rattus norvegicus*	CTTGCAACTAGCAGGGGTTC TTTAGCGTTCATTGGAGCAG	57	This thesis
EXO1	*Rattus norvegicus*	GCTGCTTTCTTATGGGGTCA TCTCGGGCTTCTGACACTTT	57	This thesis
ORC1	*Rattus norvegicus*	GGCATTTGTTAGGACGGAGA CCAGGACAGCTTCACAAACA	57	This thesis
MYC	*Rattus norvegicus*	ACGGCCTTCTCTTCTTCCTC GGTTGCCTCTTTTCCACAGA	57	This thesis
FANCD2	*Rattus norvegicus*	AAGCAACCCCTTTCCAAGTT GGACTCCAGGCCATTAACAA	57	This thesis
E2F7	*Rattus norvegicus*	ATAAGGGACCGGGAGAAGAA GGACAAGGGGTAGCTTGGAT	57	This thesis
PARPBP	*Rattus norvegicus*	TGGCGTGCTCATTGTAACTC CTCAGAGCGCAGAACAAGTG	57	This thesis

3.2.5. Chromatin immunoprecipitation (ChIP)

Chromatin immunoprecipitation technique was used to determine whether a protein is bound to DNA in a concrete region.

Generally 60 X 10^6 cells were grown. Cells were washed with PBS and fixed to cross-linked proteins and DNA with 1 % formaldehyde PBS for 10 min with gentle agitation. Next, glycine was added to a 125 mM final concentration to stop cross-linking reactions. Cells were washed with PBS, harvested by scraping and centrifuged 3 min at 1500 rpm. Cell pellet was resuspended in 1.2 ml of ChIP Lysis buffer (50 mM Tris HCl pH 8; 10 mM EDTA; 1% SDS) supplemented with 1:100 protease inhibitor cocktail (Calbiochem), passed through a G20 needle syringe 4-5 times and homogenized by pipetting up and down in ice for 10 min. Next, cell lysates were sonicated to shear chromatin in sizes of 200 to 600 bp using the Bioruptor® Plus sonication device (Diagenode). The sonication device was set at high power setting for 10-15 cycles of 30 seg on and 30 seg off). After sonication, cell lysates were centrifuged for 5 min at 14,000 rpm and supernatants containing chromatin were recollected. 50 µl of sample was taken to check DNA size after sonication and the rest was kept at -80 ^{o}C until used. The 50 µl of chromatin sample was diluted with 150 µl of ChIP Dilution buffer (0,01 % SDS; 1,1 % Triton X-100; 1,2 mM EDTA; 20 mM Tris-HCl pH 8; 150 mM NaCl) and 12 µl of 5 M NaCl and 6 µl of 10 mg/ml RNAse A was added. The mix was incubated in agitation at 65 ^{o}C overnight to reverse protein-DNA crosslinks and degrade RNA. The next day DNA fragments were purified with QIAquick PCR Purification Kit (Qiagen) following manufacturer's instructions and ran in a 1.5 % (w:v) agarose gel together with the "100 bp DNA ladder" standard to check if most DNA sizes were between 200-600 bp. If DNA fragments were higher, another round of sonication was made until appropriate DNA sizes were achieved. If DNA fragments were in the correct size, 200 µl of cell lysate (corresponding to 10 X 10^6 cells) were diluted 10 times with ChIP dilution buffer and 3 µg of specific antibody or unspecific immunoglobulins as a mock control were added. The cell lysate-antibody mix was incubated rotating overnight at 4 ^{o}C. The following day protein G-bound magnetic beads "Dynabeads®-protein G" (Invitrogen) were used to capture DNA-protein-antibody immunocomplexes since protein G has high affinity for immunoglobulins constant regions (Fc). 30 µl of "Dynabeads®-protein G" were washed with dilution buffer and recollected using the DynaMag™ magnet (Invitrogen). Magnetic beads were resuspended in 200 µl dilution buffer containing 14 µl salmon sperm DNA (Invitrogen) to block unspecific DNA binding. Beads were incubated with salmon sperm DNA rotating for 1 h at 4 ^{o}C. Next, blocked magnetic beads were added to the antibody-lysate mix and incubated rotating for 3-4 h at 4 ^{o}C. After incubation, beads-immunocomplexes were recollected with the magnet and washes of 5 min rotating at 4 ^{o}C were done sequentially with 1 ml of the following ChIP wash buffers: Low salt wash buffer (0.1 % SDS, 1.1 % Triton X-100, 2 mM EDTA, 20 mM Tris-HCl pH:8, 150 mM NaCl); High salt wash buffer (0.1 % SDS, 1.1 % Triton X-100, 2 mM EDTA, 20 mM Tris-HCl pH 8, 500 mM NaCl); LiCl wash buffer (0.25 M LiCl, 1 % IGEPAL (Sigma-Aldrich), 1 % sodium deoxycholate, 1 mM EDTA, 10 mM Tris-HCl pH 8); 2 washes with TE wash buffer (10 mM Tris-HCl pH 7.5, 1 mM EDTA).

Immunocomplexes were eluted from beads with 200 µl of ChIP elution buffer (1 % SDS; 50 mM Tris-HCl pH 7.5). At this point 50 µl of no immunoprecipitated lysate was diluted with 150 µl ChIP elution buffer

to be used as total DNA (input) for the final PCR step. 12 µl of 5 M NaCl and 6 µl of 10 mg/ml RNAse A was added to all samples and incubated in agitation at 65 ^{o}C overnight to reverse protein-DNA crosslinks and degrade RNA. The following day beads were removed using the magnet and supernatants containing DNA and proteins were collected. 2 µl 10 mg/ml proteinase K, 2 µl 0.5 M EDTA and 4 µl 1M Tris-HCl pH 6.8 was added and the mix was incubated for at least 3 h at 45 ^{o}C in agitation to degrade proteins. After protein degradation, DNA was purified with QIAquick PCR Purification Kit (Qiagen) following manufacturer's instructions and eluted in 30 µl DNA-free water.

Immunoprecipitated DNA was analysed by quantitative PCR (as described in Reverse transcription and quantitative polymerase chain reaction section) using the CFX Connect™ Real-Time PCR Detection System (Bio-Rad). 3 µl of eluted and input DNA was used for quantitative PCR. Immunoprecipitated DNA was normalized to total DNA quantity in the lysate (input) using the comparative Delta Ct (ΔCt) method:

$$\Delta Ct = 2^{(Ct\ \text{Input} - Ct\ \text{DNA immunoprecipitation})}$$

Finally, specific immunoprecipitated DNA was normalized to DNA immunoprecipitated with unspecific IgGs.

Reactions with water instead of DNA were used as negative controls to detect possible amplification signals from contaminant DNA or primer dimers.

Table 3.4- Primers for ChIP used in this Thesis

GENE REGION	NAME OF PRIMERS	SPECIE	PRIMERS SEQUENCE (5'→3')	Tm (^{o}C)	ORIGIN/REFERENCE
MNT promoter	MNT -654 bp	*R. norvegicus*	CCGCTAATACGACCCTGAAG CCGGATTTTGTCTCTGTTCC	57	This thesis
ATROGIN1 promoter	ATROGIN1 -370 bp	*R. norvegicus*	ACAAGGCGAGCCCATAAAC GGAACTGATGTGGAGGGTTG	57	This thesis
NDRG1 Transcriptional Start Site	NDRG1 TSS	*R. norvegicus*	GTCCGGAGGGCTTACCTAAC CGGACGTAAACAAACCTTGC	57	This thesis
Chromosome 13 intergenic region	chr13	*Homo sapiens*	GAGGAAGCCTGCACACCTAC AATTCAACAGCGAGGGGTAA	57	This thesis
Chromosome 14 intergenic region	chr14	*Homo sapiens*	ACACAGGGTCCTTGGTGAAA CACATCCAGCCTGAGAGTCA	57	This thesis
Chromosome 15 intergenic region	chr15	*Homo sapiens*	TGCTGAGGGTTCAAACTGTG CCTCCAGAACCACAGCAGAT	57	This thesis
Chromosome 21 intergenic region	chr21	*Homo sapiens*	ACCATGCACCAGGTCACATA CGCTTTCTGTGGAAATTGCT	57	This thesis
Chromosome 22 intergenic region	chr22a	*Homo sapiens*	CGCAGGGCTGTAGTGAAAAT GGGAGGAGGACTCCCTTCTA	57	This thesis
Chromosome 22 intergenic region	chr22b	*Homo sapiens*	CACCCAGGTTCAAGTTCTGG CCTGGCACAGTGCTCAATAA	57	This thesis

rDNA (ETS)	H1	*Homo sapiens*	GGCGGTTTGAGTGAGACGAGA ACGTGCGCTCACCGAGAGCAG	63	(Grandori et al., 2005)
rDNA (ETS)	H4	*Homo sapiens*	CGACGACCCATTCGAACGTCT CTCTCCGGAATCGAACCCTGA	63	(Grandori et al., 2005)
rDNA (ETS)	H8	*Homo sapiens*	AGTCGGGTTGCTTGGGAATGC CCCTTACGGTACTTGTTGACT	63	(Grandori et al., 2005)
rDNA (IGS)	H13	*Homo sapiens*	ACCTGGCGCTAAACCATTCGT GGACAAACCCTTGTGTCGAGG	63	(Grandori et al., 2005)
rDNA (IGS)	H18	*Homo sapiens*	GTTGACGTACAGGGTGGACTG GGAAGTTGTCTTCACGCCTGA	63	(Grandori et al., 2005)
rDNA (IGS)	H27	*Homo sapiens*	CCTTCCACGAGAGTGAGAAGCG CTCGACCTCCCGAAATCGTACA	63	(Grandori et al., 2005)
rDNA (IGS)	H32	*Homo sapiens*	GGAGTGCGATGGTGTGATCT TAAAGATTAGCTGGGCGTGG	63	(Grandori et al., 2005)
rDNA (IGS)	H42	*Homo sapiens*	AGAGGGGCTGCGTTTTCGGCC CGAGACAGATCCGGCTGGCAG	63	(Grandori et al., 2005)

3.2.6. E-box sequences in MNT gene promoter analysis

Genomic sequences of 1000 bp upstream the TSS of MNT gene from *Homo sapiens, Mus musculus* and *Rattus norvegicus* species were obtained from UCSC genome browser (http://genome.ucsc.edu) that contains the reference sequence and working draft assemblies for a large collection of genomes. The Feb. 2009 (GRCh37/hg19), Dec. 2011 (GRCm38/mm10) and Mar. 2012 (RGSC 5.0/rn5) assemblies were used for *Homo sapiens, Mus musculus* and *Rattus norvegicus* respectively.

E-box sequences described by Grandori et al. 1996 (canonical: CACGTG; Non-canonical: CATGTG; CATGCG; CACGCG; CACGAG; CAACGTG; CACATG) were searched within 1000 bp upstream the TSS of human, mouse and rat MNT genes.

3.2.7. RNA-sequencing (RNA-seq)

We took advantage of the next-generation and barcoding technologies to perform genome-wide sequencing of DNA from RNA from experimental mRNA transcripts (RNA-Seq).
DNA library preparation and data analysis were carried out as follows:
Library preparation and sequencing: 1 µg of total RNA was used to create barcoded 250 insert-size mRNA libraries using Illumina TruSeq RNA Sample Prep Kit v2 (kit RS-122-2002, Illumina) following manufacturer's instructions. After quantification, quality control on the 2100 Agilent Bioanalyzer (Agilent technologies) and normalization, a mix of four barcoded libraries per lane were submitted on a High-Seq 2000 Illumina sequencing platform following a 50 bp Single-End protocol. A minimum of 40 million reads per sample were obtained.

Data analysis: RNA sequence reads obtained from each sample were aligned against rat genome using the TopHat 2.0.1 software that uses Tophat algorithm (Trapnell et al., 2009). A set of gene model annotations and/or known transcripts in a GTF file format of rat genome (rn4) was obtained from RefSeq database through the UCSC genome browser (http://genome.ucsc.edu) and provided for TopHat alignment. Once sequence reads were aligned, Cufflinks software (Trapnell et al., 2010) was run

to assemble the alignments into a parsimonious set of transcripts to test for differential expression. Transcripts abundances were estimated based on the number of reads per transcript. Estimated expression values were represented in RPKM units (reads per kilobase per million reads) originally proposed by Ali Mortazavi et al. (Mortazavi et al., 2008).

3.2.8. Bioinformatics tools for functional analysis. Babelomics

Babelomics4 is an integrated web-based suite (http://babelomics.bioinfo.cipf.es/) of tools for the analysis of genomic data and functional profiling of the transcriptome, proteomic and genomic experiments. We used Babelomics 4.3 software to perform functional enrichment analysis of a set of experimental genes (from RNA-seq data) which expression was found to be ≥ 0.5 RPKMs with a fold change ≤ 0.6 between the conditions that were being compared using the FatiGO method with KEGG pathway and Gene Ontology (GO) databases.

3.2.9. Luciferase reporter assay

2 X 10^6 cells were transfected with a mix of DNA plasmids specific for each experiment, generally:

-1 µg of firefly (*Photinus pyralis*) luciferase gene reporter vector carrying the 5' transcription regulatory sequence that we wanted to analyse or a control vector without any specific transcription regulatory sequence.

-0.5 µg of the "pRL-null" Renilla (*Renilla reniformis*) luciferase gene construct that is constitutively expressed used as control of transfection efficiency.

-2-3 µg of the specific gene/short hairpin sequence or control constructs that we wanted to use for each experiment.

Luciferase reporter assays were carried out with the Dual-Luciferase Reporter (DLR) System (Promega) following manufacturer's instructions. Briefly, cells were harvested and lysed with 100 µl PLB (Pasive Lysis Buffer) diluted in distilled water rotating during 30 min at 4 ^{o}C. After that, cell lysates were centrifuged 15 min at 14,000 rpm and supernatants were collected for the assay.

20 µl of cell lysate was load into a 96-well plate. 100 µl of Luciferase Assay Reagent (LARII) containing the firefly luciferase substrate (luciferin) was added and luminescence was measured within 1 min after addition. After quantifying luminescence, *Firefly* luciferase reaction was quenched with 100 µl of Stop&Glo ® Reagent that also contains the *Renilla* luciferase substrate (coelenterazine) so that initiating the second luciferase reaction. Luminescence from both luciferase reactions was measured with the Mithras LB 940 Multimode Microplate Reader (Berthold technologies).

Firefly luminescence values were normalized against *Renilla* luminescence values used as control of transfection for each sample. Measurements were done in parallel duplicates and values were averaged. Relative light units (R.L.U.) were obtained of experimental values related to empty vector (control) values.

3.3. PROTEIN ANALYSIS

3.3.1. Western blot

3-5 X 10^6 cells were harvested by either trypsinization or scraping, centrifuged 5 min at 4 ^oC 1500 rpm and washed with PBS. Cells were resuspended in 100-200 µl Lysis buffer. Generally NP-40 lysis buffer (150 mM NaCl, 50 mM Tris-HCl pH 8, 1 mM EDTA, 1 % IGEPAL (Sigma-Aldrich), 0.2 % SDS, 20 mM NaF, 1:100 proteases inhibitor cocktail Set I (Calbiochem) and 1:100 phosphatases inhibitor cocktail (sigma-Aldrich)) was used. Exceptionally SDS lysis buffer (150 mM NaCl, 50 mM Tris-HCl pH8, 1 mM EDTA, 1 % SDS, 20 mM NaF, 1:100 proteases inhibitor cocktail Set I (Calbiochem) and 1:100 phosphatases inhibitor cocktail (Sigma-Aldrich)) was chosen for nucleolar proteins extraction.

Cell lysates were incubated 30 min in ice pipetting up and down every 5 min. After incubation, the lysates were sonicated using the Bioruptor® Plus sonication device (Diagenode) set at high power setting for 10-15 cycles (30 s ON, 30 s OFF). After sonication, cell lysates were centrifuged 20 min at 4 ^oC at 14,000 rpm. Supernatant containing proteins was recollected and kept until use. Protein quantification was carried out by Bradford method (Bradford et al., 1975) measuring $A_{595\ nm}$ absorbance using a micro-plate reader spectrophotometer. Protein concentration of experimental samples was estimated interpolating A_{595} values in a standard curve performed with known BSA (Bovine Serum Albumin) concentration samples.

50-100 µg of protein was mixed with distilled water and 5 X Laemli buffer (100 mM Tris-HCl pH 6.8, 8 % 2-mercaptoethanol, 4 % SDS, 0.1 % bromo phenol blue, 20 % glycerol) to 1 X final concentration. The protein samples were heated for 5-10 min at 95 ^oC to denature proteins and loaded in an 8 to 15 % (v:v) polyacrylamide-SDS (SDS-PAGE) gel depending on the protein sizes to be detected. The proteins were separated by electrophoresis in running buffer (10 % SDS, 1 X TG (10 X TG: Tris-Glycine buffer, Bio-Rad)) using a MiniProtean cuvette (Bio-Rad) with constant voltage at 180 V until desired according to the protein marker "Precision Plus Protein™ Dual Color Standards" (Bio-Rad). After gel electrophoresis, proteins were transferred to a nitrocellulose membrane (Amersham Protran Supported 0.45 NC, GE Healthcare Life Sciences) with the wet electrophoresis method in transfer buffer (10 % methanol, 1 X TG (Bio-Rad)) using the MiniProtean cuvette (Bio-Rad) with constant amperage for 1 h at 400 mA. After protein transference to nitrocellulose membrane, the polyacrylamide-SDS gels were stained with Coomassie Brilliant Blue solution (0.025 % Coomassie Brilliant Blue R-250 (w:v), 40 % methanol (v:v) and 10 % (v:v) glacial acetic acid) for 10 min at RT and distained with water until proteins bands were seen to check proteins load and integrity.

The following steps were all done in agitation. First, membrane were blocked with blocking solution (10 % non-fat dry milk (w:v) in TBS-T (20 mM Tris pH 7.5, 150 mM NaCl, 0.05 % Tween-20) for 1 h at RT to avoid unspecific antibody bindings. After incubation three washes of 10 min were done with TBS-T. Specific primary antibody solutions were prepared (1 % BSA (w:v) in TBS-T with a 1:500 to 1:3000

antibody dilution (Table 3.5) and membranes were incubated either 3 h at RT or overnight at 4 °C. Three washes of 10 min with TBS-T were followed. After that, membranes were incubated in dark conditions 1 h at RT with secondary antibody solution (1 % BSA (w:v) in TBS-T with a 1:10,000 IRDye680/IRDye800 fluorochrome-conjugated antibody dilution (LI-COR Bioscience) (Table 3.6). After incubation with the secondary antibody, membranes were washed twice with TBS-T before analysis.
Finally the proteins of interest were detected with an Odyssey Infrared Imaging System (LI-COR Bioscience). For protein loading control, primary antibody against β-Actin or α-Tubulin protein were used, alternatively stained polyacrylamide-gel was also used.

Table 3.5- Primary antibodies used in this Thesis

ANTIBODY	IMMUNOGEN	TYPE	ORIGIN/REFERENCE	USE AND DILUTION
anti-MAX (C-17)	C-terminal (human)	Rabbit polyclonal	SantaCruz biotechnology (sc-197)	WB (1:1000); IF (1:200); IP; ChIP
anti-MLX (8020.2)	Full length	Rabbit polyclonal	Ayer lab	WB (1:1000)
anti-MNT (M-132)	226-361 aa (human)	Rabbit polyclonal	SantaCruz biotechnology (sc-769)	WB (1:1000); IF (1:200); IP; ChIP
anti-MNT (F-11)	226-361 aa (human)	Mouse monoclonal	SantaCruz biotechnology (sc-376708)	WB: 1:1000
anti-MXD1 (C-19)	C-terminal (human)	Rabbit polyclonal	SantaCruz biotechnology (sc-222)	WB (1:1000); IF (1:200); IP; ChIP
anti-REL (D6)	143-184 aa (human)	Mouse monoclonal	SantaCruz biotechnology (sc-373713)	WB: 1:1000
anti-REL (N)	N-terminal (human)	Rabbit polyclonal	SantaCruz biotechnology (sc-70)	WB (1:1000); IF (1:200); IP
anti-MYC (N-262)	1-262 aa (human)	Rabbit polyclonal	SantaCruz biotechnology (sc-764)	WB (1:1000); IF (1:200)
anti-MYC (9E10)	MYC 9E10 epitope	Mouse monoclonal	J. León	WB (1:100); IP
anti-MYC (A-14)	C-terminal (human)	Rabbit polyclonal	SantaCruz biotechnology (sc-790)	WB (1:1000); IF (1:200); IP
anti-FLAG® (M2)	DYKDDDDK	Mouse monoclonal	(Sigma-Aldrich) F-1804	WB (1:1000); IF (1:200); IP
anti-NFkB p65 (F-6)	C-terminal (human)	Mouse monoclonal	SantaCruz biotechnology (sc-372)	WB (1:1000)
anti-NFkB p65 (gC-20)	1-286 aa (human)	Goat polyclonal	SantaCruz biotechnology (sc-8008)	WB (1:1000); IF (1:200); IP
anti-CCDC6 (Ab56353)	375-475 aa (human)	Mouse monoclonal	abcam®	WB (1:1000); IF (1:200); IP
anti-α-Tubulin	Human Tubulin peptid	Rabbit polyclonal	Nick Cowan	WB (1:3000)
anti-β-Actin (I-19)	C-terminal (human)	Goat polyclonal	SantaCruz biotechnology (sc-1616)	WB (1:1000)
anti-PARP1 (H-250)	764-1014 aa (human)	Rabbit polyclonal	SantaCruz biotechnology (sc-7150)	WB (1:1000)
anti-BCL-XL (54H6)	residues surrounding Asp61 of human BCL-XL	Rabbit monoclonal	Cell Signalling (#2764)	WB (1:1000)

anti-p57^{KIP2} (A120-1)	p57^{Kip2} Recombinant Human	Mouse monoclonal	BD Pharmingen^{TM} (556346)	WB (1:1000)
anti-CCNA2 (H-432)	Full length (human)	Rabbit polyclonal	SantaCruz biotechnology (sc-751)	WB (1:1000)
anti-CTCF	659-675 aa (human)	Rabbit polyclonal	07-729 (Upstate^{TM})	WB (1:1000)
anti-RhoGDI (A-20)	N-terminal (human)	Rabbit polyclonal	SantaCruz biotechnology (sc-360)	WB (1:1000)
anti-SIN3B (H-4)	172-228 aa (mouse)	Mouse monoclonal	SantaCruz biotechnology (sc-13145)	WB (1:1000)
anti-SIN3B (A-20)	N-terminal (mouse)	Rabbit polyclonal	SantaCruz biotechnology (sc-996)	WB (1:1000)
anti-UBF (F-9)	1-220 aa (human)	Mouse monoclonal	SantaCruz biotechnology (sc-13125)	WB (1:1000); IF (1:200)
anti-UBF (H-300)	1-220 aa (human)	Rabbit polyclonal	SantaCruz biotechnology (sc-9131)	WB (1:1000); IF (1:200); IP; ChIP
anti-Hemoglobin ɣ (51-7)	Full length (human)	Rabbit polyclonal	SantaCruz biotechnology (sc-21756)	IF (1:200)

Table 3.6.- Secondary antibodies used in this Thesis

ANTIBODY	IMMUNOGEN	TYPE	REFERENCE	USE AND DILUTION
Anti-Rabbit IRDye®800	rabbit heavy and light IgG	Donkey polyclonal	LI-COR (926-32213)	WB (1:10000)
Anti-Rabbit IRDye®680	rabbit heavy and light IgG	Donkey polyclonal	LI-COR (926-68073)	WB (1:10000)
Anti-Mouse IRDye®800	mouse heavy and light IgG	Donkey polyclonal	LI-COR (926-32212)	WB (1:10000)
Anti-Mouse IRDye®680	mouse heavy and light IgG	Donkey polyclonal	LI-COR (926-68072)	WB (1:10000)
Anti-Goat IRDye®800	goat heavy and light IgG	Donkey polyclonal	LI-COR (926-32214)	WB (1:10000)
Anti-Goat IRDye®680	goat heavy and light IgG	Donkey polyclonal	LI-COR (926-68074)	WB (1:10000)
Anti-Rabbit FITC	rabbit heavy and light IgG	Goat polyclonal	Jackson InmunoResearch laboratories Inc. (111-095-045)	IF (1:200)
Anti-Rabbit Texas Red	rabbit heavy and light IgG	Goat polyclonal	Jackson InmunoResearch laboratories Inc. (111-075-045)	IF (1:200)
Anti-Mouse FITC	mouse heavy and light IgG	Goat polyclonal	Jackson InmunoResearch laboratories Inc. (111-096-003)	IF (1:200)
Anti-Mouse Texas Red	mouse heavy and light IgG	Goat polyclonal	Jackson InmunoResearch laboratories Inc. (115-075-062)	IF (1:200)

3.3.2. Nuclear-cytoplasmic fractionation

3-5 X 10^6 adherent growing cells were washed with PBS. 100-200 µl of Lysis buffer 1 (10 mM HEPES pH 7; 10 mM KCl; 0.25 mM EDTA pH 8; 0.125 mM EGTA pH 8; 0.5 mM Spermidin, 0.1 % (v:v) IGEPAL (Sigma-Aldrich); 1 mM DTT; 1:100 proteases inhibitor cocktail Set I (Calbiochem)) was added to the plates and incubated in agitation for 30-40 min at 4 ^{o}C. Cells lysates were harvested by scraping and centrifuged at 4 ^{o}C 1500 rpm for 5 min. Supernatant containing cytoplasmic fraction was collected and kept at -80

°C until use. Nuclear fraction pellet was then resuspended in 50 µl of Lysis buffer 2 (20 mM HEPES; 400 mM NaCl; 0.25 mM EDTA; 1.5 mM MgCl2; 0.5 mM DTT; 1:100 proteases inhibitor cocktail Set I (Calbiochem)) and incubated rotating at 4 °C for 30 min. Nuclei lysates were centrifuged 20 min at 4 °C maximum speed in a microcentrifuge. Supernatant containing nuclear fraction was collected and kept at -80 °C until use.
Protein concentration was measured according to the Bradford method as described in Western blot section. Cytoplasmic and nuclear fraction samples were subjected to western blot assay to determine the localization of a protein of interest. To verify the enrichment of the fractions, RhoGDI, Tubulin were used as controls for cytoplasmic proteins and SIN3B and CTCF as nuclear protein.

3.3.3. Protein immunoprecipitation

5 X 10^6 cells were used for each protein immunoprecipitation assay. Cells were washed with PBS, harvested either by trypsinization or scraping method and centrifuged at 4 °C 1500 rpm for 5 min. 1 ml of Lysis buffer (50 mM Tris-HCl pH 7.5; 150 mM NaCl; 0.5 % NP40 (v:v); 1 mM EDTA; 1:100 proteases inhibitor cocktail Set I (Calbiochem)) was added to cell pellet. Cell lysate was passed through a G20 needle syringe 4-5 times and incubated rotating at 4 °C for 30 min. After incubation, cell lysate was centrifuged at 4 °C maximum speed for 20 min. Supernatant containing proteins was collected for protein immunoprecipitation of this, 25 µl of total cell lysate (input) was kept a -80 °C until use as loading control.
450 µl of cell lysate was used for a single immunoprecipitation and 3 µg of specific antibody or unspecific immunoglobulins (IgGs) used as control were added. Additional lysis buffer was added to the mix up to 1 ml final volume and they were incubated rotating overnight at 4 °C. The following day 15 µl of protein G-bound magnetic beads "Dynabeads®-protein G" (Invitrogen) previously washed with lysis buffer were used to capture protein-antibody immunocomplexes. The immunocomplexes-beads mix was incubated rotating for 2-3 h at 4 °C. After incubation, 3 rotating washing steps of 10 min at 4 °C were followed with the immunoprecipitation wash buffer (50 mM Tris-HCl pH 7.5; 150 mM NaCl) using the DynaMag™ magnet (Invitrogen) to recollect dynabeads-immunocomplexes after washes. Finally, proteins were eluted from beads with 30 µl of 2 X Laemli buffer (5 X stock: 100 mM Tris-HCl pH 6.8, 8 % 2-mercaptoethanol, 4 % SDS, 0.1 % bromo phenol blue, 20 % glycerol). At this point non-immunoprecipitated total lysate (input) was also mixed with 5 X Laemmli buffer to a 2 X final concentration. Samples were heated 10-15 min at 95 °C, beads were removed with the magnet and supernatant was collected and subjected to immunoblot analysis.

Detection of immunoprecipitated or co-immunoprecipitated proteins was determined by western blot with specific antibodies. Total lysate (input) was used as loading control.

3.3.4. Immunoprecipitation for proteomics analysis

Protein immunoprecipitation was carried out as described in protein immunoprecipitation section with the exception of the Laemli elution step. Instead, elution was carried out in Alex von Kriegsheim's laboratory (Systems Biology Ireland, Conway Institute, Dublin) according to the "On-beads digestion"

protocol used by Turriziani B. et al. (Turriziani et al., 2014). Briefly, beads-immunocomplexes were trypsinized, in order to digest the baits and the interacting proteins. After trypsinization protein samples were purified and finally resuspended in 0.1 % (v:v) trifluoroacetic acid buffer to be analysed by mass spectrometry on a Q-Exactive mass spectrometer (Thermo Scientific) connected to an Ultimate Ultra3000 chromatography system (Thermo Scientific). Mass spectra were analysed using the MaxQuant Software package of two technical replicates and biological triplicates of the experimental and control samples. Raw data files were searched against a rat database (Uniprot RAT), using a mass accuracy of 6 ppm and 0.01 false discovery rate (FDR) at both peptide and protein level.

3.3.5. Immunofluorescence analysis and fluorescence microscopy

Adherent cells were grown on glass coverslips, washed with PBS and fixed to cross-link proteins with 4 % (v:v) paraformaldehyde PBS for 15 min RT. Fixed cells were washed with PBS and incubated rotating in permeabilization buffer (1 % (v:v) Triton X-100 in PBS) during 30 min. After incubation, cells were blocked with blocking buffer (3 % (w:v)BSA; 0.1 % (v:v) Triton X-100 in PBS) for 20 min, washed 2 times with PBS 5 min and 1 min more with 0.1 % Triton X-100 (v:v) in PBS. Primary antibody solution was diluted 1:100-1:500 in blocking buffer and cells were incubated for either 3 h RT or overnight at 4 ^{o}C in a wet chamber. 2 washes of 5 min with PBS and 1 wash with 0.1 % Triton X-100 (v:v) in PBS was followed. Secondary antibody solution was prepared by diluting Texas-Red, FITC or Alexa Fluor® Flurochrome-conjugated antibodies 1:100 to 1:500 in blocking solution and cells were incubated for 1 h in a wet chamber in dark conditions. Several washes of 5 min were followed with PBS and coverslips glasses were mounted with DAPI nuclear stain incorporated ProLong® Gold Antifade Mountant (Life Technologies).

Cell samples were visualized using a Zeiss IMAGER M1 fluorescence microscope and a Leica TCS SP5 Confocal microscope equipped with UV laser diode (405 nm) and HeNe lasers (543 nm and 633 nm). Images were acquired and analysed with the ImageJ software.

3.3.6. Proximity ligation assay

This technique allows us to elucidate whether endogenous proteins interact in vivo and the subcellular location where the interaction takes place. It is based in the immunofluorescence technique. What differs from a conventional immunofluorescence is that the secondary antibodies used are conjugated to an oligonucleotide sequence (instead of a fluorophore) that recognizes regions of two additional and unconjugated probes. If both secondary antibodies are close enough, they will allow its conjugated oligonucleotides hybridize to both unconjugated additional probes. The two unconjugated probes will be hybridized to each antibody-conjugated oligonucleotide and a ligation step will ligate these two probes generating a unique circularized probe. Then, an amplification step with a DNA polymerase that follows will generate many copies of this circularized probe. Finally the addition of detection probes conjugated to a fluorophore and their hybridization to the amplified DNA will generate coloured signals when observed with a fluorescence microscope (see http://www.olink.com/products/duolink/how-

use-duolink). So that if the proteins to be analysed are interacting, positive signals (coloured dots) will be detected (Soderberg et al., 2006).

Proximity Ligation Assay (PLA®) was performed with Duolink® in situ Red Starter kit Mouse/Rabbit (Sigma-Aldrich) according to manufacturer's instructions with home-made buffers. Briefly, immunodetection with primary antibodies of proteins which interaction was going to be analysed were carried out as described in immunofluorescence section. After primary antibody incubation, 3 washes of 10 min with buffer A (0.05 % (v:v) Tween-20, 0.15 M NaCl, 0.015 M Trizma® base pH 7.4) were followed. Meanwhile oligonucleotide-conjugated secondary antibodies solution (PLA probe anti-Rabbit PLUS and anti-Mouse MINUS, Sigma-Aldrich) was prepared in blocking solution (3 % (w:v) BSA, 0.1 % (v:v) Triton X-100 in PBS) and incubated 20 min at RT before incubating them with the samples. Samples were incubated 1 h at 37 ^{o}C with secondary antibodies followed by 3 washes of 10 min with buffer A. Next, a ligation step was followed by incubating the samples with ligase solution (1 X ligation buffer containing two oligonucleotides and ligase enzyme) 30 min at 37 ^{o}C. Two additional washing steps of 10 min with buffer A were followed. After that, samples were incubated with amplification solution (1 X amplification buffer containing nucleotides and fluorochrome labelled oligonucleotides and polymerase enzyme) for 90 min at 37 ^{o}C in dark conditions. Amplification reaction was stopped by washing the samples in buffer B (0.1 M NaCl, 0.2 M Tris pH 7.5) 10 min at RT. Two additional washes with 0.01 X buffer B were done and samples were kept at 4 ^{o}C. The following day samples were mounted with DAPI nuclear stain incorporated ProLong® Gold Antifade Mountant (Life technologies). All washing steps were done in agitation and incubation steps in a wet chamber.

Cell samples were visualized using a Zeiss IMAGER M1 fluorescence microscope and a Leica TCS SP5 Confocal microscope equipped with UV laser diode (405 nm) and HeNe lasers (543 nm and 633 nm). Images were acquired and analysed with the ImageJ software.

Results

4. RESULTS

4.1. MXD1 IN GROWING AND UNDIFFERENTIATED CELLS

4.1.1. MXD1 expression and localization in growing and undifferentiated cells. MXD1 localized in the nucleolus

It is well known that MXD1 acts controlling MYC function in the differentiation and quiescent states (Eisenman, 2000) as it is in these conditions where MXD1 protein is highly expressed, contrarily to MYC proteins. However, little is known about possible roles of MXD1 protein in growing and undifferentiated conditions. We are interested in studying MXD1 protein since it is together with MNT, one of the best known biological antagonists of MYC oncoproteins.

We first asked if MXD1 was completely silent in growing and undifferentiated cells. We also wanted to study the subcellular localization of MXD1 in growing cells, which has not been reported in the literature. To do so we analysed its expression and localization by immunofluorescence using an antibody against MXD1 protein in different undifferentiated and proliferating cells. We did it in the human embryonic stem cells Val3 and Hs181.1; the human transformed mesenchymal stem cells MSC-3H (stably transfected with HPV-E6, HPV-E7 and hTERT) and in HEK293T; K562 and HeLa cells. As it can be seen in figure 4.1, MXD1 was localised in the nucleus as expected and it was detected in all growing and undifferentiated (stem cells) cells suggesting a role of MXD1 in general gene transcription regulation even when the cells are not in a differentiation or quiescent state.

It was also surprising, and never described before, that MXD1 was found localised in the nucleolus in a relevant fraction of cells (figure 4.1). To see whether this localization was common to all MXD family members in growing and undifferentiated conditions, we assessed immunofluorescence against others MXD members such as MXI1 and MNT and also against MAX proteins in Hs181.1 cells. We also studied MNT localization in Val3 cells and MNT and MAX localization in HeLa cells. We used UBF (Upstream Binding Factor) in Hs181.1 cells as a marker of nucleolar localization. As shown in figure 4.2, MXD1 was the only one of the MXD members analysed to have nucleolar localization in all types of cells studied.

To further confirm this localization we transfected HeLa cells with a GFP-MXD1 fusion gene construct to follow the localization of MXD1 in the cell. GFP construct and a GFP-MNT fusion gene construct were also transfected to see the specificity of MXD1 localization in the nucleolus. As it can be seen in figure 4.3, GFP-MXD1 fusion protein but not GFP or GFP-MNT, localized in the nucleus but also in the nucleolus in most cells. We also transfected HeLa cells with a CFP-Fibrillarin fusion gene since Fibrillarin localizes to the dense fibrillar component (DFC) of the nucleolus and assessed an immunofluorescence against MXD1 to see if it co-localised with CFP-Fibrillarin. As it can be seen in figure 4.3, endogenous MXD1 co-localized with CFP-Fibrillarin in the nucleolus. Immunofluorescence against MNT was used as a negative control of the experiment.

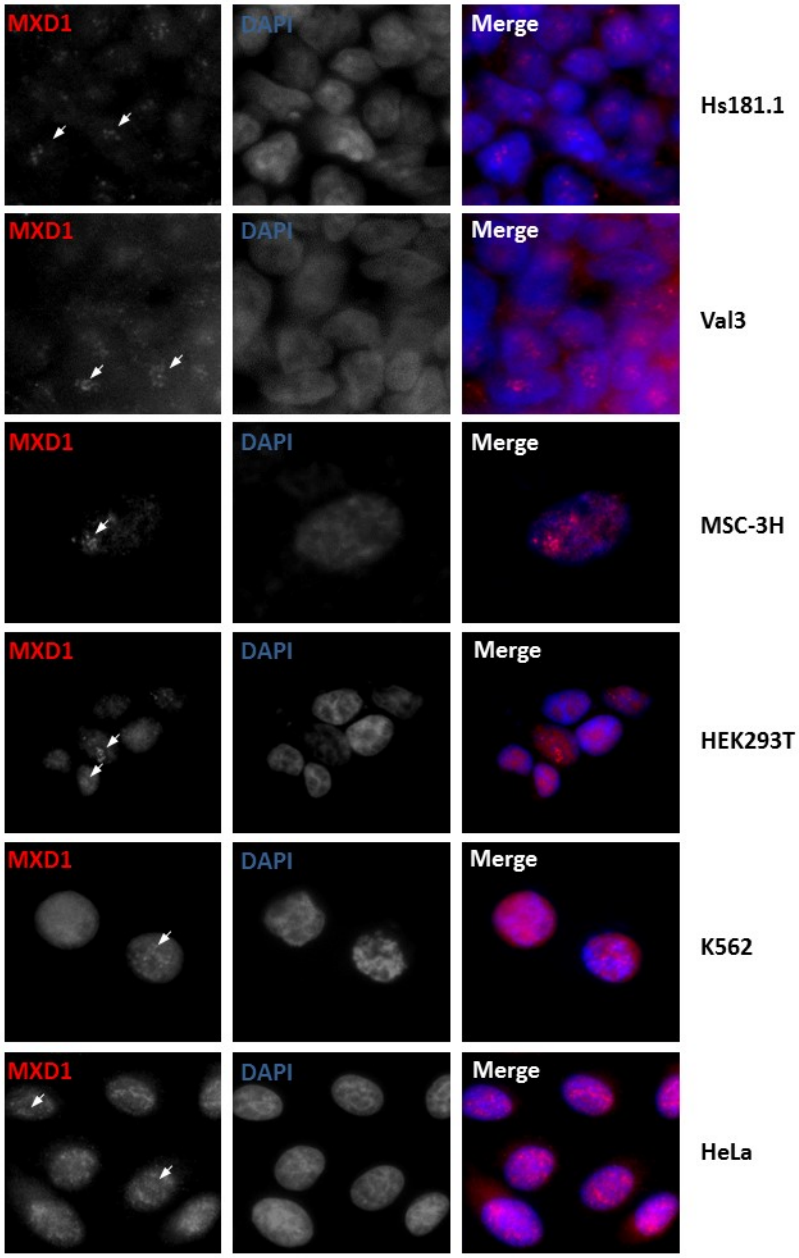

Figure 4.1.- MXD1 expression and localization in undifferentiated and proliferating cells. MXD1 immunofluorescence in different cell types: the undifferentiated embryonic cells Hs181.1; Val3; MSC-3H and 293T and the tumor cell lines K562 and HeLa. MXD1 in Hs181.1 and Val3 was mainly nucleolar meanwhile in MSC-3H, 293T, K562 and HeLa cells MXD1 was both nuclear and nucleolar. MXD1 is shown in red and DAPI staining of DNA (blue) was used to detect cell nuclei. Nucleolar regions correspond to DAPI unstained regions within the nucleus. White arrows indicate nucleoli.

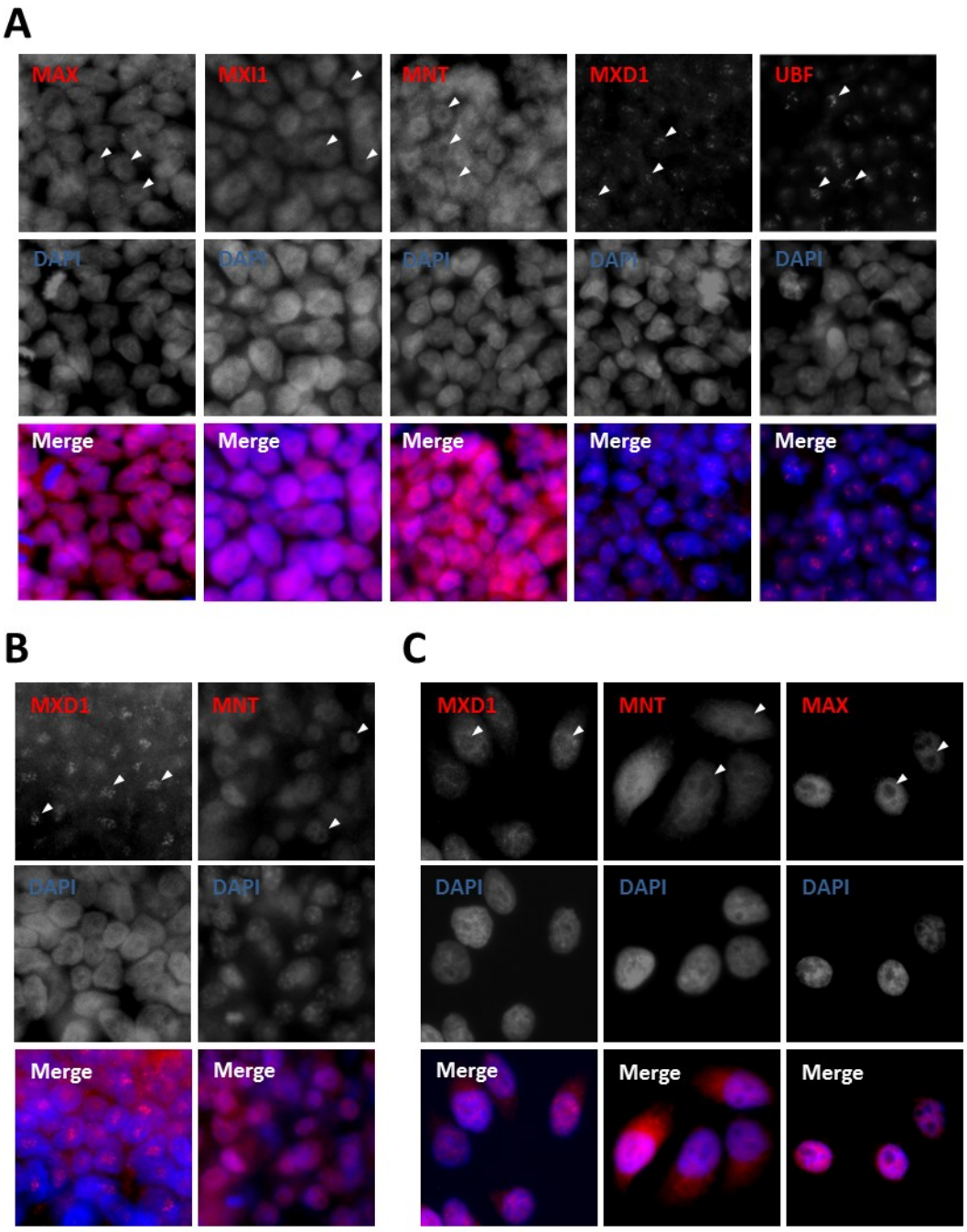

Figure 4.2.- Subcellular localization of MNT, MXD1, MXI1 and MAX. (A) Immunofluorescence against MAX, MXI1, MNT, MXD1 and UBF in the human embryonic stem cells Hs181.1. MXD1 was the only member of MXD family to localize in the nucleolus. UBF was used as a nucleolar marker. (B) Immunofluorescence against MNT and MXD1 in human embryonic stem cells Val3. MXD1 but not MNT was localized in the nucleolus. (C) Immunofluorescence against MXD1, MNT and MAX in HeLa cells. All of the proteins were nuclear but MXD1 was also nucleolar conversely to MAX and MNT. Immunofluorescence are shown in red and DAPI staining of DNA (blue) was used to detect cell nuclei. White arrows indicate nucleoli.

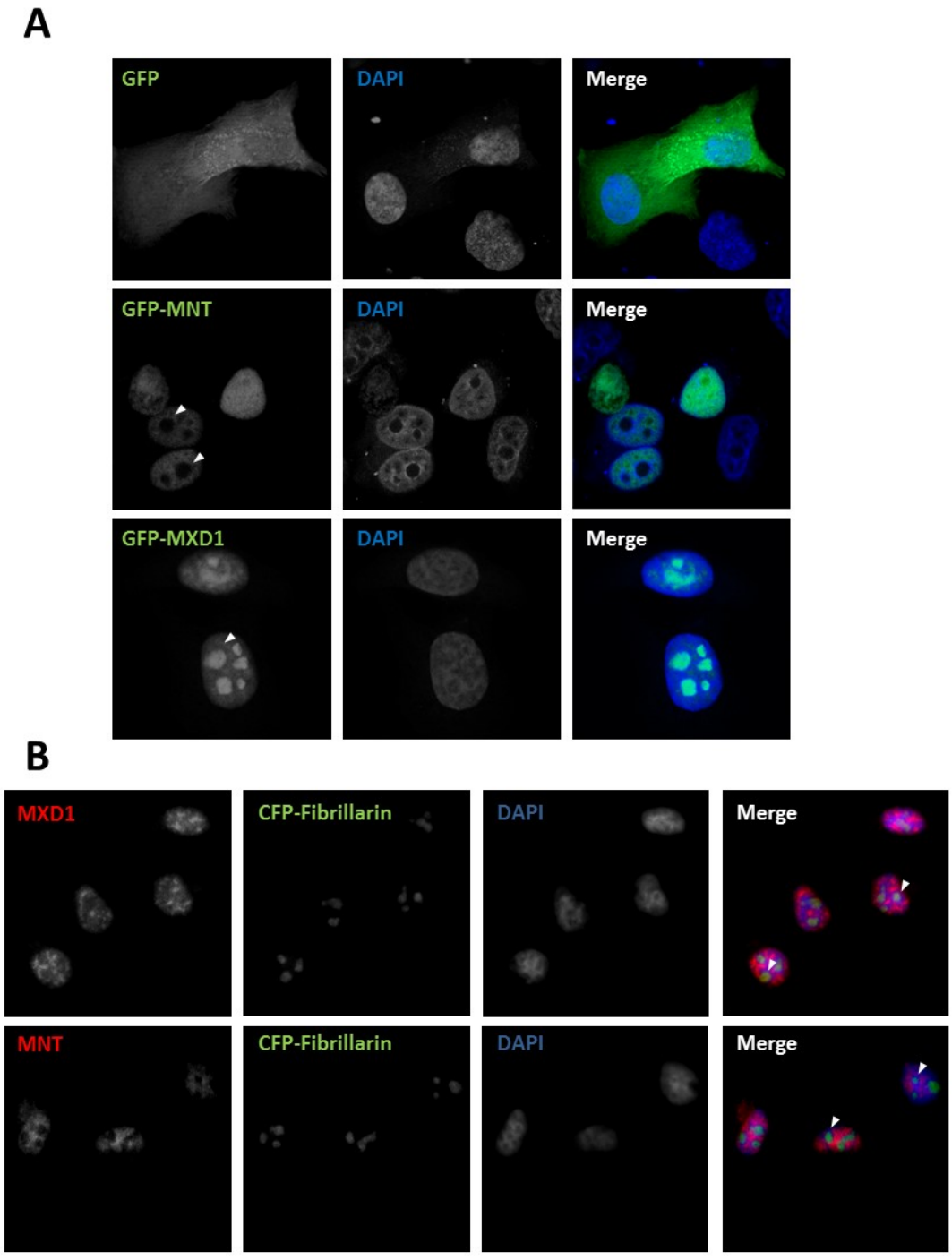

Figure 4.3.- MXD1 –GFP nucleolar localization. (A) MNT and MXD1 localization in HeLa cells transfected with GFP, GFP-MNT and GFP-MXD1 constructs (green). GFP-MXD1 protein was the only one that localized in the nucleus and nucleolus. (B) Immunofluorescence against MXD1 and MNT in HeLa cells transfected with a CFP-Fibrillarin construct (a nucleolar component). MXD1 (not MNT) and CFP-Fribrillarin shown in red and green colors respectively co-localized in the nucleolus. DAPI staining of DNA (blue) was used to detect cell nuclei. White arrows indicate nucleoli.

Furthermore, we transfected the HEK293T cells with a MXD1 expressing vector and performed an immunofluorescence against MXD1 using two different antibodies (C-19 from Santacruz Biotechnology and HPA001599 from Sigma-Aldrich). As it can be seen in figure 4.4, overexpressed MXD1 (localised in the nucleus and nucleolus of HEK293T cells) was detected with both antibodies confirming the nucleolar localization of MXD1.

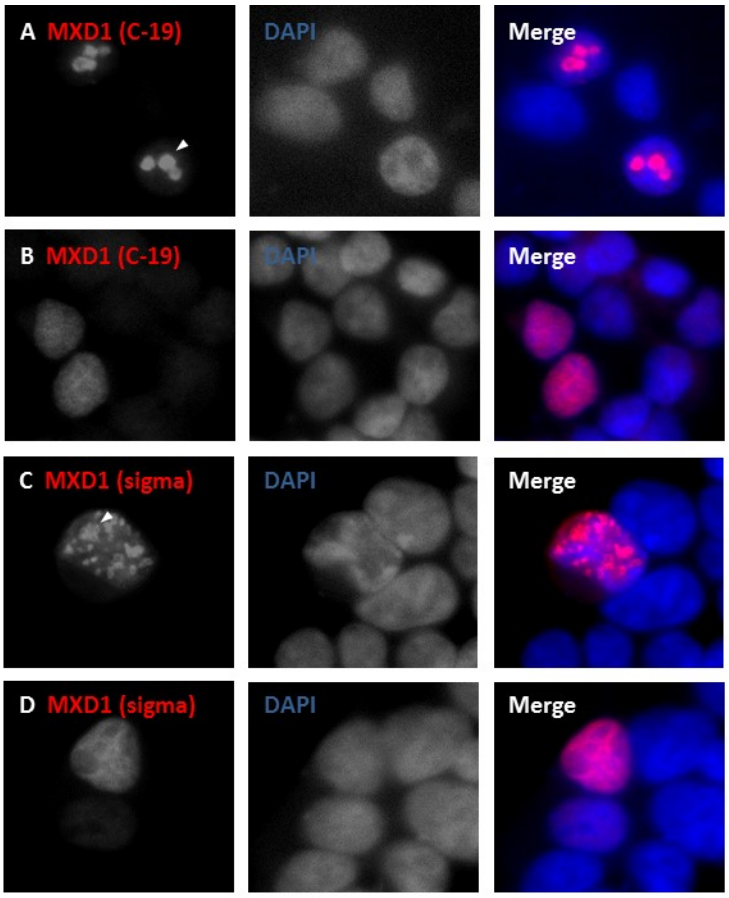

Figure 4.4.- Nuclear and nucleolar localization of overexpressed MXD1. Immunofluorescence of HEK293T cells transfected with a MXD1 expression vector using two different antibodies: (A,B) Anti-MXD1 C-19 from Santacruz Biotechnology and (C,D) anti-MXD1 from Sigma-Aldrich. Both antibodies recognized MXD1 in the nucleus and nucleolus confirming the specificity of the antibodies. DAPI staining of DNA (blue) was used to detect cell nuclei. White arrows indicate MXD1 nucleolar localization.

Moreover, MXD1 had a particular pattern of localization within the nucleolus very similar to UBF pattern. UBF, the main transcription factor regulating rDNA transcription, is known to localize in specific regions of nucleolus, the fibrillar centers (FC), where rDNA transcription takes place. This similarity in MXD1 and UBF localization made us think that MXD1 was being localised in the fibrillar centers. To confirm this localization of MXD1, we performed a double-immunofluorescence assay of MXD1 and UBF in HEK293T; HeLa; MSC-3H human transformed mesenchymal stem cells and Val3 human embryonic stem cells. We also did a co-immunofluorescence of endogenous MNT and UBF in Val3 to confirm the MNT exclusion from nucleolus. MXD1 co-localized in all cases with UBF (figure 4.5). To further confirm this co-localization, we assessed an immunofluorescence for UBF in HeLa cells transfected with the GFP-MXD1 construct to see the co-localization of the proteins (figure 4.6). Altogether, these results confirmed that MXD1 localized in the fibrillar centers of nucleolus where rDNA transcription takes place.

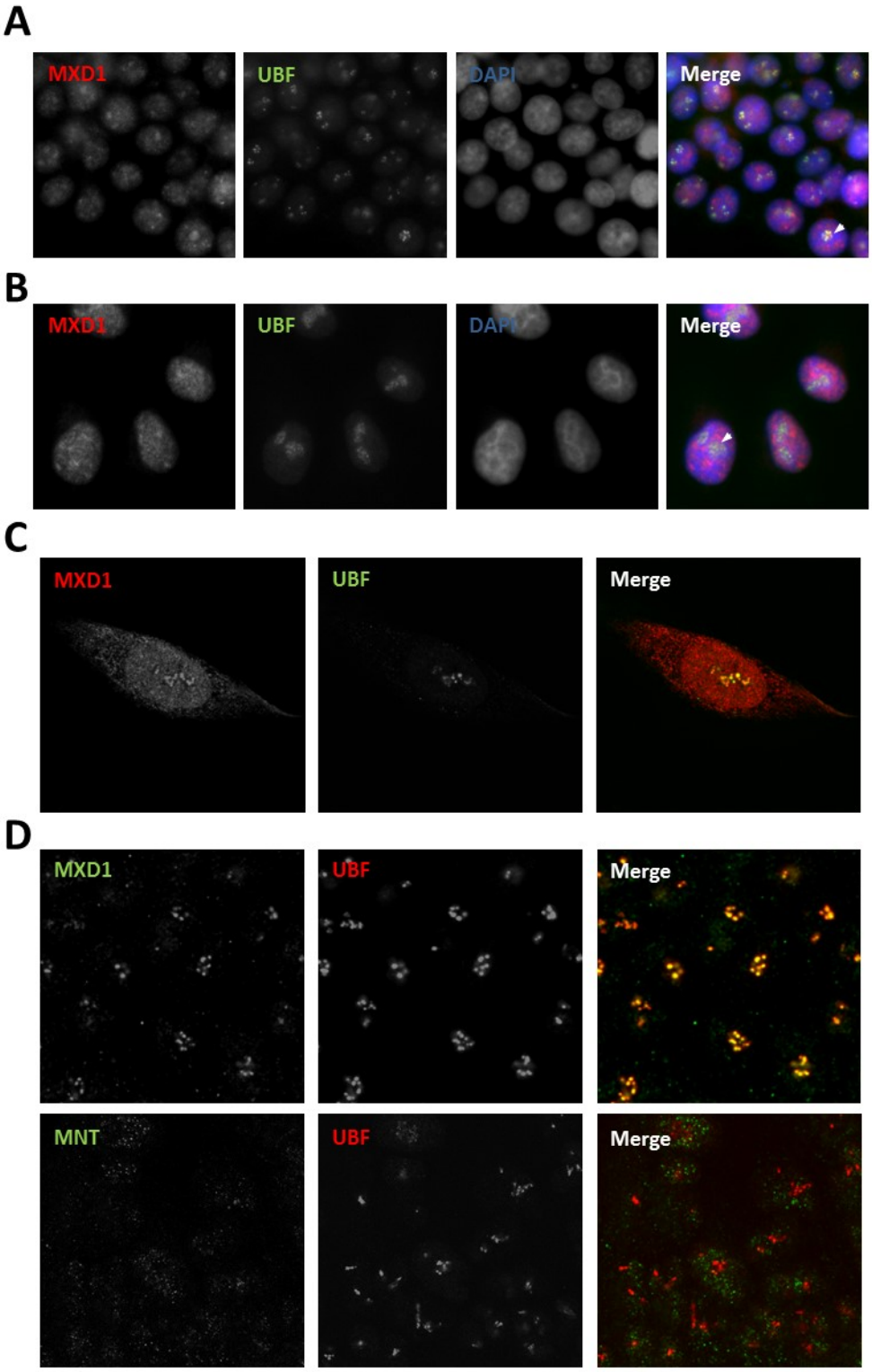

Figure 4.5.- MXD1 co-localizes with UBF in the nucleolus. (A) Immunofluorescence against MXD1 and UBF in HEK293T, (B) HeLa, (C) MSC-3H mesenchymal stem cells. MXD1 is shown in red and UBF in green. DAPI stain in blue was used to localize cell nuclei. (D) Immunofluorescence against MXD1 or MNT and UBF in Val3 embryonic stem cells. MXD1 and MNT are shown in green and UBF in red. MXD1 but not MNT and UBF co-localized in all cases in the nucleolus of cells. DAPI staining of DNA (blue) was used to detect cell nuclei. White arrows indicate MXD1 and UBF nucleolar co-localization.

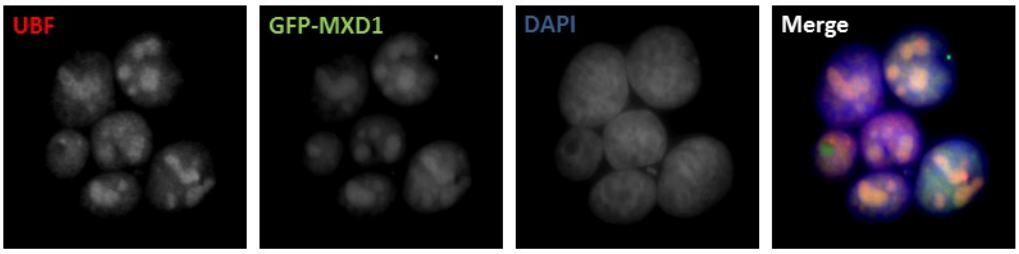

Figure 4.6.- GFP-MXD1 and UBF co-localization in the nucleolus. Immunofluorescence for endogenous UBF in HeLa cells transfected with GFP-MXD1 vector. UBF and GFP-MXD1 shown in red and green respectively localized in nucleolus. DAPI staining of DNA (blue) was used to detect cell nuclei.

4.1.2. MXD1 segregated from nucleolus when RNApol I was inhibited

Since MXD1 is a transcription factor and we saw that it localised in the fibrillar centers of nucleolus where rDNA transcription takes place, we wondered whether MXD1 might be regulating rDNA transcription. To do so we treated HEK293T cells, MSC-H and Hs181.8 cells with actinomycin D at low concentration (0.05 µg/ml) for 1 h to inhibit the RNApol I complex responsible for ribosomal RNA transcription in nucleolus (Perry and Kelley, 1970). The inhibition of rRNA synthesis following actinomycin D treatment results in a characteristic reorganization of the ultrastructural components of the nucleolus that are taking part in rRNA synthesis termed nucleolar segregation (Journey and Goldstein, 1961). After treatment with actinomycin D, immunofluorescence against MXD1 and UBF was assessed in HEK293T and MSC-3H and a co-immunofluorescence of both proteins in Hs181.1. As it can be seen in figure 4.7 all cells treated with actinomycin D showed MXD1 nucleolar segregation suggesting that MXD1 might be regulating rRNA synthesis. It is worth to note that in HEK293T cells, MXD1 was highly present in the nucleoplasm apart from the nucleolus so that after treatment with Actinomycin D, a clear nucleolar area appeared meanwhile the signal in the nucleoplasm fraction remained the same indicating the specificity of the RNApol I complex inhibition by low actinomycin D concentrations. UBF was used as positive control in Hs181.1 and HEK293T cells, as it is reported that also segregates from nucleolus after actinomycin D treatment (figure 4.7A).

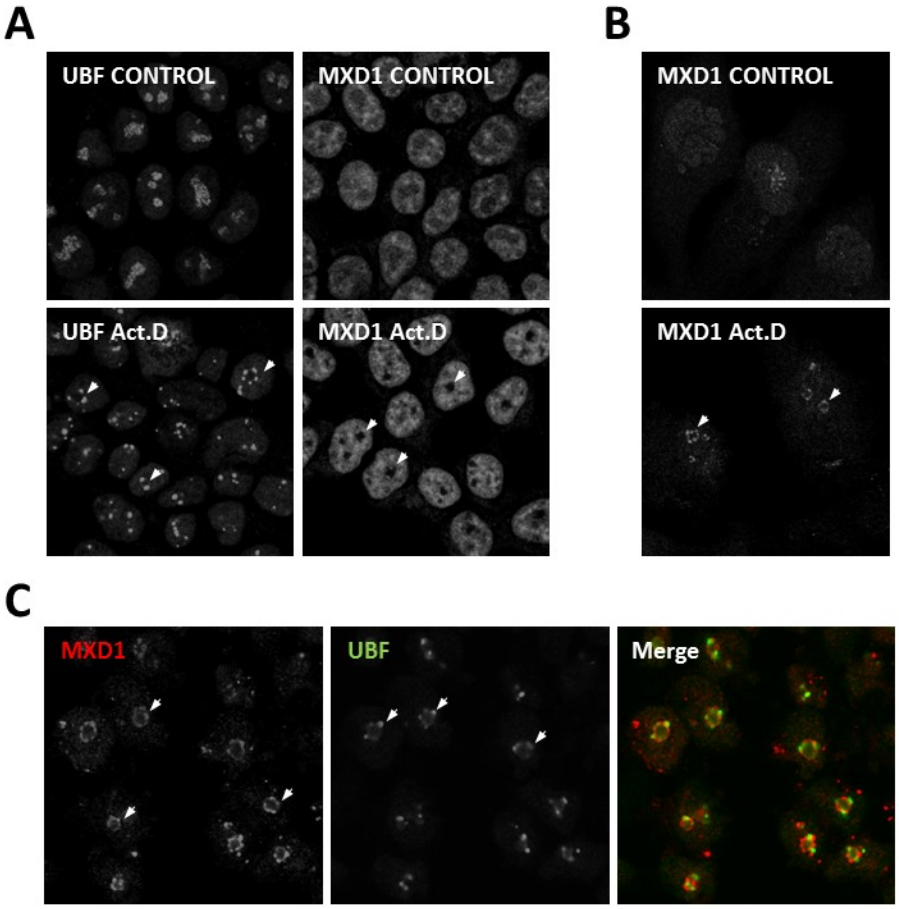

Figure 4.7.- MXD1 and UBF nucleolar segregation. (A) Immunofluorescence against UBF and MXD1 in HEK293T cells after actinomycin D treatment. (B) Immunofluorescence against MXD1 in MSC-3H cells after actinomycin D treatment. Immunofluorescence in normal conditions was assessed as control of UBF and MXD1 localization in the absence of the drug, upper panels (A,B). (C) Co-immunofluorescence against MXD1 and UBF in Hs181.1 cells after actinomycin D treatment. MXD1 and UBF are shown in red and green respectively. White arrows indicate nucleoli segregation.

4.1.3. MXD1 bound to chromatin in rDNA regions

Human rRNA genes are organized into clusters of ~43 kb repeats that are distributed among different chromosomes (chromosome 13, 14, 15, 21, 22) (see Introduction). These gene clusters in interphase localize in the fibrillar centers (FC) of nucleolus, where rRNA synthesis occurs. Since we saw that MXD1 was localizing in the fibrillar centers of nucleoli and it might be taking part in rRNA synthesis regulation, we wanted to know if it was bound to rDNA and in which regions.

To do so we performed a chromatin immunoprecipitation assay (ChIP) of MXD1 on rDNA in growing HEK293T cells. For this, we used the primers used in Grandori et al. 2005 designed for rDNA ChIP studies

and termed H1, H4, H8, H13, H18, H27, H32, H42. The distance between two TSS of the rDNA cluster is 43 kb and the names of the primers refer to the number of kb downstream from the initiation transcription region (i.e. H4 primers target a region 4 kb downstream the initiation transcription region of human rDNA repeats). With this set of primers, Grandori et al. described that UBF was bound to human rDNA in the transcription initiation and transcribed regions [H1, H4, H8, H13, H42] and less in the intergenic region (IGS)[H18, H27, H32]. We used an antibody against UBF as a positive control. Our data for UBF in HEK293T cells confirmed these previous results (Grandori et al. 2005) indicating that the ChIP technique was working properly (figure 4.8). MXD1 results were positive in respect to the unspecific rabbit immunoglobulins (IgG) used as negative control. MXD1 then was bound to rDNA. However, MXD1 bound to the rDNA in much less amounts than UBF and with a very high variability in HEK293T cells (figure 4.8).

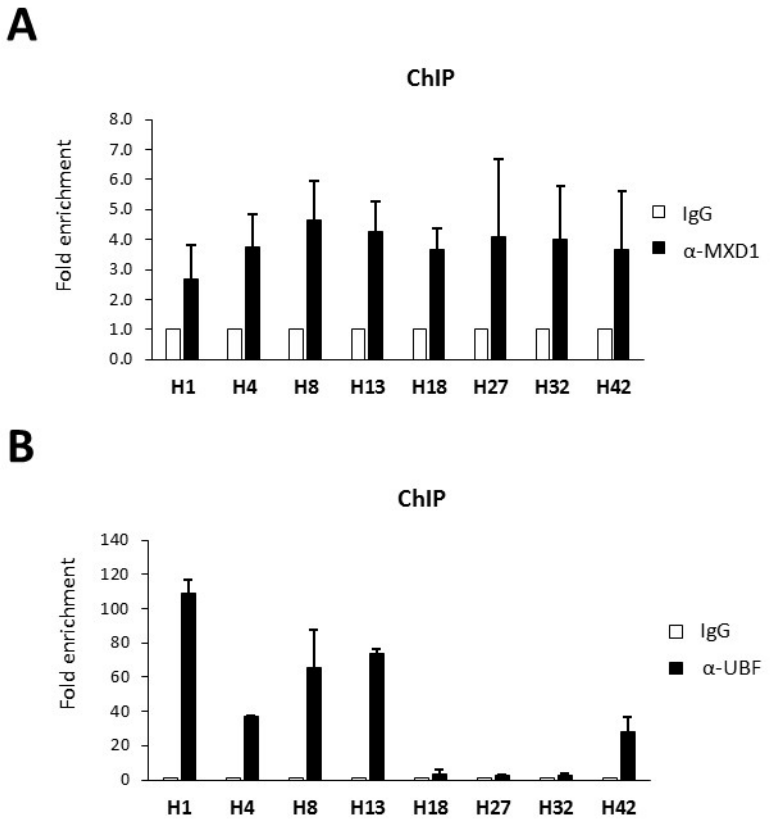

Figure 4.8.- MXD1 and UBF ChIP on rDNA in HEK293T cells. (A) Chromatin immunoprecipitation (ChIP) with anti-MXD1 antibody in HEK293T cells. The binding of MXD1 was analysed by PCR with different amplicons of the rDNA region. MXD1 bound across the entire rDNA although in less amounts in the initiation and transcribed regions H1, H4. (B) ChIP assay with anti-UBF antibody. UBF bound to DNA corresponding to the initiation and transcribed regions H1, H4, H8, H13, as described (Grandori et al. 2005).

It is described that HeLa cells deprived from serum during 48 h accumulates MXD1 due to the inactivation of the kinases responsible for MXD1 phosphorylation and consequent proteasome

degradation (Zhu et al., 2008). We confirmed this result by western blot (figure 4.9) and studied MXD1 localization in such conditions. MXD1 localization did not changed in HeLa deprived from serum (figure 4.9) being both nuclear and nucleolar as shown above. So that we decided to perform ChIP assays for

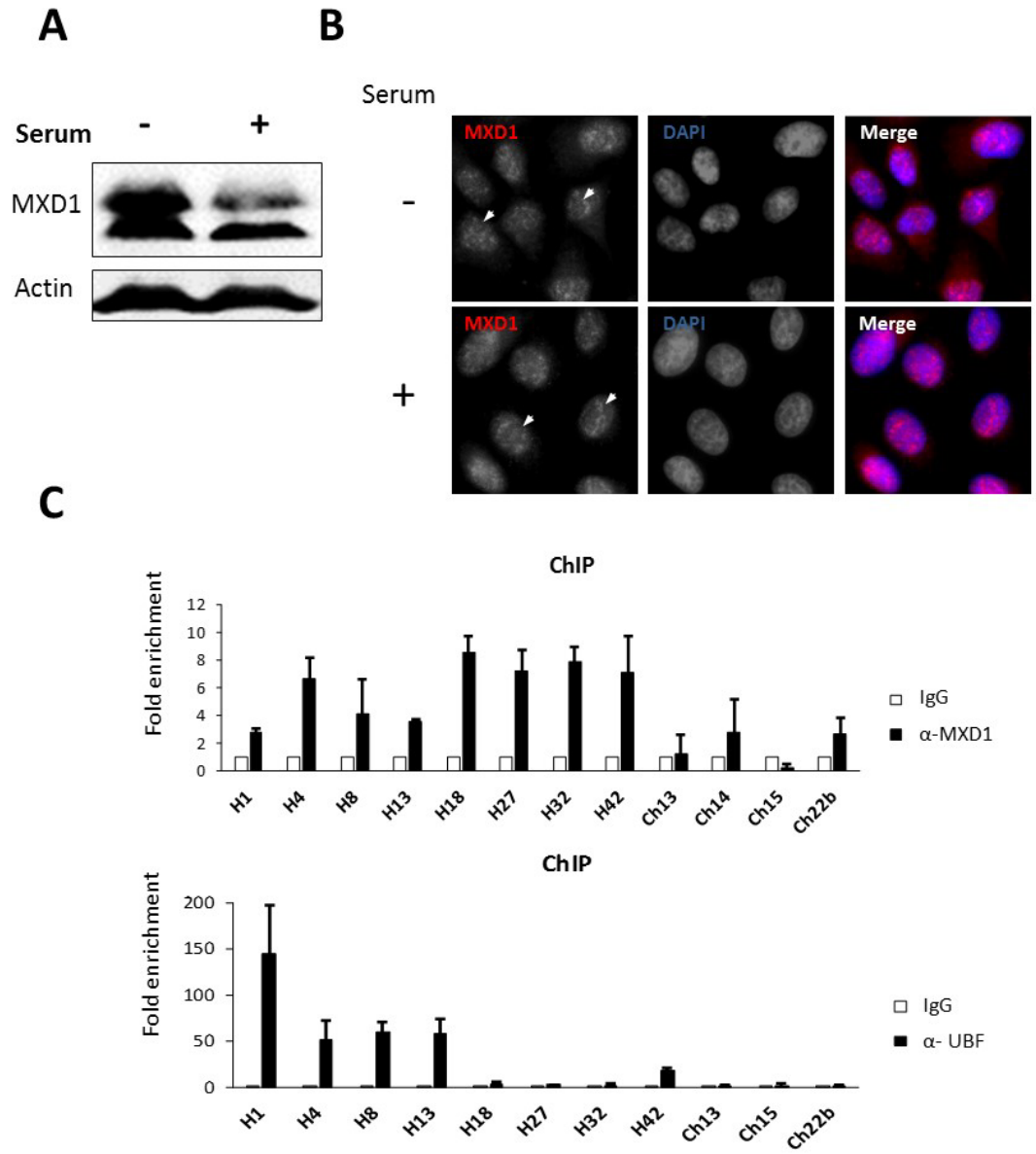

Figure 4.9.- MXD1 expression and localization in serum-derpivated HeLa cells. MXD1 ChIP on rDNA in serum-deprivated HeLa cells. (A) Western blot against MXD1 in HeLa cells after 48 h of serum deprivation and re-stimulated with 10 % serum for 5 h. MXD1 accumulated in serum deprivation conditions. (B) Immunofluorescence of MXD1 in HeLa cells 5 h with serum after being 48 h deprivated. DAPI stain in blue was used to localize cell nuclei. White arrows indicate nucleoli localization. (C) Chromatin immunoprecipitation (ChIP) of MXD1 and UBF in HeLa cells 48 h deprived from serum (to augment MXD1 expression). UBF was bound preferentially at initiation and transcribed regions within the rDNA as described (Grandori et al., 2005). MXD1 was bound acrosss the entire rDNA regions but preferentially to intergenic regions (IGS) H18, H27, H32 and H42. Ch13, Ch14, Ch15, Ch22b regions were used as negative controls refering to intergenic regions of chromosomes 13, 14, 15 and 22 respectively.

MXD1 and UBF in these conditions to try to diminish the variability of the results obtained with MXD1 in growing HEK293T cells. MXD1 was bound to the rDNA of HeLa cells in relation to unspecific rabbit IgG, again in much less amounts than UBF (positive control) (figure 4.9).

Altogether, the results above indicated that MXD1 bound across the entire rDNA but preferentially to intergenic regions (IGS) [H18, H27, H32, H42]. Primers targeting intergenic regions of human chromosome 13, 14, 15, 22 (Ch13, Ch14, Ch15, Ch22b) were used as negative controls (figure 4.9).

4.1.4. MXD1 and UBF interaction

Since UBF and MXD1 co-localized in the fibrillar centers of nucleolus and both bound to rDNA regions, we thought that MXD1 and UBF could be interacting through the formation of a transcriptional regulation complex.

To analyse this, we performed a proximity ligation assay (PLA) in HeLa cells to see whether MXD1 and UBF were interacting. This technique allows us to elucidate whether endogenous proteins interact in vivo and the subcellular location where the interaction takes place.

First, to assess the fitness of the antibodies used for PLA, we performed conventional co-immunofluorescence with the pairs of antibodies to be used: MXD1-UBF and MXD1-ɣHemoglobin (ɣHB). Expression was detected in the expected subcellular localization and ɣHemoglobin was not detected since it is not expressed in HeLa cells (figure 4.10).

As shown in figure 4.11 PLA signal was positive when antibodies against MXD1 and UBF were used suggesting that MXD1 and UBF interact. Positive signal was achieved when antibodies against MYC and MAX were used (positive control) and no signal was detected when antibodies against MXD1 and ɣHemoglobin were used as negative control. Positive signals were quantified (red dots per nuclei) and the results indicated that MXD1 and UBF do interact significantly according to the negative control (MXD1-HB) but less than the positive control MYC-MAX (figure 4.12).

To further confirm the interaction of MXD1 and UBF we performed co-immunoprecipitations assays in HeLa cells 48 h deprived from serum. We first performed an immunoprecipitation with anti-UBF to test by western blot if MXD1 was co-immunoprecipitated. In figure 4.13A is observed that MXD1 co-immunoprecipitated with UBF. Then, we tried to immunoprecipitate MXD1 to see if UBF co-immunoprecipitated with MXD1 protein. As it can be seen in figure 4.13B UBF was detected in the western blot after the immunoprecipitation of MXD1 indicating that UBF co-immunoprecipitated with MXD1. Finally, we transfected the HeLa cells with a flag-tagged UBF expressing vector and 12 h after transfection, the cells were deprived from serum for 48 h, lysed and an immunoprecipitation of MXD1 was performed. UBF, tested by western blot using an antibody against the flag epitope, co-immunoprecipitated with MXD1 (figure 4.13C).

Altogether, these results suggest that MXD1 and UBF are interacting directly or indirectly at the site of rRNA synthesis in the nucleolus.

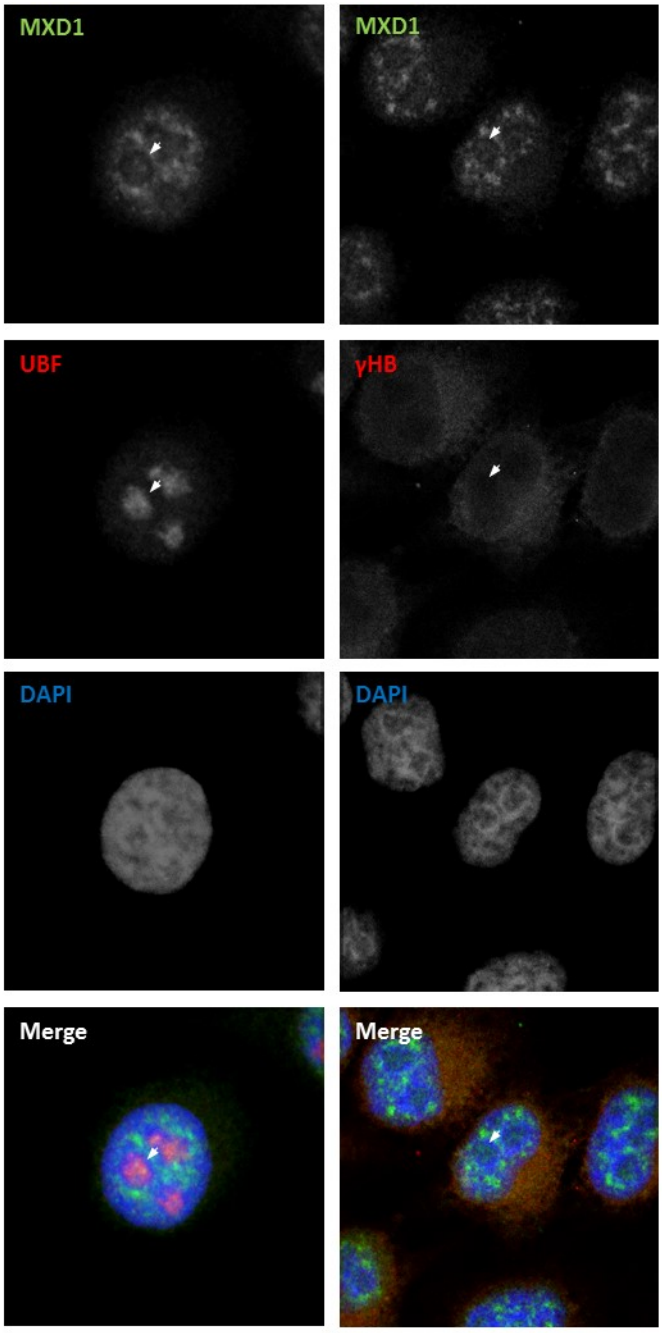

Figure 4.10.- MXD1, UBF and γHemoglobin expression in HeLa cells. Co-immunofluorescence of MXD1 with UBF and γ Hemoglobin (as a negative control) in HeLa cells with the antibodies used in the proximity ligation assay. MXD1 in green localized in the nucleoplasm and nucleolus; UBF in red localized in the nucleolus and γ Hemoglobin in red was not expressed in HeLa cells as expected. DAPI stain in blue was used to localize cell nuclei. White arrows indicate nucleoli.

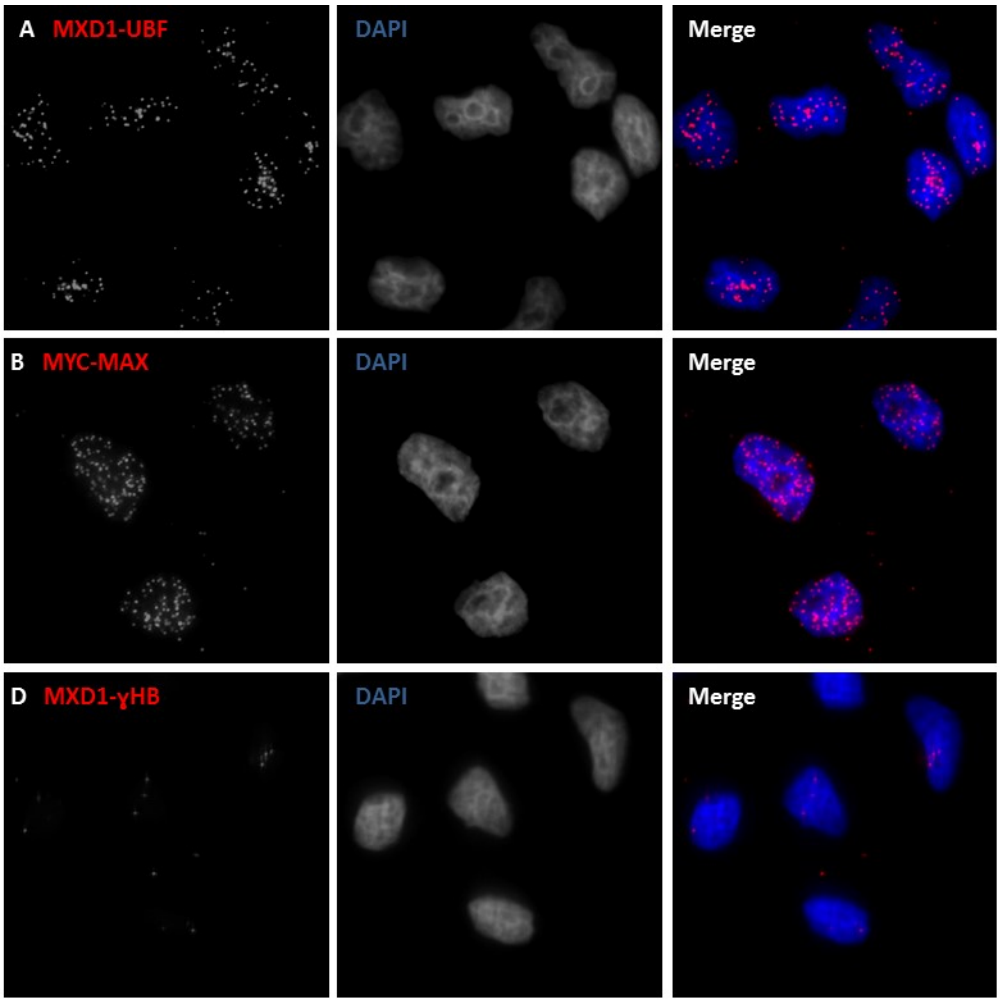

Figure 4.11.- MXD1-UBF interaction in HeLa cells. Proximity ligation assay in growing HeLa cells to test MXD1-UBF interaction. The antibodies used were anti-MXD1 and anti-UBF (A), anti-MYC and anti-MAX (as a positive control), (B) and anti-MXD1 and anti-ɣ Hemoglobin (ɣHB) (as a negative control) (C). Red dots indicating positive interaction showed MXD1-UBF interaction. DAPI staining of DNA (blue) was used to

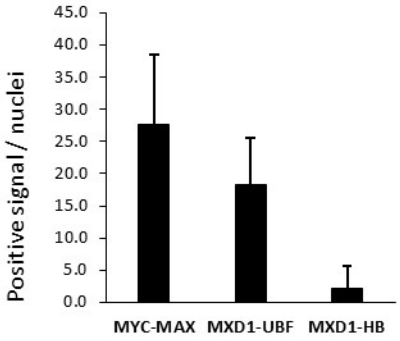

Figure 4.12.- Quantification of PLA signals. PLA positive signal per nuclei were quantified using ImageJ software for MYC-MAX, MXD1-UBF and MXD1-ɣHB conditions. At least 200 nuclei were counted for each experimental condition ($p < 0.05$ between MYC-MAX and MXD1-UBF, $p < 0.00001$ between MYC-MAX and MXD1-HB, $p<0.00001$ between MXD1-UBF and MXD1-HB)

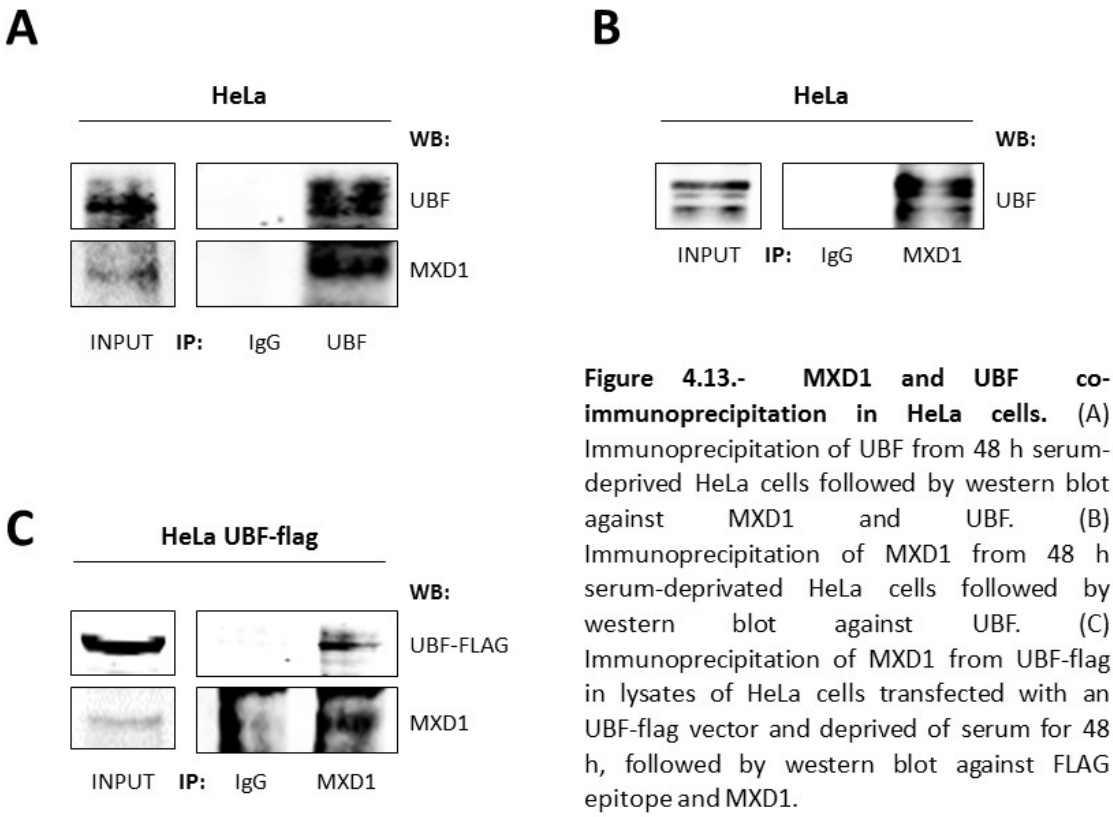

Figure 4.13.- MXD1 and UBF co-immunoprecipitation in HeLa cells. (A) Immunoprecipitation of UBF from 48 h serum-deprived HeLa cells followed by western blot against MXD1 and UBF. (B) Immunoprecipitation of MXD1 from 48 h serum-deprivated HeLa cells followed by western blot against UBF. (C) Immunoprecipitation of MXD1 from UBF-flag in lysates of HeLa cells transfected with an UBF-flag vector and deprived of serum for 48 h, followed by western blot against FLAG epitope and MXD1.

4.1.5. MXD1 knock-down upregulated total RNA production in the cell

All the above data suggests that MXD1 is regulating ribosomal DNA transcription. We decided to knock-down MXD1 expression in growing cells conditions, where we had seen MXD1 in the nucleoli, to study the effect of MXD1 silencing in ribosomal RNA production.

For this purpose we decided to use the K562 cells due to the high efficiency of transfection achieved in these cells. We transfected the K562 cells with siRNA against *MXD1* and 72 h post-transfection we counted the cells, extracted and quantified total RNA and checked MXD1 silencing by RT-qPCR and western blot (figure 4.14 A,B). Then, we estimated the amounts of total RNA per cell in MXD1 knock-down and in the control cells. Since ribosomal RNA accounts for more than 80 % of total RNA produced in the cell we assumed that if there is a change in total RNA production this is mainly due to ribosomal RNA. As shown in figure 4.14C MXD1 knock-down in K562 cells led to a slightly higher amount of total RNA in the cell compared with the control. This tendency was observed in the four experiments performed, although the difference with the control cells was not statistically significant. This result suggests that MXD1 might be acting as repressor of ribosomal RNA production.

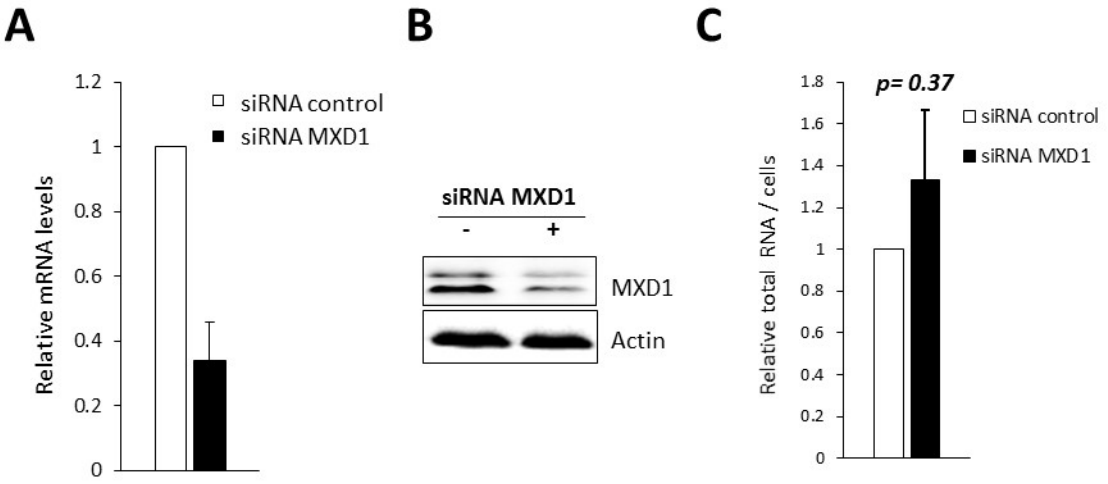

Figure 4.14.- Effect of MXD1 depletion on total RNA levels. K562 were transfected with siRNA against MXD1 to silence MXD1 expression. After 72 h of transfection MXD1 silencing was checked by quantitative PCR (A) and western blot (B). (C) Total RNA per cells from MXD1 silenced cells after 72 h of siRNA transfection was compared with that of control cells (C).

4.2. MNT AND MXD1 IN UR61 CELLS WITHOUT MAX

4.2.1. MNT and MXD1 did not affect the differentiation of UR61 cells

Previous work in our lab described that MYC overexpression in UR61 cells impairs the differentiation state triggered upon dexamethasone addition in this system without MAX (Vaque et al., 2008). MXD1 and MNT are the best characterized MXDs members; MXD1 is known to have opposite biological functions to the MYC family of proteins according to the levels and states in which they are expressed in the cell. MXD1, contrarily to MYC, is known to be upregulated when cells are in a quiescent or differentiation state, and downregulated in proliferating cells (Eisenman et al., 2000). On the other hand, MNT is thought to act as buffer on MYC activity since it has constitutive expression levels independently of cell state, it binds to E-boxes to repress gene expression and its downregulation leads to MYC-like phenotypes (Hurlin et al., 1997a).

Knowing these facts, we wondered whether MXD1 and MNT overexpression in UR61 cells in the absence of MAX would lead to an increase in the differentiation state (i.e., the opposite effect than that of MYC overexpression). We monitored the acquisition of the neuronal-like phenotype that is characterized by neurites outgrowth and upregulation of neuronal genes such as *VGF*, *GAP43*, *NGFR* or *CHGA* (Greene and Tischler, 1976; Tischler and Greene, 1978). We transfected MNT, MXD1 expressing vectors or the empty vector (Vo) together with a GFP expressing vector in a 4:1 proportion (MNT:GFP) to UR61 cells and the following day the cells were treated with 100 nM dexamethasone to induce the N-RAS oncogene expression and so trigger their differentiation. At 24 h post-treatment the induction of the differentiation phenotype in MNT and MXD1 expressing cells calculated by the percentage of GFP-positive cells with neurite outgrowth was at the same extent than in controls (Vo) (figure 4.15A).

We also investigated possible effects at the expression level of genes related to neuronal differentiation. For this purpose, we transfected the UR61 cells with MNT or MXD1 expressing vectors and the empty vectors (Vo) and at 24 h post-transfection we checked MNT and MXD1 overexpression by RT-qPCR (figure 4.15B) and looked at several neuronal markers (*CHGA*, *GAP43*, *NGFR*, *VGF*) and the *JUN (c-JUN)* transcription factor (activated through the N-RAS-MAPK pathway) by RT-qPCR. The presence of overexpressed MNT protein did not upregulate all genes analysed being only slightly upregulated *GAP43* and *JUN* and almost invariant *VGF* and *NGFR* genes (figure 4.15C). On the other hand MXD1 overexpression did not affect the expression of the *CHGA*, *GAP43* and *JUN*, and only caused a down-regulation of the *VGF* (figure 4.15D). Altogether, we can conclude that MNT and MXD1 overexpression in this system without MAX does not enhance the differentiation state.

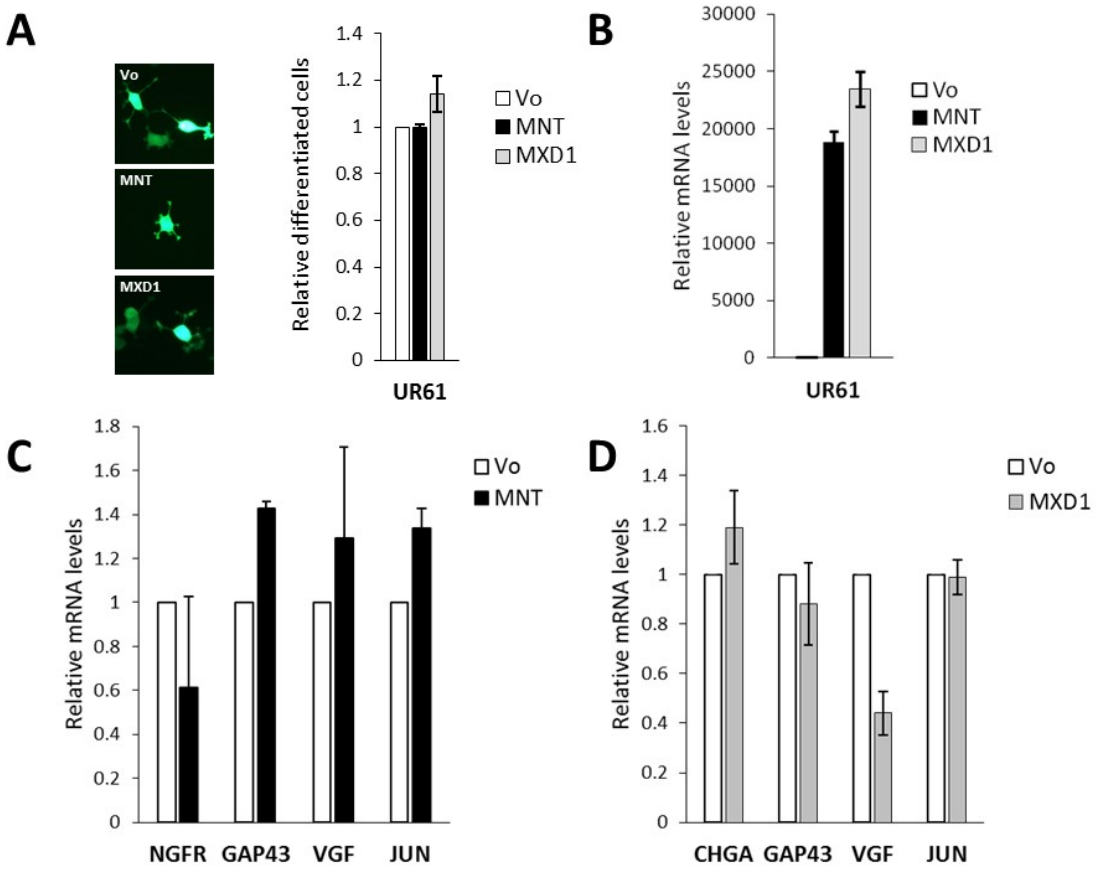

Figure 4.15. MNT and MXD1 in UR61 differentiation. (A) Pictures and percentage of neurite outgrowth of UR61 cells co-transfected with MNT, MXD1 or the empty vector (Vo) and a GFP expressing vector treated 24 h with 100 nM dexamethasone. (B) MNT and MXD1 overexpression in UR61 transfected cells measured by RT-qPCR. (C) Neuronal markers expression in UR61 cells overexpressing MNT, measured by RT-qPCR. (D) Neuronal markers expression in UR61 cells overexpressing MXD1 measured by RT-qPCR. The data are mean values of at least 3 independent experiments. The error bars are S.D.

4.2.2. MNT and MXD1 did not regulate E-box containing promoters in the absence of MAX

In an attempt to elucidate if these transcription factors can act in a MAX-independent manner we studied if they were able to regulate E-box containing promoters in the UR61 cells. To do so, luciferase assays were performed using an E-box-luciferase reporter construct containing 4 E-box sequences.

This construct was transfected together with MNT, MXD1, MAX and the empty expressing vectors alone or alternatively together with MAX overexpressing vectors as a control of the experiment. The luciferase activity was measured at 36 h post-transfection. As it can be seen in figure 4.16, MNT alone did not reduce the luciferase activity, MXD1 alone reduced the luciferase activity only slightly and MAX reduced significatively the luciferase activity consistently with its homodimerizing, E-box binding

capacity and its inert transcriptional activity. On the contrary, when MNT or MXD1 were co-transfected with MAX, they reduced significatively the luciferase activity in the absence of MAX (figure 4.16).

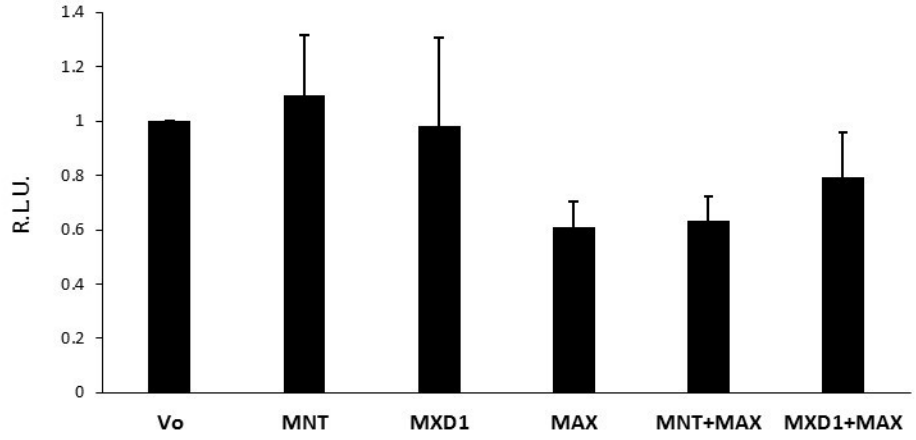

Figure 4.16. E-box luciferase assay in UR61 cells. Luciferase activity of UR61 cells co-transfected with an E-box containing luciferase reporter vector together with MNT, MXD1, MAX and the empty (Vo) expressing vectors alone or a mixture of MNT+MAX and MXD1+MAX vectors. All the experiments were done at least 3 times. R.L.U.: Relative luciferase units. The data are means values of at least 3 independent experiments. The error bars are S.D. ($p<0.05$ between MAX and Vo, between MNT+MAX and Vo and between MXD1+MAX and Vo; $p<0.05$ between MNT+MAX and MNT and $p<0.1$ between MXD1+MAX and MXD1)

Altogether, these results show that MNT and MXD1 do not regulate E-box containing promoters in the absence of MAX.

4.2.3. MNT and MXD1 expression in MAX-deficient cells

MNT, as described in the Introduction section, is a constitutively expressed protein whose levels do not change significatively among the different cell states. MXD1 on the other hand is poorly expressed in proliferating cells. We asked for the expression level of MNT and MXD1 proteins in the UR61 cells, which lack their heterodimerizing partner MAX. We studied MNT and MAX expression in different cell lines: the parental UR61 cells; the UR61MYC that constitutively express the MYC protein; the UR61-MT-MAX expressing the MAX protein upon 24 h of 100 µM Zn^{+2} addition and the control UR61-MT-Hebo that have the empty construct; the UR61 transfected with a MNT expressing vector and the UR61 and the UR61MYC treated 24 h with 100 nM dexamethasone.

As shown in figure 4.17A, MNT expression levels in the UR61 and UR61-derived cells were much higher than in the other three cell lines tested (figure 4.17). It is of note that MNT was expressed in all these proliferating cells and that MNT-transfected UR61 did not show a significant increase of MNT protein levels. Also, it is worth to consider that UR61-MT-MAX expressing MAX protein, had similar or even lower levels of MAX expression in comparison with other cell lines (figure 4.17), so that the expression levels obtained after Zn^{+2}-mediated induction of MAX in UR61-MT-MAX cells can be considered within the range of normal conditions. Regarding the rest of cell lines (HeLa, K562 and HEK293T), there was a

variation in MNT expression among the different cell lines (figure 4.17). These data show that MNT is highly expressed in the UR61 cells in spite of the absence of MAX expression.

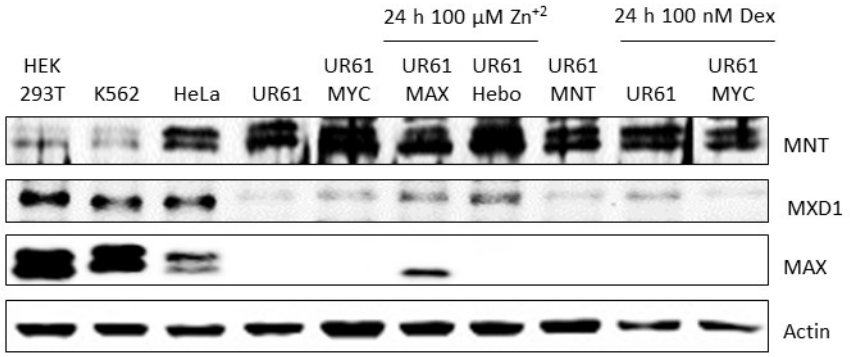

Figure 4.17. MNT, MXD1 and MAX expression in different cell lines. Western blot of MNT, MXD1 and MAX proteins in the human HEK293T, K562 and HeLa cells and the rat UR61 cells and its derived cell lines: UR61MYC (constitutively expressing MYC); UR61-MT-Hebo; UR61-MT-MAX (expressing MAX upon Zn^{+2} treatment); UR61 transiently transfected with MNT expression vector; UR61 and UR61MYC treated 24 h with 100 nM dexamethasone.

On the other hand, MXD1 expression levels in UR61 and UR61-derived cells were in general lower than those of MXD1 in the other cell lines studied (figure 4.17A). In addition, MXD1 was expressed in all growing cells (figure 4.17A). It is worth to mention that MXD1 protein levels in the UR61 cells treated with dexamethasone (i.e., differentiation) were similar to that of UR61 growing cells. These data show that MXD1 expression in UR61 cells does not increase upon the induction of N-RAS (neuronal-like differentiation inducer).

4.2.4. MXD1 did not affect cell proliferation in MAX absence

Since MXD1 does not seem to trigger differentiation of UR61 cells and its endogenous levels are low we wondered if MXD1 overexpression would affect UR61 proliferation. To do so, the UR61 cells were transfected with a MXD1 expressing vector or the empty vector together with a puromycin resistance expressing vector in five less amounts. Then, cells were selected to ensure that all cells overexpressed MXD1. Three days post-selection MXD1 overexpression was confirmed by western blot (figure 4.18A) and 6 days post-selection cells were stained with crystal violet dye. Afterwards, the dye was extracted as described in Materials and Methods section for quantification.

As shown in figure 4.18B, MXD1 overexpression did not affect UR61 cell growth. These results show that MXD1, in the absence of MAX, is not able to arrest cell proliferation.

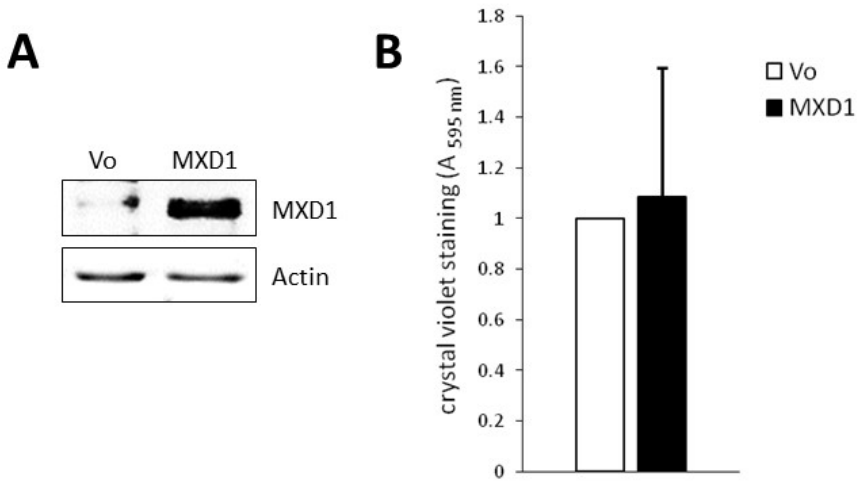

Figure 4.18. MXD1 and cell proliferation in UR61. UR61 co-transfected with a MXD1 expressing vector or the empty vector (Vo) and a puromycin resistance gene vector. Cells were selected with puromycin at 0.3 µg/ml final concentration and: (A) after 3 days of selection, MXD1 expression was confirmed by western blot; (B) after 6 days of selection, puromycin resistant cells were stained with crystal violet dye. The dye captured by stained cells was solidified and quantified according to Materials and Methods section. The data are means values of at least 3 independent experiments. The error bars are S.D.

4.3. MNT AUTO-REGULATION

4.3.1. MNT expression was altered in MAX absence

When analysing MNT expression levels in different cell lines, it was observed that MNT expression in UR61 without MAX was relatively high and that transfecting the cells with the MNT vector increased only slightly the expression of this protein (figure 4.17). Since MNT heterodimerises with MAX, we wondered whether MAX absence could affect MNT expression. We used UR61-MT-MAX and UR61-MT-Hebo cells treated for 24 h with 100 µM Zn^{+2} to induce MAX expression and we analysed MNT expression by western blot and RT-qPCR. As shown in figure 4.19A-B, MNT expression was downregulated at mRNA and protein level when MAX expression was induced. To eliminate the possibility that it was due to the particular UR61-MT-MAX clone (generated after selection with antibiotic) we transiently transfected UR61 cells with a MAX expression and empty vectors (Vo) and analysed MNT expression by western blot. As shown in figure 4.19C, the expression of MAX in UR61 cells also led to a downregulation of MNT at protein level, thus reproducing the observation in the UR61-MT-MAX cell line.

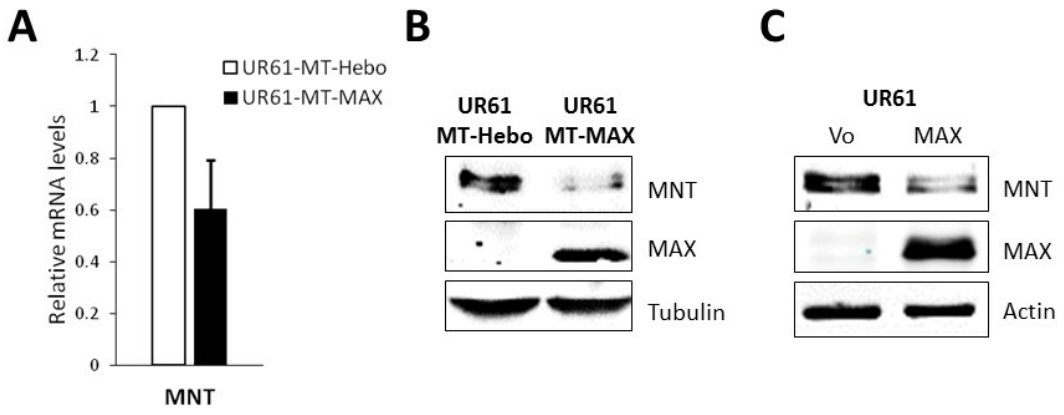

Figure 4.19. MNT expression in UR61. UR61-MT-Hebo and UR61-MT-MAX were treated 24 h with 100 µM Zn^{+2} and the MNT expression was determined by RT-qPCR (A) and western blot (B). (C) Western blot of MNT in 24 h transfected UR61 cells with a MAX expressing vector. The data are means values of at least 3 independent experiments. The error bars are S.D.

To confirm this in a different system, we transfected the human leukaemia K562 cells (that express the MAX protein) with a MAX expression vector and at 48 h post-transfection we analysed MNT expression. The western blot results showed that MAX was overexpressed and MNT downregulated at protein level (figure 4.20A). Also, we used the K562 derivative cell line Kmax12 which carries a MAX transgene regulated by the metallothionein promoter, which is activated by Zn^{+2}. We treated Kmax12 cells with 100 µM Zn^{+2} and harvested the cells at 48 h post-treatment. We showed by western blot that MAX was overexpressed and observed that MNT was downregulated at protein level (figure 4.20B). Next, we tried to confirm this finding through the opposite approach, i.e. we transfected the K562 with siRNA to

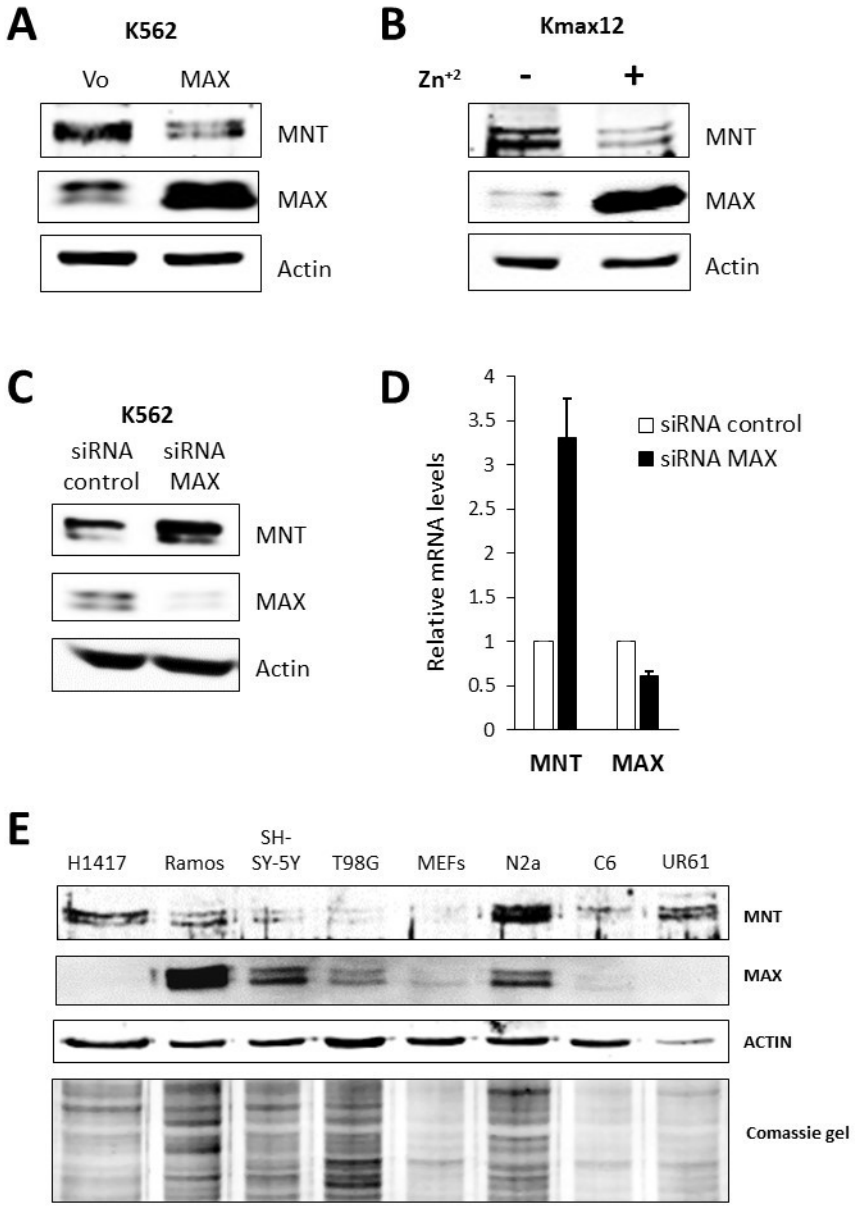

Figure 4.20. MNT expression in K562 and other cell lines. (A) MNT and MAX expression determined by western blot in K562 cells 24 h after transfection with a MAX expressing vector. (B) MNT and MAX expression measured by western blot in Kmax12 cells treated 48 h with 100 µM Zn^{+2} to induce MAX expression.(C,D) MNT and MAX expression measured by (C) western blot or (D) RT-qPCR in K562 48 h after transfection with siRNA against MAX gene. The data are mean values of two RT-qPCR determinations and the error bars are S.D. (E) MNT and MAX expression in the human cell lines H1417 (small cell lung cancer), Ramos (B-cell lymphoma), SH-SY-5Y (neuroblastoma) and T98G (glioblastoma); the mouse cell lines MEF (embryonic fibroblast) and N2a (neuroblastoma) and the rat cell lines C6 (glioma) and UR61 (pheochromocytoma).

knock-down MAX expression. After 48 h post-transfection K562 were harvested and MAX and MNT expression was analysed by western blot and RT-qPCR. As shown in figure 4.20C-D, MNT expression was upregulated when MAX protein was silenced with the siRNA.

Altogether these data showed that there is an inverse correlation between MAX and MNT expression at mRNA and protein level.

We also analysed the expression of MNT protein in different cell lines that express MAX [the human Ramos (B-cell lymphoma), SH-SY-5Y (neuroblastoma) and T98G (glioblastoma) cells; the mouse MEF (embryonic fibroblast) and N2a (neuroblastoma) cells and the rat C6 (glioma) cells] and in the small cell lung cancer H1417 cell line that was recently described to carry a mutated MAX gene and do not express the MAX protein (Romero et al., 2014) and in the UR61 cells. As shown in figure 4.20E, MNT expression was different depending on the cell type. It is of note that MNT was highly expressed in the two cell lines deficient in MAX (H1417 and UR61) in comparison with the rest of cell lines.

4.3.2. E-box sequences in MNT Promoter

Since MNT expression was altered by the presence of MAX and MAX is a co-factor that reportedly heterodimerises with MNT to bind E-boxes in the promoters of genes, we asked whether MNT expression was regulated by MAX. We first searched for the presence of E-box sequences at *MNT* promoter. We obtained 1000 bp region upstream the transcription start site (TTS) of human, mouse and rat *MNT* promoters from the UCSC genome browser database (http://genome.ucsc.edu/) and analysed the presence of canonical and non-canonical E-box sequences. As shown in figure 4.21, the *MNT* promoters of human, mouse and rat presented two E-boxes (one canonical “CACGTG” and one non-canonical “CATGTG”). These E-boxes presented a similar pattern in the different species being the canonical one the closest to the TSS. Human E-boxes are at -788 and -289 bp from the TSS; mouse E-boxes are at -595 and -123 bp from the TSS and rat E-boxes are at -593 and -123. In addition, we also did an alignment of the promoter sequences of human, mouse and rat species and found that they were highly conserved across species. All this suggested to us that *MNT* might be regulated by MAX dimers.

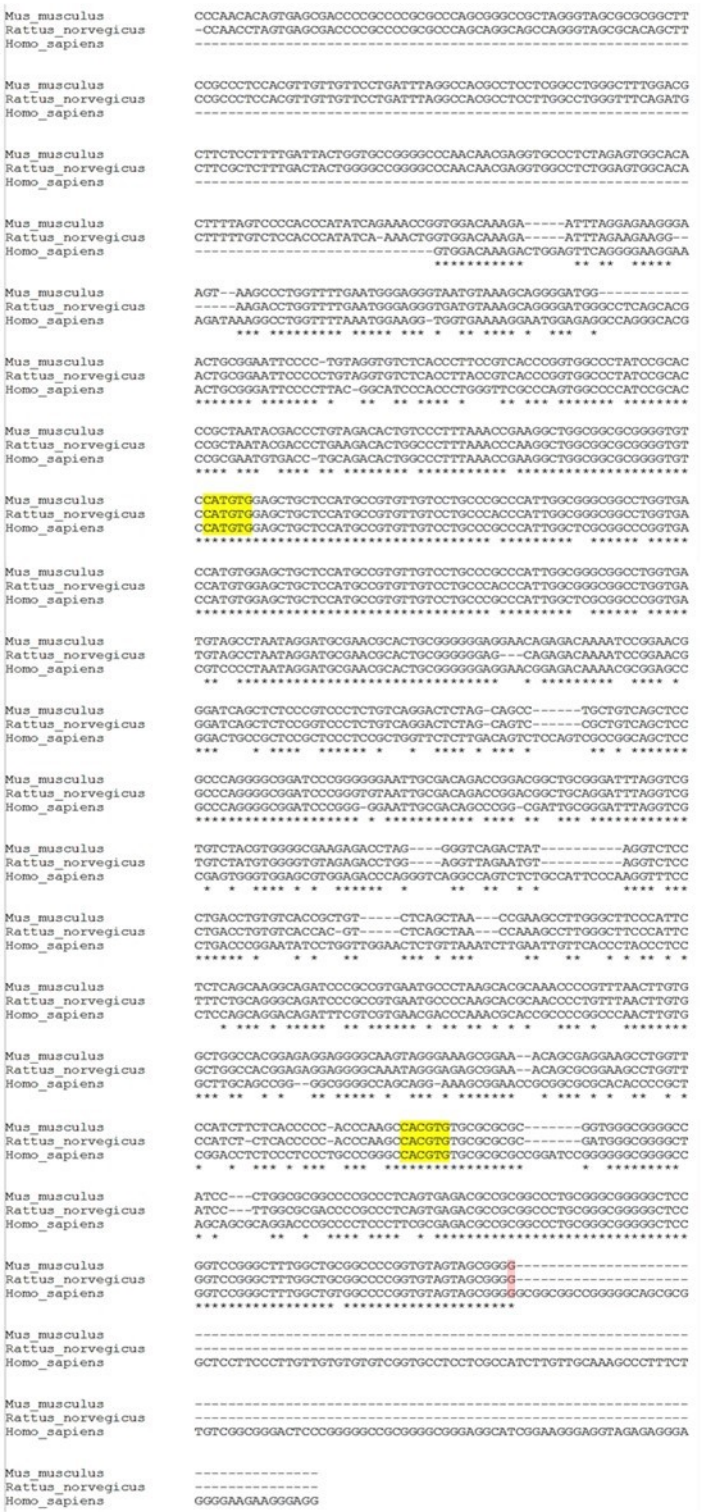

Figure 4.21. MNT gene promoter sequence. An alignment of a 1000 bp upstream the TSS of MNT gene from human, mouse and rat species. The E-box sequences are highlighted in yellow and the exact position upstream the TSS is indicated for each specie. The +1 nucleotide of *MNT* is highlighted in red for each specie.

4.3.3. Peaks of MAX/MYC in MNT promoter at ENCODE project

Once we confirmed the presence of E-box sequences in these *MNT* promoters, we analysed the ChIP-seq ENCODE data (UCSC genome browser http://genome.ucsc.edu/ENCODE/) for MAX, MYC and MXI1 in all the cell lines available in ENCODE (H1ES, K562, HeLa, NB4, A549, GM78, HEPG, SKSM and IMR90 cells). We observed that the three proteins presented peaks in similar positions near the transcription start site and in the first exon of human MNT gene. In addition, we observed that these peaks in the promoter of MNT gene contained the E-boxes identified in figure 4.21. This suggests that members of the MYC and MXD family bind and possibly regulate the promoter of *MNT* (figure 4.22).

4.3.4. MNT bound to its own promoter when MAX is present

With all the above data (MNT downregulation by enforced MAX expression, luciferase assays and the MYC-MAX-MXI1 peaks detected by ChIP-seq) it was conceivable that *MNT* was regulated by MAX-containing dimers. Since the UR61 cells highly expressed MNT and we saw that MNT was downregulated when MAX was re-expressed, we hypothesized that MNT-MAX heterodimers might bind to *MNT* promoter and down-regulate its own expression. To assess if MNT was bound to its own promoter, we did a ChIP assay with MNT and MAX antibodies in UR61-MT-Hebo and UR61-MT-MAX treated 24 h with 100 µM Zn^{+2} to induce *MAX*. We studied by qPCR the immunoprecipitated DNA for regions of the *MNT* promoter as well as the *ATROGIN-1* and *NDRG1* promoters as positive and negative controls respectively for MNT and MAX (Terragni et al., 2011). As shown in figure 4.23, MNT and MAX were bound to *MNT* promoter in UR61-MT-MAX. However, in UR61-MT-Hebo cells neither MNT nor MAX (as expected) were bound to *MNT* promoter. In the same way, MNT and MAX were bound to the positive control *ATROGIN-1* promoter in UR61-MT-MAX but not in UR61-MT-Hebo cells. No signal was found in the promoter of *NDRG1* in UR61-MT-MAX and UR61-MT-Hebo, used as negative control (figure 4.23). These data show that MNT binds to its own promoter as a heterodimer with MAX and suggest a possible negative regulation of its own expression. This also suggests that MNT has a different set of target genes when MAX is not present in the cells.

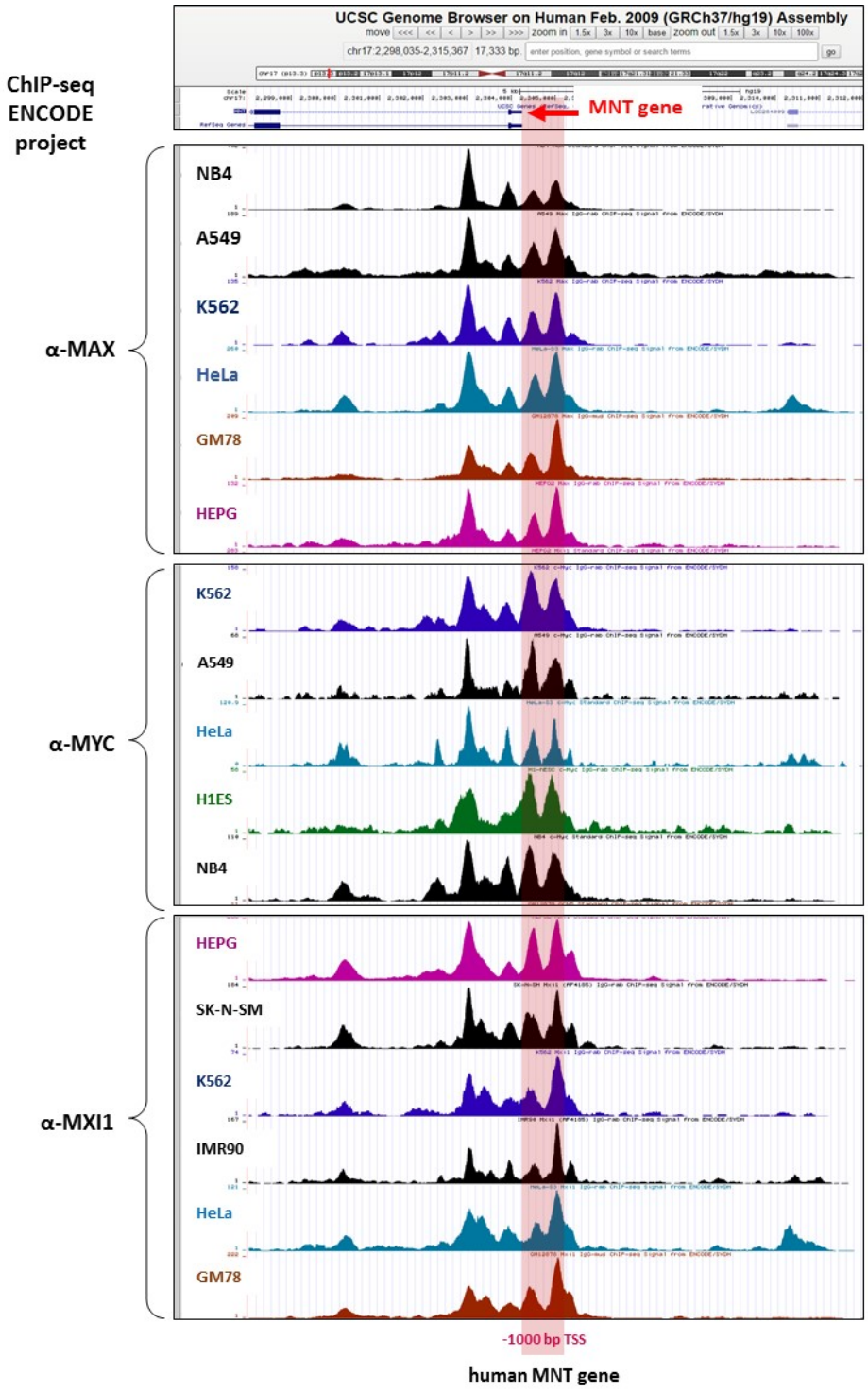

Figure 4.22. MYC, MAX and MXI1 peaks from the ChIP-seq ENCODE project. ChIP-seq peaks found in the human MNT gene corresponding to: MAX protein in NB4, A549, K562, HeLa, GM78 and HEPG cells; MYC protein in K562, A549, HeLa, H1ES and NB4 cells and MXI1 protein in HEPG, SK-N-SM, K562, IMR90, HeLa and GM78 cells. The MNT gene and its 5'→3' orientation is indicated with a red arrow and the 1000 bp upstream the TSS regions highlighted in red. The data are from the Stanford/Yale/USC/Harvard (SYDH) ENCODE project (http://genome.ucsc.edu/ENCODE/).

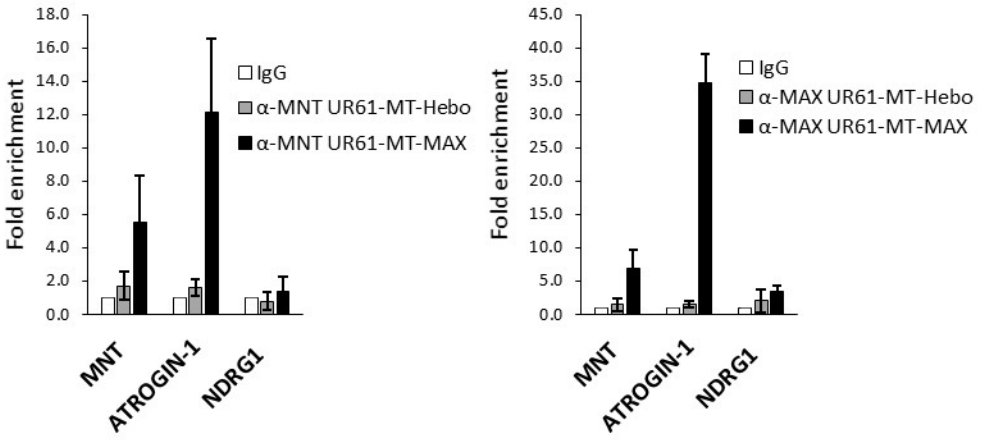

Figure 4.23. MNT and MAX ChIP on MNT promoter in UR61-MT-Hebo and UR61-MT-MAX. ChIP with anti-MNT (left) and MAX (rigth) antibodies in UR61-MT-Hebo and UR61-MT-MAX treated with 100 µM Zn^{+2} for 24 h. MNT and MAX binding to MNT gene promoter was studied by qPCR. MNT and MAX bind to MNT promoter only when MAX is expressed. ATROGIN-1 and NDRG1 genes were used as postive (in UR61-MT-MAX) and negative controls respectively, as reported in the literature. The data are means values of at 4 independent experiments. The error bars are S.D.

4.3.5. MNT repress its own promoter

The previous data showing that MNT binds to its own promoter opened the possibility of an autosuppression of its expression. To explore this possibility we cloned 800 bp upstream the transcription start site from the human MNT gene in a luciferase reporter vector and we called it "-800MNT-luc". Using this construct (figure 4.24A) we studied the activity of the human *MNT* promoter. We first transfected UR61-MT-MAX and UR61-MT-Hebo cells with the -800MNT-luc vector and 16 h later we induced the MAX expression by the addition of 100 µM Zn^{+2}. After 24 h of induction we did the luciferase assay and as it can be seen in figure 4.24B, the induction of MAX led to slightly less luciferase activity. We then transfected the UR61 cells with the -800MNT-luc vector together with MNT and MAX expression or the empty vectors and we found again that the expression of MNT and MAX led to a decrease in the luciferase activity (figure 4.24C). Since MAX protein is more stable than MNT, it is possible that the co-transfection of both expression vectors results in a predominance of MAX-MAX over MNT-MAX dimers. To test *MNT* promoter activity in response to higher levels of MNT-MAX dimers, we transfected HEK293T cells (which express MAX) with the -800MNT-luc and MNT (but not MAX) expression or the empty vectors. In this system we ensure that in the transfected cells, MNT is overexpressed and ready to form heterodimers with MAX. MNT overexpression in HEK293T cells led to a reduction in the luciferase activity in comparison with the empty vector (Vo) (figure 4.24D). Together, these data indicate that MNT-MAX negatively regulates the *MNT* promoter.

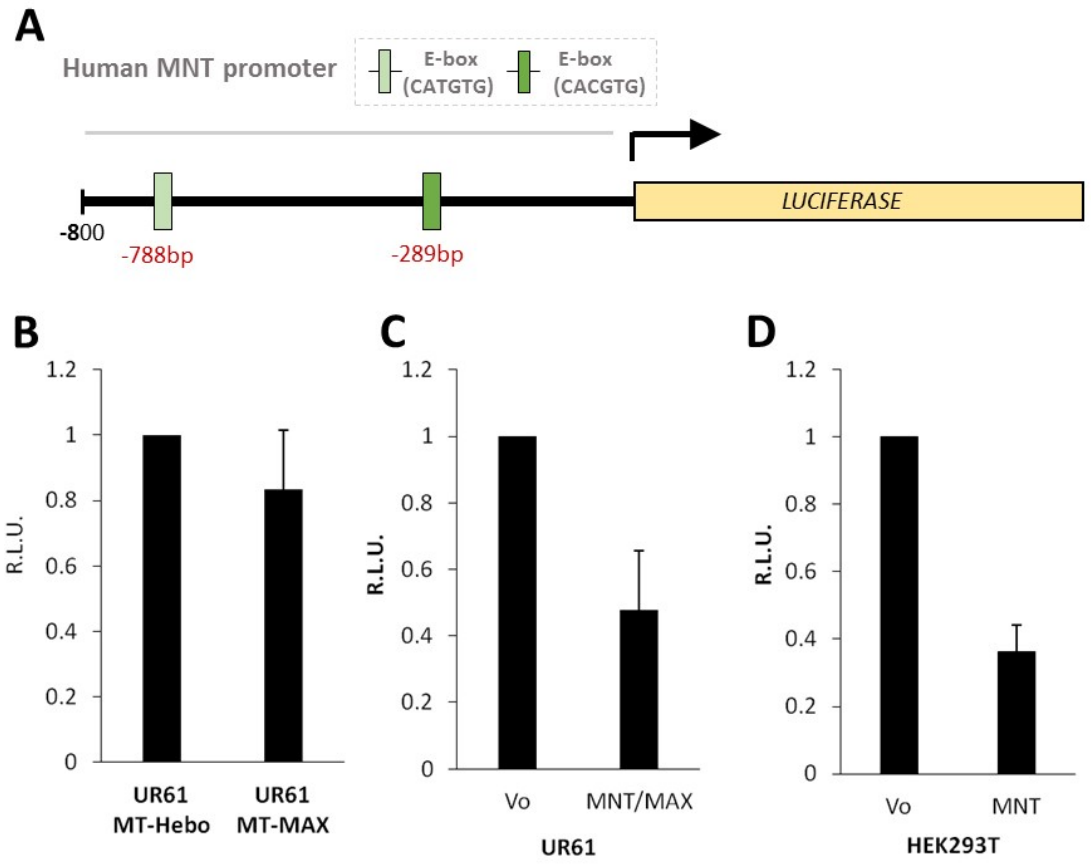

Figure 4.24. MNT regulates its own promoter. (A) Generation of the -800MNT-luc vector, containing 800 bp upstream the TSS of human MNT gene and including two coserved E-boxes. (B) Luciferase assay of UR61-MT-Hebo and UR61-MT-MAX transfected with the -800MNT-luc vector and treated for 24 h with 100 µM Zn^{+2}. (C) Luciferase assay of UR61 cells transfected with the -800MNT-luc and MNT and MAX expressing vectors. (D) Luciferase assay of HEK293T cells transfected with the -800MNT-luc and MNT expressing vectors. Luciferase activity was assayed 24 h after trasnfection. The data are means values of at least 3 independent experiments. The error bars are S.D.

4.4. MNT LOCALIZATION IN MAX-DEFICIENT CELLS

Since our results showed that the MNT protein behaves differently in MAX presence we wanted to know whether the localization of MNT changed in UR61 depending on the presence of MAX. We first treated UR61-MT-Hebo and UR61-MT-MAX cells with 100 µM Zn^{+2} to induce *MAX* expression in UR61-MT-MAX and after 24 h of treatment an immunofluorescence assay was performed. Figure 4.25A shows that MNT in UR61-MT-Hebo localised in the nucleus but also in the cytoplasm. On the contrary, in UR61-MT-MAX cells expressing MAX, MNT was mainly localised in the nucleus. UBF is a nucleolar protein used as a control. To further confirm these results, again UR61-MT-Hebo and UR61-MT-MAX cells were treated with 100 µM Zn^{+2} and 24 h post-treatment a cytoplasm/nucleus fractionation was done to analyse MNT localization by western blot. We observed that in UR61-MT-Hebo cells that do not express MAX, MNT protein was localised in the nucleus as expected but also in the cytoplasm and that it was at similar levels in the different fractions (cytoplasm and nucleus) (figure 4.25B). However, in UR61-MT-MAX expressing MAX, MNT was localised mainly in the nucleus but not in the cytoplasm and MAX was localised only in the nucleus, as expected (figure 4.25B). In addition, comparing MNT levels in the nuclear fractions of UR61-MT-Hebo and UR61-MT-MAX cells, these were very similar (figure 4.25B). To confirm these data we analysed MNT localization in cells that do normally express the MAX protein. We used HEK293T to carry out a cytoplasm/nucleus fractionation and analysed protein localization by western blot. As it can be seen in figure 4.25C, MNT and MAX were localised in the nucleus but not in the cytoplasm of the HEK293T cells. Sin3B and RhoGDI were used as nuclear and cytoplasm markers respectively. To further confirm that this MNT localization depended on MAX presence in the cell, we silenced MAX protein in the K562 cells with siRNA and after 48 h of transfection we did cytoplasm/nucleus fractionation followed by western blot. In MAX-silenced K562 cells, MNT localised in the nucleus but also in the cytoplasm. In contrast, in K562 normally expressing MAX, MNT and MAX were mainly localised in the nucleus (figure 4.25D). Again, nuclear fractions of K562 and MAX-silenced K562 presented similar levels of MNT protein. CTCF and Tubulin were used as nuclear and cytoplasmic markers respectively. These data suggest that MAX absence leads to an upregulation of MNT and that this overexpressed-MNT localises in the cytoplasm.

4.4.1. Searching for new MNT partners

MNT was found to be highly expressed in the UR61 cells and its expression and localization was different depending on the presence of MAX. We wanted to confirm whether MNT was able to interact with MAX in these cells. The UR61-MT-Hebo and UR61-MT-MAX cells were treated with 100 µM Zn^{+2} for 24 h and after treatment the interaction of MNT and MAX was assayed by co-immunoprecipitation. As shown in figure 4.27A, MNT co-immunoprecipitated with MAX only in UR61-MT-MAX when the expression of *MAX* was induced by Zn^{+2}.

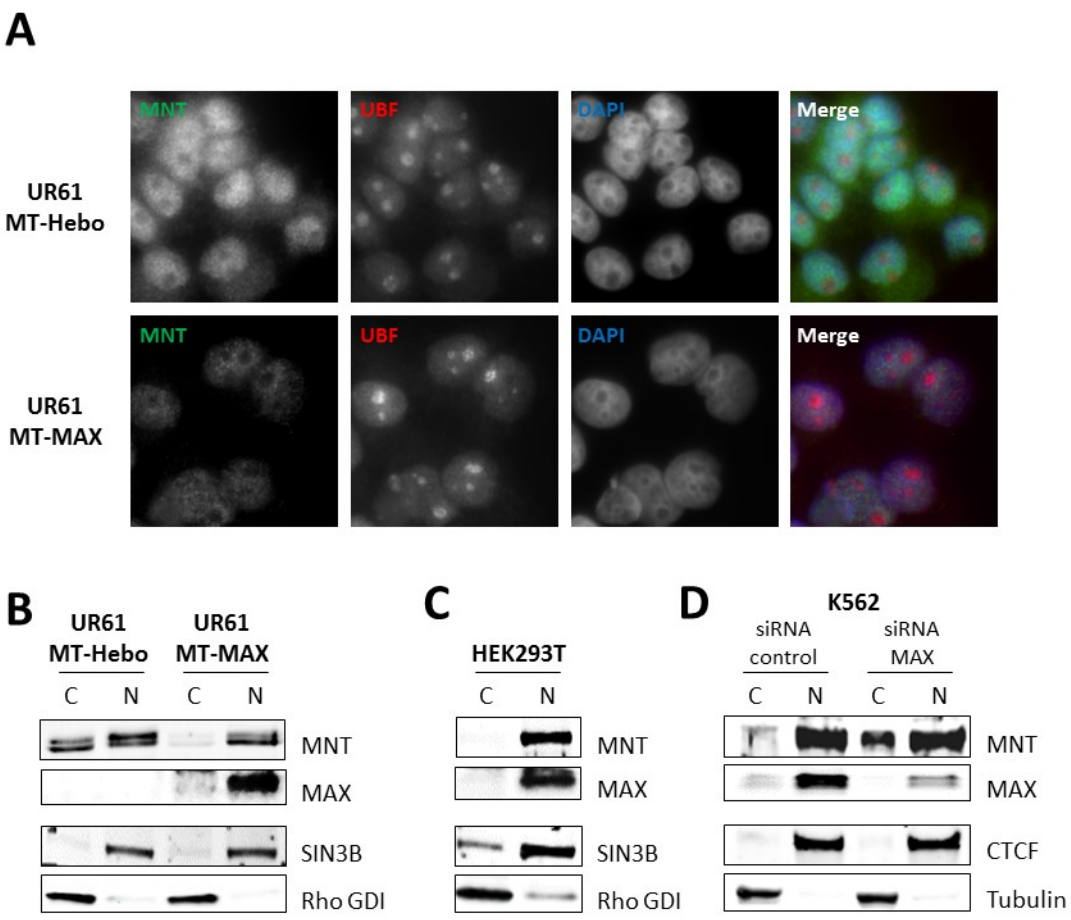

Figure 4.25. MNT localization in MAX absence. (A) Immunofluorescence for MNT in UR61-MT-Hebo and UR61-MT-MAX cells treated 24 h with 100 µM Zn^{+2} to induce MAX. MNT is shown in green, the nucleolar protein UBF used as control in red and the DNA was stained with DAPI (in blue). (B, C, D) Cell extracts were subjected to cytoplasmic/nuclear fractionation and the levels of MNT and MAX were determined in each fraction by western blot: (B) MNT distribution in UR61-MT-Hebo and UR61-MT-MAX treated 24 h with 100 µM Zn^{+2}. SIN3B and RhoGDI were used as nuclear and cytoplasmic markers respectively; (C) MNT distribution in HEK293T cells. SIN3B and RhoGDI were used as nuclear and cytoplasmic markers respectively and (D) 48 h transfected K562 with siRNA against the MAX gene. CTCF and Tubulin were used as nuclear and cytoplasmic markers respectively. C refers to cytoplasmic fraction and N to nuclear fraction.

Then, we wondered whether MNT was interacting with proteins other than MAX, taking advantage of the MAX-deficient UR61 cells. To do so, we transfected UR61-MT-Hebo and UR61-MT-MAX with a MNT expression vector to ensure higher amounts of MNT protein and 12 h later the cells were treated with 100 µM Zn^{+2} to induce *MAX* expression in UR61-MT-MAX. After 24 h of incubation the cells were lysed and the expression of MNT and MAX determined by western blot (figure 4.26B). In parallel, we immunoprecipitated MNT in UR61-MT-Hebo and UR61-MT-MAX cells by triplicate for each cell line. After MNT immunoprecipitation, in collaboration with Alex von Kriegsheim's group (Systems Biology Ireland, Conway Institute, Dublin) we analysed the immunoprecipitated proteins by mass spectrometry

as described in Materials and Methods section. Immunoprecipitated peptides with a p-value ≤ 0.05 and a fold change in peptide abundance in relation to the IgG control condition ≥ 2, were considered as positive. It was found that there were 11 proteins immunoprecipitated in MNT-UR61-MT-Hebo and 47 in MNT-UR61-MT-MAX. Five of the proteins found in MNT immunoprecipitations (REL, CCDC6, AMPD2, QSER1, TPP2) were present in both UR61-MT-Hebo and UR61-MT-MAX, meaning that they co-immunoprecipitated with MNT independently of MAX (figure 4.26C). Of these five proteins we focused on REL and CCDC6. REL is a well-known protein of the NF-κB family meanwhile CCDC6 takes part in the RET-PTC1 fusion oncoprotein as a consequence of a chromosomal rearrangement frequently found in papillary thyroid carcinoma. As a control of the technique, MAX was found in MNT immunoprecipitates from UR61-MT-MAX but not from UR61-MT-Hebo cells (table 4.1).

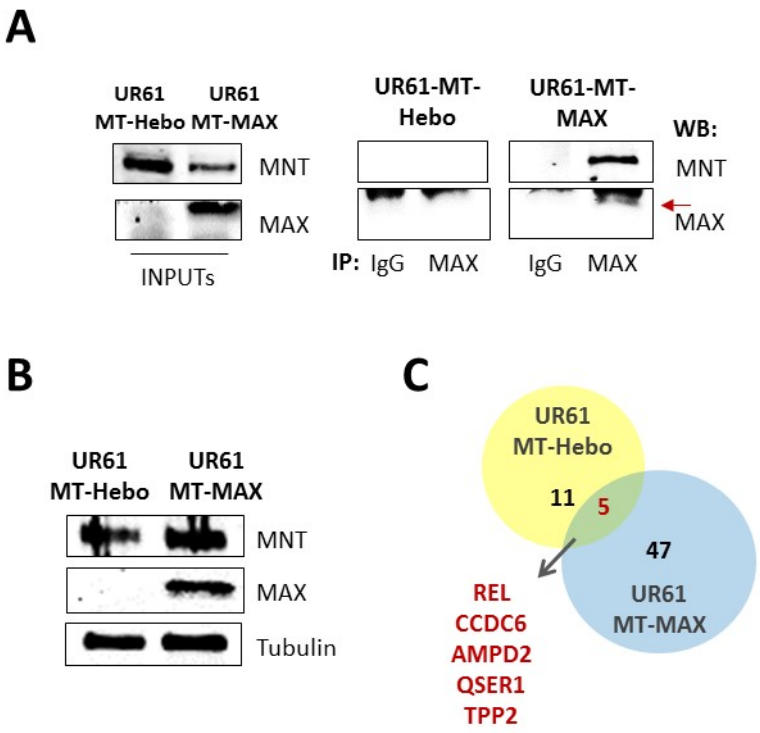

Figure 4.26. MNT interacting proteins. (A) Immunoprecipitation of MNT and MAX proteins in UR61-MT-Hebo and UR61-MT-MAX treated 24 h with 100 µM Zn^{+2}. MNT is co-immunoprecipitated with MAX in UR61-MT-MAX but not in UR61-MT-Hebo cells. The red arrow points the MAX protein and the * unspecific signal corresponding to the IgG light chains from the antibodies used. (B) Confirmation by western blot of MNT and MAX overexpression of the samples used in the proteomics assay: UR61-MT-Hebo and UR61-MT-MAX transfected with MNT expressing vector and treated for 24 h with 100 µM Zn^{+2}. (C) Schematic representation of the positive interactions found in the proteomics assay. REL, CCDC6, AMPD2, QSER1 and TPP2 were found in both UR61-MT-Hebo and UR61-MT-MAX immunoprecipitations.

To confirm the MNT-REL interaction, UR61-MT-Hebo and UR61-MT-MAX were treated with 100 µM Zn^{+2} for 24 h and endogenous MNT was immunoprecipitated followed by western blot to see if REL was co-immunoprecipitated with MNT. As a control of the technique RELA/p65 protein, another NF-κB member known to interact with REL (Hayden and Gosh, 2004), was also immunoprecipitated. As it can

be seen in figure 4.27A, REL was detected in MNT-immunoprecipitations from UR61-MT-Hebo and UR61-MT-MAX cells confirming the results obtained by proteomics and also in RELA-immunoprecipitations from UR61-MT-Hebo and UR61-MT-MAX as a positive control. The same was done to confirm MNT-CCDC6 interaction. However, endogenous CCDC6 was not found in MNT immunoprecipitations neither from UR61-MT-Hebo or UR61-MT-MAX, despite that the interaction was originally described in these cells (data not shown).

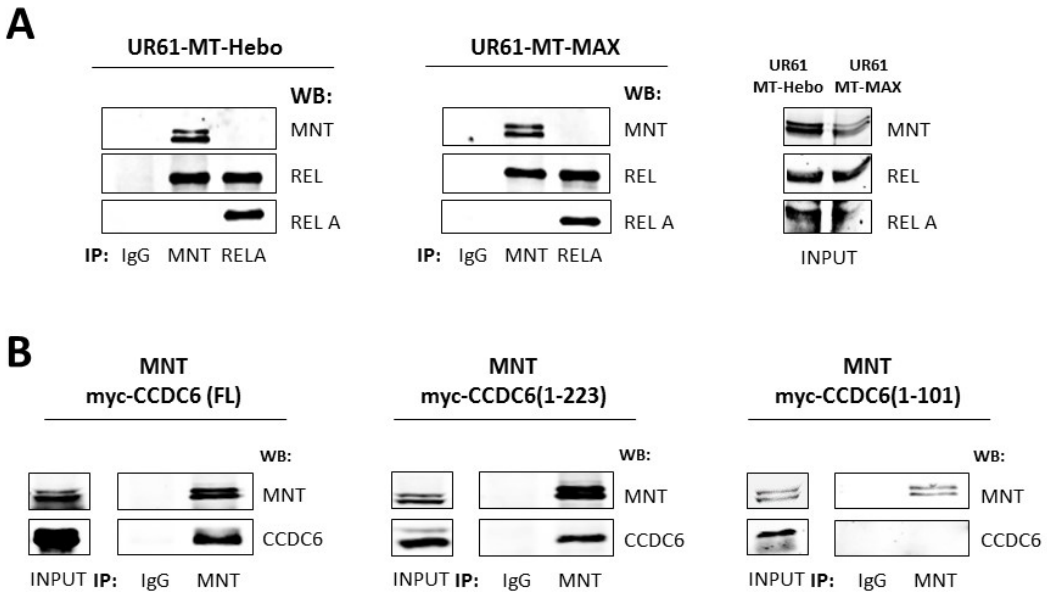

Figure 4.27. MNT immunoprecipitations. (A) Co-ilmmunoprecipitation of MNT and RELA proteins in UR61-MT-Hebo and UR61-MT-MAX treated for 24 h with 100 µM Zn^{+2}. Total lysates were subjected to immunoprecipitation with anti-MNT or anti-RELA antibodies as indicated, and the presence of MNT and REL in the immunocomplexes was assessed by western blot (B) Co-immunoprecipitation of MNT and CCDC6 in HEK293T cells. Cells were co-transfected with the MNT and the myc-tagged CCDC6 expressing vectors (full length CCDC6 and the mutants CCDC6(1-223) and CCDC6(1-101). Co-immunoprecipitated proteins were analysed as above.

To try to confirm the MNT-CCDC6 interaction we transfected the HEK293T cells with MNT and myc-tagged-CCDC6 overexpressing vectors. After 24 h of transfection an immunoprecipitation against MNT was assessed followed by western blot against the myc tag using the anti-myc (9E10) antibody; as it can be seen in figure 4.27B, CCDC6 co-immunoprecipitated with MNT in the HEK293T cells. Once confirmed that CCDC6 was co-immunoprecipitated by MNT suggesting that they were interacting, we tried to determine the region of CCDC6 responsible for MNT interaction. To do so we transfected the HEK293T cells with overexpressing vectors of MNT and two CCDC6 mutants: the CCDC6(1-223) that contained the amino acids 1 to 223 and the CCDC6(1-101) that contained amino acids 1 to 101. Both constructs were myc-tagged, detectable with the anti-myc 9E10 antibody. The vectors were transfected into the HEK293T cells and 24 h post-transfection an immunoprecipitation against MNT was performed. The co-immunoprecipitation of the CCDC6 mutants in MNT immunoprecipitations was checked by

western blot using the 9E10 antibody. As shown in figure 4.27B, CCDC6(1-223) but not the CCDC6(1-101) mutant was still co-immunoprecipitating with MNT. These results suggest that MNT-CCDC6 interaction needs at least the region between 101-223 amino acids of CCDC6 protein.

Table 4.1. MNT positive interactions in UR61-MT-Hebo and UR61-MT-MAX. A list of the MNT interacting proteins found by mass spectrometry of three MNT-immunoprecipitations from UR61-MT-Hebo and UR61-MT-MAX transfected with a MNT expressing vector and treated 24 h with 100 µM Zn^{+2}. The 5 common proteins found in MNT-UR61-MT-Hebo and MNT-UR61-MT-MAX immunoprecipitates are in light blue letters. MNT and MAX as control of the technique are highlighted in green. The fold change corresponds to the relative amount of the protein in the anti-MNT immunoprecipitates versus the IgG immunoprecipitates.

	Gene name	Protein name	Fold change (α-MNT vs IgG)	T-test (*p-value*)
UR61 MT-Hebo	AMPD2	AMP deaminase 2	919.90	0.015
	MNT	Max-binding protein MNT	182.67	0.006
	CCDC6	Coiled-coil domain-containing protein 6	49.00	0.015
	REL	Proto-oncogene c-Rel	43.57	0.004
	QSER1	Glutamine and serine-rich protein 1	13.73	0.004
	MAT2A	S-adenosylmethionine synthase isoform type-2;S-adenosylmethionine synthase	6.43	0.002
	ALB	Serum albumin	5.85	0.024
	TPP2	Tripeptidyl-peptidase 2	3.99	0.020
	KRT6B	Keratin, type II cytoskeletal 6B	3.62	0.023
	PRKRA	Interferon-inducible double stranded RNA-dependent protein kinase activator A	3.14	0.024
	PDE4DIP	Myomegalin	2.68	0.018
	PIP	Prolactin-inducible protein	2.65	0.022
UR61 MT-MAX	NISCH	Nischarin	88.70	0.000
	AMPD2	AMP deaminase 2	43.72	0.000
	REL	Proto-oncogene c-Rel	36.99	0.000
	TPP2	Tripeptidyl-peptidase 2	34.75	0.002
	CCDC6	Coiled-coil domain-containing protein 6	30.83	0.000
	MAX	Protein max	26.30	0.000
	MNT	Max-binding protein MNT	18.26	0.000
	KIF7	Kinesin-like protein KIF7	9.96	0.000
	ARPC5	Actin-related protein 2/3 complex subunit 5	8.40	0.044
	QSER1	Glutamine and serine-rich protein 1	7.80	0.000
	SMARCE1	SWI/SNF-related matrix-associated actin-dependent regulator of chromatin subfamily E member 1	7.20	0.000
	SMARCC2;SMARCC1	SWI/SNF complex subunit SMARCC2;SWI/SNF complex subunit SMARCC1	6.77	0.000
	PGK1	Phosphoglycerate kinase 1;Phosphoglycerate kinase	5.99	0.047
	CCT5	T-complex protein 1 subunit epsilon	5.90	0.012
	TUBB2A;TUBB2B	Tubulin beta-2A chain;Tubulin beta-2B chain	5.62	0.001

	GSN	Gelsolin	5.12	0.000
	VDAC2	Voltage-dependent anion-selective channel protein 2	5.10	0.019
	VDAC1	Voltage-dependent anion-selective channel protein 1	5.07	0.049
	HNRNPUL2;hCG_2044799	Heterogeneous nuclear ribonucleoprotein U-like protein 2	4.38	0.001
	HSP90AA1	Heat shock protein HSP 90-alpha	4.06	0.035
	S100A9	Protein S100-A9	4.02	0.000
	DMBT1	Deleted in malignant brain tumors 1 protein	3.78	0.005
	SBSN		3.75	0.037
	PPIA	Peptidyl-prolyl cis-trans isomerase A;Peptidyl-prolyl cis-trans	3.74	0.020
	CPSF7	Cleavage and polyadenylation specificity factor subunit 7	3.49	0.000
	PKM2	Pyruvate kinase isozymes M1/M2;Pyruvate kinase	3.47	0.021
	DSC3	Desmocollin-3	3.41	0.007
	FABP5	Fatty acid-binding protein, epidermal	3.31	0.013
	LDHA;LDHAL6A	L-lactate dehydrogenase A chain;L-lactate dehydrogenase;L-lactate dehydrogenase A-like 6A	3.27	0.007
	HSP90AB1	Heat shock protein HSP 90-beta	3.20	0.033
	SUPT16H	FACT complex subunit SPT16	3.12	0.041
	RAB39A;RAB6A;RAB6B	Ras-related protein Rab-39A;Ras-related protein Rab-6A;Ras-related protein Rab-6B	3.02	0.006
	HSPB1	Heat shock protein beta-1	2.74	0.000
	ENO1	Alpha-enolase	2.56	0.007
	PRDX1	Peroxiredoxin-1	2.51	0.011
	PPP1R12A	Protein phosphatase 1 regulatory subunit 12A	2.45	0.022
	ATP5B	ATP synthase subunit beta, mitochondrial;ATP synthase subunit beta	2.42	0.018
	HSPA8	Heat shock cognate 71 kDa protein	2.42	0.003
	AZGP1	Zinc-alpha-2-glycoprotein	2.42	0.008
	HSPA5	78 kDa glucose-regulated protein	2.29	0.000
	ATP5A1	ATP synthase subunit alpha, mitochondrial;ATP synthase subunit alpha	2.25	0.008
	ANXA2;ANXA2P2	Annexin A2;Annexin;Putative annexin A2-like protein	2.20	0.028
	CCT8	T-complex protein 1 subunit theta	2.19	0.036
	NUDT21;DKFZp313O211	Cleavage and polyadenylation specificity factor subunit 5	2.18	0.000
	METAP1	Methionine aminopeptidase 1;Methionine aminopeptidase	2.15	0.039
	CFL1	Cofilin-1	2.06	0.027
	DSG1	Desmoglein-1	2.06	0.021
	DSC1	Desmocollin-1	2.05	0.036

4.5. MNT EXPRESSION AND SURVIVAL IN UR61 CELLS

4.5.1. MNT regulation at protein level in UR61 cells

Since we failed to detect increased amounts of MNT protein upon transfection of the UR61 cells with a MNT expression vector (figure 4.17), we asked whether MNT was being controlled at protein level, so as to degrade MNT in excess over normal levels. To do so, we transfected UR61 cells with the empty vector and MNT expressing vector and after 16 h of transfection we treated the cells with 15 nM and 50 nM bortezomib to inhibit the proteasome and impair protein degradation via this pathway. As shown in figure 4.28, again in MNT-transfected UR61, the MNT protein did not increase in the untreated condition, as compared with the cells transfected with the empty vector (Vo). However, when the protein degradation was inhibited with bortezomib, the MNT protein levels were highly increased. In contrast, actin and BCL-XL (with shorter half-life) protein levels were unchanged by the proteasome inhibition, as well as the bulk of cellular proteins, as assessed by Coomassie blue staining of the gel (figure 4.28). Thus, this result showed that there is a tight control of the MNT levels in the cells. The mechanism that senses the overexpression of MNT proteins is so far unknown, but the result show that MNT degradation is carried out by proteosome-dependent mechanisms.

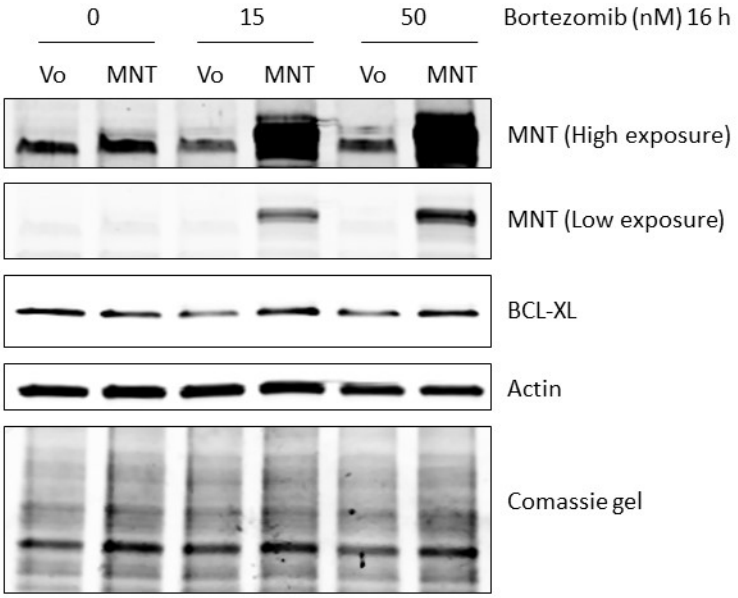

Figure 4.28. MNT expression in UR61 treated with Bortezomid. MNT expression of UR61 cells transfected with the empty vector (Vo) and MNT expression vector. 36 h after transfection the cells were treated for 16 h with 15 nM and 50 nM Bortezomib and the levels of MNT, BCL-XL and ACTIN were determined by westen blot. A picture of the gel stained with Coomasie blue is shown at the bottom.

4.5.2. MNT downregulation in UR61 impaired cell proliferation

Taking into account that enforcing the MNT expression did not lead to an increase of the protein in UR61 since this ectopic MNT is being degraded (figure 4.28), in order to continue studying MNT roles in the absence of MAX, we chose to knock-down MNT gene expression. We first tried to make stable MNT-silenced UR61 by transducing the cells with lentiviral particles containing a short hairpin construct that would express a siRNA against the rat MNT gene (herein after sh-MNT) and silence its expression. The short hairpin vector also carried a puromycin-resistance gene. We tried at least three times but we could not generate these MNT-silenced cells (data not shown). This failure to generate stably cell lines with decreased MNT levels suggested that MNT silencing was affecting UR61 cell growth and viability.

To confirm this hypothesis we decided to transiently transfect the UR61 cells with the lentiviral plasmid containing the sh-MNT vector or an empty vector (pLKO) as control. We first transfected the cells with a mixture of a GFP expression vector and the sh-MNT or pLKO vectors in a proportion 1:5 to ensure that the GFP positive cells had also incorporated the shRNA plasmid. The following day and 6 days after transfection, the fraction of GFP positive cells were analysed by flow cytometry (FACS). As it can be seen in figure 4.29A, the ratio of GFP positive cells after 6 days post-transfection was reduced to almost one half in the MNT-silenced UR61 cells in comparison with the control indicating that MNT silencing was affecting the proliferation of the GFP-positive UR61 cells.

As a second approach to elucidate whether MNT silencing in UR61 slows cell population growth we counted the cells. The UR61 cells were transfected with the sh-MNT and the control (pLKO) and cells were counted after 3, 6 and 12 days of transfection. As shown in figure 4.29B, the MNT-silenced UR61 cells grew more slowly than the control.

We also performed clonogenic assays in UR61 in parallel with the rat TGR-1 cell line. On the one hand, the UR61 cells were transfected with both the sh-MNT and a MAX overexpressing vector (in 1:3 proportions to ensure that the sh-MNT containing cells had also incorporated the MAX vector) and the empty vectors (pLKO and pCEFL). On the other hand, the TGR-1 cells that do normally express the MAX protein were transfected exclusively with the sh-MNT and the empty vector. 24 h post-transfection the cells (UR61 and TGR-1) were selected with puromycin and after 17 days of selection they were stained with crystal violet dye and picture of the plates were taken (figure 4.29C). Alternatively, crystal violet was solubilised and quantified as indicated in Material and Methods section. The results showed that the UR61 cells overexpressing the MAX protein grew more slowly than the control (figure 4.29C), an expected result (Hopewell and Ziff, 1995). The MNT-silenced UR61 cells grew even more slowly than the MAX expressing cells and a combination of MNT-silencing and MAX overexpression in the UR61 cells almost totally inhibited the UR61 cell proliferation. On the contrary, in the TGR-1 cells MNT-silencing did not only affect cell growth but led to a slightly increase of cell proliferation as expected according to Hurlin et al., 2003 data (figure 4.29C).

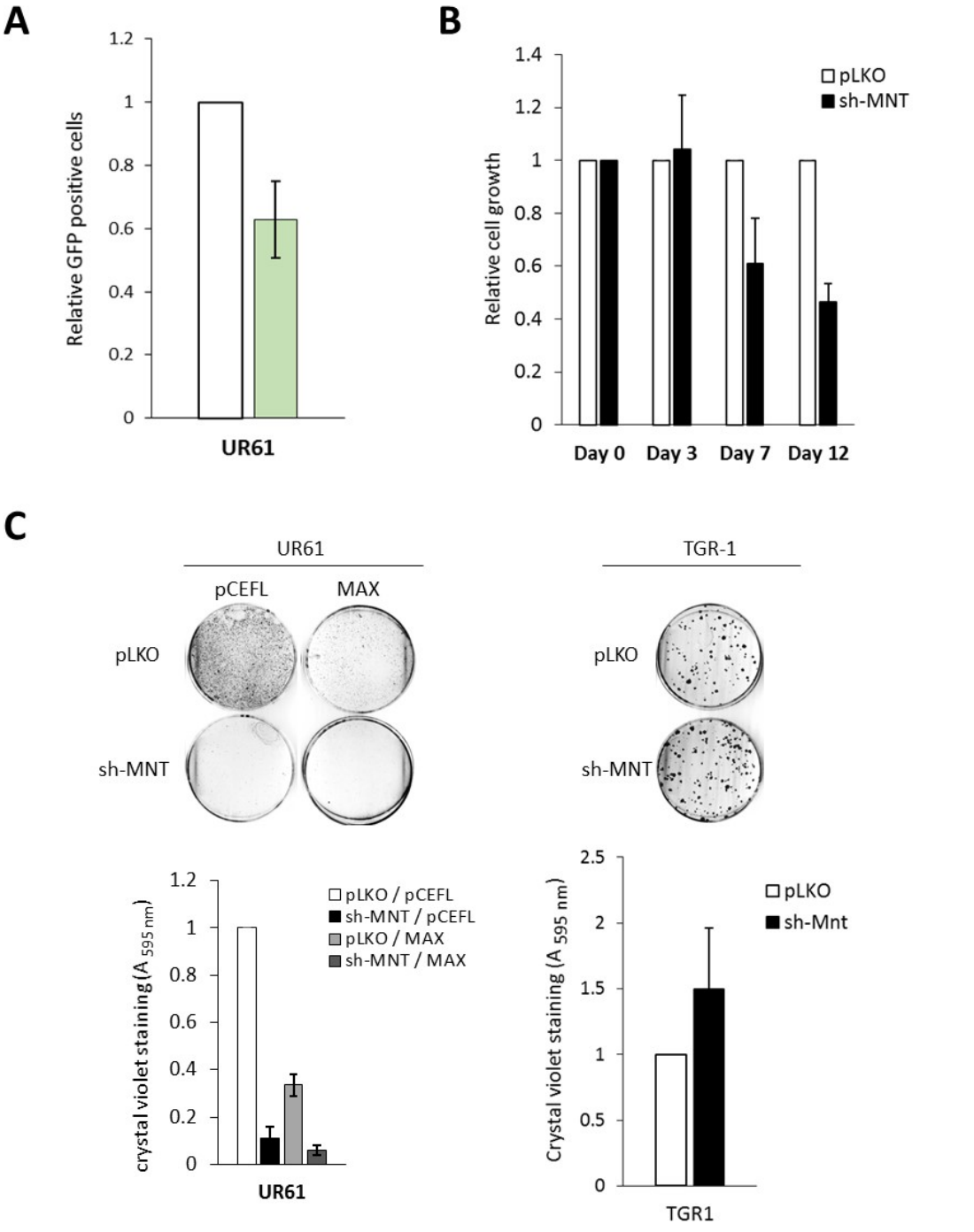

Figure 4.29 MNT knock-down in UR61 cells. (A) Fraction of GFP positive cells 7 days transfection with the sh-MNT vector. UR61 cells were co-transfected with the shRNA plasmid against MNT (sh-MNT) and a GFP expressing vector. (B) sh-MNT transfected UR61 counted after 3, 7 and 12 days of transfection. (C) Crystal violet stain and quantification of: UR61 cells co-transfected with the sh-MNT plasmid and a MAX expressing vector (left grafts) and TGR-1 cells transfected with the sh-MNT plasmid (right grafts) after 17 days of puromycin selection. The data are means values of at least 3 independent experiments. The error bars are S.D.

To assess whether MNT silencing was altering cell cycle progression in the UR61 cells we transfected UR61-MT-Hebo and also UR61-MT-MAX with the sh-MNT vector and the empty vector. Three days post-transfection and after 12 h of Zn^{+2} treatment the cells were harvested and the cell cycle proteins cyclin A2 (CCNA2) and p57 were analysed by western blot. Cyclin A2 that is needed for cell cycle progression was downregulated in the MNT-silenced cells (figure 4.30A). On the contrary, p57 that it known to arrests cell cycle progression was slightly upregulated when *MNT* was silenced in the UR61-MT-Hebo and UR61-MT-MAX cells (figure 4.30A).

Altogether, these data show that MNT downregulation impairs cell cycle progression in the UR61 and UR61-MT-MAX cells suggesting that MNT is needed for these cells to proliferate even in the absence of MAX.

4.5.3. MNT downregulation in UR61 induced cell death

Since MNT silencing in UR61 impairs the cell population growth, we wondered whether MNT silencing was also inducing cell death. To study this possibility we transfected the UR61 cells with the sh-MNT plasmid and the pLKO (empty vector) and the following day puromycin was added to the medium. After 7 days of selection, cells were harvested and stained with propidium iodide (PI) to see by flow cytometry (FACS) the fraction of cell population in subG0 phase in each condition. The subG0 phase accounts for the DNA fragmentation (less than 2n) that is observed when cells are dying. As it can be seen in figure 4.30B, the silencing of MNT led to a two-fold increase in the number of subG0 cells, indicating that MNT absence promotes cell death.

To further study this cell death observed when MNT is silenced in UR61, the UR61-MT-Hebo and UR61-MT-MAX cells were transfected with the sh-MNT and the empty vector. After 72 h of transfection and 12 h of 100 µM Zn^{+2} treatment, cells were harvested, lysed and PARP1 cleavage (indicative of apoptosis activation) and BCL-XL (an antiapoptotic protein) protein were analysed by western blot. As shown in figure 4.30A, the full length form of PARP1 (~110 kDa) was expressed in all conditions. However, the cleaved form that was observed in apoptosis activation (~89 kDa) was only observed in cells were *MNT* was silenced. Furthermore, the antiapoptotic BCL-XL protein is downregulated in such conditions.

Altogether, these data suggest that MNT silencing in the UR61 and UR61-MT-MAX cells leads to cell death at least in part by the activation of an apoptotic program.

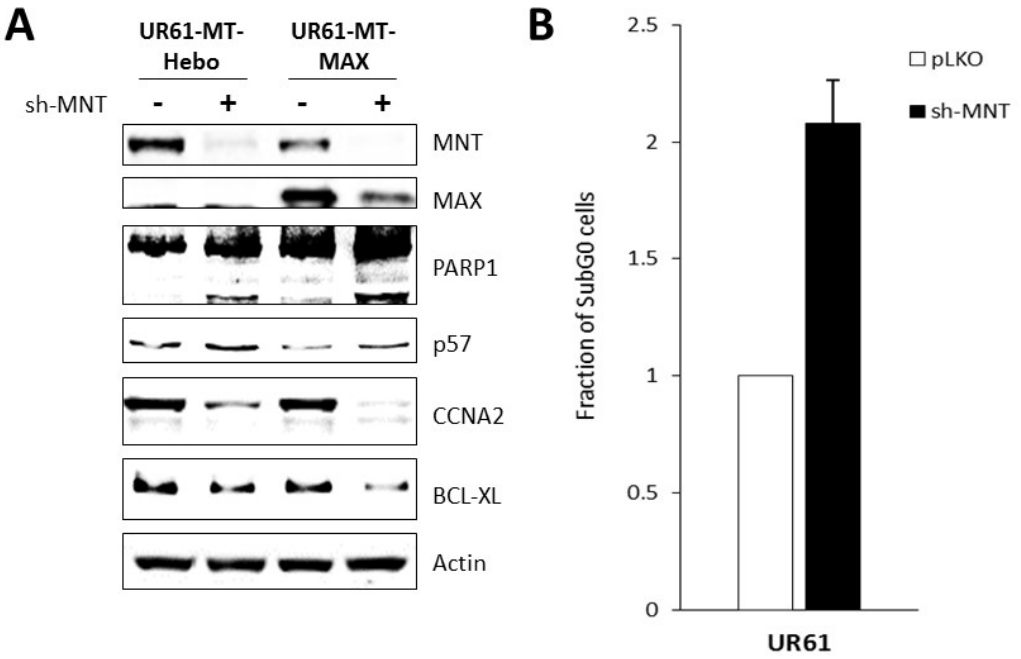

Figure 4.30. MNT knock-down in UR61 cells and the effect on cell death. (A) Western blot of sh-MNT transfected UR61-MT-Hebo and UR61-MT-MAX cells after 72 h of transfection and 12 h of 100 µM Zn^{+2} treatment. Data are form two different blots with the same protein loading. (B) UR61 cells transfected with the sh-MNT and stained with propidium iodide (PI) at day 6 of transfection and puromycin selection. The fraction of cells containing less than 2C DNA content was determined by flow cytometry. The data are means values of at least 2 independent experiments. The error bars are S.D.

4.6. MNT AND NF-κB

4.6.1. MNT modulates NF-kB gene regulation activity

Since we found that MNT interacts with REL in the UR61 cells and REL is a transcription factor, we wondered whether MNT expression levels would affect REL transcriptional regulation. To study this, we first transfected the UR61 cells with a luciferase reporter gene regulated by five κB sites (NF-κB binding sites) together with the shRNA against *MNT* to silence *MNT* expression, as well as the corresponding empty vector. After 72 h of transfection, the luciferase activity was analysed in the different conditions. As shown in the figure 4.31A, *MNT* silencing increased by about 50 % the luciferase activity of the NF-κB reporter vector.

We also carried out luciferase experiments in HeLa cells. For this, we used a stable MNT-silenced HeLa cell line and the control with the empty vector. These cells were generated by transduction with lentiviral particles containing shRNA constructs against human *MNT* (sh-MNT). MNT silencing was assessed by western blot (figure 4.31B). MNT-silenced HeLa cells and the control were transfected with the NF-κB luciferase reporter vector and 24 h post-transfection cells were harvested and the luciferase assay monitored. As it can be seen in figure 4.31C, again, *MNT* silencing in HeLa cells leads to an increase in the luciferase activity. Moreover, HeLa cells were transiently transfected with the NF-κB reporter vector together with a MNT expression and the control vector. After 24 h of transfection the luciferase activity was analysed and as it can be seen in figure 4.31D, concordantly with the results above, MNT overexpression led to a decrease in the luciferase activity.

Altogether, these data suggested that MNT expression modulated the NF-κB response in the UR61 and HeLa cells.

4.6.2. MNT depletion increases TNFα sensibility of UR61 cells

To continue studying the role of the MNT-REL interaction, we studied whether MNT expression would affect the canonical NF-κB pathway in response to a biological activator. For that, we chose the TNFα chemokine as it is one of the best known and characterized NF-kB activators. To do so, we first asked by immunofluorescence if the canonical NF-κB pathway was activated by TNFα in the UR61 cells. UR61 were treated with 100 ng/ml of TNFα and after 30 min an immunofluorescence against REL and RELA/p65 NF-κB members was performed. The results showed that REL and RELA/p65 were translocated to the nucleus upon TNFα treatment (figure 4.32A), indicating that this pathway is active in the UR61 cells.

Once that it was confirmed the activation of the pathway by TNFα treatment, we asked whether MNT modified the response to TNFα. The UR61 cells, where the REL-MNT interaction was found, were transfected with the sh-MNT plasmid and the corresponding empty vector (pLKO).

The following day, puromycin (0.3 μg/ml) was added and the cells were treated with or without the cytokine TNFα (100 ng/ml) to induce the NF-κB canonical pathway. After 7 days of treatment cells were stained with crystal violet and then it was solubilised for quantification as described in Material and

Methods section. As shown in figure 4.32B, TNFα treatment impaired the cell growth of UR61 and affect cell viability (data not shown) at levels similar to that obtained by MNT silencing. In addition, the TNFα treatment together with the *MNT* silencing increased this impairment of cell growth suggesting a synergistic effect that was consistent with the results obtained from the luciferase assays (figures 4.31A,C,D).

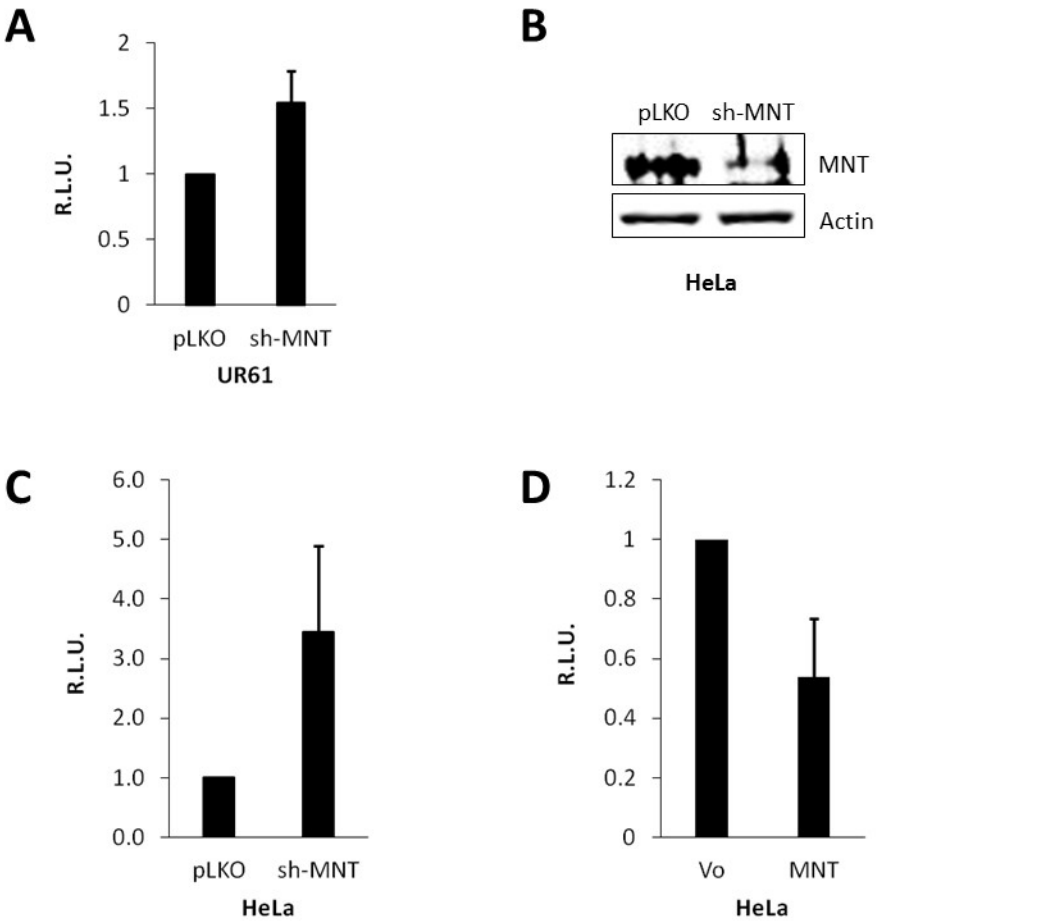

Figure 4.31. NF-κB activity in MNT-depleted cells. (A) Luciferase assay of UR61 cells 72 h after transfection with a luciferase reporter containig NF-κB sites and the sh-MNT vector. (B) Western blot to determine MNT levels in a MNT knock-down HeLa cell line established by transduction of lentiviral particles containing an shRNA sequence against human MNT gene. (C) Luciferase assay of MNT knock-down HeLa cells 24 h after transfection with the NF-κB luciferase reporterr. (D) Luciferase assay of HeLa cells 24 h after transfection with the NF-κB sites containing luciferase reporter vector and a MNT expressing vector. The data are means values of at least 3 independent experiments. The error bars are S.D.

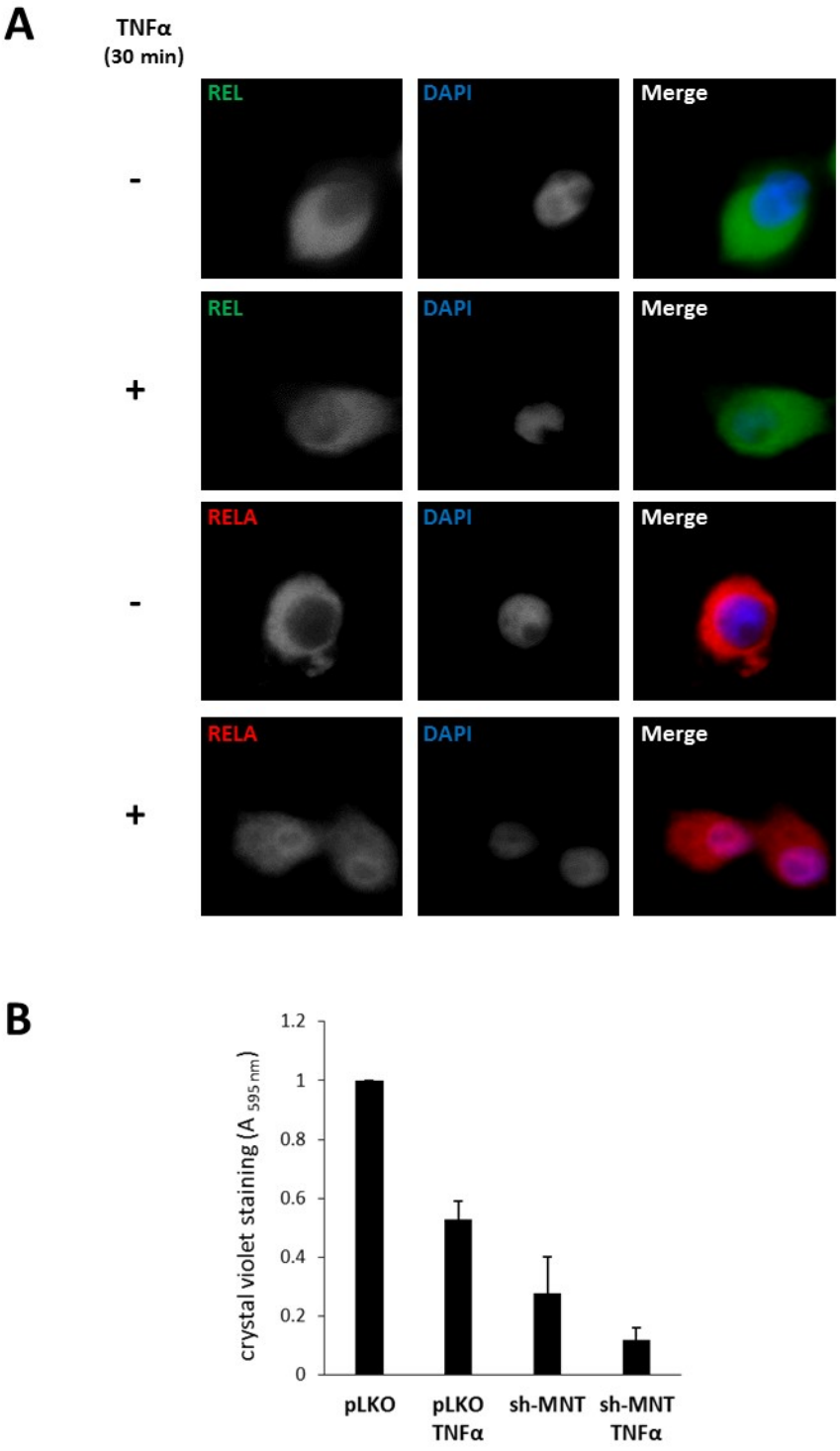

Figure 4.32. NF-κB pathway activation in UR61 cells. (A) Immunofluorescence of UR61 cells treated with 100 ng/ml TNFα for 0 and 30 min. REL is shown in green, RELA in red and the DNA (DAPI-stained) in blue. (B) Cell growth quantification based on crystal violet staining of UR61 cells. Cells were transfected with the sh-MNT and empty vector (pLKO), treated with 100 ng/ml TNFα and stained after 7 days of treatment and puromycin selection. The data are means values of at least 3 independent experiments. The error bars are S.D.

4.7. GENE REGULATION BY MNT IN THE ABSENCE OF MAX

4.7.1. MNT downregulation in UR61 alters the transcriptional program in the absence and presence of MAX

Since MNT is a transcription factor we wanted to know the expression of which genes were altered in *MNT* silencing conditions. We transfected the UR61-MT-Hebo and UR61-MT-MAX cells with the shRNA construct against the rat MNT gene (sh-MNT) and the empty vector (pLKO) as control (in duplicates). After 72 h of transfection and 24 h of 100 µM Zn^{+2} treatment, total RNA was prepared and the expression of *MNT* and *MAX* were determined at mRNA level by RT-qPCR and protein level by western blot to assess the depletion of MNT and the upregulation of MAX in response to Zn^{2+} (figure 4.33A,B). Then, total RNA was sequenced using the Illumina platform as indicated in Material and Methods and

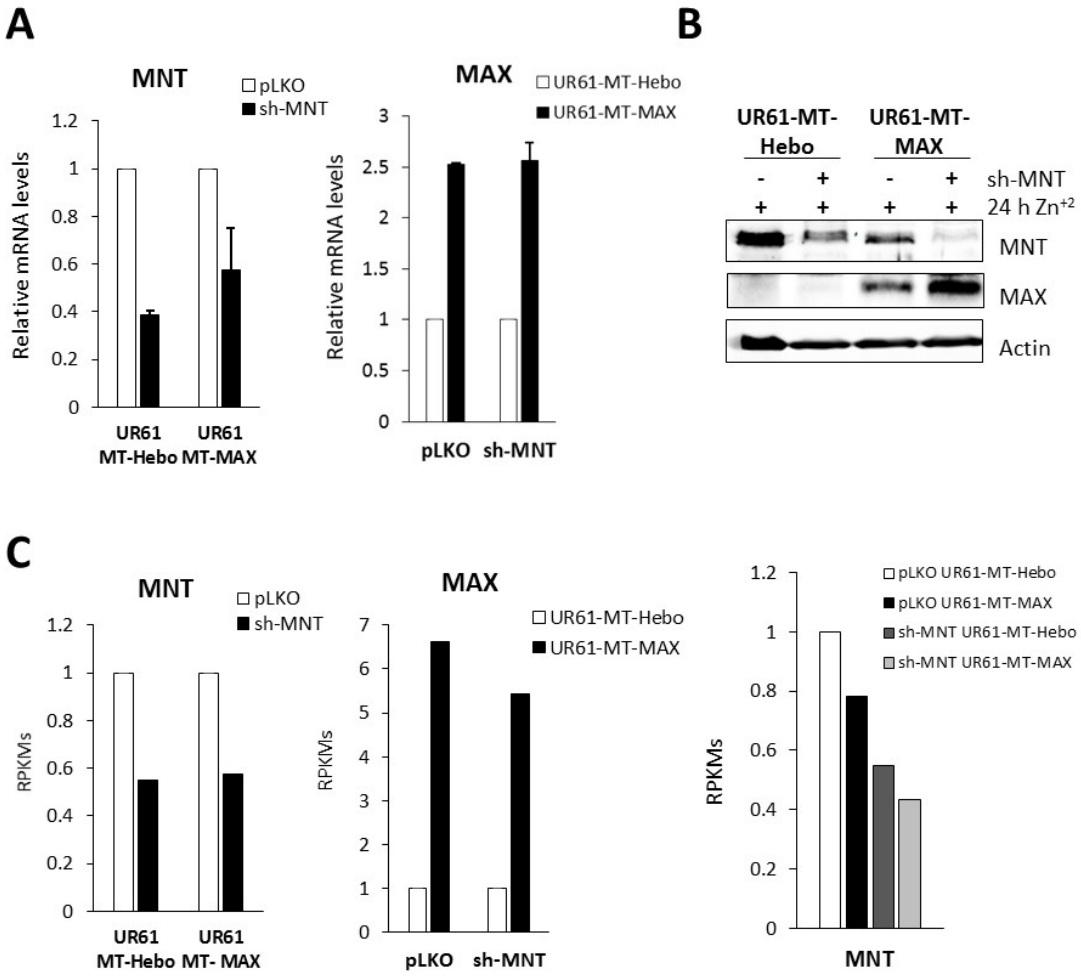

Figure 4.33. RNA-seq of MNT knock-down cells. MNT silencing and MAX expression measured by (A) RT-qPCR and (B) western blot of UR61-MT-Hebo and UR61-MT-MAX cells 72 h after transfection with sh-MNT transfection and 24 h of treatment with 100 µM Zn^{+2}. (C) MNT and MAX expression according to the RNA-seq data expressed by RPKM in UR61-MT-Hebo and UR61-MT-MAX cells.

after bioinformatics analysis mRNA levels were expressed as RPKM (Reads Per Kilobase per Million reads). The decrease in *MNT* mRNA in the UR61-MT-Hebo and UR61-MT-MAX cells was confirmed, as well as the expression of *MAX* mRNA in the UR61-MT-MAX cells (figure 4.33C). In addition, according to the previous data regarding the decrease of MNT levels when MAX is present in the UR61 cells, the RPKMs values of *MNT* in UR61-MT-MAX cells were lower than in UR61-MT-Hebo and even lower when MAX was expressed together with the shRNA against MNT (figure 4.33C). Once we showed the consistency of the RNA-seq data we grouped the genes that were highly expressed in both the MNT-silenced and the control UR61-MT-Hebo and UR61-MT-MAX (considering an RPKM mean value of the duplicates higher or equal to 0.5 with a standard deviation lower or equal to 3) and that had a fold change in the MNT-silenced conditions higher or equal to 1.7 or lower than 0.6 in relation to the control condition (UR61-MT-Hebo and UR61-MT-MAX). We considered these genes to be upregulated or downregulated respectively. With these settings we listed 240 genes in MNT-silenced UR61-MT-Hebo whose expression was altered (annex 1). Of those 37 % were upregulated and 63 % downregulated by MNT silencing (figure 4.34A). In MNT-silenced UR61-MT-MAX, a list of 351 genes whose expression was altered (annex 2) was obtained with 37 % being upregulated and 63 % downregulated (figure 4.34A).

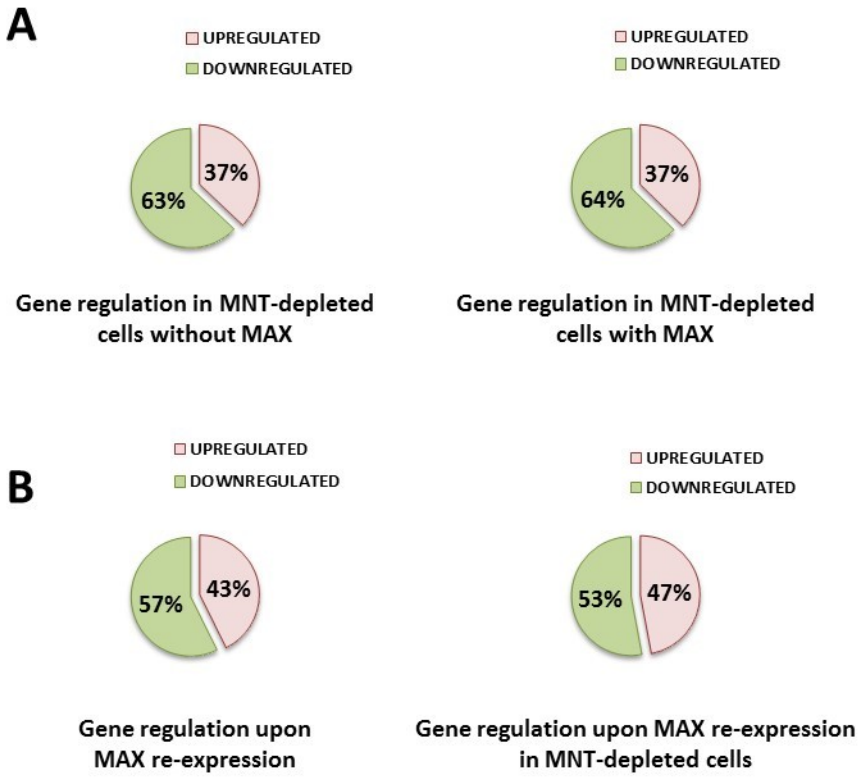

Figure 4.34. Gene expression changes in MNT knock-down cells. Percentage of upregulated and downregulated genes 72 h after transfection with the sh-MNT or pLKO vectors and 24 h of treatment with 100 µM Zn^{+2} in : (A) UR61-MT-Hebo sh-MNT vs UR61-MT-Hebo pLKO (left) or UR61-MT-MAX sh-MNT versus UR61-MT-MAX pLKO (right) and (B) UR61-MT-MAX pLKO vs UR61-MT-Hebo pLKO (left) or UR61-MT-MAX sh-MNT vs UR61-MT-Hebo sh-MNT (right).

The lists of upregulated or downregulated genes obtained in the sh-MNT UR61-MT-Hebo and sh-MNT UR61-MT-MAX cells were then classified according to biological processes using the Babelomics 4.3 software (http://babelomics.bioinfo.cipf.es/) and the KEGG pathway and Gene Ontology (GO) databases as indicated in Material and Methods section. Using this software no association with any specific function was found for the upregulated genes. Conversely, it was found that the lists of genes whose expression was downregulated in our experiments presented an enrichment of genes involved in cell cycle and DNA damage processes in comparison with the genes present in the whole genome (table 4.2). Interestingly and consistently with the previous results, genes involved in cell cycle progression and DNA replication such as *CDK6, E2F1, E2F6, E2F7, CDC6, CDC25B, ORC1* and *MCM10* were downregulated meanwhile genes involved in cell cycle arrest such as *CDKN1C* (encoding p57) were upregulated in the MNT-silenced UR61-MT-Hebo and UR61-MT-MAX cells (annex 1 and 2). In addition, genes involved in DNA repair were generally downregulated such as *PARPBP, BRCA2, RAD51, RAD54B* or *CHEK1* (annex 1 and 2).

The effect of MAX expression at transcriptional level was also analysed in UR61 and MNT-depleted UR61. The genes that were highly expressed were grouped (considering an RPKM mean value of the duplicates higher or equal to 0.5 with a standard deviation lower or equal to 3). Of these we considered the ones with a fold change in the MAX-expressed conditions higher or equal to 1.7 or lower than 0.6 related to the control condition (UR61-MT-Hebo pLKO or UR61-MT-Hebo sh-MNT cells). With these setting we obtained a list of 260 genes in UR61-MT-MAX pLKO (Annex 3). Of those, 43 % were upregulated and 57 % downregulated when MAX was present (figure 4.34B). We did the same for the MNT silenced conditions and obtained a list of 255 genes in UR61-MT-MAX sh-MNT (Annex 4). Of those, 47 % were upregulated and 53 % downregulated when MAX was present (figure 4.34B).

Then, we validated by RT-qPCR some of the genes which expression was altered in the MNT-silenced condition. We chose some genes that were involved in cell cycle and DNA repair mechanisms and validated them only in UR61-MT-Hebo since they were similar in UR61-MT-MAX according to the RNA-seq data (RPKMs). As it can be seen in figure 4.35 all the genes from the RNA-seq experiments chosen for validation (figure 4.35A) were successfully validated by RT-qPCR (figure 4.35B). Furthermore, we also studied in these validated genes the presence of E-boxes within 1000 bp upstream/downstream the TSS and the presence of positive peaks for MYC, MAX and MXI1 in the promoter regions looking at the ChIP-seq data of the ENCODE project (UCSC genome browser http://genome.ucsc.edu/ENCODE/) (annex 5).

Table 4.2. Ontology analysis of the genes changed by MNT depletion in UR61 with and without MAX. Biological processes association of the gene set downregulated in MNT knock-down UR61-MT-Hebo and UR61-MT-MAX treated with 100 µM Zn^{+2} for 24 h using the Babelomics4.2 software and the KEGG pathway and Gene Ontology (GO) databases with a p-value ≤ 0.05. No association for upregulated genes was found. Cell cycle processes are highlighted in dark green, DNA damage processes in light green and cytoskeleton processes in light blue.

UR61-MT-Hebo downregulated genes in sh-MNT condition					
KEGG pathways database					
#term	**name**	**general process**	**% genes in**		**Fold change**
			this analysis	**total genome**	
rno03440	homologous recombination	**DNA DAMAGE**	2	0.05	**40**
GO ontology database					
#term	**name process**	**general process**	**% genes in**		**Fold change**
			this analysis	**total genome**	
GO:0048599	oocyte development	**DNA DAMAGE**	2	0.07	**28.57**
GO:0009994	oocyte differentiation	**CELL CYCLE**	2	0.08	**25.00**
GO:0007126	meiotic nuclear division	**CELL CYCLE**	4.67	0.26	**17.96**
GO:0051321	meiotic cell cycle	**CELL CYCLE**	4.67	0.27	**17.30**
GO:0051329	mitotic interphase	**CELL CYCLE**	3.33	0.26	**12.81**
GO:0051325	interphase	**CELL CYCLE**	3.33	0.29	**11.48**
GO:0006310	DNA recombination	**DNA DAMAGE**	3.33	0.29	**11.48**
GO:0000226	microtubule cytoskeleton organization	**CYTOSKELETON**	4.67	0.53	**8.81**
GO:0022402	cell cycle process	**CELL CYCLE**	10.67	1.43	**7.46**
GO:0007017	microtubule-based process	**CYTOSKELETON**	7.33	1.01	**7.26**
GO:0006281	DNA repair	**DNA DAMAGE**	6	0.87	**6.90**
GO:0051726	regulation of cell cycle	**CELL CYCLE**	5.33	0.92	**5.79**
GO:0000278	mitotic cell cycle	**CELL CYCLE**	6	1.04	**5.77**
GO:0034984	cellular response to DNA damage	**DNA DAMAGE**	6	1.05	**5.71**
GO:0007049	cell cycle	**CELL CYCLE**	12.67	2.28	**5.56**
GO:0006974	cellular response to DNA damage	**DNA DAMAGE**	6	1.18	**5.08**
GO:0006259	DNA metabolic process	**DNA DAMAGE**	9.33	1.96	**4.76**

Table 4.2. (Cont.)

UR61-MT-MAX downregulated genes in sh-MNT condition					
KEGG pathways database					
#term	**name**	**general process**	**% genes in**		**Fold change**
			this analysis	**total genome**	
NO ASSOCIATION					
GO ontology database					
#term	**name process**	**general process**	**% genes in**		**Fold change**
			this analysis	**total genome**	
GO:0030048	actin filament-based movement	**CYTOSKELETON**	1.39	0.05	**27.80**
GO:0006261	DNA-dependent DNA replication	**DNA DAMAGE**	2.31	0.17	**13.59**
GO:0007059	chromosome segregation	**CELL CYCLE**	2.31	0.18	**12.83**
GO:0051329	mitotic interphase	**CELL CYCLE**	2.31	0.26	**8.88**
GO:0007126	meiotic nuclear division	**CELL CYCLE**	2.31	0.26	**8.88**
GO:0051321	meiotic cell cycle	**CELL CYCLE**	2.31	0.27	**8.56**
GO:0000087	mitotic M phase	**CELL CYCLE**	3.7	0.57	**6.49**
GO:0007067	mitotic nuclear division	**CELL CYCLE**	3.24	0.53	**6.11**
GO:0022402	cell cycle process	**CELL CYCLE**	8.33	1.41	**5.91**
GO:0000278	mitotic cell cycle	**CELL CYCLE**	6.02	1.02	**5.90**
GO:0051301	cell division	**CELL CYCLE**	3.24	0.55	**5.89**
GO:0006281	DNA repair	**DNA DAMAGE**	4.63	0.87	**5.32**
GO:0007049	cell cycle	**CELL CYCLE**	11.11	2.25	**4.94**
GO:0007017	microtubule-based process	**CYTOSKELETON**	4.63	1.02	**4.54**
GO:0034984	cellular response to DNA damage	**DNA DAMAGE**	4.63	1.05	**4.41**
GO:0006259	DNA metabolic process	**DNA DAMAGE**	8.33	1.94	**4.29**
GO:0006974	cellular response to DNA damage	**DNA DAMAGE**	4.63	1.17	**3.96**

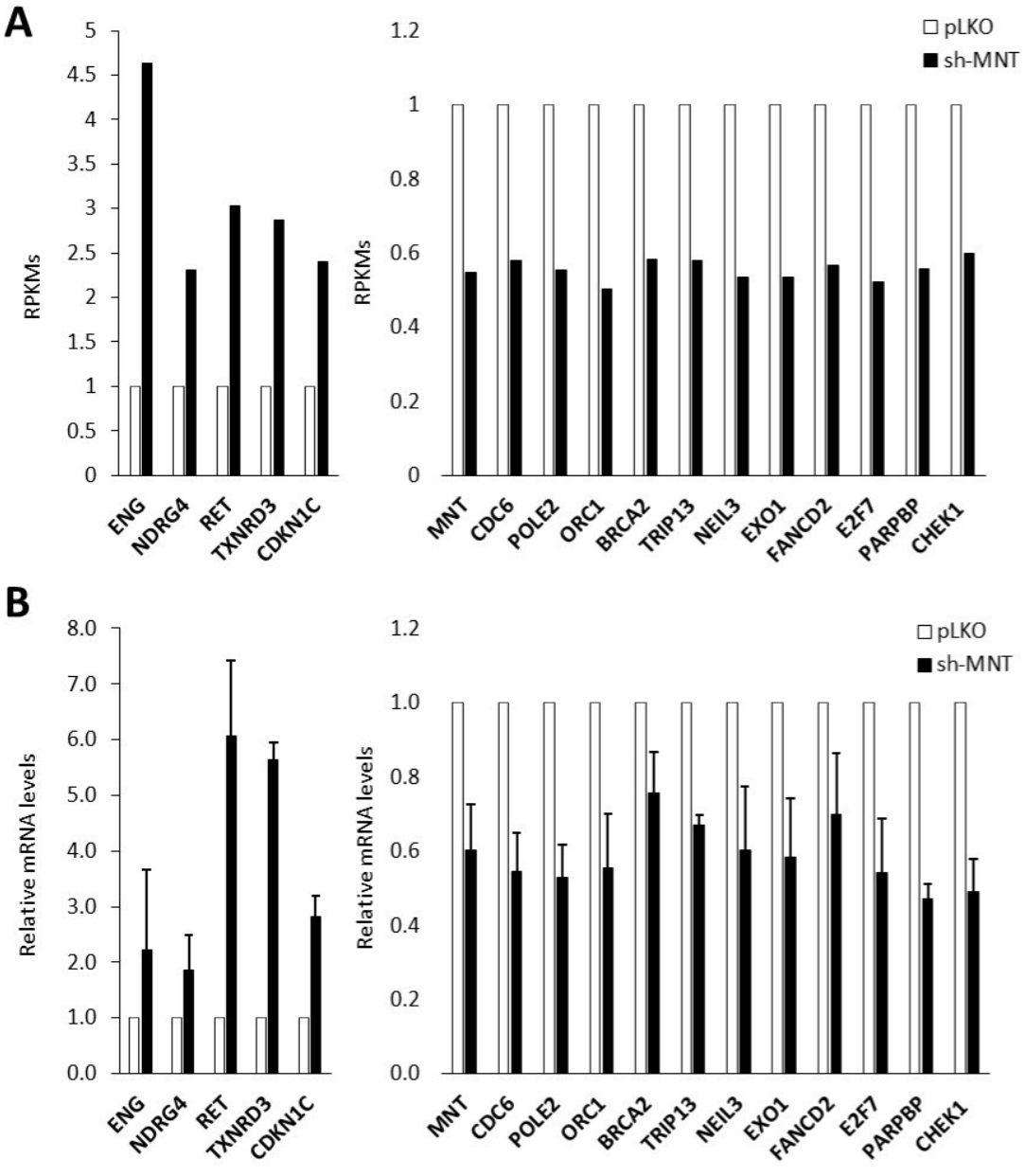

Figure 4.35. RNA seq validation in UR61 cells. (A) Gene expression (according to RNA-seq data) of the gene chosen for validation. The upregulated and downregulated genes are represented in the left and right grafts respectively. (B) Validation of the results obtained in the RNA-seq data by RT-qPCR. The upregulated and downregulated genes are represented in the left and right grafts respectively. RPKM refers to reads per kilobase per million reads.

Discussion

5. DISCUSSION

5.1. MXD1

MXD1 is the first member of the MXD family discovered and thus one of the best known MXD proteins. Its functions regarding cell cycle arrest and differentiation have been widely studied in different cell models. Its involvement in these functions is intimately related with its levels of expression among the different cell states and its opposite function, regarding transcriptional regulation, to MYC oncoprotein; for instance, MXD1 is highly expressed in arrested and differentiated cells where it regulates negatively gene transcription (see section 1.3.3 of Introduction). Due to these facts, it has been assumed since its discovery that MXD1 is not expressed in proliferating or undifferentiated cells and also that it needs MAX for such functions.

5.1.1. MXD1 does not trigger a differentiation program in UR61 cells

In this Thesis we have analysed MXD1 expression and function in the UR61 cell model. This cell model is of particular interest since UR61 cells do not express a wild type MAX protein. The MAX^{PC12} protein that is expressed in UR61 and their parental PC12 cells, lacks the H2-LZ regions of the b-HLH-LZ domain that is needed for protein interaction (Hopewell and Ziff, 1995). MAX^{PC12} then, becomes incapable of interacting neither with MYC nor with MXD members. Furthermore, UR61 cells have an inducible N-RAS oncogene, which expression is activated with dexamethasone. N-RAS induction leads to a neuronal-like phenotype (Guerrero et al., 1988).

Previous work in our laboratory described MYC functions in this MAX-deficient system. It was described that MYC oncoprotein was able to do one of its main functions that is the differentiation blockade in UR61 cells without MAX (Vaque et al., 2008). In the same way since MXD members take part in the MYC/MAX/MXD network, we wanted to know whether MXD1 maintains its functions in a MAX-independent manner or whether it achieves new properties in those conditions.

We have found that MXD1 does not affect UR61 cell differentiation since its enforced expression does not induce differentiation and does not enhance the differentiation phenotype of dexamethasone-treated UR61 cells. This is demonstrated by assaying the lack of morphological differentiation and the lack of the upregulation of neuronal markers such as *CHGA*, *GAP43* and *VGF* or the *JUN* transcription factor (involved in the neuronal-like differentiation program of UR61) (Vaque et al, 2008). In addition, MXD1 overexpressing UR61 cells do not show a significatively reduced cell proliferation, an indispensable condition for differentiation in this system.

These results show that MXD1 in the UR61 system does not function as it would be expected according to its previously reported effects in other models. That can be due to different reasons, for instance: 1) The levels of MXD1 overexpression that we achieved might not be sufficient to trigger a differentiation program as described for instance for keratinocytes (Grandori et al., 2000); 2) MXD1 might not be

capable of inducing a neuronal-like differentiation program considering that MXD1 functions regarding differentiation has been mainly observed in blood and keratinocytic lineages (see Introduction); or 3) MXD1 might need to heterodimerize with MAX for the differentiation and cell cycle arrest function since we have seen that MXD1-MAX but not MXD1 alone regulates E-box containing promoters.

5.1.2. MXD1 in proliferating and undifferentiated cells

According with the previous literature, MXD1 expression levels in proliferating and undifferentiated cells is very low or undetectable. In this Thesis we have found by western blot or immunofluorescence that MXD1 is expressed in different cell lines in growing conditions such as HEK293T, K562, HeLa and UR61 cells and also in undifferentiated human embryonic and transformed mesenchymal stem cells. This suggests that MXD1 might have a role different from inducing or maintaining a differentiation state. However, MXD1 functions in processes other that differentiation has received little attention. It is known that MXD1 is a transcription factor that acts as a repressor forming complexes with Sin3A/B and HDAC (Ge et al., 2010; Grandori et al., 2000). It is possible that MXD1 is repressing genes in those conditions that contribute to maintain the growth capacity, for instance, modulating excessive MYC activity and thus preventing MYC-mediated apoptosis.

5.1.3. MXD1 localizes to the nucleolus

MXD1 localization was known to be nuclear where it would act as repressive transcription factor. However, the subnuclear localization of MXD1 has not been reported. In this Thesis we have re-examined MXD1 localization in growing cells. Three compartments have been identified in the nucleolus: Fibrillar Centers (FC), Dense Fibrillar Centers (DFC) and the granular component (GC). Fibrillar centers are the places in nucleoli where active NORs (nucleolar organizing regions) and the rDNA transcriptional machinery localize. UBF regulates rDNA transcription and so it mainly localizes in the fibrillar centers of nucleoli. Interestingly, in undifferentiated human embryonic stem cells, MXD1 is found in the fibrillar centers of nucleoli, co-localizing with UBF. In addition, in more differentiated human mesenchymal stem cells, HEK293T, K562 and HeLa cells, MXD1 is localized in the nucleoplasm as expected but also in the fibrillar centers of nucleolus where again it also localizes with UBF. It is worth to mention that this localization is not a general fact of all MXD members since we studied the localization of other members of the MXD family like MNT and MXI1 and they were found in the nucleoplasm but not in the nucleolus. This suggests that not all the MXD members share common functions or regulate common genes as it would be expected due to their similarities in structure and expression pattern, especially for MXD1, MXI1, MXD3 and MXD4. These differences in subcellular localization suggest different functions and highlight the interest in the study of MXD members.

As mention above, MXD1 co-localizes with UBF in the nucleolus. It is known that nucleoli are dynamic structures that are sensible to external stimulus reflecting among other facts the stress that a cell is suffering. When a cell is under stress conditions such as DNA damage, protein or RNA synthesis inhibition, the nucleolus experience a phenomenon called nucleolar segregation which is a reorganization of the different compartments of nucleolus, where the fibrillar elements (FC, DFC) separate from the granular component (Journey and Goldstein, 1961). The fact that nucleoli are the

places where rRNA is synthesized, if a protein suffers a nucleolar segregation it may suggest that this protein is involved in some way or another in rRNA synthesis, either at the rDNA transcription or pre-rRNA processing level. One of the mechanism that induce cell stress and that affect nucleoli is the inhibition of RNApol I. Actinomycin D at low concentrations selectively inhibits RNApol I and leads to a segregation of nucleoli and so of UBF protein that can be observed by fluorescence microscopy. Here we have confirm this result and observe that MXD1 also segregates from nucleolus when RNApol I is inhibited by Actinomycin D in two different cell lines (HEK293T and human embryonic stem cells). This suggests that MXD1 is involved in some way or other in ribosomal RNA synthesis.

UBF regulates ribosomal RNA synthesis by activating rDNA transcription. It binds throughout the entire rDNA repeat but preferentially to the promoter and transcribed regions favouring an open chromatin conformation and enhancing the assembly of the pre-initiation complex that is needed for RNApol I to start rDNA transcription (Grandori et al., 2005; O'Sullivan et al., 2002). In addition, Grandori et al. described that there are about 8 E-box sequences within the transcribed region of the rDNA and a cluster of more than 15 E-boxes in the 3' end of the transcription termination region that extends in the intergenic region (IGS) of the rDNA repeat. Furthermore, they described that MYC binds to these regions and also to the promoter and transcription start site of the rDNA locus. In this Thesis we describe that MXD1 also binds to the rDNA and that it does it with preference for the intergenic regions (IGS) where the E-box sequences have been described. In addition, by PLA and conventional co-immunoprecipitation we have found that MXD1 interacts with UBF. We do not know yet if this interaction is direct or indirect as they could be forming a molecular complex with other intermediate proteins. These findings on MXD1 in the nucleolus suggest that MXD1 might be involved in the regulation of rDNA transcription. However, we only detected a small change in ribosomal RNA levels in MXD1 knock-down cells. The transcription of the rDNA is highly regulated by many different mechanisms that act at the transcriptional machinery and chromatin conformation levels. One explanation that could explain why knocking-down MXD1 does not lead to larger changes in RNA synthesis could be that MXD1 is not directly involved in rDNA transcriptional repression but it serves as an ancillary factor for other protein(s) of the RNApol I complex. Also the fact that MXD1 binds preferentially to IGS in the rDNA supports an indirect involvement of MXD1 in rDNA transcription regulation. Instead it might be controlling a particular chromatin conformation allowing or impairing the accession of other factors or even modifying other proteins as a consequence of the complexes that it forms with HDAC and demethylases proteins. On the other hand, it has been also described that many nuclear proteins not involved in rRNA synthesis accumulate in the nucleolus when they are not required in that moment of the cell biology or to be labelled for degradation (Arabi et al., 2003; Pederson and Tsai, 2009). Thus it is possible then that the nucleolus acts as a transient reservoir of MXD1, providing MXD1 protein when a cell receives a differentiation or cell arrest stimulus.

5.2. MNT

MNT protein is one of the best studied MXD members. It is the most divergent member of the MXD family regarding its size and expression pattern. MNT expression does not significantly fluctuate between the growing and quiescent states, instead it has a constitutive expression pattern. It is considered one of the major antagonists of MYC function since it is also expressed even when MYC expression is high, conversely to the other MXD members (see Introduction). This fact makes MNT to be considered as "buffer" of MYC activity.

5.2.1. MNT does not enhance a differentiation program in UR61 cells

As mention before, previous work in our lab described that MYC is able to block the differentiation of UR61 cells without MAX. Although MNT involvement in differentiation is not clear, it is clear the opposite effect that it has over MYC activity in proliferation and transformation (Hurlin et al., 1997a, 2003). Since the differentiation blockade is achieved when MYC is overexpressed in UR61 cells (Vaque et al., 2008) we hypothesized that MNT overexpression in this system would create a better environment for differentiation. However, MNT overexpression in UR61 cells does not enhance the differentiation phenotype induced by N-RAS and it neither leads to an upregulation of neuronal markers such as *NGFR*, *GAP43* and *VGF* or *JUN* which is a key transcriptional factor in the neuronal-like differentiation program of UR61 cells (Vaque et al., 2008). Two explanations for this might be that MNT is not directly involved in differentiation of UR61 cells or that it needs MAX for such function.

5.2.2. MNT expression and MAX

MNT shows a constitutive expression in most cells tested. We wondered whether MNT levels in UR61 cells were in the range of that observed in MAX-expressing cells. We analysed the expression of MNT in different cell lines that normally express MAX, originated from different tissues, like HEK293T, K562 and HeLa cells and in UR61 and UR61-derived cells. We found that MNT expression is higher in UR61 and UR61-derived cells in comparison with the other cell lines.

It is worth to note that in the cell lines studied with MAX expression (HEK293T, K562 and HeLa), MNT expression is lower than in UR61 cells. In addition, when MAX is expressed in UR61, MNT expression (at both mRNA and protein level) is lower than in UR61 cells without MAX. Furthermore, the MNT protein is downregulated with increasing amounts of MAX in K562 cells. On the contrary, MAX knock-down K562 cells present increase MNT expression at mRNA and protein levels. These results confirm the effect of MAX over MNT expression in different systems.

In conclusion, MAX presence leads to a downregulation of MNT. We wondered whether MNT promoter contains E-box sequences where MAX dimers (homo or heterodimers) could bind and regulate MNT gene transcription. Bioinformatics analysis of the *MNT* promoters of human, mouse and rat species have revealed that the MNT gene has two E-boxes (one canonical and one non-canonical) at -788 and

-289 bp from the human TSS; -595 and -123 bp from the mouse TSS and -593 and -123 bp from the rat TSS. In addition, an alignment of these *MNT* promoter sequences from human, mouse and rat indicates that these regions present high homology in mammals. Furthermore, these conserved E boxes in the mammal *MNT* promoters suggest a *MNT* regulation by MAX-containing dimers such as MYC-MAX or MXDs-MAX.

Taking advantage of the ChIP-seq data available from the ENCODE project, we have studied if the members of the MYC/MAX/MXD network available in the project (MAX, MYC and MXI1) bind to the human *MNT* promoter in those regions where the two E-boxes map. We have found in all cell lines used in the ENCODE project that all three MAX, MYC and MXI1 proteins present peaks in 1000 bp upstream the TSS and first exon of human MNT gene suggesting that MAX dimers whether with MYC or MXD proteins bind to human *MNT* promoter.

5.2.3. MNT autoregulation

We have shown that when MAX is present, MNT forms MNT-MAX heterodimers and bind to E-box sequences to regulate gene transcription in UR61 cells. Moreover, we found that MNT and MAX bind to the rat *MNT* promoter in UR61-MT-MAX cells that express the MAX protein but not in UR61-MT-Hebo cells without MAX suggesting that MNT needs MAX to bind and possibly regulate its own expression (figure 5.1).

This MNT autoregulation is further confirmed by the luciferase assays performed with a reporter harbouring the 800 bp upstream the TSS of human *MNT* (constructed in this Thesis). These luciferase assays were done overexpressing MAX alone or MNT together with MAX in UR61 or alternatively MNT in HEK293T (which express MAX). All the assays show that when MAX is present there is a decrease in the luciferase activity that is enhanced upon MNT transfection, suggesting that MNT-MAX heterodimers regulate negatively this *MNT* promoter.

This MNT negative autoregulation explains why MAX ectopic expression leads to a decrease in MNT levels in UR61: MNT-MAX dimers would be rapidly formed as MNT is highly and constitutively expressed in UR61 cells and they would negatively regulate *MNT* expression. On the contrary, the lack of MAX in UR61 might explain at least in part why MNT is highly expressed in UR61 cells in comparison with other cell lines since there would be no MAX-dependent negative gene regulation on MNT gene.

Moreover, we demonstrated that MNT expression is autocontrolled not only at the level of transcription but also at the level of protein stability. We observed that MNT levels did not increase upon transfection of MNT expression vectors into UR61 cells. We explored the possibility that MNT was being controlled at protein levels by transfecting a MNT expressing vector and treating the cells with bortezomib to inhibit proteosome-dependent protein degradation. The results showed that MNT levels are highly increased in the MNT-transfected UR61 cells treated with bortezomib. Altogether, our data show that MNT levels are tightly controlled in the UR61 cells so that an increase of MNT over its basal levels results in its degradation. However, the mechanism by which MNT “senses” its own protein levels is unknown.

5.2.4. MNT localizes in the nucleus and cytoplasm when it lacks MAX

It has not been described a nuclear localization signal (NLS) in MNT protein. However, due to its amino acid composition and its heterodimerization with MAX (which does have one NLS), MNT localizes in the nucleus of cells where it works as a transcriptional repressor.

We have shown that the lack of MAX leads to an upregulation of MNT protein. We have studied MNT localization when MAX is not present in UR61 and MAX-silenced K562 cells and we have found that MNT, in the absence of MAX, is nuclear but also cytoplasmic. This cytoplasmic localization seems to be a consequence of the higher amounts of MNT in those conditions since the amounts of MNT in the nucleus remains the same in MAX presence/absence but MNT levels in the cytoplasm increase when MAX is not present (figure 5.1). This suggests that when MNT is in excess, it accumulates in the cytoplasm instead of being degraded. However, as discussed above, MNT is degraded if excessive accumulation occurs. On the other hand, the existence of cytoplasmic MNT in MAX-deficient cells, suggest that it may exert functions different from that of transcriptional regulation.

5.2.5. MNT interactome dependent on MAX presence

It is well-known that MNT interacts with MAX and with the mSIN3A and B co-repressor proteins to regulate gene transcription (Hurlin et al., 1997b; Meroni et al., 1997). Also, it was described that MNT interacts with MLX (Max-Like protein X) (Meroni et al., 2000), a protein very similar to MAX that also binds to E-boxes in dimers and that takes part as the key element in another gene regulation network. MNT-MLX interaction was described to be an alternative dimer formation for MNT with capacities similar to MNT-MAX regarding E-box binding and gene regulation (Meroni et al., 2000).

In this Thesis we have analysed by MNT immunoprecipitation followed by mass spectrometry which proteins interact with MNT in UR61-MT-Hebo and UR61-MT-MAX cells expressing the MAX protein. We performed three independent immunoprecipitations for each cell line and we have found 11 proteins that interact with MNT only when MAX is not present and 47 that interact with MNT only when MAX is present (figure 5.1). Five of these proteins interact with MNT in the lysates of both cell lines. So these interactions were detected in six independent immunoprecipitation experiments in the absence and presence of MAX meaning that they likely interact with MNT in a MAX-independent manner. We focused on two of these interacting proteins: REL and CCDC6. REL is an NF-κB transcription factor and CCDC6 takes part in the RET-PTC1 fusion oncoprotein as a consequence chromosomal rearrangement frequently found in papillary thyroid carcinoma. REL and CCDC6 are proteins involved in cell survival and cancer and in basal conditions, they have cytoplasmic localization. We have confirmed MNT-REL interaction of endogenous proteins in UR61 and we have observed an effect of MNT on NF-κB signalling (discussed below.). However, we could not confirm the interaction MNT-CCDC6 possibly because the antibody used for CCDC6 is raised against human CCDC6 protein. However, we have confirmed MNT-CCDC6 interaction in HEK293T cells. In addition, we have found that the region of CCDC6 that comprised between amino acids 101 and 223 is required for MNT binding. It is noteworthy that the region of CCDC6 involved in the RET-PTC1 fusion oncoprotein (1 to 101 amino acids) does not interact with MNT.

So it is conceivable that the lack of MNT interaction contributes to the oncogenic activity of the rearranged CCDC6 gene in these thyroid carcinomas.

Interestingly, neither MLX nor mSIN3 A or B have been found in the mass spectrometry experiments

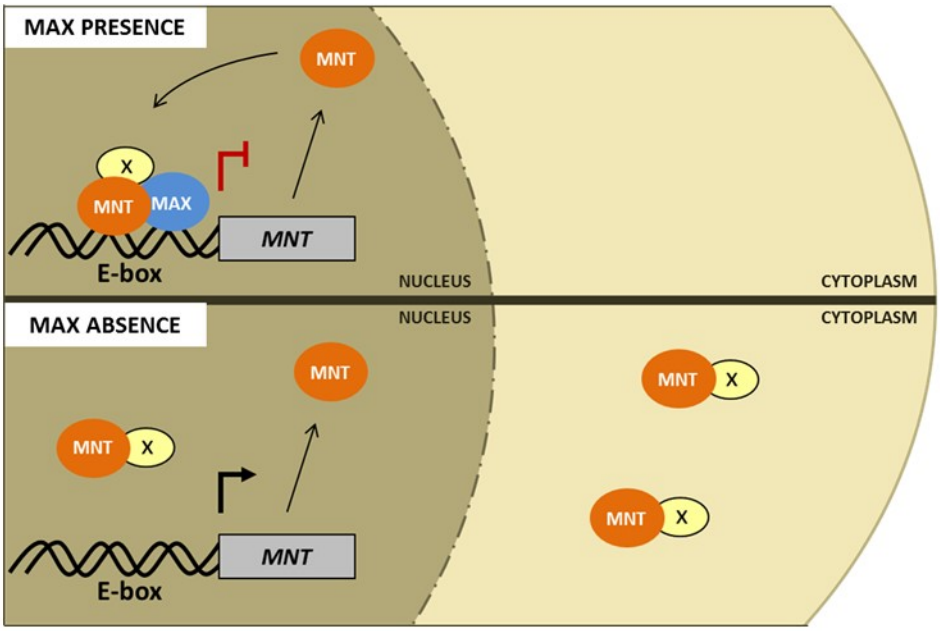

Figure 5.1.- MNT autoregulation and relocalization. MNT in heterodimerization with MAX respresses its own expression and localizes in the nucleus. MNT in the absence of MAX is not able to repress its own expression and its excessed expression goes to the cytoplasm. Different proteins interact with MNT in an MAX-independent manner (see text for details). X refers to possible MNT interactors different from MAX.

despite being expressed in UR61 cells (data not shown). In contrast, MAX was detected among the MNT immunoprecipitated proteins from UR61-MT-MAX expressing MAX confirming that the technique worked properly. The fact that MLX does not appear in these mass spectrometry experiments suggests that MLX is not supplying MAX functions in UR61 cells so that all MNT functions described in UR61 would be MAX but also MLX independent.

5.2.6. Effects of MNT silencing on UR61 growth

MNT expression, localization and interacting partners in UR61 is altered when MAX is expressed in UR61 cells. These data were suggesting that MNT has a role even in MAX absence. We have silenced MNT with a plasmid containing a shRNA against MNT.

Using this strategy we have found that the absence of MNT in MAX-deficient UR61 cells impairs cell growth. It seems that this effect is in part due to: 1) a proliferative arrest that it is accompanied by downregulation and upregulation of genes involved in cell cycle progression such as cyclin A (CCNA2) and the cdk inhibitor p57, respectively; and 2) an increase in apoptotic cell death as observed by FACS

of propidium iodide stained cells, PARP1 cleavage and the downregulation of the antiapoptotic protein BCL-XL.

The fact that MNT depletion impairs UR61 proliferation is in the opposite line of what it was observed in other cells (MEFs) that express MAX, where MNT downregulation leads to similar effects of those of MYC overexpression, i.e. increased proliferation and transformation capacities (Hurlin et al., 2003). However, re-expression of MAX in UR61 does not reverse this effect on cell proliferation and apoptosis in UR61 cells. In fact, at longer periods of MAX expression there is a cooperation with MNT depletion in proliferation arrest.

5.2.7. MNT and NF-κB

Taking into account that one of the major functions attributed to the NF-κB pathway is related to cell survival and that we have found that MNT interacts with the NF-κB member REL in UR61 cells, we have studied whether this interaction was affecting the NF-κB pathway.

On the one hand, we have found that the NF-κB canonical pathway is activated in UR61 upon TNFα treatment as assessed by REL and RELA nuclear translocation. In addition we have found that the activation of this pathway impairs UR61 cell growth. Interestingly, MNT silencing increases the antiproliferative effect of TNFα treatment in UR61. On the other hand, luciferase assays with a luciferase reporter vector containing NF-κB binding elements show that MNT silencing increases the transcriptional effect of NF-κB meanwhile MNT overexpression decreases it.

These results suggest that MNT is negatively modulating the NF-κB pathway and that it might do that throughout its interaction with the REL protein. It is possible that MNT contributes to maintain a cytoplasmic localization of the NF-κB dimers and when MNT is depleted with the shRNA plasmid, NF-κB dimers are liberated to enter the nuclei and transactivate their targets genes. Another hypothesis would be that MNT, throughout the interaction with REL leads to the formation of a repressor complex (since MNT is a transcriptional repressor) at the promoters of the genes that are normally activated by REL so that decreasing their expression levels and increasing them when MNT is silenced.

Furthermore, considering that MAX re-expression in UR61 and PC12 decreases their proliferation rate and that MAX expression in UR61 leads to a downregulation of MNT it can be also possible that in UR61 cells expressing MAX, MNT downregulation leads to a higher activation of the NF-κB pathway (that induces cell death in UR61 cells) being this fact among many others one of the reasons why MAX expression decreases UR61 cell growth capacity.

5.2.8. MNT silencing and UR61 transcriptome

We have seen that MNT silencing affects UR61 cell growth. Since MNT is a transcription factor we decided to study how MNT silencing affected generally gene expression using the RNA-seq technology.

With this approach we have found that there are several genes involved in cell cycle progression and DNA damage response (annex 1) that are downregulated in MNT-silenced cells without MAX (UR61-

MT-Hebo) and with MAX (UR61-MT-MAX treated with Zn^{+2}). Again, the re-expression of MAX protein does not provoke broader changes in the transcriptome. This is concordant with the similar effects of MNT silencing on cell growth in UR61 with and without MAX at short periods.

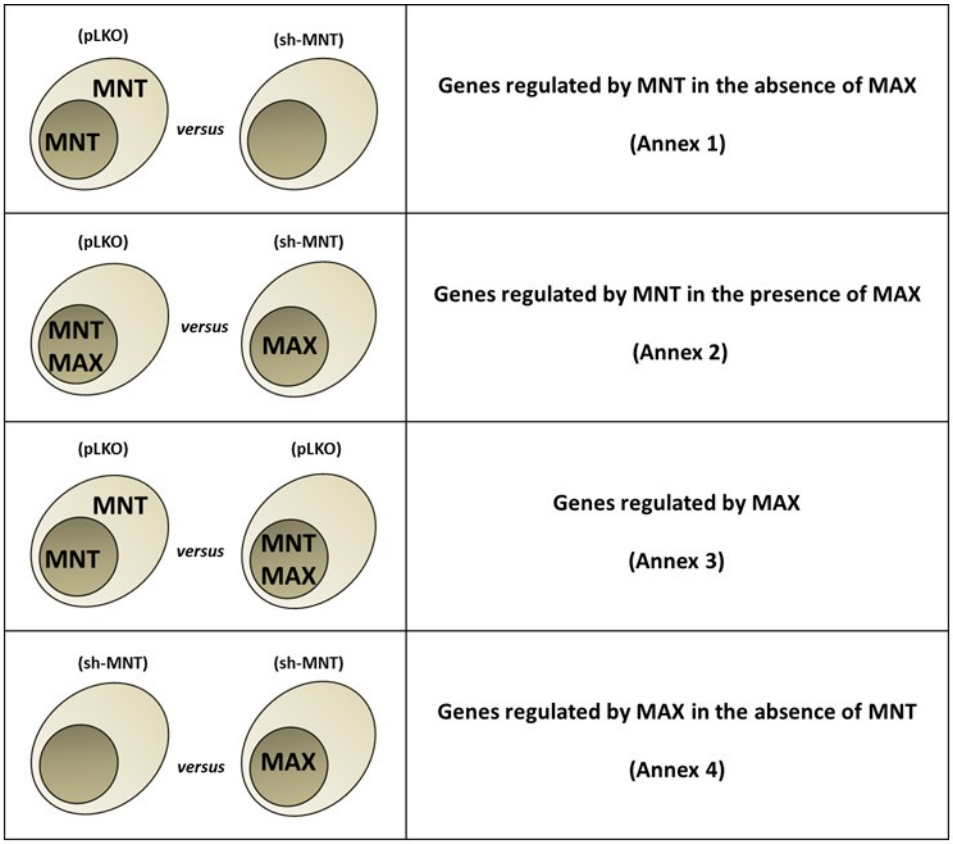

Figure 5.2.- Transcriptome analysis of MNT-depleted and MAX-restored UR61 cells. The different comparisons of the transcriptomes are indicated (see text for details).

In addition, there is also an alteration in the transcriptome provoked by MAX in UR61 cells. However, the genes altered or the direction of the alteration are different from those observed when MNT is depleted, another indirect evidence that shows that MNT silencing effects in UR61 do not depend on MAX.

In summary, it seems that MNT presence is important for UR61 cell survival and proliferation allowing the expression of genes involved in cell cycle progression and DNA repair. It might be possible that the absence of MNT leads to an increase in DNA damage by diverse mechanisms. For example it has been described the generation of reactive oxygen species (ROS) as a consequence of an altered metabolism in MNT-deficient cells (Link et al., 2012). If this is the case, the cells would stop cell cycle to try to repair this damage what is concordant with the downregulation of genes involved in cell proliferation (according to the RNA-seq data). However, this damage would not be efficiently repaired since the DNA repair genes are also downregulated when MNT is silenced in UR61 cells, leading to cell death.

Since the above results suggested that MNT is active as transcription factor in UR61, a ChIP-seq assay was done to try to find MNT target gene which regulation by MNT is independent of MAX. We have tried to validate some of the positive ChIP peaks for MNT found in UR61 with and without MAX but we have not been able to validate any of them so far. It is possible that the ChIP-seq technique has not enough sensitivity to detect reliable MNT binding to chromatin or that we need further analysis of the experiment to achieve true positive signals.

As a final conclusion, in this Thesis we have described new biological roles for MXD1 and MNT proteins. It is important to have a good knowledge of the behaviour of these proteins since they are part of the MYC/MAX/MXD network and thus they have an impact on MYC oncoprotein activity. In addition, the recent studies indicating an involvement of MAX in some tumors like human pheochromocytomas, paraganglyomas and small cell lung cancer highlighted the importance of understanding the role that these proteins play in the absence of MAX.

Conclusions

6. CONCLUSIONS

1. MXD1 is expressed in growing and undifferentiated cells and it localizes in the nucleoplasm and fibrillar centers of nucleoli.
2. MXD1 interacts with UBF, binds to rDNA and moderates rDNA transcription.
3. MXD1 in cells deficient in MAX, does not repress nor induce E-box containing promoters neither promotes UR61 cell differentiation or cell proliferation arrest.
4. MNT in the absence of MAX does not repress nor induce E-box containing promoters neither promotes UR61 cell differentiation.
5. MNT promoter is conserved in mammals and it presents two E-box sequences within 1000 bp upstream the TSS. MNT bound to MAX regulates negatively its own expression but not in the absence of MAX, leading to an upregulation of MNT expression.
6. MNT localizes in the nucleoplasm of cells but also in the cytoplasm in MAX-deficient cells.
7. Ectopic MNT expression is controlled at protein levels by proteasome degradation when it is in excess in the absence of MAX in UR61 cells.
8. MNT interacts with REL and CCDC6 in a MAX-independent manner and modulates NF-κB activity.
9. MNT presence is required for UR61 cell proliferation and viability and it regulates gene transcription of genes involved in such functions also in the absence of MAX.

Bibliography

7. BIBLIOGRAPHY:

Abrams, H.D., Rohrschneider, L.R., and Eisenman, R.N. (1982). Nuclear location of the putative transforming protein of avian myelocytomatosis virus. Cell *29*, 427-439.

Acosta, J.C., Ferrandiz, N., Bretones, G., Torrano, V., Blanco, R., Richard, C., O'Connell, B., Sedivy, J., Delgado, M.D., and Leon, J. (2008). Myc inhibits p27-induced erythroid differentiation of leukemia cells by repressing erythroid master genes without reversing p27-mediated cell cycle arrest. Molecular and cellular biology *28*, 7286-7295.

Adams, P.D. (2001). Regulation of the retinoblastoma tumor suppressor protein by cyclin/cdks. Biochimica et biophysica acta *1471*, M123-133.

Adhikari, A., Xu, M., and Chen, Z.J. (2007). Ubiquitin-mediated activation of TAK1 and IKK. Oncogene *26*, 3214-3226.

Adhikary, S., and Eilers, M. (2005). Transcriptional regulation and transformation by Myc proteins. Nature reviews *6*, 635-645.

Albert, T., Wells, J., Funk, J.O., Pullner, A., Raschke, E.E., Stelzer, G., Meisterernst, M., Farnham, P.J., and Eick, D. (2001). The chromatin structure of the dual c-myc promoter P1/P2 is regulated by separate elements. The Journal of biological chemistry *276*, 20482-20490.

Alitalo, K., and Schwab, M. (1986). Oncogene amplification in tumor cells. Advances in cancer research *47*, 235-281.

Amati, B., Brooks, M.W., Levy, N., Littlewood, T.D., Evan, G.I., and Land, H. (1993). Oncogenic activity of the c-Myc protein requires dimerization with Max. Cell *72*, 233-245.

Amati, B., Dalton, S., Brooks, M.W., Littlewood, T.D., Evan, G.I., and Land, H. (1992). Transcriptional activation by the human c-Myc oncoprotein in yeast requires interaction with Max. Nature *359*, 423-426.

Amin, C., Wagner, A.J., and Hay, N. (1993). Sequence-specific transcriptional activation by Myc and repression by Max. Molecular and cellular biology *13*, 383-390.

Andreassen, A., Oyjord, T., Hovig, E., Holm, R., Florenes, V.A., Nesland, J.M., Myklebost, O., Hoie, J., Bruland, O.S., Borresen, A.L., and et al. (1993). p53 abnormalities in different subtypes of human sarcomas. Cancer research *53*, 468-471.

Arabi, A., Rustum, C., Hallberg, E., and Wright, A.P. (2003). Accumulation of c-Myc and proteasomes at the nucleoli of cells containing elevated c-Myc protein levels. Journal of cell science *116*, 1707-1717.

Arnold, H.K., Zhang, X., Daniel, C.J., Tibbitts, D., Escamilla-Powers, J., Farrell, A., Tokarz, S., Morgan, C., and Sears, R.C. (2009). The Axin1 scaffold protein promotes formation of a degradation complex for c-Myc. The EMBO journal *28*, 500-512.

Arsura, M., Deshpande, A., Hann, S.R., and Sonenshein, G.E. (1995). Variant Max protein, derived by alternative splicing, associates with c-Myc in vivo and inhibits transactivation. Molecular and cellular biology *15*, 6702-6709.

Askew, D.S., Ashmun, R.A., Simmons, B.C., and Cleveland, J.L. (1991). Constitutive c-myc expression in an IL-3-dependent myeloid cell line suppresses cell cycle arrest and accelerates apoptosis. Oncogene *6*, 1915-1922.

Ayer, D.E., and Eisenman, R.N. (1993). A switch from Myc:Max to Mad:Max heterocomplexes accompanies monocyte/macrophage differentiation. Genes & development *7*, 2110-2119.

Ayer, D.E., Kretzner, L., and Eisenman, R.N. (1993). Mad: a heterodimeric partner for Max that antagonizes Myc transcriptional activity. Cell *72*, 211-222.

Ayer, D.E., Laherty, C.D., Lawrence, Q.A., Armstrong, A.P., and Eisenman, R.N. (1996). Mad proteins contain a dominant transcription repression domain. Molecular and cellular biology *16*, 5772-5781.

Ayer, D.E., Lawrence, Q.A., and Eisenman, R.N. (1995). Mad-Max transcriptional repression is mediated by ternary complex formation with mammalian homologs of yeast repressor Sin3. Cell *80*, 767-776.

Barth, T.F., Bentz, M., Leithauser, F., Stilgenbauer, S., Siebert, R., Schlotter, M., Schlenk, R.F., Dohner, H., and Moller, P. (2001). Molecular-cytogenetic comparison of mucosa-associated marginal zone B-cell lymphoma and large B-cell lymphoma arising in the gastro-intestinal tract. Genes, chromosomes & cancer *31*, 316-325.

Barth, T.F., Martin-Subero, J.I., Joos, S., Menz, C.K., Hasel, C., Mechtersheimer, G., Parwaresch, R.M., Lichter, P., Siebert, R., and Mooller, P. (2003). Gains of 2p involving the REL locus correlate with nuclear c-Rel protein accumulation in neoplastic cells of classical Hodgkin lymphoma. Blood *101*, 3681-3686.

Bazett-Jones, D.P., Leblanc, B., Herfort, M., and Moss, T. (1994). Short-range DNA looping by the Xenopus HMG-box transcription factor, xUBF. Science (New York, N.Y *264*, 1134-1137.

Bejarano, M.T., Albihn, A., Cornvik, T., Brijker, S.O., Asker, C., Osorio, L.M., and Henriksson, M. (2000). Inhibition of cell growth and apoptosis by inducible expression of the transcriptional repressor Mad1. Experimental cell research *260*, 61-72.

Belguise, K., and Sonenshein, G.E. (2007). PKCtheta promotes c-Rel-driven mammary tumorigenesis in mice and humans by repressing estrogen receptor alpha synthesis. The Journal of clinical investigation *117*, 4009-4021.

Berberich, S.J., and Cole, M.D. (1992). Casein kinase II inhibits the DNA-binding activity of Max homodimers but not Myc/Max heterodimers. Genes & development *6*, 166-176.

Biegel, J.A., Burk, C.D., Barr, F.G., and Emanuel, B.S. (1992). Evidence for a 17p tumor related locus distinct from p53 in pediatric primitive neuroectodermal tumors. Cancer research *52*, 3391-3395.

Biggiogera, M., Fakan, S., Kaufmann, S.H., Black, A., Shaper, J.H., and Busch, H. (1989). Simultaneous immunoelectron microscopic visualization of protein B23 and C23 distribution in the HeLa cell nucleolus. J Histochem Cytochem *37*, 1371-1374.

Billin, A.N., and Ayer, D.E. (2006). The Mlx network: evidence for a parallel Max-like transcriptional network that regulates energy metabolism. Current topics in microbiology and immunology *302*, 255-278.

Billin, A.N., Eilers, A.L., Coulter, K.L., Logan, J.S., and Ayer, D.E. (2000). MondoA, a novel basic helix-loop-helix-leucine zipper transcriptional activator that constitutes a positive branch of a max-like network. Molecular and cellular biology *20*, 8845-8854.

Billin, A.N., Eilers, A.L., Queva, C., and Ayer, D.E. (1999). Mlx, a novel Max-like BHLHZip protein that interacts with the Max network of transcription factors. The Journal of biological chemistry *274*, 36344-36350.

Bindra, R.S., and Glazer, P.M. (2007). Co-repression of mismatch repair gene expression by hypoxia in cancer cells: role of the Myc/Max network. Cancer letters *252*, 93-103.

Birrer, M.J., Raveh, L., Dosaka, H., and Segal, S. (1989). A transfected L-myc gene can substitute for c-myc in blocking murine erythroleukemia differentiation. Molecular and cellular biology *9*, 2734-2737.

Blackwood, E.M., and Eisenman, R.N. (1991). Max: a helix-loop-helix zipper protein that forms a sequence-specific DNA-binding complex with Myc. Science *251*, 1211-1217.

Blackwood, E.M., Kretzner, L., and Eisenman, R.N. (1992a). Myc and Max function as a nucleoprotein complex. Curr Opin Genet Dev *2*, 227-235.

Blackwood, E.M., Luscher, B., and Eisenman, R.N. (1992b). Myc and Max associate in vivo. Genes & development *6*, 71-80.

Boisvert, F.M., van Koningsbruggen, S., Navascues, J., and Lamond, A.I. (2007). The multifunctional nucleolus. Nature reviews *8*, 574-585.

Bouchard, C., Dittrich, O., Kiermaier, A., Dohmann, K., Menkel, A., Eilers, M., and Luscher, B. (2001). Regulation of cyclin D2 gene expression by the Myc/Max/Mad network: Myc-dependent TRRAP recruitment and histone acetylation at the cyclin D2 promoter. Genes & development *15*, 2042-2047.

Bouchard, C., Thieke, K., Maier, A., Saffrich, R., Hanley-Hyde, J., Ansorge, W., Reed, S., Sicinski, P., Bartek, J., and Eilers, M. (1999). Direct induction of cyclin D2 by Myc contributes to cell cycle progression and sequestration of p27. The EMBO journal *18*, 5321-5333.

Boult, J.K., Taniere, P., Hallissey, M.T., Campbell, M.J., and Tselepis, C. (2008). Oesophageal adenocarcinoma is associated with a deregulation in the MYC/MAX/MAD network. British journal of cancer *98*, 1985-1992.

Boxer, L.M., and Dang, C.V. (2001). Translocations involving c-myc and c-myc function. Oncogene *20*, 5595-5610.

Brenner, C., Deplus, R., Didelot, C., Loriot, A., Vire, E., De Smet, C., Gutierrez, A., Danovi, D., Bernard, D., Boon, T.*, et al.* (2005). Myc represses transcription through recruitment of DNA methyltransferase corepressor. The EMBO journal *24*, 336-346.

Bretones, G., Delgado, M.D., and Leon, J. (2014). Myc and cell cycle control. Biochimica et biophysica acta.

Brewer, G., and Ross, J. (1988). Poly(A) shortening and degradation of the 3' A+U-rich sequences of human c-myc mRNA in a cell-free system. Molecular and cellular biology *8*, 1697-1708.

Burnichon, N., Cascon, A., Schiavi, F., Morales, N.P., Comino-Mendez, I., Abermil, N., Inglada-Perez, L., de Cubas, A.A., Amar, L., Barontini, M.*, et al.* (2012). MAX mutations cause hereditary and sporadic pheochromocytoma and paraganglioma. Clin Cancer Res *18*, 2828-2837.

Bush, A., Mateyak, M., Dugan, K., Obaya, A., Adachi, S., Sedivy, J., and Cole, M. (1998). c-myc null cells misregulate cad and gadd45 but not other proposed c-Myc targets. Genes & development *12*, 3797-3802.

Caburet, S., Conti, C., Schurra, C., Lebofsky, R., Edelstein, S.J., and Bensimon, A. (2005). Human ribosomal RNA gene arrays display a broad range of palindromic structures. Genome research *15*, 1079-1085.

Cairo, S., Merla, G., Urbinati, F., Ballabio, A., and Reymond, A. (2001). WBSCR14, a gene mapping to the Williams--Beuren syndrome deleted region, is a new member of the Mlx transcription factor network. Human molecular genetics *10*, 617-627.

Cannell, I.G., Kong, Y.W., Johnston, S.J., Chen, M.L., Collins, H.M., Dobbyn, H.C., Elia, A., Kress, T.R., Dickens, M., Clemens, M.J.*, et al.* (2010). p38 MAPK/MK2-mediated induction of miR-34c following DNA damage prevents Myc-dependent DNA replication. Proceedings of the National Academy of Sciences of the United States of America *107*, 5375-5380.

Celetti, A., Cerrato, A., Merolla, F., Vitagliano, D., Vecchio, G., and Grieco, M. (2004). H4(D10S170), a gene frequently rearranged with RET in papillary thyroid carcinomas: functional characterization. Oncogene *23*, 109-121.

Cerni, C., Skrzypek, B., Popov, N., Sasgary, S., Schmidt, G., Larsson, L.G., Luscher, B., and Henriksson, M. (2002). Repression of in vivo growth of Myc/Ras transformed tumor cells by Mad1. Oncogene *21*, 447-459.

Cetinkaya, C., Hultquist, A., Su, Y., Wu, S., Bahram, F., Pahlman, S., Guzhova, I., and Larsson, L.G. (2007). Combined IFN-gamma and retinoic acid treatment targets the N-Myc/Max/Mad1 network resulting in repression of N-Myc target genes in MYCN-amplified neuroblastoma cells. Molecular cancer therapeutics *6*, 2634-2641.

Charron, J., Malynn, B.A., Fisher, P., Stewart, V., Jeannotte, L., Goff, S.P., Robertson, E.J., and Alt, F.W. (1992). Embryonic lethality in mice homozygous for a targeted disruption of the N-myc gene. Genes & development *6*, 2248-2257.

Chen, X., Kandasamy, K., and Srivastava, R.K. (2003). Differential roles of RelA (p65) and c-Rel subunits of nuclear factor kappa B in tumor necrosis factor-related apoptosis-inducing ligand signaling. Cancer research *63*, 1059-1066.

Cheng, S.W., Davies, K.P., Yung, E., Beltran, R.J., Yu, J., and Kalpana, G.V. (1999). c-MYC interacts with INI1/hSNF5 and requires the SWI/SNF complex for transactivation function. Nature genetics *22*, 102-105.

Chin, L., Schreiber-Agus, N., Pellicer, I., Chen, K., Lee, H.W., Dudast, M., Cordon-Cardo, C., and DePinho, R.A. (1995). Contrasting roles for Myc and Mad proteins in cellular growth and differentiation. Proceedings of the National Academy of Sciences of the United States of America *92*, 8488-8492.

Cho, K., Shin, H.W., Kim, Y.I., Cho, C.H., Chun, Y.S., Kim, T.Y., and Park, J.W. (2013). Mad1 mediates hypoxia-induced doxorubicin resistance in colon cancer cells by inhibiting mitochondrial function. Free radical biology & medicine *60*, 201-210.

Cole, M.D. (1986). The myc oncogene: its role in transformation and differentiation. Annual review of genetics *20*, 361-384.

Coller, H.A., Grandori, C., Tamayo, P., Colbert, T., Lander, E.S., Eisenman, R.N., and Golub, T.R. (2000). Expression analysis with oligonucleotide microarrays reveals that MYC regulates genes involved in growth, cell cycle, signaling, and adhesion. Proceedings of the National Academy of Sciences of the United States of America *97*, 3260-3265.

Comai, L., Tanese, N., and Tjian, R. (1992). The TATA-binding protein and associated factors are integral components of the RNA polymerase I transcription factor, SL1. Cell *68*, 965-976.

Comai, L., Zomerdijk, J.C., Beckmann, H., Zhou, S., Admon, A., and Tjian, R. (1994). Reconstitution of transcription factor SL1: exclusive binding of TBP by SL1 or TFIID subunits. Science (New York, N.Y *266*, 1966-1972.

Comino-Mendez, I., Gracia-Aznarez, F.J., Schiavi, F., Landa, I., Leandro-Garcia, L.J., Leton, R., Honrado, E., Ramos-Medina, R., Caronia, D., Pita, G.*, et al.* (2011). Exome sequencing identifies MAX mutations as a cause of hereditary pheochromocytoma. Nature genetics *43*, 663-667.

Conacci-Sorrell, M., Ngouenet, C., and Eisenman, R.N. (2010). Myc-nick: a cytoplasmic cleavage product of Myc that promotes alpha-tubulin acetylation and cell differentiation. Cell *142*, 480-493.

Copenhaver, G.P., Putnam, C.D., Denton, M.L., and Pikaard, C.S. (1994). The RNA polymerase I transcription factor UBF is a sequence-tolerant HMG-box protein that can recognize structured nucleic acids. Nucleic acids research *22*, 2651-2657.

Coppola, J.A., and Cole, M.D. (1986). Constitutive c-myc oncogene expression blocks mouse erythroleukaemia cell differentiation but not commitment. Nature *320*, 760-763.

Cornelius, P., MacDougald, O.A., and Lane, M.D. (1994). Regulation of adipocyte development. Annual review of nutrition *14*, 99-129.

Cory, S. (1986). Activation of cellular oncogenes in hemopoietic cells by chromosome translocation. Advances in cancer research *47*, 189-234.

Cowley, S., Paterson, H., Kemp, P., and Marshall, C.J. (1994). Activation of MAP kinase kinase is necessary and sufficient for PC12 differentiation and for transformation of NIH 3T3 cells. Cell *77*, 841-852.

Cowling, V.H., Chandriani, S., Whitfield, M.L., and Cole, M.D. (2006). A conserved Myc protein domain, MBIV, regulates DNA binding, apoptosis, transformation, and G2 arrest. Molecular and cellular biology *26*, 4226-4239.

Crews, S., Barth, R., Hood, L., Prehn, J., and Calame, K. (1982). Mouse c-myc oncogene is located on chromosome 15 and translocated to chromosome 12 in plasmacytomas. Science (New York, N.Y *218*, 1319-1321.

Cultraro, C.M., Bino, T., and Segal, S. (1997a). Function of the c-Myc antagonist Mad1 during a molecular switch from proliferation to differentiation. Molecular and cellular biology *17*, 2353-2359.

Cultraro, C.M., Bino, T., and Segal, S. (1997b). Regulated expression and function of the c-Myc antagonist, Mad1, during a molecular switch from proliferation to differentiation. Current topics in microbiology and immunology *224*, 149-158.

Curry, C.V., Ewton, A.A., Olsen, R.J., Logan, B.R., Preti, H.A., Liu, Y.C., Perkins, S.L., and Chang, C.C. (2009). Prognostic impact of C-REL expression in diffuse large B-cell lymphoma. Journal of hematopathology *2*, 20-26.

Cvekl, A., Jr., Zavadil, J., Birshtein, B.K., Grotzer, M.A., and Cvekl, A. (2004). Analysis of transcripts from 17p13.3 in medulloblastoma suggests ROX/MNT as a potential tumour suppressor gene. Eur J Cancer *40*, 2525-2532.

Dalla-Favera, R., Bregni, M., Erikson, J., Patterson, D., Gallo, R.C., and Croce, C.M. (1982a). Human c-myc onc gene is located on the region of chromosome 8 that is translocated in Burkitt lymphoma cells. Proceedings of the National Academy of Sciences of the United States of America *79*, 7824-7827.

Dalla-Favera, R., Gelmann, E.P., Martinotti, S., Franchini, G., Papas, T.S., Gallo, R.C., and Wong-Staal, F. (1982b). Cloning and characterization of different human sequences related to the onc gene (v-myc) of avian myelocytomatosis virus (MC29). Proceedings of the National Academy of Sciences of the United States of America *79*, 6497-6501.

Dang, C.V. (2012). MYC on the path to cancer. Cell *149*, 22-35.

Dang, C.V., and Lee, W.M. (1988). Identification of the human c-myc protein nuclear translocation signal. Molecular and cellular biology *8*, 4048-4054.

Dang, C.V., McGuire, M., Buckmire, M., and Lee, W.M. (1989). Involvement of the 'leucine zipper' region in the oligomerization and transforming activity of human c-myc protein. Nature *337*, 664-666.

Dang, C.V., O'Donnell, K.A., Zeller, K.I., Nguyen, T., Osthus, R.C., and Li, F. (2006). The c-Myc target gene network. Seminars in cancer biology *16*, 253-264.

Dansen, T.B., Whitfield, J., Rostker, F., Brown-Swigart, L., and Evan, G.I. (2006). Specific requirement for Bax, not Bak, in Myc-induced apoptosis and tumor suppression in vivo. The Journal of biological chemistry *281*, 10890-10895.

Dejardin, E., Droin, N.M., Delhase, M., Haas, E., Cao, Y., Makris, C., Li, Z.W., Karin, M., Ware, C.F., and Green, D.R. (2002). The lymphotoxin-beta receptor induces different patterns of gene expression via two NF-kappaB pathways. Immunity *17*, 525-535.

Delgado, M.D., Chernukhin, I.V., Bigas, A., Klenova, E.M., and Leon, J. (1999). Differential expression and phosphorylation of CTCF, a c-myc transcriptional regulator, during differentiation of human myeloid cells. FEBS Lett *444*, 5-10.

Delgado, M.D., Lerga, A., Canelles, M., Gomez-Casares, M.T., and Leon, J. (1995). Differential regulation of Max and role of c-Myc during erythroid and myelomonocytic differentiation of K562 cells. Oncogene *10*, 1659-1665.

Delmore, J.E., Issa, G.C., Lemieux, M.E., Rahl, P.B., Shi, J., Jacobs, H.M., Kastritis, E., Gilpatrick, T., Paranal, R.M., Qi, J.*, et al.* (2011). BET bromodomain inhibition as a therapeutic strategy to target c-Myc. Cell *146*, 904-917.

DePinho, R.A., Schreiber-Agus, N., and Alt, F.W. (1991). myc family oncogenes in the development of normal and neoplastic cells. Adv Cancer Res *57*, 1-46.

Devilee, P., van den Broek, M., Kuipers-Dijkshoorn, N., Kolluri, R., Khan, P.M., Pearson, P.L., and Cornelisse, C.J. (1989). At least four different chromosomal regions are involved in loss of heterozygosity in human breast carcinoma. Genomics *5*, 554-560.

Dezfouli, S., Bakke, A., Huang, J., Wynshaw-Boris, A., and Hurlin, P.J. (2006). Inflammatory disease and lymphomagenesis caused by deletion of the Myc antagonist Mnt in T cells. Molecular and cellular biology *26*, 2080-2092.

Di Cristofano, A., and Pandolfi, P.P. (2000). The multiple roles of PTEN in tumor suppression. Cell *100*, 387-390.

Dubois, N.C., Adolphe, C., Ehninger, A., Wang, R.A., Robertson, E.J., and Trumpp, A. (2008). Placental rescue reveals a sole requirement for c-Myc in embryonic erythroblast survival and hematopoietic stem cell function. Development *135*, 2455-2465.

Duesberg, P.H., and Vogt, P.K. (1979). Avian acute leukemia viruses MC29 and MH2 share specific RNA sequences: evidence for a second class of transforming genes. Proceedings of the National Academy of Sciences of the United States of America *76*, 1633-1637.

Eberhardy, S.R., D'Cunha, C.A., and Farnham, P.J. (2000). Direct examination of histone acetylation on Myc target genes using chromatin immunoprecipitation. The Journal of biological chemistry *275*, 33798-33805.

Eberhardy, S.R., and Farnham, P.J. (2001). c-Myc mediates activation of the cad promoter via a post-RNA polymerase II recruitment mechanism. The Journal of biological chemistry *276*, 48562-48571.

Edelmann, J., Holzmann, K., Miller, F., Winkler, D., Buhler, A., Zenz, T., Bullinger, L., Kuhn, M.W., Gerhardinger, A., Bloehdorn, J.*, et al.* (2012). High-resolution genomic profiling of chronic lymphocytic leukemia reveals new recurrent genomic alterations. Blood *120*, 4783-4794.

Eilers, M., and Eisenman, R.N. (2008). Myc's broad reach. Genes & development *22*, 2755-2766.

Eilers, M., Picard, D., Yamamoto, K.R., and Bishop, J.M. (1989). Chimaeras of myc oncoprotein and steroid receptors cause hormone-dependent transformation of cells. Nature *340*, 66-68.

Eilers, M., Schirm, S., and Bishop, J.M. (1991). The MYC protein activates transcription of the alpha-prothymosin gene. The EMBO journal *10*, 133-141.

Eisenman, R.N. (2000). The Max network: coordinated transcriptional regulation of cell growth and proliferation. Harvey lectures *96*, 1-32.

Eisenman, R.N., and Hann, S.R. (1985). Proteins expressed by the c-myc oncogene in lymphomas of human and avian origin. Proc R Soc Lond B Biol Sci *226*, 73-78.

Ekholm, S.V., and Reed, S.I. (2000). Regulation of G(1) cyclin-dependent kinases in the mammalian cell cycle. Current opinion in cell biology *12*, 676-684.

Evan, G.I., Wyllie, A.H., Gilbert, C.S., Littlewood, T.D., Land, H., Brooks, M., Waters, C.M., Penn, L.Z., and Hancock, D.C. (1992). Induction of apoptosis in fibroblasts by c-myc protein. Cell *69*, 119-128.

Facchini, L.M., Chen, S., Marhin, W.W., Lear, J.N., and Penn, L.Z. (1997). The Myc negative autoregulation mechanism requires Myc-Max association and involves the c-myc P2 minimal promoter. Molecular and cellular biology *17*, 100-114.

Faiola, F., Liu, X., Lo, S., Pan, S., Zhang, K., Lymar, E., Farina, A., and Martinez, E. (2005). Dual regulation of c-Myc by p300 via acetylation-dependent control of Myc protein turnover and coactivation of Myc-induced transcription. Molecular and cellular biology *25*, 10220-10234.

Fajas, L., Fruchart, J.C., and Auwerx, J. (1998). Transcriptional control of adipogenesis. Current opinion in cell biology *10*, 165-173.

Fernandez-Capetillo, O., Lee, A., Nussenzweig, M., and Nussenzweig, A. (2004). H2AX: the histone guardian of the genome. DNA repair *3*, 959-967.

Foley, K.P., McArthur, G.A., Queva, C., Hurlin, P.J., Soriano, P., and Eisenman, R.N. (1998). Targeted disruption of the MYC antagonist MAD1 inhibits cell cycle exit during granulocyte differentiation. The EMBO journal *17*, 774-785.

Frank, S.R., Parisi, T., Taubert, S., Fernandez, P., Fuchs, M., Chan, H.M., Livingston, D.M., and Amati, B. (2003). MYC recruits the TIP60 histone acetyltransferase complex to chromatin. EMBO Rep *4*, 575-580.

Frank, S.R., Schroeder, M., Fernandez, P., Taubert, S., and Amati, B. (2001). Binding of c-Myc to chromatin mediates mitogen-induced acetylation of histone H4 and gene activation. Genes & development *15*, 2069-2082.

Freytag, S.O. (1988). Enforced expression of the c-myc oncogene inhibits cell differentiation by precluding entry into a distinct predifferentiation state in G0/G1. Molecular and cellular biology *8*, 1614-1624.

Freytag, S.O., Dang, C.V., and Lee, W.M. (1990). Definition of the activities and properties of c-myc required to inhibit cell differentiation. Cell Growth Differ *1*, 339-343.

Freytag, S.O., and Geddes, T.J. (1992). Reciprocal regulation of adipogenesis by Myc and C/EBP alpha. Science *256*, 379-382.

Friedrich, J.K., Panov, K.I., Cabart, P., Russell, J., and Zomerdijk, J.C. (2005). TBP-TAF complex SL1 directs RNA polymerase I pre-initiation complex formation and stabilizes upstream binding factor at the rDNA promoter. The Journal of biological chemistry *280*, 29551-29558.

Fruehauf, J.P., and Meyskens, F.L., Jr. (2007). Reactive oxygen species: a breath of life or death? Clin Cancer Res *13*, 789-794.

Fu, T.J., Peng, J., Lee, G., Price, D.H., and Flores, O. (1999). Cyclin K functions as a CDK9 regulatory subunit and participates in RNA polymerase II transcription. The Journal of biological chemistry *274*, 34527-34530.

Fullard, N., Wilson, C.L., and Oakley, F. (2012). Roles of c-Rel signalling in inflammation and disease. The international journal of biochemistry & cell biology *44*, 851-860.

Gandarillas, A., and Watt, F.M. (1995). Changes in expression of members of the fos and jun families and myc network during terminal differentiation of human keratinocytes. Oncogene *11*, 1403-1407.

Garcia-Sanz, P., Quintanilla, A., Lafita, M.C., Moreno-Bueno, G., Garcia-Gutierrez, L., Tabor, V., Varela, I., Shiio, Y., Larsson, L.G., Portillo, F., and Leon, J. (2014). Sin3b interacts with Myc and decreases Myc levels. The Journal of biological chemistry *289*, 22221-22236.

Gartel, A.L., Ye, X., Goufman, E., Shianov, P., Hay, N., Najmabadi, F., and Tyner, A.L. (2001). Myc represses the p21(WAF1/CIP1) promoter and interacts with Sp1/Sp3. Proceedings of the National Academy of Sciences of the United States of America *98*, 4510-4515.

Gautier, T., Fomproix, N., Masson, C., Azum-Gelade, M.C., Gas, N., and Hernandez-Verdun, D. (1994). Fate of specific nucleolar perichromosomal proteins during mitosis: cellular distribution and association with U3 snoRNA. Biology of the cell / under the auspices of the European Cell Biology Organization *82*, 81-93.

Gavine, P.R., Neil, J.C., and Crouch, D.H. (1999). Protein stabilization: a common consequence of mutations in independently derived v-Myc alleles. Oncogene *18*, 7552-7558.

Ge, Z., Li, W., Wang, N., Liu, C., Zhu, Q., Bjorkholm, M., Gruber, A., and Xu, D. (2010). Chromatin remodeling: recruitment of histone demethylase RBP2 by Mad1 for transcriptional repression of a Myc target gene, telomerase reverse transcriptase. Faseb J *24*, 579-586.

Gebrane-Younes, J., Fomproix, N., and Hernandez-Verdun, D. (1997). When rDNA transcription is arrested during mitosis, UBF is still associated with non-condensed rDNA. Journal of cell science *110 (Pt 19)*, 2429-2440.

Gehring, S., Rottmann, S., Menkel, A.R., Mertsching, J., Krippner-Heidenreich, A., and Luscher, B. (2000). Inhibition of proliferation and apoptosis by the transcriptional repressor Mad1. Repression of Fas-induced caspase-8 activation. The Journal of biological chemistry *275*, 10413-10420.

Gerondakis, S., Strasser, A., Metcalf, D., Grigoriadis, G., Scheerlinck, J.Y., and Grumont, R.J. (1996). Rel-deficient T cells exhibit defects in production of interleukin 3 and granulocyte-macrophage colony-stimulating factor. Proceedings of the National Academy of Sciences of the United States of America *93*, 3405-3409.

Gilmore, T.D. (1999). The Rel/NF-kappaB signal transduction pathway: introduction. Oncogene *18*, 6842-6844.

Gomez-Roman, N., Grandori, C., Eisenman, R.N., and White, R.J. (2003). Direct activation of RNA polymerase III transcription by c-Myc. Nature *421*, 290-294.

Gonda, T.J., and Metcalf, D. (1984). Expression of myb, myc and fos proto-oncogenes during the differentiation of a murine myeloid leukaemia. Nature *310*, 249-251.

Gonzalez, I.L., and Sylvester, J.E. (1995). Complete sequence of the 43-kb human ribosomal DNA repeat: analysis of the intergenic spacer. Genomics *27*, 320-328.

Gorski, J.J., Pathak, S., Panov, K., Kasciukovic, T., Panova, T., Russell, J., and Zomerdijk, J.C. (2007). A novel TBP-associated factor of SL1 functions in RNA polymerase I transcription. The EMBO journal *26*, 1560-1568.

Grandori, C., Cowley, S.M., James, L.P., and Eisenman, R.N. (2000). The Myc/Max/Mad network and the transcriptional control of cell behavior. Annual review of cell and developmental biology *16*, 653-699.

Grandori, C., Gomez-Roman, N., Felton-Edkins, Z.A., Ngouenet, C., Galloway, D.A., Eisenman, R.N., and White, R.J. (2005). c-Myc binds to human ribosomal DNA and stimulates transcription of rRNA genes by RNA polymerase I. Nature cell biology *7*, 311-318.

Greenberg, R.A., O'Hagan, R.C., Deng, H., Xiao, Q., Hann, S.R., Adams, R.R., Lichtsteiner, S., Chin, L., Morin, G.B., and DePinho, R.A. (1999). Telomerase reverse transcriptase gene is a direct target of c-Myc but is not functionally equivalent in cellular transformation. Oncogene *18*, 1219-1226.

Greene, L.A., and Rukenstein, A. (1981). Regulation of acetylcholinesterase activity by nerve growth factor. Role of transcription and dissociation from effects on proliferation and neurite outgrowth. The Journal of biological chemistry *256*, 6363-6367.

Greene, L.A., and Tischler, A.S. (1976). Establishment of a noradrenergic clonal line of rat adrenal pheochromocytoma cells which respond to nerve growth factor. Proceedings of the National Academy of Sciences of the United States of America *73*, 2424-2428.

Gregory, M.A., and Hann, S.R. (2000). c-Myc proteolysis by the ubiquitin-proteasome pathway: stabilization of c-Myc in Burkitt's lymphoma cells. Molecular and cellular biology *20*, 2423-2435.

Grieco, M., Cerrato, A., Santoro, M., Fusco, A., Melillo, R.M., and Vecchio, G. (1994). Cloning and characterization of H4 (D10S170), a gene involved in RET rearrangements in vivo. Oncogene *9*, 2531-2535.

Grosso, L.E., and Pitot, H.C. (1985). Transcriptional regulation of c-myc during chemically induced differentiation of HL-60 cultures. Cancer research *45*, 847-850.

Grozdanov, P., Georgiev, O., and Karagyozov, L. (2003). Complete sequence of the 45-kb mouse ribosomal DNA repeat: analysis of the intergenic spacer. Genomics *82*, 637-643.

Grummt, I. (2003). Life on a planet of its own: regulation of RNA polymerase I transcription in the nucleolus. Genes & development *17*, 1691-1702.

Grummt, I. (2007). Different epigenetic layers engage in complex crosstalk to define the epigenetic state of mammalian rRNA genes. Human molecular genetics *16 Spec No 1*, R21-27.

Grummt, I., Kuhn, A., Bartsch, I., and Rosenbauer, H. (1986a). A transcription terminator located upstream of the mouse rDNA initiation site affects rRNA synthesis. Cell *47*, 901-911.

Grummt, I., Maier, U., Ohrlein, A., Hassouna, N., and Bachellerie, J.P. (1985). Transcription of mouse rDNA terminates downstream of the 3' end of 28S RNA and involves interaction of factors with repeated sequences in the 3' spacer. Cell *43*, 801-810.

Grummt, I., Rosenbauer, H., Niedermeyer, I., Maier, U., and Ohrlein, A. (1986b). A repeated 18 bp sequence motif in the mouse rDNA spacer mediates binding of a nuclear factor and transcription termination. Cell *45*, 837-846.

Grumont, R.J., Richardson, I.B., Gaff, C., and Gerondakis, S. (1993). rel/NF-kappa B nuclear complexes that bind kB sites in the murine c-rel promoter are required for constitutive c-rel transcription in B-cells. Cell Growth Differ *4*, 731-743.

Grumont, R.J., Rourke, I.J., and Gerondakis, S. (1999). Rel-dependent induction of A1 transcription is required to protect B cells from antigen receptor ligation-induced apoptosis. Genes & development *13*, 400-411.

Grumont, R.J., Rourke, I.J., O'Reilly, L.A., Strasser, A., Miyake, K., Sha, W., and Gerondakis, S. (1998). B lymphocytes differentially use the Rel and nuclear factor kappaB1 (NF-kappaB1) transcription factors to regulate cell cycle progression and apoptosis in quiescent and mitogen-activated cells. The Journal of experimental medicine *187*, 663-674.

Gu, W., Cechova, K., Tassi, V., and Dalla-Favera, R. (1993). Opposite regulation of gene transcription and cell proliferation by c-Myc and Max. Proceedings of the National Academy of Sciences of the United States of America *90*, 2935-2939.

Guerrero, I., Pellicer, A., and Burstein, D.E. (1988). Dissociation of c-fos from ODC expression and neuronal differentiation in a PC12 subline stably transfected with an inducible N-ras oncogene. Biochemical and biophysical research communications *150*, 1185-1192.

Gugasyan, R., Grumont, R., Grossmann, M., Nakamura, Y., Pohl, T., Nesic, D., and Gerondakis, S. (2000). Rel/NF-kappaB transcription factors: key mediators of B-cell activation. Immunological reviews *176*, 134-140.

Gunes, C., Lichtsteiner, S., Vasserot, A.P., and Englert, C. (2000). Expression of the hTERT gene is regulated at the level of transcriptional initiation and repressed by Mad1. Cancer research *60*, 2116-2121.

Guo, X.L., Pan, L., Zhang, X.J., Suo, X.H., Niu, Z.Y., Zhang, J.Y., Wang, F., Dong, Z.R., Da, W., and Ohno, R. (2007). Expression and mutation analysis of genes that encode the Myc antagonists Mad1, Mxi1 and Rox in acute leukaemia. Leukemia & lymphoma *48*, 1200-1207.

Gupta, S., Seth, A., and Davis, R.J. (1993). Transactivation of gene expression by Myc is inhibited by mutation at the phosphorylation sites Thr-58 and Ser-62. Proceedings of the National Academy of Sciences of the United States of America *90*, 3216-3220.

Haaf, T., Hayman, D.L., and Schmid, M. (1991). Quantitative determination of rDNA transcription units in vertebrate cells. Experimental cell research *193*, 78-86.

Halleck, M.S., Pownall, S., Harder, K.W., Duncan, A.M., Jirik, F.R., and Schlegel, R.A. (1995). A widely distributed putative mammalian transcriptional regulator containing multiple paired amphipathic helices, with similarity to yeast SIN3. Genomics *26*, 403-406.

Haltiner, M.M., Smale, S.T., and Tjian, R. (1986). Two distinct promoter elements in the human rRNA gene identified by linker scanning mutagenesis. Molecular and cellular biology *6*, 227-235.

Han, S., Park, K., Kim, H.Y., Lee, M.S., Kim, H.J., Kim, Y.D., Yuh, Y.J., Kim, S.R., and Suh, H.S. (2000). Clinical implication of altered expression of Mad1 protein in human breast carcinoma. Cancer *88*, 1623-1632.

Hanahan, D., and Weinberg, R.A. (2011). Hallmarks of cancer: the next generation. Cell *144*, 646-674.

Hann, S.R. (2006). Role of post-translational modifications in regulating c-Myc proteolysis, transcriptional activity and biological function. Semin Cancer Biol *16*, 288-302.

Hann, S.R., Abrams, H.D., Rohrschneider, L.R., and Eisenman, R.N. (1983). Proteins encoded by v-myc and c-myc oncogenes: identification and localization in acute leukemia virus transformants and bursal lymphoma cell lines. Cell *34*, 789-798.

Hann, S.R., King, M.W., Bentley, D.L., Anderson, C.W., and Eisenman, R.N. (1988). A non-AUG translational initiation in c-myc exon 1 generates an N-terminally distinct protein whose synthesis is disrupted in Burkitt's lymphomas. Cell *52*, 185-195.

Hann, S.R., Thompson, C.B., and Eisenman, R.N. (1985). c-myc oncogene protein synthesis is independent of the cell cycle in human and avian cells. Nature *314*, 366-369.

Hannan, K.M., Brandenburger, Y., Jenkins, A., Sharkey, K., Cavanaugh, A., Rothblum, L., Moss, T., Poortinga, G., McArthur, G.A., Pearson, R.B., and Hannan, R.D. (2003). mTOR-dependent regulation of ribosomal gene transcription requires S6K1 and is mediated by phosphorylation of the carboxy-terminal activation domain of the nucleolar transcription factor UBF. Molecular and cellular biology *23*, 8862-8877.

Harrington, E.A., Bennett, M.R., Fanidi, A., and Evan, G.I. (1994). c-Myc-induced apoptosis in fibroblasts is inhibited by specific cytokines. The EMBO journal *13*, 3286-3295.

Hayashi, K., Makino, R., Kawamura, H., Arisawa, A., and Yoneda, K. (1987). Characterization of rat c-myc and adjacent regions. Nucleic acids research *15*, 6419-6436.

Hayden, M.S., and Ghosh, S. (2004). Signaling to NF-kappaB. Genes & development *18*, 2195-2224.

He, L., Liu, J., Collins, I., Sanford, S., O'Connell, B., Benham, C.J., and Levens, D. (2000). Loss of FBP function arrests cellular proliferation and extinguishes c-myc expression. The EMBO journal *19*, 1034-1044.

Heinzel, T., Lavinsky, R.M., Mullen, T.M., Soderstrom, M., Laherty, C.D., Torchia, J., Yang, W.M., Brard, G., Ngo, S.D., Davie, J.R*., et al.* (1997). A complex containing N-CoR, mSin3 and histone deacetylase mediates transcriptional repression. Nature *387*, 43-48.

Heix, J., Zomerdijk, J.C., Ravanpay, A., Tjian, R., and Grummt, I. (1997). Cloning of murine RNA polymerase I-specific TAF factors: conserved interactions between the subunits of the species-specific transcription initiation factor TIF-IB/SL1. Proceedings of the National Academy of Sciences of the United States of America *94*, 1733-1738.

Henderson, A.S., Warburton, D., and Atwood, K.C. (1972). Location of ribosomal DNA in the human chromosome complement. Proceedings of the National Academy of Sciences of the United States of America *69*, 3394-3398.

Henderson, S., and Sollner-Webb, B. (1986). A transcriptional terminator is a novel element of the promoter of the mouse ribosomal RNA gene. Cell *47*, 891-900.

Henriksson, M., and Luscher, B. (1996). Proteins of the Myc network: essential regulators of cell growth and differentiation. Adv Cancer Res *68*, 109-182.

Herbst, A., Hemann, M.T., Tworkowski, K.A., Salghetti, S.E., Lowe, S.W., and Tansey, W.P. (2005). A conserved element in Myc that negatively regulates its proapoptotic activity. EMBO Rep *6*, 177-183.

Herkert, B., and Eilers, M. (2010). Transcriptional repression: the dark side of myc. Genes & cancer *1*, 580-586.

Hermeking, H., and Eick, D. (1994). Mediation of c-Myc-induced apoptosis by p53. Science *265*, 2091-2093.

Hermeking, H., Rago, C., Schuhmacher, M., Li, Q., Barrett, J.F., Obaya, A.J., O'Connell, B.C., Mateyak, M.K., Tam, W., Kohlhuber, F*., et al.* (2000). Identification of CDK4 as a target of c-MYC. Proceedings of the National Academy of Sciences of the United States of America *97*, 2229-2234.

Hoffmann, A., Natoli, G., and Ghosh, G. (2006). Transcriptional regulation via the NF-kappaB signaling module. Oncogene *25*, 6706-6716.

Holt, J.T., Redner, R.L., and Nienhuis, A.W. (1988). An oligomer complementary to c-myc mRNA inhibits proliferation of HL-60 promyelocytic cells and induces differentiation. Molecular and cellular biology *8*, 963-973.

Hooker, C.W., and Hurlin, P.J. (2006). Of Myc and Mnt. J Cell Sci *119*, 208-216.

Hopewell, R., and Ziff, E.B. (1995). The nerve growth factor-responsive PC12 cell line does not express the Myc dimerization partner Max. Molecular and cellular biology *15*, 3470-3478.

Houldsworth, J., Mathew, S., Rao, P.H., Dyomina, K., Louie, D.C., Parsa, N., Offit, K., and Chaganti, R.S. (1996). REL proto-oncogene is frequently amplified in extranodal diffuse large cell lymphoma. Blood *87*, 25-29.

Hourihan, R.N., O'Sullivan, G.C., and Morgan, J.G. (2003). Transcriptional gene expression profiles of oesophageal adenocarcinoma and normal oesophageal tissues. Anticancer research *23*, 161-165.

Hu, S.S., Duesberg, P.H., Lai, M.M., and Vogt, P.K. (1979). Avian oncovirus MH2: preferential growth in macrophages and exact size of the genome. Virology *96*, 302-306.

Hurlin, P.J., and Dezfouli, S. (2004). Functions of myc:max in the control of cell proliferation and tumorigenesis. International review of cytology *238*, 183-226.

Hurlin, P.J., Foley, K.P., Ayer, D.E., Eisenman, R.N., Hanahan, D., and Arbeit, J.M. (1995a). Regulation of Myc and Mad during epidermal differentiation and HPV-associated tumorigenesis. Oncogene *11*, 2487-2501.

Hurlin, P.J., and Huang, J. (2006). The MAX-interacting transcription factor network. Semin Cancer Biol *16*, 265-274.

Hurlin, P.J., Queva, C., and Eisenman, R.N. (1997a). Mnt, a novel Max-interacting protein is coexpressed with Myc in proliferating cells and mediates repression at Myc binding sites. Genes & development *11*, 44-58.

Hurlin, P.J., Queva, C., and Eisenman, R.N. (1997b). Mnt: a novel Max-interacting protein and Myc antagonist. Current topics in microbiology and immunology *224*, 115-121.

Hurlin, P.J., Queva, C., Koskinen, P.J., Steingrimsson, E., Ayer, D.E., Copeland, N.G., Jenkins, N.A., and Eisenman, R.N. (1995b). Mad3 and Mad4: novel Max-interacting transcriptional repressors that suppress c-myc dependent transformation and are expressed during neural and epidermal differentiation. The EMBO journal *14*, 5646-5659.

Hurlin, P.J., Steingrimsson, E., Copeland, N.G., Jenkins, N.A., and Eisenman, R.N. (1999). Mga, a dual-specificity transcription factor that interacts with Max and contains a T-domain DNA-binding motif. The EMBO journal *18*, 7019-7028.

Hurlin, P.J., Zhou, Z.Q., Toyo-oka, K., Ota, S., Walker, W.L., Hirotsune, S., and Wynshaw-Boris, A. (2003). Deletion of Mnt leads to disrupted cell cycle control and tumorigenesis. The EMBO journal *22*, 4584-4596.

Hurlin, P.J., Zhou, Z.Q., Toyo-Oka, K., Ota, S., Walker, W.L., Hirotsune, S., and Wynshaw-Boris, A. (2004). Evidence of mnt-myc antagonism revealed by mnt gene deletion. Cell cycle (Georgetown, Tex *3*, 97-99.

Hwang, C.S., Loftus, T.M., Mandrup, S., and Lane, M.D. (1997). Adipocyte differentiation and leptin expression. Annual review of cell and developmental biology *13*, 231-259.

Imoto, I., Yang, Z.Q., Pimkhaokham, A., Tsuda, H., Shimada, Y., Imamura, M., Ohki, M., and Inazawa, J. (2001). Identification of cIAP1 as a candidate target gene within an amplicon at 11q22 in esophageal squamous cell carcinomas. Cancer research *61*, 6629-6634.

Iritani, B.M., Delrow, J., Grandori, C., Gomez, I., Klacking, M., Carlos, L.S., and Eisenman, R.N. (2002). Modulation of T-lymphocyte development, growth and cell size by the Myc antagonist and transcriptional repressor Mad1. The EMBO journal *21*, 4820-4830.

Iritani, B.M., and Eisenman, R.N. (1999). c-Myc enhances protein synthesis and cell size during B lymphocyte development. Proceedings of the National Academy of Sciences of the United States of America *96*, 13180-13185.

Ishikawa, H., Claudio, E., Dambach, D., Raventos-Suarez, C., Ryan, C., and Bravo, R. (1998). Chronic inflammation and susceptibility to bacterial infections in mice lacking the polypeptide (p)105 precursor (NF-kappaB1) but expressing p50. The Journal of experimental medicine *187*, 985-996.

James, L., and Eisenman, R.N. (2002). Myc and Mad bHLHZ domains possess identical DNA-binding specificities but only partially overlapping functions in vivo. Proceedings of the National Academy of Sciences of the United States of America *99*, 10429-10434.

Jhiang, S.M. (2000). The RET proto-oncogene in human cancers. Oncogene *19*, 5590-5597.

Jiang, G., Espeseth, A., Hazuda, D.J., and Margolis, D.M. (2007). c-Myc and Sp1 contribute to proviral latency by recruiting histone deacetylase 1 to the human immunodeficiency virus type 1 promoter. Journal of virology *81*, 10914-10923.

Jiang, K., Hein, N., Eckert, K., Luscher-Firzlaff, J., and Luscher, B. (2008). Regulation of the MAD1 promoter by G-CSF. Nucleic acids research *36*, 1517-1531.

Johnston, L.A., Prober, D.A., Edgar, B.A., Eisenman, R.N., and Gallant, P. (1999). Drosophila myc regulates cellular growth during development. Cell *98*, 779-790.

Jones, T.R., and Cole, M.D. (1987). Rapid cytoplasmic turnover of c-myc mRNA: requirement of the 3' untranslated sequences. Molecular and cellular biology *7*, 4513-4521.

Journey, L.J., and Goldstein, M.N. (1961). Electron microscope studies on HeLa cell lines sensitive and resistant to actinomycin D. Cancer research *21*, 929-932.

Juergens, K., Rust, B., Pieler, T., and Henningfeld, K.A. (2005). Isolation and comparative expression analysis of the Myc-regulatory proteins Mad1, Mad3, and Mnt during Xenopus development. Dev Dyn *233*, 1554-1559.

Kanazawa, S., Soucek, L., Evan, G., Okamoto, T., and Peterlin, B.M. (2003). c-Myc recruits P-TEFb for transcription, cellular proliferation and apoptosis. Oncogene *22*, 5707-5711.

Karin, M., and Ben-Neriah, Y. (2000). Phosphorylation meets ubiquitination: the control of NF-[kappa]B activity. Annual review of immunology *18*, 621-663.

Kato, G.J., Barrett, J., Villa-Garcia, M., and Dang, C.V. (1990). An amino-terminal c-myc domain required for neoplastic transformation activates transcription. Molecular and cellular biology *10*, 5914-5920.

Kato, G.J., Lee, W.M., Chen, L.L., and Dang, C.V. (1992). Max: functional domains and interaction with c-Myc. Genes & development *6*, 81-92.

Kenneth, N.S., Ramsbottom, B.A., Gomez-Roman, N., Marshall, L., Cole, P.A., and White, R.J. (2007). TRRAP and GCN5 are used by c-Myc to activate RNA polymerase III transcription. Proceedings of the National Academy of Sciences of the United States of America *104*, 14917-14922.

Kiermaier, A., and Eilers, M. (1997). Transcriptional control: calling in histone deacetylase. Curr Biol *7*, R505-507.

Kim, H.H., Kuwano, Y., Srikantan, S., Lee, E.K., Martindale, J.L., and Gorospe, M. (2009). HuR recruits let-7/RISC to repress c-Myc expression. Genes & development *23*, 1743-1748.

Kim, J.W., Zeller, K.I., Wang, Y., Jegga, A.G., Aronow, B.J., O'Donnell, K.A., and Dang, C.V. (2004). Evaluation of myc E-box phylogenetic footprints in glycolytic genes by chromatin immunoprecipitation assays. Molecular and cellular biology *24*, 5923-5936.

Kim, S., Li, Q., Dang, C.V., and Lee, L.A. (2000). Induction of ribosomal genes and hepatocyte hypertrophy by adenovirus-mediated expression of c-Myc in vivo. Proceedings of the National Academy of Sciences of the United States of America *97*, 11198-11202.

King, M.W., Blackwood, E.M., and Eisenman, R.N. (1993). Expression of two distinct homologues of Xenopus Max during early development. Cell Growth Differ *4*, 85-92.

Knoepfler, P.S., and Eisenman, R.N. (1999). Sin meets NuRD and other tails of repression. Cell *99*, 447-450.

Kohl, N.E., Kanda, N., Schreck, R.R., Bruns, G., Latt, S.A., Gilbert, F., and Alt, F.W. (1983). Transposition and amplification of oncogene-related sequences in human neuroblastomas. Cell *35*, 359-367.

Koskinen, P.J., Ayer, D.E., and Eisenman, R.N. (1995). Repression of Myc-Ras cotransformation by Mad is mediated by multiple protein-protein interactions. Cell Growth Differ *6*, 623-629.

Koskinen, P.J., Vastrik, I., Makela, T.P., Eisenman, R.N., and Alitalo, K. (1994). Max activity is affected by phosphorylation at two NH2-terminal sites. Cell Growth Differ *5*, 313-320.

Kretzner, L., Blackwood, E.M., and Eisenman, R.N. (1992a). Myc and Max proteins possess distinct transcriptional activities. Nature *359*, 426-429.

Kretzner, L., Blackwood, E.M., and Eisenman, R.N. (1992b). Transcriptional activities of the Myc and Max proteins in mammalian cells. Curr Top Microbiol Immunol *182*, 435-443.

Kuhn, A., Voit, R., Stefanovsky, V., Evers, R., Bianchi, M., and Grummt, I. (1994). Functional differences between the two splice variants of the nucleolar transcription factor UBF: the second HMG box determines specificity of DNA binding and transcriptional activity. The EMBO journal *13*, 416-424.

Kulkarni, S., Heath, C., Parker, S., Chase, A., Iqbal, S., Pocock, C.F., Kaeda, J., Cwynarski, K., Goldman, J.M., and Cross, N.C. (2000). Fusion of H4/D10S170 to the platelet-derived growth factor receptor beta in BCR-ABL-negative myeloproliferative disorders with a t(5;10)(q33;q21). Cancer research *60*, 3592-3598.

Kurland, J.F., and Tansey, W.P. (2008). Myc-mediated transcriptional repression by recruitment of histone deacetylase. Cancer research *68*, 3624-3629.

La Rocca, S.A., Grossi, M., Falcone, G., Alema, S., and Tato, F. (1989). Interaction with normal cells suppresses the transformed phenotype of v-myc-transformed quail muscle cells. Cell *58*, 123-131.

Lachman, H.M., and Skoultchi, A.I. (1984). Expression of c-myc changes during differentiation of mouse erythroleukaemia cells. Nature *310*, 592-594.

Laherty, C.D., Yang, W.M., Sun, J.M., Davie, J.R., Seto, E., and Eisenman, R.N. (1997). Histone deacetylases associated with the mSin3 corepressor mediate mad transcriptional repression. Cell *89*, 349-356.

Lahoz, E.G., Xu, L., Schreiber-Agus, N., and DePinho, R.A. (1994). Suppression of Myc, but not E1a, transformation activity by Max-associated proteins, Mad and Mxi1. Proceedings of the National Academy of Sciences of the United States of America *91*, 5503-5507.

Landschulz, W.H., Johnson, P.F., and McKnight, S.L. (1988). The leucine zipper: a hypothetical structure common to a new class of DNA binding proteins. Science (New York, N.Y *240*, 1759-1764.

Larsson, L.G., Ivhed, I., Gidlund, M., Pettersson, U., Vennstrom, B., and Nilsson, K. (1988). Phorbol ester-induced terminal differentiation is inhibited in human U-937 monoblastic cells expressing a v-myc oncogene. Proceedings of the National Academy of Sciences of the United States of America *85*, 2638-2642.

Larsson, L.G., Pettersson, M., Oberg, F., Nilsson, K., and Luscher, B. (1994). Expression of mad, mxi1, max and c-myc during induced differentiation of hematopoietic cells: opposite regulation of mad and c-myc. Oncogene *9*, 1247-1252.

Laurenti, E., Varnum-Finney, B., Wilson, A., Ferrero, I., Blanco-Bose, W.E., Ehninger, A., Knoepfler, P.S., Cheng, P.F., MacDonald, H.R., Eisenman, R.N.*, et al.* (2008). Hematopoietic stem cell function and survival depend on c-Myc and N-Myc activity. Cell Stem Cell *3*, 611-624.

Lawrence, R.J., and Pikaard, C.S. (2004). Chromatin turn ons and turn offs of ribosomal RNA genes. Cell cycle (Georgetown, Tex *3*, 880-883.

Learned, R.M., Learned, T.K., Haltiner, M.M., and Tjian, R.T. (1986). Human rRNA transcription is modulated by the coordinate binding of two factors to an upstream control element. Cell *45*, 847-857.

Leeman, J.R., Weniger, M.A., Barth, T.F., and Gilmore, T.D. (2008). Deletion analysis and alternative splicing define a transactivation inhibitory domain in human oncoprotein REL. Oncogene *27*, 6770-6781.

Leone, V., Mansueto, G., Pierantoni, G.M., Tornincasa, M., Merolla, F., Cerrato, A., Santoro, M., Grieco, M., Scaloni, A., Celetti, A., and Fusco, A. (2010). CCDC6 represses CREB1 activity by recruiting histone deacetylase 1 and protein phosphatase 1. Oncogene *29*, 4341-4351.

Leung, T.H., Hoffmann, A., and Baltimore, D. (2004). One nucleotide in a kappaB site can determine cofactor specificity for NF-kappaB dimers. Cell *118*, 453-464.

Levens, D. (2010). You Don't Muck with MYC. Genes & cancer *1*, 547-554.

Li, F., Wang, Y., Zeller, K.I., Potter, J.J., Wonsey, D.R., O'Donnell, K.A., Kim, J.W., Yustein, J.T., Lee, L.A., and Dang, C.V. (2005). Myc stimulates nuclearly encoded mitochondrial genes and mitochondrial biogenesis. Molecular and cellular biology *25*, 6225-6234.

Li, J., Langst, G., and Grummt, I. (2006). NoRC-dependent nucleosome positioning silences rRNA genes. The EMBO journal *25*, 5735-5741.

Lin, C.Y., Navarro, S., Reddy, S., and Comai, L. (2006). CK2-mediated stimulation of Pol I transcription by stabilization of UBF-SL1 interaction. Nucleic acids research *34*, 4752-4766.

Lindblom, A., Rotstein, S., Skoog, L., Nordenskjold, M., and Larsson, C. (1993). Deletions on chromosome 16 in primary familial breast carcinomas are associated with development of distant metastases. Cancer research *53*, 3707-3711.

Link, J.M., Ota, S., Zhou, Z.Q., Daniel, C.J., Sears, R.C., and Hurlin, P.J. (2012). A critical role for Mnt in Myc-driven T-cell proliferation and oncogenesis. Proceedings of the National Academy of Sciences of the United States of America *109*, 19685-19690.

Liou, H.C., Jin, Z., Tumang, J., Andjelic, S., Smith, K.A., and Liou, M.L. (1999). c-Rel is crucial for lymphocyte proliferation but dispensable for T cell effector function. International immunology *11*, 361-371.

Littlewood, T.D., Amati, B., Land, H., and Evan, G.I. (1992). Max and c-Myc/Max DNA-binding activities in cell extracts. Oncogene *7*, 1783-1792.

Liu, J., and Levens, D. (2006). Making myc. Current topics in microbiology and immunology *302*, 1-32.

Liu, Y.C., Li, F., Handler, J., Huang, C.R., Xiang, Y., Neretti, N., Sedivy, J.M., Zeller, K.I., and Dang, C.V. (2008). Global regulation of nucleotide biosynthetic genes by c-Myc. PloS one *3*, e2722.

Lo Nigro, C., Venesio, T., Reymond, A., Meroni, G., Alberici, P., Cainarca, S., Enrico, F., Stack, M., Ledbetter, D.H., Liscia, D.S*., et al.* (1998). The human ROX gene: genomic structure and mutation analysis in human breast tumors. Genomics *49*, 275-282.

Loo, L.W., Secombe, J., Little, J.T., Carlos, L.S., Yost, C., Cheng, P.F., Flynn, E.M., Edgar, B.A., and Eisenman, R.N. (2005). The transcriptional repressor dMnt is a regulator of growth in Drosophila melanogaster. Molecular and cellular biology *25*, 7078-7091.

Lorenz, V.N., Schon, M.P., and Seitz, C.S. (2014). c-Rel downregulation affects cell cycle progression of human keratinocytes. The Journal of investigative dermatology *134*, 415-422.

Lu, H., Yang, X., Duggal, P., Allen, C.T., Yan, B., Cohen, J., Nottingham, L., Romano, R.A., Sinha, S., King, K.E*., et al.* (2011). TNF-alpha promotes c-REL/DeltaNp63alpha interaction and TAp73 dissociation from key genes that mediate growth arrest and apoptosis in head and neck cancer. Cancer research *71*, 6867-6877.

Luo, Q., Li, J., Cenkci, B., and Kretzner, L. (2004). Autorepression of c-myc requires both initiator and E2F-binding site elements and cooperation with the p107 gene product. Oncogene *23*, 1088-1097.

Luscher, B. (2012). MAD1 and its life as a MYC antagonist: an update. European journal of cell biology *91*, 506-514.

Luscher, B., and Vervoorts, J. (2012). Regulation of gene transcription by the oncoprotein MYC. Gene *494*, 145-160.

Lymboussaki, A., Kaipainen, A., Hatva, E., Vastrik, I., Jeskanen, L., Jalkanen, M., Werner, S., Stenback, F., and Alitalo, R. (1996). Expression of Mad, an antagonist of Myc oncoprotein function, in differentiating keratinocytes during tumorigenesis of the skin. British journal of cancer *73*, 1347-1355.

Mackay, J., Elder, P.A., Porteous, D.J., Steel, C.M., Hawkins, R.A., Going, J.J., and Chetty, U. (1988a). Partial deletion of chromosome 11p in breast cancer correlates with size of primary tumour and oestrogen receptor level. British journal of cancer *58*, 710-714.

Mackay, J., Steel, C.M., Elder, P.A., Forrest, A.P., and Evans, H.J. (1988b). Allele loss on short arm of chromosome 17 in breast cancers. Lancet *2*, 1384-1385.

Magrath, I. (1990). The pathogenesis of Burkitt's lymphoma. Adv Cancer Res *55*, 133-270.

Makela, T.P., Koskinen, P.J., Vastrik, I., and Alitalo, K. (1992). Alternative forms of Max as enhancers or suppressors of Myc-ras cotransformation. Science (New York, N.Y *256*, 373-377.

Mao, D.Y., Watson, J.D., Yan, P.S., Barsyte-Lovejoy, D., Khosravi, F., Wong, W.W., Farnham, P.J., Huang, T.H., and Penn, L.Z. (2003). Analysis of Myc Bound Loci Identified by CpG Island Arrays Shows that Max Is Essential for Myc-Dependent Repression. Curr Biol *13*, 882-886.

Martin-Subero, J.I., Gesk, S., Harder, L., Sonoki, T., Tucker, P.W., Schlegelberger, B., Grote, W., Novo, F.J., Calasanz, M.J., Hansmann, M.L*., et al.* (2002). Recurrent involvement of the REL and BCL11A loci in classical Hodgkin lymphoma. Blood *99*, 1474-1477.

Martin, A.G., San-Antonio, B., and Fresno, M. (2001). Regulation of nuclear factor kappa B transactivation. Implication of phosphatidylinositol 3-kinase and protein kinase C zeta in c-Rel activation by tumor necrosis factor alpha. The Journal of biological chemistry *276*, 15840-15849.

Mates, J.M., Segura, J.A., Alonso, F.J., and Marquez, J. (2008). Intracellular redox status and oxidative stress: implications for cell proliferation, apoptosis, and carcinogenesis. Archives of toxicology *82*, 273-299.

Mateyak, M.K., Obaya, A.J., Adachi, S., and Sedivy, J.M. (1997). Phenotypes of c-Myc-deficient rat fibroblasts isolated by targeted homologous recombination. Cell Growth Differ *8*, 1039-1048.

Mayer, C., Schmitz, K.M., Li, J., Grummt, I., and Santoro, R. (2006). Intergenic transcripts regulate the epigenetic state of rRNA genes. Molecular cell *22*, 351-361.

McDonald, J.D., Daneshvar, L., Willert, J.R., Matsumura, K., Waldman, F., and Cogen, P.H. (1994). Physical mapping of chromosome 17p13.3 in the region of a putative tumor suppressor gene important in medulloblastoma. Genomics *23*, 229-232.

McMahon, S.B., Van Buskirk, H.A., Dugan, K.A., Copeland, T.D., and Cole, M.D. (1998). The novel ATM-related protein TRRAP is an essential cofactor for the c-Myc and E2F oncoproteins. Cell *94*, 363-374.

McStay, B., and Grummt, I. (2008). The epigenetics of rRNA genes: from molecular to chromosome biology. Annual review of cell and developmental biology *24*, 131-157.

McStay, B., and Reeder, R.H. (1986). A termination site for Xenopus RNA polymerase I also acts as an element of an adjacent promoter. Cell *47*, 913-920.

Menssen, A., Hydbring, P., Kapelle, K., Vervoorts, J., Diebold, J., Luscher, B., Larsson, L.G., and Hermeking, H. (2012). The c-MYC oncoprotein, the NAMPT enzyme, the SIRT1-inhibitor DBC1, and the SIRT1 deacetylase form a positive feedback loop. Proceedings of the National Academy of Sciences of the United States of America *109*, E187-196.

Meraner, J., Lechner, M., Loidl, A., Goralik-Schramel, M., Voit, R., Grummt, I., and Loidl, P. (2006). Acetylation of UBF changes during the cell cycle and regulates the interaction of UBF with RNA polymerase I. Nucleic acids research *34*, 1798-1806.

Merolla, F., Luise, C., Muller, M.T., Pacelli, R., Fusco, A., and Celetti, A. (2012). Loss of CCDC6, the first identified RET partner gene, affects pH2AX S139 levels and accelerates mitotic entry upon DNA damage. PloS one *7*, e36177.

Merolla, F., Pentimalli, F., Pacelli, R., Vecchio, G., Fusco, A., Grieco, M., and Celetti, A. (2007). Involvement of H4(D10S170) protein in ATM-dependent response to DNA damage. Oncogene *26*, 6167-6175.

Meroni, G., Cairo, S., Merla, G., Messali, S., Brent, R., Ballabio, A., and Reymond, A. (2000). Mlx, a new Max-like bHLHZip family member: the center stage of a novel transcription factors regulatory pathway? Oncogene *19*, 3266-3277.

Meroni, G., Reymond, A., Alcalay, M., Borsani, G., Tanigami, A., Tonlorenzi, R., Lo Nigro, C., Messali, S., Zollo, M., Ledbetter, D.H.*, et al.* (1997). Rox, a novel bHLHZip protein expressed in quiescent cells that heterodimerizes with Max, binds a non-canonical E box and acts as a transcriptional repressor. The EMBO journal *16*, 2892-2906.

Mertz, J.A., Conery, A.R., Bryant, B.M., Sandy, P., Balasubramanian, S., Mele, D.A., Bergeron, L., and Sims, R.J., 3rd (2011). Targeting MYC dependence in cancer by inhibiting BET bromodomains. Proceedings of the National Academy of Sciences of the United States of America *108*, 16669-16674.

Miner, J.H., and Wold, B.J. (1991). c-myc inhibition of MyoD and myogenin-initiated myogenic differentiation. Molecular and cellular biology *11*, 2842-2851.

Mortazavi, A., Williams, B.A., McCue, K., Schaeffer, L., and Wold, B. (2008). Mapping and quantifying mammalian transcriptomes by RNA-Seq. Nature methods *5*, 621-628.

Mosialos, G., and Gilmore, T.D. (1993). v-Rel and c-Rel are differentially affected by mutations at a consensus protein kinase recognition sequence. Oncogene *8*, 721-730.

Mosialos, G., Hamer, P., Capobianco, A.J., Laursen, R.A., and Gilmore, T.D. (1991). A protein kinase-A recognition sequence is structurally linked to transformation by p59v-rel and cytoplasmic retention of p68c-rel. Molecular and cellular biology *11*, 5867-5877.

Moss, T., Langlois, F., Gagnon-Kugler, T., and Stefanovsky, V. (2007). A housekeeper with power of attorney: the rRNA genes in ribosome biogenesis. Cell Mol Life Sci *64*, 29-49.

Muchardt, C., and Yaniv, M. (1999). ATP-dependent chromatin remodelling: SWI/SNF and Co. are on the job. Journal of molecular biology *293*, 187-198.

Munz, B., Smola, H., Engelhardt, F., Bleuel, K., Brauchle, M., Lein, I., Evans, L.W., Huylebroeck, D., Balling, R., and Werner, S. (1999). Overexpression of activin A in the skin of transgenic mice reveals new activities of activin in epidermal morphogenesis, dermal fibrosis and wound repair. The EMBO journal *18*, 5205-5215.

Murphy, M.J., Wilson, A., and Trumpp, A. (2005). More than just proliferation: Myc function in stem cells. Trends Cell Biol *15*, 128-137.

Murre, C., McCaw, P.S., Vaessin, H., Caudy, M., Jan, L.Y., Jan, Y.N., Cabrera, C.V., Buskin, J.N., Hauschka, S.D., Lassar, A.B., and et al. (1989). Interactions between heterologous helix-loop-helix proteins generate complexes that bind specifically to a common DNA sequence. Cell *58*, 537-544.

Nagy, Z., and Tora, L. (2007). Distinct GCN5/PCAF-containing complexes function as co-activators and are involved in transcription factor and global histone acetylation. Oncogene *26*, 5341-5357.

Nascimento, E.M., Cox, C.L., MacArthur, S., Hussain, S., Trotter, M., Blanco, S., Suraj, M., Nichols, J., Kubler, B., Benitah, S.A*., et al.* (2011). The opposing transcriptional functions of Sin3a and c-Myc are required to maintain tissue homeostasis. Nature cell biology *13*, 1395-1405.

Nau, M.M., Brooks, B.J., Battey, J., Sausville, E., Gazdar, A.F., Kirsch, I.R., McBride, O.W., Bertness, V., Hollis, G.F., and Minna, J.D. (1985). L-myc, a new myc-related gene amplified and expressed in human small cell lung cancer. Nature *318*, 69-73.

Neel, B.G., Gasic, G.P., Rogler, C.E., Skalka, A.M., Ju, G., Hishinuma, F., Papas, T., Astrin, S.M., and Hayward, W.S. (1982). Molecular analysis of the c-myc locus in normal tissue and in avian leukosis virus-induced lymphomas. Journal of virology *44*, 158-166.

Nesbit, C.E., Tersak, J.M., and Prochownik, E.V. (1999). MYC oncogenes and human neoplastic disease. Oncogene *18*, 3004-3016.

Nikiforov, M.A., Popov, N., Kotenko, I., Henriksson, M., and Cole, M.D. (2003). The Mad and Myc basic domains are functionally equivalent. The Journal of biological chemistry *278*, 11094-11099.

Nilsson, J.A., and Cleveland, J.L. (2004). Mnt: master regulator of the Max network. Cell cycle (Georgetown, Tex *3*, 588-590.

Nilsson, J.A., Maclean, K.H., Keller, U.B., Pendeville, H., Baudino, T.A., and Cleveland, J.L. (2004). Mnt loss triggers Myc transcription targets, proliferation, apoptosis, and transformation. Molecular and cellular biology *24*, 1560-1569.

O'Mahony, D.J., and Rothblum, L.I. (1991). Identification of two forms of the RNA polymerase I transcription factor UBF. Proceedings of the National Academy of Sciences of the United States of America *88*, 3180-3184.

O'Sullivan, A.C., Sullivan, G.J., and McStay, B. (2002). UBF binding in vivo is not restricted to regulatory sequences within the vertebrate ribosomal DNA repeat. Molecular and cellular biology *22*, 657-668.

Ogawa, H., Ishiguro, K., Gaubatz, S., Livingston, D.M., and Nakatani, Y. (2002). A complex with chromatin modifiers that occupies E2F- and Myc-responsive genes in G0 cells. Science (New York, N.Y *296*, 1132-1136.

Orian, A., van Steensel, B., Delrow, J., Bussemaker, H.J., Li, L., Sawado, T., Williams, E., Loo, L.W., Cowley, S.M., Yost, C*., et al.* (2003). Genomic binding by the Drosophila Myc, Max, Mad/Mnt transcription factor network. Genes & development *17*, 1101-1114.

Oster, S.K., Mao, D.Y., Kennedy, J., and Penn, L.Z. (2003). Functional analysis of the N-terminal domain of the Myc oncoprotein. Oncogene *22*, 1998-2010.

Owyang, A.M., Tumang, J.R., Schram, B.R., Hsia, C.Y., Behrens, T.W., Rothstein, T.L., and Liou, H.C. (2001). c-Rel is required for the protection of B cells from antigen receptor-mediated, but not Fas-mediated, apoptosis. J Immunol *167*, 4948-4956.

Patel, J.H., Du, Y., Ard, P.G., Phillips, C., Carella, B., Chen, C.J., Rakowski, C., Chatterjee, C., Lieberman, P.M., Lane, W.S.*, et al.* (2004). The c-MYC oncoprotein is a substrate of the acetyltransferases hGCN5/PCAF and TIP60. Molecular and cellular biology *24*, 10826-10834.

Pederson, T., and Tsai, R.Y. (2009). In search of nonribosomal nucleolar protein function and regulation. The Journal of cell biology *184*, 771-776.

Perez-Roger, I., Kim, S.H., Griffiths, B., Sewing, A., and Land, H. (1999). Cyclins D1 and D2 mediate myc-induced proliferation via sequestration of p27(Kip1) and p21(Cip1). The EMBO journal *18*, 5310-5320.

Perkins, N.D. (1997). Achieving transcriptional specificity with NF-kappa B. The international journal of biochemistry & cell biology *29*, 1433-1448.

Perkins, N.D. (2007). Integrating cell-signalling pathways with NF-kappaB and IKK function. Nature reviews *8*, 49-62.

Perry, R.P., and Kelley, D.E. (1970). Inhibition of RNA synthesis by actinomycin D: characteristic dose-response of different RNA species. Journal of cellular physiology *76*, 127-139.

Persson, H., Hennighausen, L., Taub, R., DeGrado, W., and Leder, P. (1984). Antibodies to human c-myc oncogene product: evidence of an evolutionarily conserved protein induced during cell proliferation. Science (New York, N.Y *225*, 687-693.

Phillips, N., Ziegler, M., Saha, B., and Xynos, F. (1993). Allelic loss on chromosome 17 in human ovarian cancer. International journal of cancer *54*, 85-91.

Pierotti, M.A., Santoro, M., Jenkins, R.B., Sozzi, G., Bongarzone, I., Grieco, M., Monzini, N., Miozzo, M., Herrmann, M.A., Fusco, A., and et al. (1992). Characterization of an inversion on the long arm of chromosome 10 juxtaposing D10S170 and RET and creating the oncogenic sequence RET/PTC. Proceedings of the National Academy of Sciences of the United States of America *89*, 1616-1620.

Pietenpol, J.A., Holt, J.T., Stein, R.W., and Moses, H.L. (1990). Transforming growth factor beta 1 suppression of c-myc gene transcription: role in inhibition of keratinocyte proliferation. Proceedings of the National Academy of Sciences of the United States of America *87*, 3758-3762.

Pomerantz, M.M., Beckwith, C.A., Regan, M.M., Wyman, S.K., Petrovics, G., Chen, Y., Hawksworth, D.J., Schumacher, F.R., Mucci, L., Penney, K.L.*, et al.* (2009). Evaluation of the 8q24 prostate cancer risk locus and MYC expression. Cancer research *69*, 5568-5574.

Popov, N., Wahlstrom, T., Hurlin, P.J., and Henriksson, M. (2005). Mnt transcriptional repressor is functionally regulated during cell cycle progression. Oncogene *24*, 8326-8337.

Prendergast, G.C., Lawe, D., and Ziff, E.B. (1991). Association of Myn, the murine homolog of max, with c-Myc stimulates methylation-sensitive DNA binding and ras cotransformation. Cell *65*, 395-407.

Prendergast, G.C., and Ziff, E.B. (1989). DNA-binding motif. Nature *341*, 392.

Pulverer, B., Sommer, A., McArthur, G.A., Eisenman, R.N., and Luscher, B. (2000). Analysis of Myc/Max/Mad network members in adipogenesis: inhibition of the proliferative burst and differentiation by ectopically expressed Mad1. J Cell Physiol *183*, 399-410.

Putnam, C.D., Copenhaver, G.P., Denton, M.L., and Pikaard, C.S. (1994). The RNA polymerase I transactivator upstream binding factor requires its dimerization domain and high-mobility-group (HMG) box 1 to bend, wrap, and positively supercoil enhancer DNA. Molecular and cellular biology *14*, 6476-6488.

Puxeddu, E., Zhao, G., Stringer, J.R., Medvedovic, M., Moretti, S., and Fagin, J.A. (2005). Characterization of novel non-clonal intrachromosomal rearrangements between the H4 and PTEN genes (H4/PTEN) in human thyroid cell lines and papillary thyroid cancer specimens. Mutation research *570*, 17-32.

Queva, C., Hurlin, P.J., Foley, K.P., and Eisenman, R.N. (1998). Sequential expression of the MAD family of transcriptional repressors during differentiation and development. Oncogene *16*, 967-977.

Queva, C., McArthur, G.A., Ramos, L.S., and Eisenman, R.N. (1999). Dwarfism and dysregulated proliferation in mice overexpressing the MYC antagonist MAD1. Cell Growth Differ *10*, 785-796.

Rabbitts, P.H., Watson, J.V., Lamond, A., Forster, A., Stinson, M.A., Evan, G., Fischer, W., Atherton, E., Sheppard, R., and Rabbitts, T.H. (1985). Metabolism of c-myc gene products: c-myc mRNA and protein expression in the cell cycle. The EMBO journal *4*, 2009-2015.

Rao, S., Gerondakis, S., Woltring, D., and Shannon, M.F. (2003). c-Rel is required for chromatin remodeling across the IL-2 gene promoter. J Immunol *170*, 3724-3731.

Reddy, C.D., Dasgupta, P., Saikumar, P., Dudek, H., Rauscher, F.J., 3rd, and Reddy, E.P. (1992). Mutational analysis of Max: role of basic, helix-loop-helix/leucine zipper domains in DNA binding, dimerization and regulation of Myc-mediated transcriptional activation. Oncogene *7*, 2085-2092.

Reisman, D., Glaros, S., and Thompson, E.A. (2009). The SWI/SNF complex and cancer. Oncogene *28*, 1653-1668.

Reuss, D.E., Mucha, J., Hagenlocher, C., Ehemann, V., Kluwe, L., Mautner, V., and von Deimling, A. (2013). Sensitivity of malignant peripheral nerve sheath tumor cells to TRAIL is augmented by loss of NF1 through modulation of MYC/MAD and is potentiated by curcumin through induction of ROS. PloS one *8*, e57152.

Ribon, V., Leff, T., and Saltiel, A.R. (1994). c-Myc does not require max for transcriptional activity in PC-12 cells. Molecular and cellular neurosciences *5*, 277-282.

Rogakou, E.P., Pilch, D.R., Orr, A.H., Ivanova, V.S., and Bonner, W.M. (1998). DNA double-stranded breaks induce histone H2AX phosphorylation on serine 139. The Journal of biological chemistry *273*, 5858-5868.

Romero, O.A., Torres-Diz, M., Pros, E., Savola, S., Gomez, A., Moran, S., Saez, C., Iwakawa, R., Villanueva, A., Montuenga, L.M.*, et al.* (2014). MAX inactivation in small cell lung cancer disrupts MYC-SWI/SNF programs and is synthetic lethal with BRG1. Cancer discovery *4*, 292-303.

Rottmann, S., Menkel, A.R., Bouchard, C., Mertsching, J., Loidl, P., Kremmer, E., Eilers, M., Luscher-Firzlaff, J., Lilischkis, R., and Luscher, B. (2005). Mad1 function in cell proliferation and transcriptional repression is antagonized by cyclin E/CDK2. The Journal of biological chemistry *280*, 15489-15492.

Rottmann, S., Speckgens, S., Luscher-Firzlaff, J., and Luscher, B. (2008). Inhibition of apoptosis by MAD1 is mediated by repression of the PTEN tumor suppressor gene. Faseb J *22*, 1124-1134.

Roussel, M.F., Ashmun, R.A., Sherr, C.J., Eisenman, R.N., and Ayer, D.E. (1996). Inhibition of cell proliferation by the Mad1 transcriptional repressor. Molecular and cellular biology *16*, 2796-2801.

Rudolph, B., Hueber, A.O., and Evan, G.I. (2001). Expression of Mad1 in T cells leads to reduced thymic cellularity and impaired mitogen-induced proliferation. Oncogene *20*, 1164-1175.

Russell, J., and Zomerdijk, J.C. (2005). RNA-polymerase-I-directed rDNA transcription, life and works. Trends Biochem Sci *30*, 87-96.

Ryan, K.M., and Birnie, G.D. (1997). Analysis of E-box DNA binding during myeloid differentiation reveals complexes that contain Mad but not Max. The Biochemical journal *325 (Pt 1)*, 79-85.

Saccani, S., Pantano, S., and Natoli, G. (2003). Modulation of NF-kappaB activity by exchange of dimers. Molecular cell *11*, 1563-1574.

Sachdeva, M., Zhu, S., Wu, F., Wu, H., Walia, V., Kumar, S., Elble, R., Watabe, K., and Mo, Y.Y. (2009). p53 represses c-Myc through induction of the tumor suppressor miR-145. Proceedings of the National Academy of Sciences of the United States of America *106*, 3207-3212.

Sakamuro, D., Eviner, V., Elliott, K.J., Showe, L., White, E., and Prendergast, G.C. (1995). c-Myc induces apoptosis in epithelial cells by both p53-dependent and p53-independent mechanisms. Oncogene *11*, 2411-2418.

Salghetti, S.E., Kim, S.Y., and Tansey, W.P. (1999). Destruction of Myc by ubiquitin-mediated proteolysis: cancer-associated and transforming mutations stabilize Myc. The EMBO journal *18*, 717-726.

Sanij, E., Poortinga, G., Sharkey, K., Hung, S., Holloway, T.P., Quin, J., Robb, E., Wong, L.H., Thomas, W.G., Stefanovsky, V.*, et al.* (2008). UBF levels determine the number of active ribosomal RNA genes in mammals. The Journal of cell biology *183*, 1259-1274.

Saxena, A., Clark, W.C., Robertson, J.T., Ikejiri, B., Oldfield, E.H., and Ali, I.U. (1992). Evidence for the involvement of a potential second tumor suppressor gene on chromosome 17 distinct from p53 in malignant astrocytomas. Cancer research *52*, 6716-6721.

Scheer, U., and Hock, R. (1999). Structure and function of the nucleolus. Current opinion in cell biology *11*, 385-390.

Schreiber-Agus, N., Chin, L., Chen, K., Torres, R., Rao, G., Guida, P., Skoultchi, A.I., and DePinho, R.A. (1995). An amino-terminal domain of Mxi1 mediates anti-Myc oncogenic activity and interacts with a homolog of the yeast transcriptional repressor SIN3. Cell *80*, 777-786.

Schreiber-Agus, N., and DePinho, R.A. (1998). Repression by the Mad(Mxi1)-Sin3 complex. Bioessays *20*, 808-818.

Schuhmacher, M., Kohlhuber, F., Holzel, M., Kaiser, C., Burtscher, H., Jarsch, M., Bornkamm, G.W., Laux, G., Polack, A., Weidle, U.H., and Eick, D. (2001). The transcriptional program of a human B cell line in response to Myc. Nucleic Acids Res *29*, 397-406.

Schwab, M., Alitalo, K., Klempnauer, K.H., Varmus, H.E., Bishop, J.M., Gilbert, F., Brodeur, G., Goldstein, M., and Trent, J. (1983). Amplified DNA with limited homology to myc cellular oncogene is shared by human neuroblastoma cell lines and a neuroblastoma tumour. Nature *305*, 245-248.

Schwaller, J., Anastasiadou, E., Cain, D., Kutok, J., Wojiski, S., Williams, I.R., LaStarza, R., Crescenzi, B., Sternberg, D.W., Andreasson, P*., et al.* (2001). H4(D10S170), a gene frequently rearranged in papillary thyroid carcinoma, is fused to the platelet-derived growth factor receptor beta gene in atypical chronic myeloid leukemia with t(5;10)(q33;q22). Blood *97*, 3910-3918.

Schwarzacher, H.G., and Wachtler, F. (1991). The functional significance of nucleolar structures. Annales de genetique *34*, 151-160.

Sears, R., Nuckolls, F., Haura, E., Taya, Y., Tamai, K., and Nevins, J.R. (2000). Multiple Ras-dependent phosphorylation pathways regulate Myc protein stability. Genes & development *14*, 2501-2514.

Sears, R.C. (2004). The life cycle of C-myc: from synthesis to degradation. Cell Cycle *3*, 1133-1137.

Secombe, J., and Eisenman, R.N. (2007). The function and regulation of the JARID1 family of histone H3 lysine 4 demethylases: the Myc connection. Cell Cycle *6*, 1324-1328.

Secombe, J., Li, L., Carlos, L., and Eisenman, R.N. (2007). The Trithorax group protein Lid is a trimethyl histone H3K4 demethylase required for dMyc-induced cell growth. Genes & development *21*, 537-551.

Seishima, M., Nojiri, M., Esaki, C., Yoneda, K., Eto, Y., and Kitajima, Y. (1999). Activin A induces terminal differentiation of cultured human keratinocytes. The Journal of investigative dermatology *112*, 432-436.

Shaw, P.J., Highett, M.I., Beven, A.F., and Jordan, E.G. (1995). The nucleolar architecture of polymerase I transcription and processing. The EMBO journal *14*, 2896-2906.

Shaw, P.J., and Jordan, E.G. (1995). The nucleolus. Annual review of cell and developmental biology *11*, 93-121.

Sheiness, D., and Bishop, J.M. (1979). DNA and RNA from uninfected vertebrate cells contain nucleotide sequences related to the putative transforming gene of avian myelocytomatosis virus. J Virol *31*, 514-521.

Sherr, C.J., and Roberts, J.M. (1999). CDK inhibitors: positive and negative regulators of G1-phase progression. Genes & development *13*, 1501-1512.

Shilatifard, A. (2012). The COMPASS family of histone H3K4 methylases: mechanisms of regulation in development and disease pathogenesis. Annual review of biochemistry *81*, 65-95.

Shim, H., Dolde, C., Lewis, B.C., Wu, C.S., Dang, G., Jungmann, R.A., Dalla-Favera, R., and Dang, C.V. (1997). c-Myc transactivation of LDH-A: implications for tumor metabolism and growth. Proceedings of the National Academy of Sciences of the United States of America *94*, 6658-6663.

Shimizu, A., Kato, M., Nakao, A., Imamura, T., ten Dijke, P., Heldin, C.H., Kawabata, M., Shimada, S., and Miyazono, K. (1998). Identification of receptors and Smad proteins involved in activin signalling in a human epidermal keratinocyte cell line. Genes Cells *3*, 125-134.

Siegel, R., Eskdale, J., and Gallagher, G. (2011). Regulation of IFN-lambda1 promoter activity (IFN-lambda1/IL-29) in human airway epithelial cells. J Immunol *187*, 5636-5644.

Smith, A.G., Popov, N., Imreh, M., Axelson, H., and Henriksson, M. (2004). Expression and DNA-binding activity of MYCN/Max and Mnt/Max during induced differentiation of human neuroblastoma cells. Journal of cellular biochemistry *92*, 1282-1295.

Solomon, D.L., Amati, B., and Land, H. (1993). Distinct DNA binding preferences for the c-Myc/Max and Max/Max dimers. Nucleic acids research *21*, 5372-5376.

Sommer, A., Bousset, K., Kremmer, E., Austen, M., and Luscher, B. (1998). Identification and characterization of specific DNA-binding complexes containing members of the Myc/Max/Mad network of transcriptional regulators. The Journal of biological chemistry *273*, 6632-6642.

Sommer, A., Waha, A., Tonn, J., Sorensen, N., Hurlin, P.J., Eisenman, R.N., Luscher, B., and Pietsch, T. (1999). Analysis of the Max-binding protein MNT in human medulloblastomas. Int J Cancer *82*, 810-816.

Sotelo, J., Esposito, D., Duhagon, M.A., Banfield, K., Mehalko, J., Liao, H., Stephens, R.M., Harris, T.J., Munroe, D.J., and Wu, X. (2010). Long-range enhancers on 8q24 regulate c-Myc. Proceedings of the National Academy of Sciences of the United States of America *107*, 3001-3005.

Sovak, M.A., Bellas, R.E., Kim, D.W., Zanieski, G.J., Rogers, A.E., Traish, A.M., and Sonenshein, G.E. (1997). Aberrant nuclear factor-kappaB/Rel expression and the pathogenesis of breast cancer. The Journal of clinical investigation *100*, 2952-2960.

Spotts, G.D., Patel, S.V., Xiao, Q., and Hann, S.R. (1997). Identification of downstream-initiated c-Myc proteins which are dominant-negative inhibitors of transactivation by full-length c-Myc proteins. Molecular and cellular biology *17*, 1459-1468.

Stack, M., Jones, D., White, G., Liscia, D.S., Venesio, T., Casey, G., Crichton, D., Varley, J., Mitchell, E., Heighway, J., and et al. (1995). Detailed mapping and loss of heterozygosity analysis suggests a suppressor locus involved in sporadic breast cancer within a distal region of chromosome band 17p13.3. Human molecular genetics *4*, 2047-2055.

Staller, P., Peukert, K., Kiermaier, A., Seoane, J., Lukas, J., Karsunky, H., Moroy, T., Bartek, J., Massague, J., Hanel, F., and Eilers, M. (2001). Repression of p15INK4b expression by Myc through association with Miz-1. Nat Cell Biol *3*, 392-399.

Starczynowski, D.T., Reynolds, J.G., and Gilmore, T.D. (2003). Deletion of either C-terminal transactivation subdomain enhances the in vitro transforming activity of human transcription factor REL in chicken spleen cells. Oncogene *22*, 6928-6936.

Starczynowski, D.T., Reynolds, J.G., and Gilmore, T.D. (2005). Mutations of tumor necrosis factor alpha-responsive serine residues within the C-terminal transactivation domain of human transcription factor REL enhance its in vitro transforming ability. Oncogene *24*, 7355-7368.

Stefanovsky, V., Langlois, F., Gagnon-Kugler, T., Rothblum, L.I., and Moss, T. (2006). Growth factor signaling regulates elongation of RNA polymerase I transcription in mammals via UBF phosphorylation and r-chromatin remodeling. Molecular cell *21*, 629-639.

Stefanovsky, V.Y., Pelletier, G., Bazett-Jones, D.P., Crane-Robinson, C., and Moss, T. (2001). DNA looping in the RNA polymerase I enhancesome is the result of non-cooperative in-phase bending by two UBF molecules. Nucleic acids research *29*, 3241-3247.

Steiger, D., Furrer, M., Schwinkendorf, D., and Gallant, P. (2008). Max-independent functions of Myc in Drosophila melanogaster. Nature genetics *40*, 1084-1091.

Stone, J., de Lange, T., Ramsay, G., Jakobovits, E., Bishop, J.M., Varmus, H., and Lee, W. (1987). Definition of regions in human c-myc that are involved in transformation and nuclear localization. Molecular and cellular biology *7*, 1697-1709.

Sylla, B.S., and Temin, H.M. (1986). Activation of oncogenicity of the c-rel proto-oncogene. Molecular and cellular biology *6*, 4709-4716.

Takahashi, K., and Yamanaka, S. (2006). Induction of pluripotent stem cells from mouse embryonic and adult fibroblast cultures by defined factors. Cell *126*, 663-676.

Takahashi, T., Konishi, H., Kozaki, K., Osada, H., Saji, S., Takahashi, T., and Takahashi, T. (1998). Molecular analysis of a Myc antagonist, ROX/Mnt, at 17p13.3 in human lung cancers. Jpn J Cancer Res *89*, 347-351.

Tao, H., and Umek, R.M. (1999). Reciprocal regulation of gadd45 by C/EBP alpha and c-Myc. DNA and cell biology *18*, 75-84.

Taub, R., Kirsch, I., Morton, C., Lenoir, G., Swan, D., Tronick, S., Aaronson, S., and Leder, P. (1982). Translocation of the c-myc gene into the immunoglobulin heavy chain locus in human Burkitt lymphoma and murine plasmacytoma cells. Proceedings of the National Academy of Sciences of the United States of America *79*, 7837-7841.

Terragni, J., Nayak, G., Banerjee, S., Medrano, J.L., Graham, J.R., Brennan, J.F., Sepulveda, S., and Cooper, G.M. (2011). The E-box binding factors Max/Mnt, MITF, and USF1 act coordinately with FoxO to regulate expression of proapoptotic and cell cycle control genes by phosphatidylinositol 3-kinase/Akt/glycogen synthase kinase 3 signaling. The Journal of biological chemistry *286*, 36215-36227.

Thanasopoulou, A., Stravopodis, D.J., Dimas, K.S., Schwaller, J., and Anastasiadou, E. (2012). Loss of CCDC6 affects cell cycle through impaired intra-S-phase checkpoint control. PloS one *7*, e31007.

Thomas, L.R., and Tansey, W.P. (2011). Proteolytic control of the oncoprotein transcription factor Myc. Advances in cancer research *110*, 77-106.

Thompson, C.B., Challoner, P.B., Neiman, P.E., and Groudine, M. (1985). Levels of c-myc oncogene mRNA are invariant throughout the cell cycle. Nature *314*, 363-366.

Thompson, C.B., Humphries, E.H., Carlson, L.M., Chen, C.L., and Neiman, P.E. (1987). The effect of alterations in myc gene expression on B cell development in the bursa of Fabricius. Cell *51*, 371-381.

Tian, W., and Liou, H.C. (2009). RNAi-mediated c-Rel silencing leads to apoptosis of B cell tumor cells and suppresses antigenic immune response in vivo. PloS one *4*, e5028.

Tischler, A.S., and Greene, L.A. (1978). Morphologic and cytochemical properties of a clonal line of rat adrenal pheochromocytoma cells which respond to nerve growth factor. Laboratory investigation; a journal of technical methods and pathology *39*, 77-89.

Tong, Q., Xing, S., and Jhiang, S.M. (1997). Leucine zipper-mediated dimerization is essential for the PTC1 oncogenic activity. The Journal of biological chemistry *272*, 9043-9047.

Tonissen, K.F., and Krieg, P.A. (1994). Analysis of a variant Max sequence expressed in Xenopus laevis. Oncogene *9*, 33-38.

Torrano, V., Chernukhin, I., Docquier, F., D'Arcy, V., Leon, J., Klenova, E., and Delgado, M.D. (2005). CTCF regulates growth and erythroid differentiation of human myeloid leukemia cells. The Journal of biological chemistry *280*, 28152-28161.

Toyo-oka, K., Bowen, T.J., Hirotsune, S., Li, Z., Jain, S., Ota, S., Escoubet-Lozach, L., Garcia-Bassets, I., Lozach, J., Rosenfeld, M.G*., et al.* (2006). Mnt-deficient mammary glands exhibit impaired involution and tumors with characteristics of myc overexpression. Cancer research *66*, 5565-5573.

Toyo-oka, K., Hirotsune, S., Gambello, M.J., Zhou, Z.Q., Olson, L., Rosenfeld, M.G., Eisenman, R., Hurlin, P., and Wynshaw-Boris, A. (2004). Loss of the Max-interacting protein Mnt in mice results in decreased viability, defective embryonic growth and craniofacial defects: relevance to Miller-Dieker syndrome. Human molecular genetics *13*, 1057-1067.

Trapnell, C., Pachter, L., and Salzberg, S.L. (2009). TopHat: discovering splice junctions with RNA-Seq. Bioinformatics (Oxford, England) *25*, 1105-1111.

Trapnell, C., Williams, B.A., Pertea, G., Mortazavi, A., Kwan, G., van Baren, M.J., Salzberg, S.L., Wold, B.J., and Pachter, L. (2010). Transcript assembly and quantification by RNA-Seq reveals unannotated transcripts and isoform switching during cell differentiation. Nature biotechnology *28*, 511-515.

Tuan, J.C., Zhai, W., and Comai, L. (1999). Recruitment of TATA-binding protein-TAFI complex SL1 to the human ribosomal DNA promoter is mediated by the carboxy-terminal activation domain of upstream binding factor (UBF) and is regulated by UBF phosphorylation. Molecular and cellular biology *19*, 2872-2879.

Tumang, J.R., Hsia, C.Y., Tian, W., Bromberg, J.F., and Liou, H.C. (2002). IL-6 rescues the hyporesponsiveness of c-Rel deficient B cells independent of Bcl-xL, Mcl-1, and Bcl-2. Cellular immunology *217*, 47-57.

Turriziani, B., Garcia-Munoz, A., Pilkington, R., Raso, C., Kolch, W., and von Kriegsheim, A. (2014). On-beads digestion in conjunction with data-dependent mass spectrometry: a shortcut to quantitative and dynamic interaction proteomics. Biology *3*, 320-332.

Tuupanen, S., Turunen, M., Lehtonen, R., Hallikas, O., Vanharanta, S., Kivioja, T., Bjorklund, M., Wei, G., Yan, J., Niittymaki, I.*, et al.* (2009). The common colorectal cancer predisposition SNP rs6983267 at chromosome 8q24 confers potential to enhanced Wnt signaling. Nature genetics *41*, 885-890.

Udalova, I.A., Mott, R., Field, D., and Kwiatkowski, D. (2002). Quantitative prediction of NF-kappa B DNA-protein interactions. Proceedings of the National Academy of Sciences of the United States of America *99*, 8167-8172.

Ullius, A., Luscher-Firzlaff, J., Costa, I.G., Walsemann, G., Forst, A.H., Gusmao, E.G., Kapelle, K., Kleine, H., Kremmer, E., Vervoorts, J., and Luscher, B. The interaction of MYC with the trithorax protein ASH2L promotes gene transcription by regulating H3K27 modification. Nucleic acids research *42*, 6901-6920.

van Riggelen, J., Yetil, A., and Felsher, D.W. (2010). MYC as a regulator of ribosome biogenesis and protein synthesis. Nature reviews *10*, 301-309.

Vaque, J.P., Fernandez-Garcia, B., Garcia-Sanz, P., Ferrandiz, N., Bretones, G., Calvo, F., Crespo, P., Marin, M.C., and Leon, J. (2008). c-Myc inhibits Ras-mediated differentiation of pheochromocytoma cells by blocking c-Jun up-regulation. Mol Cancer Res *6*, 325-339.

Vaque, J.P., Navascues, J., Shiio, Y., Laiho, M., Ajenjo, N., Mauleon, I., Matallanas, D., Crespo, P., and Leon, J. (2005). Myc antagonizes Ras-mediated growth arrest in leukemia cells through the inhibition of the Ras-ERK-p21Cip1 pathway. The Journal of biological chemistry *280*, 1112-1122.

Vastrik, I., Kaipainen, A., Penttila, T.L., Lymboussakis, A., Alitalo, R., Parvinen, M., and Alitalo, K. (1995). Expression of the mad gene during cell differentiation in vivo and its inhibition of cell growth in vitro. The Journal of cell biology *128*, 1197-1208.

Vastrik, I., Koskinen, P.J., Alitalo, R., and Makela, T.P. (1993). Alternative mRNA forms and open reading frames of the max gene. Oncogene *8*, 503-507.

Vennstrom, B., Sheiness, D., Zabielski, J., and Bishop, J.M. (1982). Isolation and characterization of c-myc, a cellular homolog of the oncogene (v-myc) of avian myelocytomatosis virus strain 29. Journal of virology *42*, 773-779.

Verma, I.M., Stevenson, J.K., Schwarz, E.M., Van Antwerp, D., and Miyamoto, S. (1995). Rel/NF-kappa B/I kappa B family: intimate tales of association and dissociation. Genes & development *9*, 2723-2735.

Vermeer, M.H., van Doorn, R., Dijkman, R., Mao, X., Whittaker, S., van Voorst Vader, P.C., Gerritsen, M.J., Geerts, M.L., Gellrich, S., Soderberg, O.*, et al.* (2008). Novel and highly recurrent chromosomal alterations in Sezary syndrome. Cancer research *68*, 2689-2698.

Vervoorts, J., Luscher-Firzlaff, J., and Luscher, B. (2006). The ins and outs of MYC regulation by posttranslational mechanisms. The Journal of biological chemistry *281*, 34725-34729.

Vervoorts, J., Luscher-Firzlaff, J.M., Rottmann, S., Lilischkis, R., Walsemann, G., Dohmann, K., Austen, M., and Luscher, B. (2003). Stimulation of c-MYC transcriptional activity and acetylation by recruitment of the cofactor CBP. EMBO Rep *4*, 484-490.

Voigt, P., and Reinberg, D. (2013). Epigenome editing. Nature biotechnology *31*, 1097-1099.

Wagner, A.J., Kokontis, J.M., and Hay, N. (1994). Myc-mediated apoptosis requires wild-type p53 in a manner independent of cell cycle arrest and the ability of p53 to induce p21waf1/cip1. Genes & development *8*, 2817-2830.

Wahlstrom, T., Belikov, S., and Arsenian Henriksson, M. (2013). Chromatin dynamics at the hTERT promoter during transcriptional activation and repression by c-Myc and Mnt in Xenopus leavis oocytes. Experimental cell research *319*, 3160-3169.

Walker, W., Zhou, Z.Q., Ota, S., Wynshaw-Boris, A., and Hurlin, P.J. (2005). Mnt-Max to Myc-Max complex switching regulates cell cycle entry. The Journal of cell biology *169*, 405-413.

Wang, H., Nicholson, P.R., and Stillman, D.J. (1990). Identification of a Saccharomyces cerevisiae DNA-binding protein involved in transcriptional regulation. Molecular and cellular biology *10*, 1743-1753.

Wang, J., Xie, L.Y., Allan, S., Beach, D., and Hannon, G.J. (1998). Myc activates telomerase. Genes & development *12*, 1769-1774.

Wang, R., Dillon, C.P., Shi, L.Z., Milasta, S., Carter, R., Finkelstein, D., McCormick, L.L., Fitzgerald, P., Chi, H., Munger, J., and Green, D.R. (2011). The transcription factor Myc controls metabolic reprogramming upon T lymphocyte activation. Immunity *35*, 871-882.

Werner, S., Beer, H.D., Mauch, C., Luscher, B., and Werner, S. (2001). The Mad1 transcription factor is a novel target of activin and TGF-beta action in keratinocytes: possible role of Mad1 in wound repair and psoriasis. Oncogene *20*, 7494-7504.

West, M.J., Stoneley, M., and Willis, A.E. (1998). Translational induction of the c-myc oncogene via activation of the FRAP/TOR signalling pathway. Oncogene *17*, 769-780.

Wierstra, I., and Alves, J. (2008). The c-myc promoter: still MysterY and challenge. Advances in cancer research *99*, 113-333.

Wietek, C., and O'Neill, L.A. (2007). Diversity and regulation in the NF-kappaB system. Trends in biochemical sciences *32*, 311-319.

Wilhelmsen, K.C., Eggleton, K., and Temin, H.M. (1984). Nucleic acid sequences of the oncogene v-rel in reticuloendotheliosis virus strain T and its cellular homolog, the proto-oncogene c-rel. Journal of virology *52*, 172-182.

Williamson, M.P., Elder, P.A., and Knowles, M.A. (1994). The spectrum of TP53 mutations in bladder carcinoma. Genes, chromosomes & cancer *9*, 108-118.

Wright, C.W., and Duckett, C.S. (2005). Reawakening the cellular death program in neoplasia through the therapeutic blockade of IAP function. The Journal of clinical investigation *115*, 2673-2678.

Wu, K.J., Grandori, C., Amacker, M., Simon-Vermot, N., Polack, A., Lingner, J., and Dalla-Favera, R. (1999). Direct activation of TERT transcription by c-MYC. Nature genetics *21*, 220-224.

Wu, S., Cetinkaya, C., Munoz-Alonso, M.J., von der Lehr, N., Bahram, F., Beuger, V., Eilers, M., Leon, J., and Larsson, L.G. (2003). Myc represses differentiation-induced p21CIP1 expression via Miz-1-dependent interaction with the p21 core promoter. Oncogene *22*, 351-360.

Xiao, Q., Claassen, G., Shi, J., Adachi, S., Sedivy, J., and Hann, S.R. (1998). Transactivation-defective c-MycS retains the ability to regulate proliferation and apoptosis. Genes & development *12*, 3803-3808.

Xu, D., Popov, N., Hou, M., Wang, Q., Bjorkholm, M., Gruber, A., Menkel, A.R., and Henriksson, M. (2001). Switch from Myc/Max to Mad1/Max binding and decrease in histone acetylation at the telomerase reverse transcriptase promoter during differentiation of HL60 cells. Proceedings of the National Academy of Sciences of the United States of America *98*, 3826-3831.

Xu, L., Zhu, J., Hu, X., Zhu, H., Kim, H.T., LaBaer, J., Goldberg, A., and Yuan, J. (2007). c-IAP1 cooperates with Myc by acting as a ubiquitin ligase for Mad1. Molecular cell *28*, 914-922.

Yamamoto, Y., and Gaynor, R.B. (2004). IkappaB kinases: key regulators of the NF-kappaB pathway. Trends in biochemical sciences *29*, 72-79.

Yuan, J., Tirabassi, R.S., Bush, A.B., and Cole, M.D. (1998). The C. elegans MDL-1 and MXL-1 proteins can functionally substitute for vertebrate MAD and MAX. Oncogene *17*, 1109-1118.

Zervos, A.S., Gyuris, J., and Brent, R. (1993). Mxi1, a protein that specifically interacts with Max to bind Myc-Max recognition sites. Cell *72*, 223-232.

Zhu, J., Blenis, J., and Yuan, J. (2008). Activation of PI3K/Akt and MAPK pathways regulates Myc-mediated transcription by phosphorylating and promoting the degradation of Mad1. Proceedings of the National Academy of Sciences of the United States of America *105*, 6584-6589.

Zindy, F., Eischen, C.M., Randle, D.H., Kamijo, T., Cleveland, J.L., Sherr, C.J., and Roussel, M.F. (1998). Myc signaling via the ARF tumor suppressor regulates p53-dependent apoptosis and immortalization. Genes & development *12*, 2424-2433.

Zomerdijk, J.C., Beckmann, H., Comai, L., and Tjian, R. (1994). Assembly of transcriptionally active RNA polymerase I initiation factor SL1 from recombinant subunits. Science (New York, N.Y *266*, 2015-2018.

Resumen en castellano

8. RESUMEN EN CASTELLANO

8.1. INTRODUCCIÓN

La red MYC/MAX/MXD es una red de factores de transcripción que se encarga de regular la expresión génica de múltiples genes implicados en diferentes procesos biológicos como pueden ser la diferenciación celular, proliferación, crecimiento celular, apoptosis o el metabolismo. Esta red está formada fundamentalmente por tres familias de proteínas, las proteínas MYC, MAX y MXD. Todas ellas tienen un dominio en común que es el dominio b-HLH-LZ (básico, hélice-lazo-hélice, cremallera de leucinas) a través del cual son capaces de dimerizar (por la segunda hélice y la cremallera de leucinas) y unirse al DNA (por la región básica y la primera hélice). (Eisenman 2000). Las proteínas MYC y MXD necesitan heterodimerizar con MAX para unirse al DNA. Estos heterodímeros y homodímeros se unen al DNA en secuencias específicas denominadas "cajas E" (E-box) que se encuentran en regiones reguladoras del genoma. De esta manera, los heterodímeros MYC-MAX se unen a las cajas E actuando principalmente como activadores transcripcionales mientras que los heterodímeros MXD-MAX actúan como represores de sus genes diana comunes. Por otra parte, los homodímeros MAX se unen a estas regiones pero no presentan actividad transcripcional (Eisenman, 2000).

La familia MYC está compuesta por las proteínas c-MYC (MYC en adelante), N-MYC y L-MYC. MYC fue el primer factor de transcripción identificado con capacidad oncogénica. Su papel en tumorogénesis ha sido evidenciado en multitud de neoplasmas (linfomas, carcinomas de pulmón de células pequeñas, neuroblastomas, etc.) y su desregulación a causa de diversos mecanismos (alteraciones genómicas, desregulación del promotor, estabilización de la proteína) es considerada una de las alteraciones oncogénicas más comunes en cáncer (Eilers and Eisenman, 2008; Vervoorts et al., 2006). Las proteínas MYC presentan una localización nuclear, tienen una vida media corta y su expresión se encuentra directamente relacionada con proliferación y progresión del ciclo celular e inversamente relacionada con estados de parada de ciclo celular y diferenciación (Grandori et al., 2000). Las proteínas MYC activan la transcripción génica a través de su interacción con diversas proteínas capaces de remodelar la cromatina como son los complejos SWI/SNF, proteínas histona acetil-tranferasas o metiltranferasas. Estas proteínas permiten una conformación adecuada de la cromatina para que los complejos RNA polimerasas (I, II y III) puedan acceder e iniciar la transcripción génica (Vervoots et al., 2003). Por otra parte, también se han descrito mecanismos de represión transcripcional mediada por MYC a través de la interacción con proteínas histona deacetil-transferasas, otras metiltransferasas o impidiendo la formación de complejos transactivadores a través de su interacción con los factores de transcripción MIZ1 o SP1 (Brenner et al., 2005; Mao et al., 2003; Wu et al., 2003). De esta manera, MYC puede regular la transcripción génica en ambas direcciones (activando o reprimiendo la transcripción génica) lo que hace de MYC un factor de transcripción de amplio espectro capaz de regular múltiples genes y por lo tanto múltiples funciones celulares.

La familia MXD está compuesta por las proteínas MXD1, MXI1 (MXD2), MXD3, MXD4 y MNT. Todas ellas presentan dos dominios comunes, el b-HLH-LZ y el domino SID (Dominio de interacción con la proteína SIN3). Las proteínas MXD1, MXI1, MXD3 y MXD4 son homólogas (Hurlin et al., 1995b) siendo la proteína MNT la que presenta menor homología. La expresión de las proteínas MXD (fundamentalmente MXD1-4) se encuentra altamente ligada a procesos de quiescencia y diferenciación celular mientras que sus niveles de expresión en procesos de proliferación celular e indiferenciación son muy bajos e incluso indetectables (Luscher, 2012). Por el contrario, MNT se expresa de forma constitutiva en los diferentes estados celulares (Hurlin et al., 1997b). Las proteínas MXD a través de su domino SID, interaccionan con los corepresores SIN3A y SIN3B, que a su vez interaccionan con diversas proteínas con actividad deacetil-transferasas o demetilasas que provocan una compactación de la cromatina impidiendo el acceso de la maquinaria de transcripción. De esta manera, las proteínas MXD a través de su interacción con las proteínas SIN3 forman complejos represores regulando negativamente la transcripción génica de sus genes diana (Eisenman, 2000).

Las proteínas MAX son los únicos miembros de la red capaces de homodimerizar y unirse al DNA a través del dominio b-HLH-LZ. Sin embargo, no presentan capacidad transcripcional al carecer de dominios transactivadores o represores. Además, presentan una región de localización nuclear (NLS) (Kato et al., 1992) que contribuye a que los homodímeros y heterodímeros presenten una localización nuclear. Las proteínas MAX se expresan de forma constitutiva independientemente del estado celular y presentan una alta estabilidad a nivel de proteína. De esta manera, MAX es un elemento clave de la red MYC/MAX/MXD al interaccionar con las proteínas MYC y MXD en los distintos estados celulares y permitir que sean capaces de unirse al DNA en las cajas E regulando así la transcripción génica. Sin embargo, se han descrito casos donde la proteína MAX es inactiva por reorganización génica o por mutaciones inactivadoras (Hopewell and Ziff, 1995; Comino-Mendez et al., 2011, Romero et al., 2014) sugiriendo una desestabilización de la red MYC/MAX/MXD y su implicación en tumorogénesis.

La línea celular de feocromocitoma de rata PC12 fue el primer ejemplo identificado donde la proteína MAX no es funcional a causa de una alteración génica. Esta alteración da lugar a una proteína MAX truncada a la que le falta la segunda hélice y la cremallera de leucinas del dominio b-HLH-LZ. De esta manera esta proteína MAX^{PC12} es incapaz de homodimerizar y heterodimerizar (Hopewell and Ziff, 1995). La línea UR61 es una línea derivada de la línea PC12. Esta línea celular presenta como característica la presencia de un gen N-RAS constitutivamente activo cuya expresión es inducible por dexametasona. La inducción de la vía RAS-MAPK en esta línea celular desencadena un proceso de diferenciación celular en el cual se adquiere un fenotipo de tipo neuronal (Guerrero et al., 1988). Con este modelo, en nuestro laboratorio se descubrió que MYC era capaz de mantener una de sus principales funciones como es la inhibición de la diferenciación celular, de forma independiente a su heterodimerización con MAX (Vaqué et al., 2008). Además, en nuestro laboratorio se crearon dos líneas celulares (denominadas UR61-MT-MAX y UR61-MT-Hebo) donde la expresión de MAX (UR61-MT-MAX) o su control vacío (UR61-MT-Hebo) estaba inducida por la presencia de Zn_2SO_4.

8.2. OBJETIVOS

El estudio de la red MYC/MAX/MXD es de considerable importancia ya que a través de la regulación génica, está implicada en múltiples procesos celulares. De esta manera, el desequilibrio de la red como consecuencia de alteraciones en los diferentes elementos de la red (MYC, MAX y MXD) da lugar a una desregulación génica y por lo tanto de la biología celular que podría llevar a procesos tumorogénicos y cáncer.

En este trabajo nos propusimos estudiar la parte MXD (concretamente de los miembros MXD1 y MNT) de la red MYC/MAX/MXD con los siguientes objetivos:

1. Estudiar la localización subcelular de MXD1 y MNT en células con y sin MAX.
2. Explorar funciones de MXD1 y MNT en proliferación y diferenciación independientes de MAX.
3. Estudiar el papel de MNT en la regulación transcripcional en células con y sin MAX.
4. Identificar nuevas y relevantes interacciones de MNT con otras proteínas.

8.3. RESULTADOS Y DISCUSIÓN

8.3.1. Otras funciones de MXD1

MXD1 se ha visto implicado en diferenciación y parada de ciclo celular, sin embargo, su papel fuera de estos procesos biológicos no ha sido estudiado en profundidad. En este trabajo hemos descubierto que MXD1 se encuentra expresado en diferentes tipos celulares en condiciones de proliferación e indiferenciación celular como son las líneas de células madre embrionarias humanas Hs181.1 y Val3; la línea de células madre mesenquimales humanas MSC-3H transformada con HPV-E6, HPV-E7 and hTERT (Funes et al., 2007) y la líneas celulares HEK293T (epiteliales humanas), UR61 (feocromocitoma de rata) y derivadas de UR61. Además, hemos analizado la localización subnuclear de MXD1 en estas condiciones y hemos visto que MXD1 se localiza en el nucleoplasma y en los centros fibrilares (FC) del nucleolo colocalizando con el marcador nucleolar UBF (figura 4.5). Los centros fibrilares es donde tiene lugar la regulación transcripcional del DNA ribosomal (rDNA). Hemos estudiado el papel de MXD1 en esta localización subnuclear y hemos descubierto que MXD1 interacciona con UBF y que se une a lo largo del rDNA aunque con mayor afinidad por la regiones intergénicas (figura 4.8-10). Por otra parte, hemos visto que el silenciamiento de MXD1 en estas condiciones provoca un ligero aumento en la cantidad total de RNA en la célula. Teniendo en cuenta que más del 80 % del RNA es rRNA, este resultado sugiere que MXD1 con su localización nucleolar podría estar modulando la transcripción y síntesis del rRNA.

8.3.2. MXD1 y MNT en ausencia de MAX

En nuestro laboratorio y otros se descubrió que MYC era capaz de ejercer alguna función en ausencia de MAX (Vaque et al., 2008), así pues, quisimos saber si las proteínas MXD1 y MNT también tenían funciones independientes de MAX. Para ello usamos el modelo celular UR61 en el que se induce la diferenciación neuronal al inducir la expresión del oncogén N-RAS con dexametasona. En primer lugar estudiamos dos de las principales funciones de las proteínas MXD como son su implicación en diferenciación celular y la represión transcripcional a través de la unión a cajas E. Transfectamos vectores de expresión de MXD1 y MNT a las células UR61 e indujimos la diferenciación con 100 nM dexametasona. A las 24 h después del tratamiento y 36 h post-transfección, analizamos la diferenciación celular mediante observación del fenotipo celular pero no encontramos cambios en comparación con el control. Alternativamente, transfectamos las células UR61 de forma transitoria con vectores de expresión de MXD1 y MNT y a las 24 h post-transfección analizamos mediante RT-qPCR la expresión de marcadores neuronales (*GAP43*, *VGF*, *NGFR*, *CHGA* o el factor de transcripción *c-JUN* implicado en este proceso (Vaqué et al., 2008). La presencia de MXD1 y MNT no provocó un aumento de la expresión de los marcadores neuronales en comparación con el control (figura 4.15). Estos resultados nos indican que las proteínas MXD1 y MNT en ausencia de MAX no favorecen la diferenciación celular de la línea UR61. En segundo lugar, analizamos su papel como reguladores transcripcionales en ausencia de MAX. Para ello hicimos ensayos luciferasas con un vector reportero que contenía 4 cajas E en la región reguladora. De esta manera, transfectamos las células UR61 con los vectores luciferasa y vectores de expresión de MXD1, MNT y MAX por separado o MNT y MXD1 junto con MAX y a las 36 h post-transfección realizamos los ensayos luciferasa. Los resultados nos indicaron

que MNT y MXD1 no son capaces de regular negativamente la transcripción génica a través de cajas E pero sí cuando están en presencia de MAX. Además, también estudiamos si la sobreexpresión de MXD1 era capaz de provocar una parada de la proliferación en las células UR61. Para ello transfectamos las células con un vector de expresión de MXD1 o el vector vacío junto con un vector con resistencia a puromicina en una relación 5:1. A las 24 h post-transfección seleccionamos las células con puromicina de manera que las células resistentes fuesen las que hubiesen incorporado los dos vectores (el de expresión de MXD1 y resistencia a puromicina). A los 6 días post-selección analizamos mediante tinción con cristal violeta la proliferación celular y vimos que no había diferencias en la proliferación celular con respecto al control indicándonos que al menos en ausencia de MAX, MXD1 no es capaz de inducir una parada de la proliferación en este modelo celular (figura 4.18).

También quisimos estudiar qué papel tenía MNT en las células UR61 ya que vimos que se encontraba altamente expresado en estas células que no expresan MAX. Además, intentamos varias veces incrementar todavía más los niveles de MNT mediante el uso de vectores de expresión pero no conseguimos aumentar su expresión. Lo primero que hicimos fue analizar la expresión de MNT en presencia de MAX. Para ello transfectamos un vector de expresión de MAX o indujimos la expresión de MAX con 100 µM Zn_2SO_4 en las UR61-MT-MAX y a las 24 h post-transfección/tratamiento analizamos la expresión de MNT mediante western blot y RT-qPCR. Los resultados mostraron que MNT en presencia de MAX baja su expresión a nivel de proteína y RNA (figura 4.19). Además, en las células humanas de leucemia K562, la sobreexpresión de MAX (por transfección transitoria con un vector de expresión) también hizo disminuir los niveles de MNT, mientras que el silenciamiento de MAX (mediante siRNAs) provocó aumento de la expresión de MNT a nivel de RNA y proteína, reproduciendo por tanto los resultados observados en las células UR61. Posteriormente mediante un análisis bioinformático, estudiamos la presencia de cajas E en el promotor de *MNT* de humano, ratón y rata. Las tres especies presentaron dos cajas E (una canónica y otra no canónica) a menos de 1000 pb del inicio de transcripción de *MNT*. Además estudiamos la homología del promotor en estas especies y vimos que el promotor de *MNT* está altamente conservado en mamíferos. Como MNT heterodimeriza con MAX y reprime la transcripción génica a través de la unión a caja E, analizamos si MNT era capaza de regular su propia expresión. En primer lugar nos preguntamos si MNT y MAX podrían unirse al promotor de *MNT*. Para ello analizamos los estudios de ChIP-seq presentes en el proyecto ENCODE para las proteínas de la red MYC/MAX/MXD (MYC, MAX y MXI1) en distintas líneas celulares. Este análisis nos indicó que los miembros de la red presentaban picos de unión al promotor de *MNT* humano a menos de 1000 pb del inicio de transcripción que incluían dichas cajas E (figura 4.22). Posteriormente, seguimos analizando mediante inmunoprecipitación de cromatina (ChIP) si MNT y MAX se unían al promotor de *MNT* en las UR61 con o sin MAX. Los resultados nos indicaron que MNT se une a su promotor únicamente cuando MAX está presente y no en las células UR61 sin MAX (figura 4.23). Además, hicimos ensayos luciferasas para medir la actividad del promotor. Construimos un vector luciferasa que tenía como región reguladora 800 pb del promotor de *MNT* humano y lo co-transfectamos con MAX únicamente o con MAX y MNT en las células UR61 y con un vector de expresión de MNT en las HEK293T que ya expresan MAX. Los resultados nos indicaron que la presencia de MNT y MAX disminuía la actividad luciferasa por lo tanto que MAX regula negativamente el promotor de *MNT*.

También demostramos una autoregulacion negativa de *MNT* pues la expresión forzada de MNT disminuye la actividad de su propio promotor (figura 4.24).

Para profundizar en el comportamiento de MNT en presencia y ausencia de MAX, sobreexpresamos MAX en las células UR61 y silenciamos MAX en la línea K562. Posteriormente analizamos mediante inmunofluorescencia (en las UR61) o fraccionamiento núcleo-citoplama (en las UR61 y K562) la localización de MNT en presencia o ausencia de MAX. Además, también hicimos un fraccionamiento de la línea celular HEK293T que expresa MAX. Los resultados nos indicaron que en presencia de MAX, MNT presenta una localización nuclear mientras que en ausencia de MAX, MNT aumenta su expresión y se localiza en el núcleo y en el citoplasma (figura 4.25). Habíamos visto que MNT en las UR61 sin MAX estaba altamente expresado y además no conseguíamos incrementar sus niveles mediante vectores de expresión. Esto nos hacía pensar que estaba habiendo una autoregulación negativa de MNT a nivel transcripcional o de estabilidad proteica. Por otra parte, habíamos visto que MNT únicamente era capaz de regular su expresión en presencia de MAX. Por este motivo, nos preguntamos si MNT estaba siendo regulado a nivel de proteína. Para ello, transfectamos las UR61 con un vector de expresión de MNT o el vector vacío y a las 16 post-transfección inhibimos la degradación de proteínas vía proteasoma con 15 nM y 50 nM bortezomib durante 16 h para ver si el MNT ectópico estaba siendo degradado. Los resultados nos indicaron que el MNT ectópico en las células UR61 que ya expresan altos niveles de MNT, estaba siendo degradado vía proteasoma y que por lo tanto había una regulación negativa de MNT a nivel de proteína (figura 4.28).

También quisimos saber con qué proteínas podría estar interaccionando MNT en ausencia de MAX. Para ello transfectamos un vector de expresión de MNT en las células UR61 con y sin MAX con intención de aumentar los niveles de MNT. A las 24 h post-transfección hicimos una inmunoprecipitación de MNT y analizamos mediante espectrometría de masas qué proteínas habían co-inmunoprecipitado con MNT en presencia y ausencia de MAX. Este experimento se hizo por triplicado en las dos situaciones (sin y con MAX) y los resultados nos indicaron que 11 proteínas co-inmunoprecipitaron con MNT cuando no estaba MAX y 47 proteínas cuando estaba MAX. Además, había 5 proteínas presentes en ambas condiciones, lo que indicaba que estaban interaccionando con MNT de forma independiente a la presencia de MAX (tabla 4.1). De estas 5 proteínas nos centramos en REL y CCDC6, dos proteínas que en condiciones normales se encuentran localizadas en el citoplasma. REL forma parte de la famila NF-κB mientras que CCDC6, debido a una translocacion, forma parte (aminoácidos del 1 al 101) de la proteína de fusión oncogénica RET-PTC1 frecuente en carcinoma de tiroides. Además, CCDC6 está implicada en apoptosis y respuesta a daño al DNA. Para confirmar los resultados obtenidos por proteómica, hicimos immunoprecipitaciones de MNT en UR61 y detectamos mediante western blot que REL co-inmunoprecipitaba con MNT en UR61. Sin embargo, no pudimos confirmar los resultados de CCDC6 en las UR61. Por ello, transfectamos vectores de expresión de CCDC6 (etiquetados con un epítopo de Myc) y MNT en la línea celular HEK293T. Posteriormente, inmunoprecipitamos MNT y detectamos mediante western blot que CCDC6 co-inmunoprecipitaba con MNT. Además, transfectamos dos mutantes de CCDC6 etiquetados con el epítopo Myc (CCDC6(1-101) y CCDC6(1-223) que contienen los aminoácidos 1 al 101 y 1 al 223 respectivamente) para intentar encontrar la región

de interacción de CCDC6 con MNT. Con estos mutantes vimos que el CCDC6(1-223) pero no el CCDC6(1-101) co-inmunoprecipitaba con MNT, indicándonos que CCDC6 necesita al menos los primeros 223 aminoácidos para interaccionar con MNT (figura 4.27).

Como MNT estaba altamente regulado y el incremento de MNT no era posible debido a esa degradación vía proteasoma, quisimos estudiar los efectos de silenciar MNT en las células UR61 para intentar elucidar qué papel estaba teniendo MNT en esta línea celular. Para ello, en primer lugar transfectamos las células UR61 con un vector que llevaba una secuencia shRNA (short hairpin RNA) contra el gen MNT (sh-MNT) o el vector vacío (pLKO) junto con un vector de expresión GFP en una proporción 5:1 (para asegurarnos que la gran mayoría de las células GFP-positivas habían sido también transfectadas con sh-MNT o pLKO). Al cabo de 6 días post-transfección analizamos la proporción de células GFP-positivas. De esta manera vimos que las células transfectadas con el sh-MNT presentaban menor proporción de células GFP positivas indicándonos que la presencia del vector sh-MNT reducía la proliferación de las células GFP positivas en comparación con el pLKO. Además, también transfectamos las células UR61 con los plásmidos sh-MNT y pLKO y analizamos la proliferación celular mediante contaje celular a los 3, 6 y 12 días post-transfección. Los resultados nos indicaron que las células UR61 transfectadas con el sh-MNT presentaban una menor tasa de crecimiento en comparación con las transfectadas con el pLKO. Para seguir confirmando el efecto de silenciamiento en el proliferación celular de las células UR61 y si éste se modificaba en presencia MAX, transfectamos los plásmidos sh-MNT y pLKO junto con un vector de expresión de MAX o su vector vacío (pCEFL). Al día siguiente añadimos puromicina para seleccionar las células con el sh-MNT y pLKO y a los 17 días post-selección analizamos mediante tinción con cristal violeta la proliferación de las células UR61. Los resultados nos mostraron que el silenciamiento de MNT en la línea UR61 frena la proliferación celular y que la presencia de MAX junto con el silenciamiento de MNT tiene un efecto aditivo a este efecto (figura 4.29). Además, el silenciamiento de MNT en las UR61 provocaba un aumento del doble de células en fase subG0 del ciclo celular (indicativa de muerte celular). Y el silenciamiento de MNT en las UR61 en presencia o ausencia de MAX, provocaba una bajada de expresión de la ciclina A2 (CCNA2) implicada en la progresión del ciclo celular, una bajada de la proteína antiapoptótica BCL-XL y una rotura de la proteína PARP1 indicadora de activación de apoptosis. Estos resultados sugieren que el silenciamiento de MNT frena el crecimiento celular al impedir una progresión del ciclo celular y provocar una activación de la apoptosis (figura 4.30).

Habíamos visto que el silenciamiento de MNT impedía la progresión del ciclo celular y una activación de la apoptosis y por otra parte que MNT interaccionaba con REL en las células UR61. Como la vía de NF-κB está implicada en la supervivencia celular (Fullard et al., 2012) quisimos estudiar si la interacción MNT-REL estaba modulando la vía de NF-κB. Para ello, hicimos ensayos luciferasa con un vector luciferasa cuya región reguladora consta de 5 regiones Iκ (regiones de unión al DNA de los miembros de NF-κB). Transfectamos las células UR61 con este vector luciferasa y el plásmido sh-MNT o pLKO y a las 72 h post-transfección analizamos la actividad luciferasa. Los resultados nos indicaron que el silenciamiento de MNT provoca un aumento de la actividad luciferasa. Para confirmar este resultado, hicimos ensayos luciferasa en la línea celular HeLa silenciando o sobreexpresando MNT (figura 4.31). Los resultados nos indicaron que la actividad luciferasa aumentaba o disminuía cuando MNT estaba

silenciado o sobreexpresado respectivamente. Para seguir estudiando los posibles efectos de la interacción MNT-REL en las células UR61, silenciamos MNT y analizamos los efectos sobre proliferación en las células tratadas con la citoquina TNFα (activadora de la vía canónica de NF-κB) (Fullard et al, 2012.). Para ello transfectamos las células UR61 con el sh-MNT o el vector vacío y tratamos las células con 100 ng/ml de TNFα durante 7 días. Transcurrido ese tiempo, analizamos los efectos en la proliferación mediante tinción con cristal violeta. Los resultados nos indicaron que las células UR61 disminuyen la proliferación con el tratamiento de TNFα y que esta disminución se incrementa en condiciones donde MNT está silenciado (figura 4.32). Estos resultados sugieren que MNT está frenando la actividad NF-κB por algún mecanismo y que el silenciamiento de MNT provoca una activación de la vía induciendo una parada de la proliferación o muerte celular.

Como MNT es un factor de transcripción y parece que su presencia en las células UR61 es crucial para su capacidad proliferativa y supervivencia, decidimos analizar el transcriptoma de las UR61 donde habíamos silenciado MNT en presencia o ausencia de MAX. Para ello transfectamos las UR61-MT-Hebo o UR61-MT-MAX con el vector sh-MNT y a las 48 h indujimos la expresión de MAX durante 24 h con 100 µM Zn_2SO_4. Extrajimos el RNA y analizamos el transcriptoma por RNA-seq. Los resultados obtenidos nos indicaron que el silenciamiento de MNT provoca un cambio transcripcional (figura 4.34). Además, el silenciamiento de MNT (independientemente de la presencia o ausencia de MAX en las UR61) altera la expresión de muchos genes implicados en la progresión del ciclo celular, disminuyendo la expresión de aquellos implicados en la progresión del ciclo celular y replicación del DNA como *CDK6*, *E2F1*, *ORC1* o *MCM10* y aumentando la expresión de genes implicados en la parada del ciclo celular como el inhibidor de cdk p57 (*CDKN1C*) (anexo 1-2). Además, el silenciamiento de MNT también provoca una disminución de genes implicados en la reparación de daño al DNA como son *CHEK1*, *BRCA2* o *FANCD2* (anexo 1-2). Estos cambios de expresión son consistentes con el descenso proliferativo que provoca el silenciamiento de MNT en estas células. El análisis del RNA-seq nos hace plantearnos la siguiente hipótesis. Podría ser que el silenciamiento de MNT lleve a un incremento del daño al DNA por diversos mecanismos como podría ser el incremento de especies reactivas de oxígeno (ROS) a consecuencia de una alteración del metabolismo como describen Link et al., 2012. Si este fuese el caso, las células pararían el ciclo celular para intentar reparar este daño, lo que es consistente con la disminución de la expresión de genes implicados en la proliferación celular (según los datos del RNA-seq). Sin embargo, este daño no podría ser eficientemente reparado ya que la expresión de genes implicados en la reparación del daño al DNA también se encuentra disminuida cuando MNT está silenciado (según los datos del RNA-seq), lo que llevaría a la muerte celular.

Como conclusión final, en esta Tesis hemos descrito nuevos papeles biológicos de las proteínas MXD1 y MNT. Es de considerable importancia tener un buen conocimiento del comportamiento de estas proteínas ya que forman parte de la red MYC/MAX/MXD que a consecuencia de la oncoproteína MYC está altamente involucrada en el desarrollo y progresión del cáncer. Además, estudios recientes donde se describe la implicación de MAX en algunos tumores humanos como feocromocitomas, paragangliomas o cáncer de pulmón de células pequeñas incrementan la importancia del conocimiento de esta parte de la red y del papel que éstas juegan en ausencia de MAX.

Annexes

Annex 1.- Gene expression changes upon MNT depletion in UR61 cells. mRNA levels of the whole transcriptome were determined by RNA-seq. The table includes genes showing differential expression upon MNT depletion in UR61 cells by transfection of the sh-MNT vector. The transcriptomes of UR61-MT-Hebo sh-MNT and UR61-MT-Hebo pLKO were compared. Data are mean of two independent experiments with RPKM values ≥ 0.5 and S.D. ≤ 3. The RPKMs of each experiment ("Exp.") are indicated. The fold-change thresholds between both conditions were set as ≥ 1.7 and < 0.6. The mean of the expression data and S.D. of the fold-changes are highlighted in green at the top of the table. The genes which expression changes were validated by RT-qPCR are highlighted in light green.

	RPKM				RPKM				Fold Change
	UR61-MT-Hebo pLKO		UR61-MT-Hebo sh-MNT		UR61-MT-Hebo pLKO		UR61-MT-Hebo sh-MNT		UR61-MT-Hebo
GENE	Exp.1	Exp.2	Exp.1	Exp.2	mean	S.D.	media	S.D.	sh-MNT vs pLKO
Ccl7	0.60	0.60	8.66	7.35	**0.60**	**0.00**	**8.01**	**0.92**	**13.36**
Spp2	3.76	0.94	13.29	10.44	**2.35**	**1.99**	**11.86**	**2.01**	**5.05**
Eng	0.53	0.57	2.03	3.08	**0.55**	**0.03**	**2.55**	**0.74**	**4.64**
Camta1	0.72	0.39	2.22	1.91	**0.56**	**0.23**	**2.06**	**0.22**	**3.72**
Fetub	1.44	0.34	4.29	1.83	**0.89**	**0.78**	**3.06**	**1.74**	**3.44**
Ppp2r2b	0.01	1.25	0.75	3.10	**0.63**	**0.87**	**1.93**	**1.66**	**3.05**
Ret	2.27	2.09	8.28	4.93	**2.18**	**0.12**	**6.61**	**2.37**	**3.03**
Kcng2	0.97	0.22	3.24	0.28	**0.60**	**0.53**	**1.76**	**2.09**	**2.94**
Cxcl9	0.40	1.39	2.35	2.83	**0.89**	**0.70**	**2.59**	**0.34**	**2.90**
Txnrd3	2.28	4.52	7.97	11.56	**3.40**	**1.58**	**9.76**	**2.53**	**2.87**
Ret	1.50	1.87	6.02	3.53	**1.69**	**0.26**	**4.78**	**1.76**	**2.83**
Cyp4b1	0.73	1.52	2.32	4.01	**1.12**	**0.56**	**3.17**	**1.20**	**2.82**
LOC100910973	0.89	0.26	2.81	0.35	**0.58**	**0.45**	**1.58**	**1.74**	**2.75**
Lat2	0.61	0.41	1.69	1.10	**0.51**	**0.14**	**1.39**	**0.42**	**2.72**
Ndrg4	0.40	1.72	1.09	4.62	**1.06**	**0.94**	**2.85**	**2.49**	**2.69**
Spock1	1.79	0.08	4.43	0.50	**0.93**	**1.21**	**2.47**	**2.78**	**2.64**
Plk3	2.67	2.87	8.70	5.82	**2.77**	**0.14**	**7.26**	**2.03**	**2.62**
Amacr	14.04	15.66	38.01	39.75	**14.85**	**1.14**	**38.88**	**1.23**	**2.62**
Lilrb4	0.50	0.63	0.80	2.14	**0.56**	**0.09**	**1.47**	**0.95**	**2.61**
Thoc7	1.76	1.29	4.30	3.66	**1.53**	**0.33**	**3.98**	**0.45**	**2.60**
Riiad1	1.95	1.31	3.21	5.09	**1.63**	**0.46**	**4.15**	**1.33**	**2.55**
LOC100362783	0.97	1.22	2.40	3.10	**1.09**	**0.18**	**2.75**	**0.50**	**2.51**
LOC100362783	0.97	1.22	2.40	3.10	**1.09**	**0.18**	**2.75**	**0.50**	**2.51**
Ndrg4	1.22	1.43	2.31	4.31	**1.33**	**0.15**	**3.31**	**1.42**	**2.49**
Snap25	2.04	0.43	3.87	2.29	**1.24**	**1.14**	**3.08**	**1.12**	**2.49**
Krt23	0.65	2.05	2.12	4.54	**1.35**	**0.98**	**3.33**	**1.72**	**2.46**
Shbg	0.49	0.53	1.38	1.13	**0.51**	**0.03**	**1.26**	**0.18**	**2.45**
Cdkn1c	1.79	1.53	3.65	4.34	**1.66**	**0.19**	**4.00**	**0.48**	**2.40**
P2ry12	1.76	0.38	3.66	1.38	**1.07**	**0.97**	**2.52**	**1.62**	**2.35**
Ndrg4	2.28	1.42	5.15	3.37	**1.85**	**0.61**	**4.26**	**1.26**	**2.30**
Ccl27	0.53	0.97	1.27	2.18	**0.75**	**0.31**	**1.73**	**0.64**	**2.29**
Gls2	0.88	0.40	2.04	0.85	**0.64**	**0.34**	**1.45**	**0.84**	**2.26**
Gpr1	1.14	0.67	2.37	1.68	**0.90**	**0.33**	**2.03**	**0.49**	**2.25**
LOC100359977	0.51	1.01	1.60	1.77	**0.76**	**0.35**	**1.68**	**0.12**	**2.21**
Egr1	2.17	1.30	4.81	2.65	**1.73**	**0.62**	**3.73**	**1.53**	**2.15**
Catsperd	0.36	0.98	0.87	2.00	**0.67**	**0.44**	**1.43**	**0.80**	**2.14**
Slc24a6	2.80	2.94	5.39	6.41	**2.87**	**0.10**	**5.90**	**0.72**	**2.06**
Tmem169	1.32	1.04	2.56	2.26	**1.18**	**0.20**	**2.41**	**0.21**	**2.03**
Nsmf	0.98	2.14	3.95	2.34	**1.56**	**0.82**	**3.14**	**1.14**	**2.01**
Ptbp2	4.51	4.70	7.24	11.29	**4.61**	**0.13**	**9.26**	**2.86**	**2.01**
Lcn2	1.00	0.25	2.00	0.50	**0.63**	**0.53**	**1.25**	**1.06**	**2.00**
Ehbp1l1	1.01	0.57	1.95	1.22	**0.79**	**0.31**	**1.58**	**0.52**	**2.00**
Thumpd3	1.05	0.35	1.16	1.61	**0.70**	**0.50**	**1.39**	**0.32**	**1.98**

Gramd1c	1.23	1.13	2.11	2.54	**1.18**	**0.07**	**2.33**	**0.30**	**1.97**
Plekhh1	2.84	3.46	5.38	7.00	**3.15**	**0.44**	**6.19**	**1.14**	**1.97**
Slc25a35	1.17	1.28	2.67	2.11	**1.23**	**0.08**	**2.39**	**0.39**	**1.95**
Adcyap1r1	0.77	0.46	1.27	1.09	**0.61**	**0.22**	**1.18**	**0.12**	**1.92**
Etv5	1.77	3.42	3.91	5.97	**2.59**	**1.17**	**4.94**	**1.46**	**1.90**
Mylpf	1.39	1.87	3.59	2.60	**1.63**	**0.34**	**3.09**	**0.69**	**1.90**
Smim17	0.59	0.85	0.87	1.86	**0.72**	**0.18**	**1.36**	**0.70**	**1.89**
Sts	8.02	7.92	15.24	14.78	**7.97**	**0.07**	**15.01**	**0.33**	**1.88**
Ly6c	0.42	0.84	1.35	1.01	**0.63**	**0.30**	**1.18**	**0.24**	**1.87**
Ly6c	0.42	0.84	1.35	1.01	**0.63**	**0.30**	**1.18**	**0.24**	**1.87**
Gpx4	0.58	1.39	1.95	1.73	**0.99**	**0.57**	**1.84**	**0.16**	**1.87**
Gipr	2.94	4.21	5.81	7.50	**3.57**	**0.90**	**6.66**	**1.19**	**1.86**
RGD1305938	8.17	5.87	14.26	11.85	**7.02**	**1.63**	**13.05**	**1.71**	**1.86**
Ypel4	6.39	3.11	9.80	7.83	**4.75**	**2.31**	**8.81**	**1.39**	**1.85**
Crem	0.73	0.52	1.79	0.53	**0.62**	**0.15**	**1.16**	**0.89**	**1.85**
Acbd7	3.31	4.44	6.58	7.66	**3.87**	**0.80**	**7.12**	**0.76**	**1.84**
Clybl	1.64	1.72	3.47	2.66	**1.68**	**0.06**	**3.07**	**0.57**	**1.83**
Ptprr	3.67	2.15	6.65	3.95	**2.91**	**1.08**	**5.30**	**1.91**	**1.82**
Myo9b	3.47	3.37	6.01	6.43	**3.42**	**0.07**	**6.22**	**0.30**	**1.82**
Tank	1.48	2.97	3.78	4.31	**2.22**	**1.05**	**4.04**	**0.37**	**1.82**
Csf2ra	1.39	1.70	1.98	3.63	**1.54**	**0.21**	**2.80**	**1.16**	**1.82**
Map3k8	0.68	1.09	0.87	2.32	**0.88**	**0.29**	**1.59**	**1.02**	**1.81**
Lin7b	1.93	2.67	3.87	4.39	**2.30**	**0.53**	**4.13**	**0.37**	**1.80**
Spry4	0.67	1.12	1.55	1.65	**0.89**	**0.32**	**1.60**	**0.07**	**1.79**
Maged2	1.36	1.36	1.90	2.98	**1.36**	**0.00**	**2.44**	**0.76**	**1.79**
Bles03	1.65	2.13	4.00	2.78	**1.89**	**0.34**	**3.39**	**0.86**	**1.79**
Pnkd	4.49	3.75	6.27	8.41	**4.12**	**0.52**	**7.34**	**1.51**	**1.78**
Dlgap1	0.84	0.49	1.36	0.99	**0.66**	**0.25**	**1.18**	**0.26**	**1.78**
Rab7b	4.24	4.29	7.79	7.37	**4.26**	**0.03**	**7.58**	**0.30**	**1.78**
Acadsb	0.44	0.85	0.87	1.43	**0.65**	**0.29**	**1.15**	**0.40**	**1.78**
Stc1	1.86	0.58	3.77	0.56	**1.22**	**0.91**	**2.16**	**2.27**	**1.78**
Il3ra	4.46	8.33	9.55	13.13	**6.40**	**2.73**	**11.34**	**2.53**	**1.77**
Dcun1d4	2.03	2.90	3.69	4.95	**2.47**	**0.61**	**4.32**	**0.89**	**1.75**
Hrh3	1.21	0.03	0.56	1.61	**0.62**	**0.83**	**1.08**	**0.74**	**1.75**
Nkx1-2	0.51	0.71	1.12	1.01	**0.61**	**0.14**	**1.07**	**0.08**	**1.75**
Tpm1	1.31	1.46	3.11	1.72	**1.39**	**0.10**	**2.42**	**0.99**	**1.74**
Klf11	8.60	5.85	13.62	11.55	**7.23**	**1.95**	**12.58**	**1.47**	**1.74**
Kcnj11	0.76	0.37	1.40	0.56	**0.56**	**0.28**	**0.98**	**0.60**	**1.74**
Cyp46a1	0.74	1.00	1.17	1.85	**0.87**	**0.18**	**1.51**	**0.48**	**1.74**
Nnat	3.91	0.00	5.00	1.80	**1.96**	**2.77**	**3.40**	**2.26**	**1.74**
Lpar3	1.26	2.02	3.19	2.51	**1.64**	**0.53**	**2.85**	**0.48**	**1.74**
Kif5a	4.18	4.81	5.89	9.69	**4.50**	**0.45**	**7.79**	**2.69**	**1.73**
Bcmo1	1.39	2.50	2.33	4.40	**1.95**	**0.79**	**3.36**	**1.46**	**1.73**
Sapcd1	0.85	0.64	1.39	1.18	**0.74**	**0.14**	**1.28**	**0.15**	**1.73**
Ercc8	0.76	0.38	0.85	1.08	**0.57**	**0.27**	**0.97**	**0.16**	**1.71**
Kifc2	3.58	4.61	5.33	8.63	**4.09**	**0.73**	**6.98**	**2.33**	**1.70**
Nme4	5.75	5.41	3.40	3.30	**5.58**	**0.24**	**3.35**	**0.07**	**0.60**
Smim1	8.40	7.65	5.83	3.80	**8.02**	**0.53**	**4.81**	**1.44**	**0.60**
Rims2	0.80	1.46	0.52	0.84	**1.13**	**0.46**	**0.68**	**0.23**	**0.60**
Ripply3	1.53	1.34	0.98	0.74	**1.43**	**0.14**	**0.86**	**0.17**	**0.60**
Nrarp	11.75	7.86	7.47	4.24	**9.81**	**2.75**	**5.85**	**2.28**	**0.60**
Fbxo5	10.07	9.56	6.36	5.35	**9.82**	**0.36**	**5.86**	**0.71**	**0.60**
Josd2	16.64	16.16	11.22	8.35	**16.40**	**0.34**	**9.78**	**2.03**	**0.60**
RGD1560010	8.36	7.42	5.39	4.01	**7.89**	**0.66**	**4.70**	**0.97**	**0.60**
Myo1b	16.37	13.86	9.37	8.64	**15.11**	**1.77**	**9.01**	**0.52**	**0.60**
Chek1	15.31	12.91	8.29	8.52	**14.11**	**1.70**	**8.41**	**0.16**	**0.60**
Dsn1	12.46	13.01	7.30	7.87	**12.73**	**0.39**	**7.59**	**0.40**	**0.60**
Rad51ap1	5.78	5.92	3.53	3.43	**5.85**	**0.10**	**3.48**	**0.06**	**0.59**
Rad54b	1.04	0.70	0.56	0.48	**0.87**	**0.24**	**0.52**	**0.06**	**0.59**
Cep63	0.80	1.51	1.00	0.37	**1.15**	**0.50**	**0.69**	**0.44**	**0.59**

Il1rn	3.13	3.30	2.20	1.62	**3.22**	**0.12**	**1.91**	**0.40**	**0.59**
Slfn13	13.13	13.44	7.89	7.89	**13.29**	**0.22**	**7.89**	**0.00**	**0.59**
Cdc20	42.70	41.64	25.90	24.15	**42.17**	**0.75**	**25.02**	**1.24**	**0.59**
Gmnn	11.86	13.65	7.14	7.97	**12.75**	**1.27**	**7.56**	**0.59**	**0.59**
Fam212b	4.56	6.10	3.19	3.12	**5.33**	**1.08**	**3.16**	**0.05**	**0.59**
B3gnt7	7.31	7.41	4.90	3.82	**7.36**	**0.07**	**4.36**	**0.76**	**0.59**
E2f1	24.15	21.14	14.16	12.64	**22.64**	**2.13**	**13.40**	**1.08**	**0.59**
Carm1	13.65	14.92	8.11	8.78	**14.28**	**0.90**	**8.45**	**0.47**	**0.59**
Hmgn3	0.78	2.90	0.73	1.44	**1.84**	**1.50**	**1.09**	**0.50**	**0.59**
Troap	12.59	15.40	7.68	8.84	**14.00**	**1.99**	**8.26**	**0.82**	**0.59**
Birc5	62.08	62.75	37.89	35.73	**62.41**	**0.48**	**36.81**	**1.53**	**0.59**
Ccp110	8.70	7.81	4.95	4.77	**8.25**	**0.63**	**4.86**	**0.12**	**0.59**
Polq	1.60	1.16	0.96	0.67	**1.38**	**0.31**	**0.81**	**0.20**	**0.59**
Cdh1	1.03	1.62	0.85	0.71	**1.33**	**0.42**	**0.78**	**0.10**	**0.59**
Duoxa1	1.51	1.42	0.87	0.85	**1.46**	**0.06**	**0.86**	**0.02**	**0.59**
Rad51	35.70	31.98	21.18	18.54	**33.84**	**2.63**	**19.86**	**1.86**	**0.59**
Depdc1b	5.58	5.50	3.11	3.38	**5.54**	**0.06**	**3.25**	**0.19**	**0.59**
Kif20b	13.09	10.65	7.74	6.16	**11.87**	**1.73**	**6.95**	**1.12**	**0.59**
Mlf1	2.30	3.47	1.72	1.66	**2.89**	**0.83**	**1.69**	**0.04**	**0.58**
Brca2	2.33	1.34	1.29	0.85	**1.84**	**0.70**	**1.07**	**0.31**	**0.58**
Cenpi	9.94	7.66	5.75	4.51	**8.80**	**1.61**	**5.13**	**0.88**	**0.58**
Cenpt	17.61	16.48	10.54	9.32	**17.05**	**0.80**	**9.93**	**0.87**	**0.58**
Cit	4.52	2.96	2.58	1.77	**3.74**	**1.10**	**2.18**	**0.57**	**0.58**
Ube2t	26.51	28.07	16.06	15.68	**27.29**	**1.11**	**15.87**	**0.27**	**0.58**
Flrt1	1.57	0.71	0.86	0.46	**1.14**	**0.61**	**0.66**	**0.28**	**0.58**
Cdc6	14.41	15.38	8.32	8.99	**14.89**	**0.69**	**8.65**	**0.48**	**0.58**
Tacc3	39.57	38.14	23.62	21.46	**38.86**	**1.01**	**22.54**	**1.53**	**0.58**
Rad54l	3.41	2.33	1.97	1.36	**2.87**	**0.77**	**1.66**	**0.44**	**0.58**
Gen1	3.29	2.41	1.84	1.46	**2.85**	**0.62**	**1.65**	**0.27**	**0.58**
Mgme1	5.65	5.90	3.44	3.25	**5.78**	**0.17**	**3.34**	**0.13**	**0.58**
Trip13	14.88	14.37	8.69	8.25	**14.62**	**0.36**	**8.47**	**0.31**	**0.58**
Notch2	2.47	1.58	1.40	0.95	**2.03**	**0.63**	**1.17**	**0.32**	**0.58**
Nfyc	11.32	11.27	6.77	6.30	**11.30**	**0.04**	**6.54**	**0.33**	**0.58**
Cdk6	5.14	2.09	2.87	1.30	**3.61**	**2.16**	**2.08**	**1.11**	**0.58**
Nr1i3	2.66	3.32	2.27	1.17	**2.99**	**0.47**	**1.72**	**0.78**	**0.58**
Lgalsl	20.09	17.45	11.60	9.96	**18.77**	**1.87**	**10.78**	**1.16**	**0.57**
RGD1561149	9.04	7.49	5.47	4.03	**8.26**	**1.09**	**4.75**	**1.02**	**0.57**
Podxl	1.69	1.13	1.02	0.61	**1.41**	**0.39**	**0.81**	**0.29**	**0.57**
Ska1	11.96	10.12	6.26	6.39	**11.04**	**1.30**	**6.32**	**0.10**	**0.57**
Melk	8.87	8.05	5.05	4.63	**8.46**	**0.58**	**4.84**	**0.30**	**0.57**
Mff	15.75	16.00	8.85	9.30	**15.87**	**0.18**	**9.08**	**0.32**	**0.57**
Mff	15.75	16.00	8.85	9.30	**15.87**	**0.18**	**9.08**	**0.32**	**0.57**
Cdca2	12.06	11.79	6.70	6.92	**11.92**	**0.19**	**6.81**	**0.16**	**0.57**
Chtf18	12.00	10.80	6.64	6.39	**11.40**	**0.85**	**6.51**	**0.17**	**0.57**
LOC100910802	1.62	1.28	1.07	0.58	**1.45**	**0.24**	**0.83**	**0.35**	**0.57**
Rfx2	2.40	1.50	1.20	1.02	**1.95**	**0.64**	**1.11**	**0.13**	**0.57**
Fhl1	3.64	1.15	2.32	0.41	**2.40**	**1.76**	**1.36**	**1.36**	**0.57**
Socs1	1.86	1.51	1.24	0.67	**1.68**	**0.25**	**0.96**	**0.40**	**0.57**
Serpinb2	0.86	0.92	0.49	0.52	**0.89**	**0.04**	**0.51**	**0.02**	**0.57**
Fancd2	6.38	4.54	3.63	2.57	**5.46**	**1.30**	**3.10**	**0.75**	**0.57**
Cndp1	3.70	4.40	2.22	2.37	**4.05**	**0.49**	**2.30**	**0.11**	**0.57**
Ttk	18.89	15.71	10.55	9.10	**17.30**	**2.25**	**9.82**	**1.03**	**0.57**
Tonsl	6.38	5.55	3.58	3.19	**5.97**	**0.59**	**3.39**	**0.28**	**0.57**
Gpsm1	11.31	7.90	6.73	4.17	**9.61**	**2.41**	**5.45**	**1.81**	**0.57**
Kif20a	37.42	40.29	21.48	22.44	**38.85**	**2.03**	**21.96**	**0.67**	**0.57**
March8	12.30	11.36	7.01	6.36	**11.83**	**0.66**	**6.69**	**0.46**	**0.56**
Spc25	41.86	43.53	24.65	23.58	**42.69**	**1.18**	**24.12**	**0.76**	**0.56**
Rrad	1.69	1.20	0.97	0.66	**1.45**	**0.35**	**0.82**	**0.21**	**0.56**
Cenpf	4.96	2.59	2.67	1.58	**3.78**	**1.67**	**2.13**	**0.77**	**0.56**
Slc19a1	8.60	8.03	5.43	3.92	**8.32**	**0.40**	**4.68**	**1.07**	**0.56**

Hist1h2af	3.98	3.52	2.79	1.43	**3.75**	**0.32**	**2.11**	**0.96**	**0.56**
RGD1559690	6.59	5.75	3.78	3.15	**6.17**	**0.59**	**3.47**	**0.44**	**0.56**
Slco4a1	1.65	2.15	1.02	1.11	**1.90**	**0.35**	**1.06**	**0.06**	**0.56**
LOC500034	14.92	11.36	7.80	6.92	**13.14**	**2.51**	**7.36**	**0.62**	**0.56**
Ckap2	32.62	35.81	18.32	20.01	**34.21**	**2.25**	**19.16**	**1.19**	**0.56**
Kif2c	7.56	7.29	4.31	4.01	**7.42**	**0.19**	**4.16**	**0.21**	**0.56**
Aspm	6.45	3.91	3.46	2.32	**5.18**	**1.80**	**2.89**	**0.81**	**0.56**
Parpbp	2.83	2.38	1.62	1.29	**2.61**	**0.32**	**1.45**	**0.23**	**0.56**
Psrc1	14.11	15.50	8.07	8.40	**14.80**	**0.98**	**8.24**	**0.23**	**0.56**
LOC303566	4.00	3.95	2.13	2.28	**3.97**	**0.03**	**2.21**	**0.10**	**0.56**
Tmem9	1.88	1.53	0.61	1.28	**1.71**	**0.25**	**0.95**	**0.47**	**0.55**
Pole2	8.36	8.40	4.92	4.35	**8.38**	**0.03**	**4.63**	**0.41**	**0.55**
Efemp2	1.79	2.16	1.09	1.09	**1.97**	**0.26**	**1.09**	**0.00**	**0.55**
Mxd3	19.42	19.88	11.45	10.24	**19.65**	**0.32**	**10.85**	**0.86**	**0.55**
Ccnf	12.19	11.31	6.72	6.25	**11.75**	**0.62**	**6.48**	**0.33**	**0.55**
Arf2	10.69	11.13	6.07	5.94	**10.91**	**0.31**	**6.00**	**0.09**	**0.55**
Jade3	5.81	4.23	3.32	2.21	**5.02**	**1.12**	**2.76**	**0.78**	**0.55**
Ugt1a2	5.23	3.15	2.80	1.81	**4.19**	**1.47**	**2.30**	**0.70**	**0.55**
Sgol2	9.43	7.38	5.06	4.19	**8.41**	**1.45**	**4.62**	**0.61**	**0.55**
Mnt	20.26	18.96	10.63	10.89	**19.61**	**0.92**	**10.76**	**0.18**	**0.55**
Gsta1	1.07	2.72	0.66	1.42	**1.89**	**1.17**	**1.04**	**0.54**	**0.55**
Hist2h3c2	1.89	3.17	1.57	1.20	**2.53**	**0.91**	**1.38**	**0.26**	**0.55**
Ska3	14.13	14.23	7.70	7.81	**14.18**	**0.08**	**7.76**	**0.08**	**0.55**
Foxm1	8.50	7.93	4.32	4.65	**8.21**	**0.40**	**4.48**	**0.24**	**0.55**
Tgif2	1.71	1.99	1.08	0.92	**1.85**	**0.20**	**1.00**	**0.11**	**0.54**
Kif18b	19.25	16.67	10.82	8.65	**17.96**	**1.82**	**9.73**	**1.54**	**0.54**
Recql4	6.96	8.48	3.96	4.40	**7.72**	**1.07**	**4.18**	**0.31**	**0.54**
Mt3	2.10	0.74	0.75	0.78	**1.42**	**0.97**	**0.77**	**0.02**	**0.54**
Timm9	0.71	1.19	0.56	0.46	**0.95**	**0.34**	**0.51**	**0.07**	**0.54**
E2f6	32.33	36.09	19.15	17.73	**34.21**	**2.65**	**18.44**	**1.00**	**0.54**
Zfp385a	21.38	24.06	12.76	11.71	**22.72**	**1.89**	**12.24**	**0.74**	**0.54**
Neil3	2.66	2.47	1.17	1.58	**2.57**	**0.13**	**1.38**	**0.28**	**0.54**
Exo1	3.15	2.79	1.74	1.44	**2.97**	**0.25**	**1.59**	**0.21**	**0.54**
Asf1b	36.25	33.84	19.24	18.24	**35.05**	**1.71**	**18.74**	**0.70**	**0.53**
Etnk2	3.37	4.28	2.07	2.01	**3.82**	**0.65**	**2.04**	**0.04**	**0.53**
Gipc2	3.41	2.99	1.92	1.50	**3.20**	**0.30**	**1.71**	**0.30**	**0.53**
Ccdc28a	7.08	7.93	3.75	4.24	**7.50**	**0.60**	**4.00**	**0.34**	**0.53**
Slc18a2	3.53	2.53	1.90	1.31	**3.03**	**0.71**	**1.61**	**0.42**	**0.53**
Cenpu	18.60	17.61	10.10	9.13	**18.11**	**0.70**	**9.62**	**0.68**	**0.53**
Rnf24	12.08	9.36	6.84	4.47	**10.72**	**1.92**	**5.65**	**1.68**	**0.53**
E2f7	5.37	3.71	2.59	2.17	**4.54**	**1.17**	**2.38**	**0.30**	**0.52**
Morn2	2.52	2.89	0.01	2.82	**2.71**	**0.26**	**1.42**	**1.98**	**0.52**
Xkr5	5.48	4.69	3.02	2.30	**5.09**	**0.56**	**2.66**	**0.50**	**0.52**
Lrr1	1.71	1.82	1.02	0.82	**1.76**	**0.08**	**0.92**	**0.14**	**0.52**
Pls1	12.05	12.65	6.88	6.02	**12.35**	**0.43**	**6.45**	**0.61**	**0.52**
Mcm10	5.39	3.93	2.95	1.91	**4.66**	**1.04**	**2.43**	**0.73**	**0.52**
Kif15	8.22	7.04	3.94	4.02	**7.63**	**0.84**	**3.98**	**0.06**	**0.52**
Srek1ip1	13.38	11.54	6.82	6.16	**12.46**	**1.31**	**6.49**	**0.46**	**0.52**
Nnat	1.71	0.45	0.36	0.76	**1.08**	**0.89**	**0.56**	**0.29**	**0.52**
Rab11fip1	8.38	9.91	4.10	5.34	**9.14**	**1.08**	**4.72**	**0.88**	**0.52**
Zmpste24	17.66	13.48	9.95	6.09	**15.57**	**2.96**	**8.02**	**2.73**	**0.52**
Pask	1.76	1.79	0.86	0.96	**1.78**	**0.02**	**0.91**	**0.08**	**0.51**
Nxt2	1.28	1.41	0.71	0.66	**1.34**	**0.09**	**0.68**	**0.03**	**0.51**
Kcnh3	2.41	0.99	1.22	0.51	**1.70**	**1.00**	**0.86**	**0.51**	**0.51**
Espl1	11.59	9.08	5.76	4.69	**10.33**	**1.77**	**5.23**	**0.76**	**0.51**
Rasl11a	2.58	4.72	0.86	2.82	**3.65**	**1.51**	**1.84**	**1.39**	**0.50**
Orc1	4.32	4.33	2.34	2.03	**4.33**	**0.01**	**2.18**	**0.22**	**0.50**
Pspn	1.57	2.22	0.89	1.01	**1.89**	**0.46**	**0.95**	**0.08**	**0.50**
Tagln	5.10	4.62	2.15	2.74	**4.86**	**0.34**	**2.44**	**0.42**	**0.50**
Tiam1	6.79	4.40	3.39	2.21	**5.59**	**1.69**	**2.80**	**0.83**	**0.50**

Eme1	4.95	4.39	2.52	2.12	**4.67**	**0.40**	**2.32**	**0.28**	**0.50**
Hrh3	1.63	2.11	1.01	0.85	**1.87**	**0.34**	**0.93**	**0.11**	**0.50**
Clspn	6.88	5.39	3.24	2.86	**6.14**	**1.05**	**3.05**	**0.27**	**0.50**
LOC689574	0.73	2.24	0.72	0.75	**1.48**	**1.07**	**0.74**	**0.02**	**0.50**
Mybl2	19.88	16.27	9.57	8.06	**18.08**	**2.55**	**8.82**	**1.07**	**0.49**
Mns1	4.51	4.70	2.02	2.33	**4.60**	**0.14**	**2.17**	**0.23**	**0.47**
Spi1	0.83	1.47	0.44	0.63	**1.15**	**0.45**	**0.54**	**0.14**	**0.46**
Fam98c	1.56	2.72	1.87	0.00	**2.14**	**0.82**	**0.94**	**1.32**	**0.44**
Tmem80	1.52	1.32	0.81	0.34	**1.42**	**0.14**	**0.58**	**0.34**	**0.40**
Shisa2	1.96	0.56	0.63	0.39	**1.26**	**0.99**	**0.51**	**0.17**	**0.40**
Xbp1	5.88	5.01	2.34	2.05	**5.44**	**0.61**	**2.20**	**0.21**	**0.40**
Fxyd5	1.88	1.69	0.72	0.69	**1.79**	**0.13**	**0.71**	**0.02**	**0.40**
Batf3	0.84	2.99	0.55	0.91	**1.92**	**1.52**	**0.73**	**0.26**	**0.38**
Pdlim3	1.43	3.31	0.48	1.12	**2.37**	**1.33**	**0.80**	**0.46**	**0.34**
Patz1	3.92	6.86	0.01	3.22	**5.39**	**2.08**	**1.62**	**2.27**	**0.30**
Esd	3.62	3.67	2.04	0.00	**3.64**	**0.03**	**1.02**	**1.44**	**0.28**
Znrd1	1.86	5.29	0.00	1.60	**3.58**	**2.43**	**0.80**	**1.13**	**0.22**

Annex 2.- Gene expression changes upon MNT depletion in UR61 cells expressing MAX. mRNA levels of the whole transcriptome were determined by RNA-seq. The table includes genes showing differential expression upon MNT depletion by transfection of the sh-MNT vector in UR61 cells expressing MAX.The transcriptomes of UR61-MT-MAX sh-MNT and UR61-MT-MAX pLKO, both treated with 100 µM Zn^{2+} for 24 h, were compared. Data are mean of two independent experiments with RPKM values ≥ 0.5 and S.D. ≤ 3. The RPKMs of each experiment ("Exp.") are indicated. The fold-change thresholds between both conditions were set as ≥ 1.7 and < 0.6. The mean of the expression data and S.D. of the fold-changes are highlighted in green at the top of the table.

	RPKM				RPKM				Fold Change
	UR61-MT-MAX pLKO		UR61-MT-MAX sh-MNT		UR61-MT-MAX pLKO		UR61-MT-MAX sh-MNT		UR61-MT-MAX
GENE	Exp.1	Exp.2	Exp.1	Exp.2	mean	S.D.	mean	S.D.	sh-MNT vs pLKO
Ndrg4	1.03	1.85	4.77	6.00	**1.44**	**0.58**	**5.38**	**0.87**	**3.74**
Riiad1	0.79	1.35	3.58	4.35	**1.07**	**0.40**	**3.96**	**0.54**	**3.71**
LOC100362783	0.92	1.10	3.91	3.42	**1.01**	**0.13**	**3.67**	**0.35**	**3.64**
LOC100362783	0.92	1.10	3.91	3.42	**1.01**	**0.13**	**3.67**	**0.35**	**3.64**
Slc18a1	0.96	0.36	3.32	0.97	**0.66**	**0.43**	**2.15**	**1.66**	**3.25**
Lilrb4	0.46	0.58	1.81	1.44	**0.52**	**0.08**	**1.63**	**0.26**	**3.13**
Slc6a2	2.92	2.81	9.65	7.48	**2.86**	**0.08**	**8.57**	**1.53**	**2.99**
Patz1	1.13	4.30	7.47	8.05	**2.71**	**2.25**	**7.76**	**0.41**	**2.86**
Cast	8.69	7.99	25.21	22.43	**8.34**	**0.49**	**23.82**	**1.96**	**2.86**
Tpm1	0.76	1.10	3.14	2.15	**0.93**	**0.24**	**2.65**	**0.70**	**2.85**
Cyp26b1	0.70	0.79	2.51	1.58	**0.75**	**0.07**	**2.04**	**0.66**	**2.74**
Ret	2.83	3.05	8.57	7.32	**2.94**	**0.16**	**7.95**	**0.89**	**2.70**
Ret	1.78	2.32	5.83	5.21	**2.05**	**0.38**	**5.52**	**0.44**	**2.69**
Mylpf	1.67	1.24	4.01	3.65	**1.46**	**0.30**	**3.83**	**0.25**	**2.63**
Shbg	0.76	0.68	1.84	1.73	**0.72**	**0.05**	**1.79**	**0.07**	**2.48**
Bmf	3.49	3.93	10.93	7.46	**3.71**	**0.31**	**9.20**	**2.45**	**2.48**
Ypel4	3.68	3.26	10.48	6.72	**3.47**	**0.30**	**8.60**	**2.65**	**2.48**
Gipr	1.39	1.72	3.63	4.07	**1.56**	**0.23**	**3.85**	**0.31**	**2.48**
Bcl2l11	3.75	1.54	6.21	6.74	**2.65**	**1.56**	**6.48**	**0.38**	**2.45**
Mafb	2.93	2.26	7.53	5.16	**2.59**	**0.47**	**6.35**	**1.67**	**2.45**
Maged2	6.11	4.81	14.02	12.66	**5.46**	**0.91**	**13.34**	**0.96**	**2.44**
Slc4a8	2.06	0.90	5.63	1.51	**1.48**	**0.82**	**3.57**	**2.92**	**2.41**
Zpbp2	0.42	0.78	1.45	1.44	**0.60**	**0.26**	**1.45**	**0.01**	**2.41**
S100a5	2.95	1.73	6.56	4.68	**2.34**	**0.86**	**5.62**	**1.33**	**2.41**
Camta1	1.49	1.59	3.50	3.88	**1.54**	**0.07**	**3.69**	**0.27**	**2.39**
St6galnac3	1.05	1.09	2.54	2.57	**1.07**	**0.03**	**2.55**	**0.02**	**2.39**
Txnrd3	4.04	4.88	10.42	10.84	**4.46**	**0.60**	**10.63**	**0.29**	**2.38**
Ptbp2	4.98	5.45	11.58	13.26	**5.22**	**0.33**	**12.42**	**1.19**	**2.38**
Ccdc28b	3.03	2.94	7.21	6.85	**2.98**	**0.06**	**7.03**	**0.26**	**2.36**
Sapcd1	0.56	0.62	1.59	1.19	**0.59**	**0.04**	**1.39**	**0.28**	**2.34**
Dclk1	2.05	1.15	5.74	1.68	**1.60**	**0.64**	**3.71**	**2.88**	**2.32**
Krt23	0.51	0.62	1.49	1.13	**0.57**	**0.07**	**1.31**	**0.25**	**2.31**
Lrcol1	0.50	0.54	1.13	1.23	**0.52**	**0.03**	**1.18**	**0.07**	**2.27**
Gramd1c	1.09	1.00	2.22	2.52	**1.05**	**0.07**	**2.37**	**0.21**	**2.26**
Maged2	0.31	2.53	3.46	2.87	**1.42**	**1.57**	**3.16**	**0.42**	**2.22**
Cacng2	1.70	0.91	3.83	1.97	**1.31**	**0.56**	**2.90**	**1.32**	**2.22**
Ankrd37	12.44	13.09	29.78	26.82	**12.76**	**0.46**	**28.30**	**2.09**	**2.22**
Ces1a	1.62	1.28	3.03	3.35	**1.45**	**0.23**	**3.19**	**0.23**	**2.20**
Ccl27	0.69	0.90	1.76	1.75	**0.80**	**0.15**	**1.76**	**0.00**	**2.20**
Zfp180	2.88	0.02	2.15	4.21	**1.45**	**2.02**	**3.18**	**1.46**	**2.19**
Acyp1	4.24	4.78	8.99	10.70	**4.51**	**0.38**	**9.85**	**1.21**	**2.18**
Atat1	9.12	9.69	21.30	19.71	**9.40**	**0.41**	**20.51**	**1.12**	**2.18**

Ggn	0.57	0.94	1.83	1.47	**0.76**	**0.26**	**1.65**	**0.25**	**2.18**
Dcun1d4	2.04	2.42	4.79	4.68	**2.23**	**0.27**	**4.73**	**0.08**	**2.12**
Cyp4b1	1.04	0.83	2.63	1.33	**0.93**	**0.14**	**1.98**	**0.92**	**2.12**
Pdp1	6.08	4.45	10.63	11.62	**5.27**	**1.15**	**11.13**	**0.70**	**2.11**
Cdkn1c	0.86	0.88	2.09	1.59	**0.87**	**0.01**	**1.84**	**0.36**	**2.11**
Fam132a	0.34	1.13	0.38	2.71	**0.74**	**0.55**	**1.54**	**1.65**	**2.10**
Sh2d3c	0.41	0.70	1.25	1.08	**0.56**	**0.21**	**1.17**	**0.12**	**2.09**
Trim67	1.88	0.74	3.95	1.50	**1.31**	**0.81**	**2.72**	**1.73**	**2.08**
Erg	0.97	0.79	2.19	1.47	**0.88**	**0.13**	**1.83**	**0.51**	**2.07**
Kif5a	2.79	4.43	6.67	8.25	**3.61**	**1.16**	**7.46**	**1.12**	**2.07**
Atcay	1.61	1.28	3.27	2.69	**1.44**	**0.23**	**2.98**	**0.41**	**2.06**
Rab7b	3.24	3.71	8.42	5.87	**3.47**	**0.33**	**7.15**	**1.80**	**2.06**
Plekhh1	2.14	3.15	4.98	5.91	**2.64**	**0.72**	**5.44**	**0.65**	**2.06**
MGC93861	0.80	0.80	1.67	1.62	**0.80**	**0.00**	**1.64**	**0.03**	**2.05**
Dmkn	1.24	0.76	2.29	1.82	**1.00**	**0.34**	**2.06**	**0.33**	**2.05**
Elavl4	4.80	3.18	9.79	6.57	**3.99**	**1.15**	**8.18**	**2.27**	**2.05**
Cend1	11.50	10.25	21.29	22.98	**10.87**	**0.88**	**22.13**	**1.19**	**2.04**
Cend1	11.50	10.25	21.31	22.96	**10.87**	**0.88**	**22.13**	**1.16**	**2.04**
Ric3	2.62	1.06	3.93	3.57	**1.84**	**1.10**	**3.75**	**0.26**	**2.04**
Acbd7	2.57	3.93	7.37	5.84	**3.25**	**0.96**	**6.61**	**1.08**	**2.03**
Timm9	0.90	0.62	1.99	1.07	**0.76**	**0.19**	**1.53**	**0.65**	**2.01**
Tmem169	1.22	0.74	2.10	1.83	**0.98**	**0.33**	**1.96**	**0.19**	**2.00**
Jph4	4.81	3.37	10.29	6.05	**4.09**	**1.02**	**8.17**	**3.00**	**2.00**
Sec23a	15.75	15.63	32.80	29.57	**15.69**	**0.09**	**31.18**	**2.28**	**1.99**
Cmah	0.72	1.08	2.21	1.37	**0.90**	**0.25**	**1.79**	**0.60**	**1.99**
Smad2	1.87	0.74	2.20	2.96	**1.31**	**0.80**	**2.58**	**0.54**	**1.97**
Fam98c	1.84	1.44	2.53	3.92	**1.64**	**0.28**	**3.23**	**0.98**	**1.97**
Gpr155	0.89	0.79	1.74	1.55	**0.84**	**0.07**	**1.64**	**0.13**	**1.95**
Ptprr	3.03	2.11	6.63	3.41	**2.57**	**0.65**	**5.02**	**2.28**	**1.95**
Spaca5	0.70	0.44	0.98	1.24	**0.57**	**0.19**	**1.11**	**0.18**	**1.94**
Atp7a	15.92	11.83	28.76	24.84	**13.87**	**2.89**	**26.80**	**2.77**	**1.93**
Catsperd	0.54	1.15	1.28	2.00	**0.85**	**0.43**	**1.64**	**0.51**	**1.93**
RGD1309808	0.60	0.72	1.52	1.01	**0.66**	**0.09**	**1.26**	**0.36**	**1.92**
RGD1309808	0.60	0.72	1.52	1.01	**0.66**	**0.09**	**1.26**	**0.36**	**1.92**
Ankrd42	2.20	2.63	4.46	4.73	**2.42**	**0.30**	**4.60**	**0.20**	**1.90**
Igsf9	4.19	3.75	6.87	8.14	**3.97**	**0.31**	**7.50**	**0.90**	**1.89**
Mospd1	16.98	21.09	36.52	35.37	**19.03**	**2.91**	**35.95**	**0.81**	**1.89**
Slc26a6	4.38	6.24	9.06	10.90	**5.31**	**1.31**	**9.98**	**1.30**	**1.88**
Gtpbp6	4.14	4.41	7.87	8.19	**4.28**	**0.19**	**8.03**	**0.23**	**1.88**
Gtpbp6	4.14	4.41	7.87	8.19	**4.28**	**0.19**	**8.03**	**0.23**	**1.88**
Kifc2	2.93	4.93	6.90	7.85	**3.93**	**1.41**	**7.38**	**0.67**	**1.88**
Cyp46a1	1.19	1.42	2.54	2.33	**1.30**	**0.16**	**2.44**	**0.15**	**1.87**
Map9	6.21	5.17	11.48	9.77	**5.69**	**0.74**	**10.63**	**1.21**	**1.87**
Spats1	1.44	1.33	2.77	2.38	**1.38**	**0.08**	**2.58**	**0.28**	**1.87**
Fbxo24	0.49	0.65	1.05	1.08	**0.57**	**0.11**	**1.06**	**0.02**	**1.86**
Scfd2	3.55	3.06	6.84	5.41	**3.31**	**0.34**	**6.12**	**1.01**	**1.85**
Pip4k2a	11.68	10.73	22.80	18.67	**11.21**	**0.67**	**20.73**	**2.92**	**1.85**
Crb3	2.61	4.21	6.17	6.45	**3.41**	**1.13**	**6.31**	**0.20**	**1.85**
Nek11	0.66	0.47	1.34	0.74	**0.56**	**0.14**	**1.04**	**0.42**	**1.84**
Per2	3.53	2.42	6.00	4.96	**2.97**	**0.79**	**5.48**	**0.74**	**1.84**
Taf9	1.24	2.11	2.63	3.46	**1.68**	**0.62**	**3.05**	**0.59**	**1.82**
B3gntl1	1.11	1.91	2.36	3.09	**1.51**	**0.57**	**2.73**	**0.51**	**1.80**
Prr24	3.24	1.88	5.23	4.01	**2.56**	**0.96**	**4.62**	**0.86**	**1.80**
Dlgap1	0.80	0.62	1.58	0.98	**0.71**	**0.13**	**1.28**	**0.42**	**1.80**
Actn3	1.76	1.19	2.96	2.36	**1.48**	**0.40**	**2.66**	**0.42**	**1.80**
Prr18	1.62	0.55	2.81	1.10	**1.09**	**0.76**	**1.95**	**1.21**	**1.80**
Clybl	2.43	2.89	5.16	4.39	**2.66**	**0.33**	**4.77**	**0.54**	**1.79**
Spred3	1.83	1.88	3.37	3.27	**1.85**	**0.03**	**3.32**	**0.07**	**1.79**
Tcte1	1.26	1.06	2.57	1.57	**1.16**	**0.14**	**2.07**	**0.71**	**1.79**
Nsmf	1.80	1.57	2.99	3.04	**1.69**	**0.16**	**3.01**	**0.04**	**1.79**

Paqr9	3.41	2.97	6.73	4.65	**3.19**	**0.31**	**5.69**	**1.47**	**1.79**
Mblac2	6.72	4.34	10.55	9.16	**5.53**	**1.68**	**9.86**	**0.98**	**1.78**
Stk32a	0.78	1.30	1.11	2.57	**1.04**	**0.37**	**1.84**	**1.03**	**1.78**
Ethe1	17.30	19.40	33.19	31.99	**18.35**	**1.49**	**32.59**	**0.85**	**1.78**
Zfp238	15.83	13.98	25.80	27.09	**14.91**	**1.31**	**26.45**	**0.91**	**1.77**
Klhl29	4.77	3.14	8.39	5.65	**3.96**	**1.15**	**7.02**	**1.93**	**1.77**
Asmtl	14.22	14.24	25.73	24.65	**14.23**	**0.02**	**25.19**	**0.76**	**1.77**
P2ry12	1.59	0.38	2.39	1.08	**0.98**	**0.86**	**1.74**	**0.93**	**1.76**
Dpp6	3.63	1.75	6.49	3.00	**2.69**	**1.32**	**4.74**	**2.47**	**1.76**
Flot2	6.67	7.94	14.34	11.35	**7.30**	**0.89**	**12.84**	**2.11**	**1.76**
RGD1309821	2.38	2.65	4.40	4.42	**2.51**	**0.19**	**4.41**	**0.01**	**1.75**
Ypel2	5.56	5.85	9.31	10.67	**5.70**	**0.20**	**9.99**	**0.97**	**1.75**
Cdkl2	3.19	3.12	5.21	5.81	**3.15**	**0.05**	**5.51**	**0.42**	**1.75**
Wipi1	12.26	10.05	21.09	17.80	**11.15**	**1.56**	**19.45**	**2.33**	**1.74**
Itsn1	2.15	1.38	3.46	2.69	**1.77**	**0.55**	**3.08**	**0.54**	**1.74**
Bmp2	13.52	13.15	22.64	23.80	**13.33**	**0.26**	**23.22**	**0.82**	**1.74**
Fn3k	5.75	4.25	9.38	7.99	**5.00**	**1.06**	**8.69**	**0.98**	**1.74**
Rab40b	7.70	6.33	13.98	10.33	**7.01**	**0.97**	**12.15**	**2.58**	**1.73**
Dync1i2	1.31	0.44	2.10	0.93	**0.87**	**0.61**	**1.51**	**0.83**	**1.73**
LOC100366054	0.82	0.71	1.31	1.33	**0.76**	**0.08**	**1.32**	**0.02**	**1.73**
Glmn	2.61	3.08	4.85	4.97	**2.84**	**0.33**	**4.91**	**0.08**	**1.73**
Sycp3	0.68	0.53	1.09	0.99	**0.61**	**0.11**	**1.04**	**0.07**	**1.72**
Kdm5a	1.24	0.00	1.90	0.23	**0.62**	**0.87**	**1.07**	**1.18**	**1.72**
Samd14	2.95	1.88	5.46	2.83	**2.41**	**0.76**	**4.14**	**1.86**	**1.72**
Fa2h	0.93	0.98	1.78	1.50	**0.96**	**0.03**	**1.64**	**0.19**	**1.72**
Lrrc73	3.64	2.52	6.29	4.28	**3.08**	**0.79**	**5.28**	**1.42**	**1.71**
Kcng2	0.94	0.34	1.84	0.34	**0.64**	**0.42**	**1.09**	**1.06**	**1.71**
Fbxo41	0.91	0.84	1.83	1.16	**0.88**	**0.05**	**1.50**	**0.48**	**1.71**
Bcmo1	0.89	1.44	1.82	2.13	**1.16**	**0.39**	**1.97**	**0.22**	**1.70**
Myl9	14.92	15.83	10.35	8.07	**15.37**	**0.65**	**9.21**	**1.61**	**0.60**
Akap12	0.37	1.80	0.67	0.62	**1.08**	**1.01**	**0.65**	**0.03**	**0.60**
Rad51ap1	5.95	7.76	3.00	5.20	**6.85**	**1.27**	**4.10**	**1.55**	**0.60**
Tmem189	95.06	99.10	57.03	59.02	**97.08**	**2.86**	**58.03**	**1.40**	**0.60**
Cdc25b	29.47	28.47	16.09	18.49	**28.97**	**0.71**	**17.29**	**1.69**	**0.60**
Traf6	7.58	5.62	4.29	3.58	**6.60**	**1.39**	**3.94**	**0.50**	**0.60**
Timeless	14.27	14.78	7.38	9.94	**14.52**	**0.35**	**8.66**	**1.80**	**0.60**
Txk	1.29	1.53	0.67	1.01	**1.41**	**0.17**	**0.84**	**0.24**	**0.60**
Notch2	4.28	2.55	2.42	1.65	**3.41**	**1.22**	**2.03**	**0.55**	**0.60**
Rnf24	7.89	9.30	5.24	4.99	**8.59**	**1.00**	**5.11**	**0.18**	**0.59**
Afap1	5.98	4.09	3.40	2.59	**5.04**	**1.34**	**2.99**	**0.57**	**0.59**
Wars2	6.98	7.05	3.67	4.66	**7.02**	**0.05**	**4.17**	**0.70**	**0.59**
Raph1	6.05	4.48	3.21	3.04	**5.27**	**1.11**	**3.12**	**0.12**	**0.59**
Incenp	26.70	25.09	13.67	17.02	**25.89**	**1.14**	**15.35**	**2.36**	**0.59**
Plk4	11.57	11.03	5.84	7.55	**11.30**	**0.38**	**6.70**	**1.21**	**0.59**
Rmrp	11.93	14.36	6.58	8.99	**13.15**	**1.72**	**7.79**	**1.70**	**0.59**
Hmgn3	4.12	6.17	2.63	3.46	**5.14**	**1.45**	**3.04**	**0.58**	**0.59**
Pigh	6.21	6.13	3.47	3.83	**6.17**	**0.06**	**3.65**	**0.25**	**0.59**
Sec24b	11.55	9.95	6.70	6.03	**10.75**	**1.13**	**6.36**	**0.48**	**0.59**
Pkmyt1	19.38	20.71	10.69	12.93	**20.04**	**0.94**	**11.81**	**1.59**	**0.59**
Pola1	12.53	11.74	6.54	7.74	**12.13**	**0.56**	**7.14**	**0.84**	**0.59**
Kif18a	5.00	5.18	2.49	3.50	**5.09**	**0.12**	**2.99**	**0.71**	**0.59**
Nup210	8.12	7.10	4.59	4.36	**7.61**	**0.72**	**4.47**	**0.16**	**0.59**
Mgat4a	4.05	2.56	2.60	1.29	**3.31**	**1.05**	**1.94**	**0.93**	**0.59**
Net1	4.82	4.65	2.44	3.12	**4.74**	**0.12**	**2.78**	**0.48**	**0.59**
Hells	5.19	5.42	2.54	3.69	**5.31**	**0.16**	**3.11**	**0.82**	**0.59**
Hells	5.19	5.42	2.54	3.69	**5.31**	**0.16**	**3.11**	**0.82**	**0.59**
Jade3	5.69	5.15	2.72	3.64	**5.42**	**0.39**	**3.18**	**0.65**	**0.59**
Pid1	1.05	0.95	0.41	0.75	**1.00**	**0.06**	**0.58**	**0.24**	**0.58**
Angptl4	1.05	1.86	0.74	0.95	**1.45**	**0.57**	**0.85**	**0.15**	**0.58**
Rtkn2	1.46	1.12	0.66	0.84	**1.29**	**0.24**	**0.75**	**0.13**	**0.58**

Serpinb8	1.55	1.18	0.77	0.82	**1.37**	**0.26**	**0.79**	**0.03**	**0.58**
Myc	1.41	0.61	0.73	0.44	**1.01**	**0.57**	**0.58**	**0.20**	**0.58**
Nav2	6.09	4.22	3.24	2.73	**5.15**	**1.33**	**2.98**	**0.37**	**0.58**
Arhgef39	7.95	9.03	4.34	5.48	**8.49**	**0.76**	**4.91**	**0.81**	**0.58**
Ankrd34a	7.30	5.52	4.29	3.13	**6.41**	**1.26**	**3.71**	**0.83**	**0.58**
Zfp496	18.31	15.86	10.29	9.46	**17.08**	**1.73**	**9.87**	**0.58**	**0.58**
Mgme1	5.15	5.04	2.67	3.22	**5.09**	**0.08**	**2.94**	**0.39**	**0.58**
Relt	3.99	3.57	1.96	2.40	**3.78**	**0.29**	**2.18**	**0.31**	**0.58**
Chm	10.38	8.84	5.55	5.51	**9.61**	**1.09**	**5.53**	**0.03**	**0.58**
Tmem86a	4.94	5.07	2.97	2.79	**5.00**	**0.09**	**2.88**	**0.13**	**0.58**
Fam212b	5.05	4.97	2.64	3.11	**5.01**	**0.06**	**2.87**	**0.33**	**0.57**
Mnt	14.44	16.17	9.10	8.45	**15.30**	**1.23**	**8.78**	**0.46**	**0.57**
Cdc7	4.93	3.99	2.05	3.06	**4.46**	**0.66**	**2.55**	**0.71**	**0.57**
Fzd6	16.20	15.02	8.91	8.97	**15.61**	**0.84**	**8.94**	**0.04**	**0.57**
Gtse1	13.93	14.67	7.26	9.11	**14.30**	**0.53**	**8.18**	**1.30**	**0.57**
Stau2	1.38	0.78	0.00	1.23	**1.08**	**0.42**	**0.62**	**0.87**	**0.57**
Dctd	0.41	1.43	0.37	0.68	**0.92**	**0.72**	**0.53**	**0.22**	**0.57**
Cdc42se1	73.61	73.78	42.51	41.45	**73.69**	**0.12**	**41.98**	**0.76**	**0.57**
Mfap5	2.74	5.90	0.86	4.05	**4.32**	**2.23**	**2.45**	**2.25**	**0.57**
Pole	11.19	10.15	5.52	6.57	**10.67**	**0.74**	**6.05**	**0.75**	**0.57**
Mad2l1	20.29	20.49	10.01	13.08	**20.39**	**0.14**	**11.55**	**2.17**	**0.57**
Rbmx2	25.27	21.56	12.50	14.02	**23.42**	**2.62**	**13.26**	**1.07**	**0.57**
Mycl	0.90	0.90	0.70	0.32	**0.90**	**0.01**	**0.51**	**0.27**	**0.56**
Lctl	3.03	3.17	1.57	1.93	**3.10**	**0.09**	**1.75**	**0.25**	**0.56**
Mns1	3.71	4.36	1.44	3.11	**4.03**	**0.46**	**2.28**	**1.18**	**0.56**
Ccnf	10.95	12.54	5.43	7.83	**11.74**	**1.12**	**6.63**	**1.70**	**0.56**
Rassf9	1.75	1.68	1.05	0.88	**1.71**	**0.05**	**0.97**	**0.12**	**0.56**
Fam83d	20.02	16.27	10.39	10.06	**18.14**	**2.65**	**10.23**	**0.23**	**0.56**
Naa40	12.25	12.46	6.23	7.70	**12.35**	**0.15**	**6.96**	**1.04**	**0.56**
Schip1	2.77	1.80	1.78	0.79	**2.28**	**0.69**	**1.29**	**0.70**	**0.56**
Chek1	12.56	13.84	6.09	8.76	**13.20**	**0.90**	**7.42**	**1.89**	**0.56**
Carm1	13.66	12.86	8.45	6.46	**13.26**	**0.56**	**7.46**	**1.41**	**0.56**
Aurkb	38.29	38.96	19.96	23.46	**38.62**	**0.48**	**21.71**	**2.47**	**0.56**
Sapcd2	18.99	18.74	9.66	11.47	**18.86**	**0.17**	**10.56**	**1.28**	**0.56**
Btbd10	23.11	26.47	11.94	15.80	**24.79**	**2.38**	**13.87**	**2.73**	**0.56**
Fignl1	8.93	7.77	4.26	5.08	**8.35**	**0.82**	**4.67**	**0.58**	**0.56**
Sphk2	25.78	24.26	14.96	12.98	**25.02**	**1.08**	**13.97**	**1.40**	**0.56**
Cxcl10	2.53	3.09	1.82	1.32	**2.81**	**0.40**	**1.57**	**0.35**	**0.56**
RGD1306227	6.27	6.02	3.11	3.75	**6.15**	**0.17**	**3.43**	**0.45**	**0.56**
Emp1	2.14	2.14	0.80	1.59	**2.14**	**0.00**	**1.19**	**0.56**	**0.56**
LOC292543	2.10	3.78	0.75	2.52	**2.94**	**1.19**	**1.63**	**1.25**	**0.55**
Ehd1	26.36	24.90	14.81	13.61	**25.63**	**1.03**	**14.21**	**0.85**	**0.55**
Casc5	12.29	9.47	5.56	6.50	**10.88**	**2.00**	**6.03**	**0.67**	**0.55**
Dhx36	19.36	17.70	9.97	10.54	**18.53**	**1.18**	**10.26**	**0.40**	**0.55**
Tagln	4.23	7.22	2.71	3.60	**5.72**	**2.12**	**3.16**	**0.63**	**0.55**
Rad54b	0.88	1.32	0.58	0.64	**1.10**	**0.31**	**0.61**	**0.04**	**0.55**
Cdca2	10.92	13.12	5.13	8.10	**12.02**	**1.56**	**6.62**	**2.10**	**0.55**
Nxt2	1.25	1.50	0.62	0.89	**1.38**	**0.17**	**0.76**	**0.19**	**0.55**
Cenpl	2.68	2.78	0.80	2.19	**2.73**	**0.08**	**1.50**	**0.99**	**0.55**
Tex33	1.15	1.44	0.74	0.68	**1.30**	**0.20**	**0.71**	**0.05**	**0.55**
RGD1561149	10.30	9.08	5.48	5.12	**9.69**	**0.87**	**5.30**	**0.25**	**0.55**
Irs3	3.78	4.46	2.57	1.93	**4.12**	**0.48**	**2.25**	**0.45**	**0.55**
Ccsap	10.83	8.16	5.18	5.19	**9.50**	**1.89**	**5.19**	**0.01**	**0.55**
Serpinb1a	1.29	0.91	0.75	0.45	**1.10**	**0.27**	**0.60**	**0.21**	**0.55**
Ccp110	6.45	6.85	3.21	4.04	**6.65**	**0.28**	**3.62**	**0.59**	**0.55**
Kif2c	7.43	8.49	3.63	5.05	**7.96**	**0.75**	**4.34**	**1.00**	**0.55**
Rlim	21.67	18.43	10.32	11.54	**20.05**	**2.29**	**10.93**	**0.86**	**0.54**
Ercc6l	7.49	7.21	3.52	4.48	**7.35**	**0.20**	**4.00**	**0.68**	**0.54**
Elmo1	19.70	16.74	10.28	9.56	**18.22**	**2.10**	**9.92**	**0.51**	**0.54**
Usp4	4.23	4.17	2.11	2.46	**4.20**	**0.04**	**2.28**	**0.25**	**0.54**

Rassf2	0.89	1.06	0.43	0.64	**0.98**	**0.12**	**0.53**	**0.15**	**0.54**
Nsl1	8.53	9.00	4.15	5.37	**8.77**	**0.33**	**4.76**	**0.86**	**0.54**
Srek1ip1	14.95	14.08	8.23	7.54	**14.52**	**0.61**	**7.88**	**0.49**	**0.54**
Mastl	6.16	5.88	2.90	3.64	**6.02**	**0.20**	**3.27**	**0.53**	**0.54**
Lzts3	2.95	2.77	1.62	1.47	**2.86**	**0.13**	**1.55**	**0.11**	**0.54**
Ska1	12.11	13.01	5.19	8.38	**12.56**	**0.63**	**6.78**	**2.26**	**0.54**
Tmem43	30.96	29.76	17.94	14.72	**30.36**	**0.85**	**16.33**	**2.28**	**0.54**
Zfp385a	29.27	28.05	14.59	16.22	**28.66**	**0.86**	**15.40**	**1.15**	**0.54**
Rcn2	59.09	55.85	29.92	31.71	**57.47**	**2.29**	**30.82**	**1.27**	**0.54**
Psrc1	16.85	18.20	7.77	11.03	**17.53**	**0.96**	**9.40**	**2.31**	**0.54**
Fbxo5	9.76	12.69	4.62	7.41	**11.22**	**2.07**	**6.01**	**1.97**	**0.54**
Tnnt2	1.78	2.36	0.68	1.54	**2.07**	**0.41**	**1.11**	**0.60**	**0.54**
Chtf18	11.47	11.92	5.66	6.85	**11.70**	**0.32**	**6.26**	**0.85**	**0.53**
Shisa2	1.74	0.99	0.63	0.83	**1.36**	**0.53**	**0.73**	**0.14**	**0.53**
Pask	2.65	3.05	1.23	1.81	**2.85**	**0.29**	**1.52**	**0.41**	**0.53**
LOC303566	4.25	3.72	1.81	2.44	**3.98**	**0.37**	**2.12**	**0.44**	**0.53**
Pold1	15.60	14.93	7.48	8.79	**15.27**	**0.48**	**8.14**	**0.92**	**0.53**
Slfn13	10.11	12.31	4.37	7.57	**11.21**	**1.56**	**5.97**	**2.27**	**0.53**
RGD1305645	5.92	3.94	3.49	1.75	**4.93**	**1.40**	**2.62**	**1.24**	**0.53**
Vegfa	0.43	1.99	0.57	0.72	**1.21**	**1.11**	**0.64**	**0.10**	**0.53**
March8	13.23	12.13	6.64	6.82	**12.68**	**0.78**	**6.73**	**0.13**	**0.53**
Podxl	3.26	2.80	1.51	1.70	**3.03**	**0.33**	**1.61**	**0.14**	**0.53**
Gemin8	11.38	10.76	5.99	5.76	**11.07**	**0.44**	**5.87**	**0.16**	**0.53**
Cit	4.22	4.28	2.03	2.48	**4.25**	**0.05**	**2.26**	**0.32**	**0.53**
Gpsm1	12.04	9.09	5.98	5.19	**10.57**	**2.09**	**5.58**	**0.56**	**0.53**
Nfyc	12.73	12.08	5.76	7.34	**12.41**	**0.46**	**6.55**	**1.12**	**0.53**
Gen1	3.51	3.46	1.79	1.88	**3.48**	**0.04**	**1.84**	**0.07**	**0.53**
Ugt1a2	4.60	4.31	2.19	2.50	**4.45**	**0.21**	**2.34**	**0.22**	**0.53**
LOC500034	15.26	14.84	6.94	8.84	**15.05**	**0.30**	**7.89**	**1.35**	**0.52**
Dio2	4.96	1.59	2.79	0.62	**3.27**	**2.38**	**1.71**	**1.53**	**0.52**
Aif1l	28.14	31.84	13.64	17.65	**29.99**	**2.62**	**15.64**	**2.83**	**0.52**
Dbil5	3.74	3.55	1.92	1.88	**3.65**	**0.13**	**1.90**	**0.03**	**0.52**
Tnnc1	9.40	7.85	4.02	4.94	**8.62**	**1.09**	**4.48**	**0.65**	**0.52**
Spi1	0.96	1.23	0.46	0.68	**1.10**	**0.19**	**0.57**	**0.15**	**0.52**
Serpinb9	1.41	1.17	0.74	0.60	**1.29**	**0.17**	**0.67**	**0.10**	**0.52**
Kif18b	17.53	18.56	7.93	10.76	**18.04**	**0.73**	**9.35**	**2.00**	**0.52**
Rad54l	3.05	3.17	1.49	1.73	**3.11**	**0.09**	**1.61**	**0.18**	**0.52**
Bub1	21.07	20.93	8.78	12.91	**21.00**	**0.10**	**10.84**	**2.92**	**0.52**
Traip	7.95	9.14	3.89	4.92	**8.55**	**0.84**	**4.40**	**0.72**	**0.52**
Nusap1	27.33	27.61	12.69	15.61	**27.47**	**0.20**	**14.15**	**2.07**	**0.52**
Park7	0.81	1.14	0.07	0.94	**0.97**	**0.24**	**0.50**	**0.62**	**0.51**
Kif11	21.27	17.17	9.05	10.71	**19.22**	**2.90**	**9.88**	**1.18**	**0.51**
Cdc6	14.94	17.00	6.18	10.22	**15.97**	**1.46**	**8.20**	**2.86**	**0.51**
E2f1	24.08	21.42	10.02	13.23	**22.75**	**1.88**	**11.62**	**2.27**	**0.51**
Kcnip3	8.28	6.07	4.08	3.25	**7.17**	**1.56**	**3.66**	**0.59**	**0.51**
Melk	9.48	10.23	4.20	5.87	**9.86**	**0.53**	**5.03**	**1.18**	**0.51**
Tonsl	6.98	7.27	3.26	4.02	**7.13**	**0.20**	**3.64**	**0.54**	**0.51**
Ttk	16.91	16.12	6.57	10.24	**16.51**	**0.56**	**8.41**	**2.59**	**0.51**
Ska2	25.55	27.72	12.16	14.91	**26.63**	**1.54**	**13.53**	**1.94**	**0.51**
Dlgap5	28.19	27.44	12.69	15.55	**27.81**	**0.53**	**14.12**	**2.02**	**0.51**
Aspm	6.69	5.92	3.00	3.39	**6.30**	**0.54**	**3.19**	**0.27**	**0.51**
Smndc1	0.66	2.77	0.36	1.38	**1.72**	**1.49**	**0.87**	**0.72**	**0.51**
Cdt1	22.42	21.37	10.14	11.88	**21.90**	**0.74**	**11.01**	**1.23**	**0.50**
Dio1	4.36	2.09	2.18	1.06	**3.22**	**1.61**	**1.62**	**0.79**	**0.50**
Rnh1	6.54	5.60	3.59	2.50	**6.07**	**0.66**	**3.05**	**0.77**	**0.50**
Pif1	1.20	1.35	0.46	0.81	**1.27**	**0.10**	**0.64**	**0.25**	**0.50**
Kif15	7.33	8.48	2.88	5.05	**7.91**	**0.81**	**3.97**	**1.53**	**0.50**
Knstrn	36.88	38.91	16.93	21.09	**37.90**	**1.44**	**19.01**	**2.94**	**0.50**
Xkr5	5.45	6.02	2.50	3.25	**5.73**	**0.40**	**2.87**	**0.53**	**0.50**
Sgol2	9.12	9.95	3.91	5.62	**9.53**	**0.58**	**4.76**	**1.21**	**0.50**

Kif20b	11.90	11.76	4.85	6.96	**11.83**	**0.10**	**5.90**	**1.50**	**0.50**
Pbk	22.43	21.55	9.03	12.87	**21.99**	**0.62**	**10.95**	**2.71**	**0.50**
Bard1	13.37	11.99	5.32	7.30	**12.68**	**0.98**	**6.31**	**1.40**	**0.50**
Kntc1	11.82	9.49	4.99	5.58	**10.65**	**1.65**	**5.28**	**0.42**	**0.50**
Rab11fip1	12.19	10.83	5.97	5.45	**11.51**	**0.96**	**5.71**	**0.37**	**0.50**
E2f6	25.55	26.30	11.96	13.67	**25.93**	**0.53**	**12.82**	**1.21**	**0.49**
Acta2	11.55	8.99	6.34	3.78	**10.27**	**1.81**	**5.06**	**1.81**	**0.49**
Dsn1	12.90	15.00	4.84	8.89	**13.95**	**1.48**	**6.86**	**2.86**	**0.49**
Etnk2	3.60	3.78	1.86	1.77	**3.69**	**0.13**	**1.82**	**0.06**	**0.49**
Cenpf	5.12	4.07	2.11	2.41	**4.60**	**0.74**	**2.26**	**0.21**	**0.49**
Slc18a2	3.17	2.12	1.36	1.23	**2.65**	**0.74**	**1.30**	**0.09**	**0.49**
Rap1gds1	27.75	24.87	13.14	12.58	**26.31**	**2.04**	**12.86**	**0.39**	**0.49**
Tcf19	70.80	69.80	32.41	36.31	**70.30**	**0.71**	**34.36**	**2.75**	**0.49**
Fam111a	3.76	3.52	1.47	2.09	**3.64**	**0.17**	**1.78**	**0.44**	**0.49**
Arg2	15.09	17.07	7.05	8.59	**16.08**	**1.41**	**7.82**	**1.09**	**0.49**
Arf2	12.69	11.89	5.54	6.40	**12.29**	**0.56**	**5.97**	**0.61**	**0.49**
RGD1559690	5.96	4.85	2.12	3.13	**5.41**	**0.79**	**2.62**	**0.71**	**0.49**
Ccdc28a	5.67	6.71	2.92	3.07	**6.19**	**0.74**	**3.00**	**0.11**	**0.48**
Cdca5	13.54	14.03	5.50	7.77	**13.78**	**0.35**	**6.64**	**1.61**	**0.48**
Foxm1	10.91	12.31	4.40	6.73	**11.61**	**0.99**	**5.57**	**1.65**	**0.48**
Sec14l1	28.16	24.03	13.33	11.61	**26.10**	**2.92**	**12.47**	**1.21**	**0.48**
Cx3cl1	1.67	0.98	0.68	0.58	**1.33**	**0.48**	**0.63**	**0.07**	**0.48**
Fancd2	6.59	6.96	2.80	3.67	**6.78**	**0.26**	**3.23**	**0.62**	**0.48**
E2f7	5.65	5.26	2.05	3.14	**5.45**	**0.27**	**2.59**	**0.77**	**0.48**
Polq	1.80	1.59	0.67	0.94	**1.69**	**0.15**	**0.80**	**0.19**	**0.47**
Bin3	19.34	21.41	8.49	10.83	**20.37**	**1.46**	**9.66**	**1.66**	**0.47**
Cenpu	11.96	13.58	4.36	7.75	**12.77**	**1.15**	**6.05**	**2.40**	**0.47**
Tiam1	6.08	4.74	2.85	2.27	**5.41**	**0.95**	**2.56**	**0.41**	**0.47**
Rab11fip1	13.58	13.96	5.83	7.17	**13.77**	**0.27**	**6.50**	**0.95**	**0.47**
Zmpste24	19.33	15.70	9.16	7.36	**17.51**	**2.57**	**8.26**	**1.28**	**0.47**
Exo1	3.14	3.28	1.26	1.76	**3.21**	**0.09**	**1.51**	**0.35**	**0.47**
Espl1	12.18	12.00	4.87	6.48	**12.09**	**0.13**	**5.67**	**1.14**	**0.47**
Depdc1b	5.77	7.04	2.30	3.70	**6.40**	**0.89**	**3.00**	**0.99**	**0.47**
Ska3	14.25	16.60	6.02	8.42	**15.42**	**1.66**	**7.22**	**1.70**	**0.47**
Cenpi	10.67	9.09	4.00	5.25	**9.88**	**1.11**	**4.62**	**0.88**	**0.47**
Cenpt	19.05	21.40	7.59	11.33	**20.23**	**1.66**	**9.46**	**2.65**	**0.47**
Pls1	10.37	9.47	4.72	4.55	**9.92**	**0.63**	**4.64**	**0.12**	**0.47**
Clspn	6.99	7.42	2.74	3.93	**7.21**	**0.31**	**3.33**	**0.84**	**0.46**
Mcm10	5.46	5.08	1.95	2.92	**5.27**	**0.26**	**2.43**	**0.69**	**0.46**
Il1rn	6.00	4.18	1.98	2.71	**5.09**	**1.29**	**2.34**	**0.52**	**0.46**
Arhgap11a	20.12	18.16	7.21	10.29	**19.14**	**1.39**	**8.75**	**2.18**	**0.46**
Pole2	8.74	8.53	2.95	4.75	**8.63**	**0.15**	**3.85**	**1.27**	**0.45**
Neil3	2.68	3.15	0.88	1.70	**2.92**	**0.33**	**1.29**	**0.58**	**0.44**
Pelo	9.41	7.67	4.24	3.30	**8.54**	**1.23**	**3.77**	**0.67**	**0.44**
Mybl2	19.70	20.64	7.28	10.53	**20.17**	**0.67**	**8.90**	**2.30**	**0.44**
Hjurp	15.17	14.59	5.49	7.62	**14.88**	**0.41**	**6.55**	**1.51**	**0.44**
Orc1	3.62	4.46	1.28	2.20	**4.04**	**0.59**	**1.74**	**0.66**	**0.43**
Recql4	7.68	10.68	2.99	4.88	**9.18**	**2.12**	**3.94**	**1.34**	**0.43**
Parpbp	3.60	3.41	1.29	1.71	**3.50**	**0.13**	**1.50**	**0.30**	**0.43**
Ston1	2.40	2.54	1.16	0.94	**2.47**	**0.10**	**1.05**	**0.15**	**0.43**
Crabp2	1.49	1.58	0.46	0.85	**1.54**	**0.06**	**0.66**	**0.27**	**0.43**
Iqgap3	16.55	15.37	6.11	7.41	**15.96**	**0.84**	**6.76**	**0.92**	**0.42**
Map2k6	0.81	1.71	0.53	0.53	**1.26**	**0.64**	**0.53**	**0.00**	**0.42**
Nsmf	5.40	2.75	2.03	1.42	**4.07**	**1.87**	**1.72**	**0.43**	**0.42**
Sftpd	3.37	2.70	1.15	1.34	**3.04**	**0.47**	**1.25**	**0.14**	**0.41**
Dmd	1.93	2.05	0.32	1.26	**1.99**	**0.08**	**0.79**	**0.66**	**0.40**
Fhl1	3.26	1.02	0.91	0.78	**2.14**	**1.58**	**0.85**	**0.10**	**0.40**
Eme1	4.55	5.75	1.59	2.47	**5.15**	**0.85**	**2.03**	**0.62**	**0.39**
Ccl20	2.31	2.93	0.53	1.50	**2.62**	**0.44**	**1.02**	**0.68**	**0.39**
Nr1i3	1.26	1.38	1.00	0.00	**1.32**	**0.08**	**0.50**	**0.71**	**0.38**

Icam1	3.45	2.02	0.79	1.27	**2.74**	**1.01**	**1.03**	**0.34**	**0.38**
RGD1559903	2.32	2.34	0.69	1.01	**2.33**	**0.02**	**0.85**	**0.23**	**0.36**
Plec	4.81	3.36	1.73	1.21	**4.08**	**1.03**	**1.47**	**0.37**	**0.36**
Thumpd3	2.78	0.30	0.00	1.05	**1.54**	**1.76**	**0.53**	**0.74**	**0.34**
Gbp2	2.57	1.16	0.71	0.47	**1.87**	**1.00**	**0.59**	**0.17**	**0.32**
Gsta1	3.74	2.71	1.16	0.82	**3.23**	**0.72**	**0.99**	**0.24**	**0.31**
Patz1	5.67	7.43	0.24	2.71	**6.55**	**1.25**	**1.48**	**1.75**	**0.23**
Patz1	9.84	9.41	0.99	2.02	**9.63**	**0.31**	**1.50**	**0.73**	**0.16**

Annex 3.- Gene expression changes upon MAX re-expression in UR61 cells. mRNA levels of the whole transcriptome were determined by RNA-seq. The table includes genes showing differential expression upon MAX expression in UR61 cells. The transcriptomes of UR61-MT-MAX pLKO and UR61-MT-Hebo pLKO both treated with 100 µM Zn^{2+} for 24 h, were compared. Data are mean of two independent experiments with RPKM values ≥ 0.5 and S.D. ≤ 3. The RPKMs of each experiment ("Exp.") are indicated. The fold-change thresholds between both conditions were set as ≥ 1.7 and < 0.6. The mean of the expression data and S.D. of the fold-changes are highlighted in green at the top of the table.

	RPKM				RPKM				Fold Change
	UR61-MT-Hebo pLKO		UR61-MT-MAX pLKO		UR61-MT-Hebo pLKO		UR61-MT-MAX pLKO		pLKO
GENE	Exp.1	Exp.2	Exp.1	Exp.2	mean	S.D.	media	S.D.	MAX vs Hebo
Col6a2	0.63	0.64	7.14	6.24	**0.63**	**0.00**	**6.69**	**0.64**	**10.55**
Arhgdib	0.21	1.42	3.98	5.12	**0.81**	**0.85**	**4.55**	**0.80**	**5.59**
Zcchc12	2.12	2.01	7.64	10.49	**2.06**	**0.07**	**9.06**	**2.02**	**4.39**
Slc26a7	0.34	0.68	1.60	2.60	**0.51**	**0.24**	**2.10**	**0.71**	**4.14**
Cox8b	1.43	4.69	11.41	13.46	**3.06**	**2.31**	**12.43**	**1.45**	**4.07**
Ston1	0.51	0.80	2.40	2.54	**0.65**	**0.21**	**2.47**	**0.10**	**3.78**
RT1-Db1	0.61	1.00	2.75	3.25	**0.81**	**0.27**	**3.00**	**0.36**	**3.72**
Car9	1.62	0.92	5.17	3.12	**1.27**	**0.50**	**4.14**	**1.45**	**3.26**
Kifc3	1.45	3.46	6.80	8.12	**2.45**	**1.42**	**7.46**	**0.93**	**3.04**
Slc5a5	4.83	4.23	13.96	13.28	**4.53**	**0.42**	**13.62**	**0.48**	**3.01**
Ccl7	0.60	0.60	2.08	1.49	**0.60**	**0.00**	**1.79**	**0.42**	**2.98**
Wif1	2.45	1.94	6.93	5.79	**2.19**	**0.36**	**6.36**	**0.81**	**2.90**
Stc1	1.86	0.58	3.78	3.20	**1.22**	**0.91**	**3.49**	**0.41**	**2.86**
Gpx4	0.58	1.39	3.34	2.19	**0.99**	**0.57**	**2.76**	**0.81**	**2.80**
Fgfr1	4.29	3.89	11.61	11.20	**4.09**	**0.28**	**11.40**	**0.28**	**2.79**
Camta1	0.72	0.39	1.49	1.59	**0.56**	**0.23**	**1.54**	**0.07**	**2.78**
Nsmf	0.90	2.10	5.40	2.75	**1.50**	**0.85**	**4.07**	**1.87**	**2.72**
Rest	1.21	1.31	3.73	2.84	**1.26**	**0.07**	**3.29**	**0.63**	**2.61**
Zmynd11	0.39	1.18	4.03	0.00	**0.79**	**0.56**	**2.02**	**2.85**	**2.57**
Sema6d	4.66	4.19	11.66	10.35	**4.42**	**0.33**	**11.00**	**0.93**	**2.49**
Iffo2	1.92	1.72	4.80	3.96	**1.82**	**0.14**	**4.38**	**0.59**	**2.40**
Schip1	0.90	1.01	2.77	1.80	**0.96**	**0.08**	**2.28**	**0.69**	**2.39**
Hist2h2ab	2.80	5.82	10.97	9.54	**4.31**	**2.13**	**10.26**	**1.01**	**2.38**
Synpo	1.82	1.48	3.83	3.93	**1.65**	**0.24**	**3.88**	**0.07**	**2.35**
Patz1	4.80	3.58	9.84	9.41	**4.19**	**0.86**	**9.63**	**0.31**	**2.30**
Acta1	1.89	1.17	2.23	4.69	**1.53**	**0.51**	**3.46**	**1.74**	**2.26**
Snai2	4.12	5.55	12.05	9.75	**4.83**	**1.01**	**10.90**	**1.63**	**2.26**
Usp4	1.94	1.81	4.23	4.17	**1.88**	**0.10**	**4.20**	**0.04**	**2.24**
RGD1562018	1.43	1.44	3.19	3.22	**1.44**	**0.01**	**3.20**	**0.02**	**2.23**
Hist1h2ak	0.39	1.14	1.44	1.97	**0.77**	**0.53**	**1.71**	**0.37**	**2.23**
Thumpd3	1.05	0.35	2.78	0.30	**0.70**	**0.50**	**1.54**	**1.76**	**2.20**
Sult1a1	0.36	1.31	1.13	2.55	**0.83**	**0.68**	**1.84**	**1.00**	**2.20**
Crabp2	0.74	0.67	1.49	1.58	**0.70**	**0.05**	**1.54**	**0.06**	**2.18**
Map2k6	0.34	0.83	0.81	1.71	**0.58**	**0.35**	**1.26**	**0.64**	**2.17**
Nr4a2	0.42	0.64	0.92	1.39	**0.53**	**0.15**	**1.15**	**0.33**	**2.16**
Lbh	2.20	2.44	4.84	5.19	**2.32**	**0.17**	**5.01**	**0.25**	**2.16**
Fzd1	1.38	1.50	3.25	2.96	**1.44**	**0.09**	**3.10**	**0.21**	**2.16**
Slc2a4	1.04	0.97	2.17	2.14	**1.00**	**0.05**	**2.16**	**0.02**	**2.15**
Podxl	1.69	1.13	3.26	2.80	**1.41**	**0.39**	**3.03**	**0.33**	**2.14**
Flrt1	1.57	0.71	3.25	1.59	**1.14**	**0.61**	**2.42**	**1.17**	**2.12**
Gpr56	11.40	11.47	25.47	22.84	**11.43**	**0.05**	**24.15**	**1.86**	**2.11**
Stap2	1.08	2.10	3.03	3.70	**1.59**	**0.72**	**3.36**	**0.47**	**2.11**
Sh3tc1	6.29	7.88	15.87	14.03	**7.08**	**1.13**	**14.95**	**1.30**	**2.11**
Dmrtc1a	1.02	1.39	2.03	3.04	**1.20**	**0.26**	**2.53**	**0.72**	**2.10**

Mycn	1.38	0.70	2.37	1.99	**1.04**	**0.48**	**2.18**	**0.27**	**2.09**
Gata4	1.68	2.23	3.60	4.57	**1.95**	**0.39**	**4.08**	**0.69**	**2.09**
Marcks	1.09	2.33	2.76	4.35	**1.71**	**0.88**	**3.55**	**1.12**	**2.08**
Smtnl2	1.61	1.56	3.49	3.02	**1.59**	**0.03**	**3.25**	**0.33**	**2.05**
Alk	0.78	0.78	1.79	1.39	**0.78**	**0.00**	**1.59**	**0.28**	**2.04**
Serpinb8	0.88	0.47	1.55	1.18	**0.67**	**0.29**	**1.37**	**0.26**	**2.03**
Kcnip3	3.18	3.90	8.28	6.07	**3.54**	**0.51**	**7.17**	**1.56**	**2.03**
Pip5k1c	1.26	0.58	1.91	1.78	**0.92**	**0.48**	**1.85**	**0.09**	**2.00**
Pard6g	0.62	1.08	1.65	1.72	**0.85**	**0.32**	**1.68**	**0.05**	**1.99**
Sipa1l2	2.84	2.91	5.14	6.26	**2.87**	**0.05**	**5.70**	**0.79**	**1.98**
Radil	5.65	6.72	12.11	12.37	**6.19**	**0.75**	**12.24**	**0.19**	**1.98**
Tmem176b	11.12	9.07	18.97	20.79	**10.10**	**1.45**	**19.88**	**1.29**	**1.97**
Mtus2	1.70	2.65	4.74	3.80	**2.17**	**0.68**	**4.27**	**0.66**	**1.96**
Icam1	0.90	1.90	3.45	2.02	**1.40**	**0.71**	**2.74**	**1.01**	**1.96**
Bdh2	1.82	5.09	5.42	8.11	**3.45**	**2.32**	**6.77**	**1.90**	**1.96**
Vasn	4.73	3.98	10.11	6.88	**4.35**	**0.54**	**8.49**	**2.29**	**1.95**
Igf2	5.08	4.31	10.44	7.77	**4.69**	**0.54**	**9.10**	**1.89**	**1.94**
Ctsr	0.48	0.77	1.82	0.60	**0.62**	**0.21**	**1.21**	**0.86**	**1.94**
Nnat	3.91	0.00	2.47	5.05	**1.96**	**2.77**	**3.76**	**1.83**	**1.92**
LOC292543	0.54	2.53	2.10	3.78	**1.53**	**1.41**	**2.94**	**1.19**	**1.92**
Ext1	11.66	10.42	22.17	20.04	**11.04**	**0.88**	**21.10**	**1.51**	**1.91**
Nr1i3	1.10	0.29	1.26	1.38	**0.69**	**0.57**	**1.32**	**0.08**	**1.91**
Bend6	2.42	3.94	6.37	5.75	**3.18**	**1.07**	**6.06**	**0.44**	**1.90**
Gpld1	1.83	2.59	4.16	4.25	**2.21**	**0.54**	**4.20**	**0.06**	**1.90**
Wnt11	0.75	0.64	1.48	1.15	**0.70**	**0.08**	**1.32**	**0.23**	**1.89**
Smad3	1.67	2.00	4.05	2.89	**1.84**	**0.23**	**3.47**	**0.83**	**1.89**
Acadsb	0.44	0.85	1.22	1.23	**0.65**	**0.29**	**1.22**	**0.01**	**1.89**
Cdk10	0.78	1.95	2.07	3.07	**1.37**	**0.83**	**2.57**	**0.71**	**1.88**
Hint3	1.11	0.91	2.21	1.60	**1.01**	**0.14**	**1.90**	**0.43**	**1.88**
Tmco4	0.67	0.76	1.43	1.24	**0.71**	**0.06**	**1.33**	**0.13**	**1.87**
Syt13	0.88	1.08	1.98	1.69	**0.98**	**0.14**	**1.83**	**0.20**	**1.87**
Fcgrt	5.58	6.15	11.90	9.97	**5.86**	**0.41**	**10.93**	**1.36**	**1.87**
Serpinb1a	0.60	0.58	1.29	0.91	**0.59**	**0.02**	**1.10**	**0.27**	**1.86**
Enpep	0.93	0.50	1.52	1.12	**0.71**	**0.31**	**1.32**	**0.29**	**1.86**
Cd274	1.83	3.01	3.59	5.38	**2.42**	**0.83**	**4.48**	**1.26**	**1.85**
Dmd	0.37	1.79	1.93	2.05	**1.08**	**1.00**	**1.99**	**0.08**	**1.85**
Nlgn3	0.68	0.91	1.22	1.70	**0.79**	**0.16**	**1.46**	**0.34**	**1.84**
Arhgap17	0.43	1.02	0.84	1.83	**0.73**	**0.41**	**1.33**	**0.70**	**1.84**
Acacb	0.76	0.79	1.31	1.53	**0.77**	**0.02**	**1.42**	**0.15**	**1.83**
Anks6	0.85	0.81	1.18	1.83	**0.83**	**0.03**	**1.50**	**0.46**	**1.81**
Aplf	0.67	1.05	1.34	1.79	**0.86**	**0.27**	**1.56**	**0.32**	**1.81**
Capn6	0.38	0.99	1.02	1.46	**0.69**	**0.43**	**1.24**	**0.31**	**1.81**
Mboat2	4.59	7.64	10.82	11.27	**6.11**	**2.16**	**11.05**	**0.32**	**1.81**
Ptpn13	3.42	3.88	5.55	7.65	**3.65**	**0.33**	**6.60**	**1.49**	**1.81**
Efna4	3.84	5.36	8.05	8.55	**4.60**	**1.08**	**8.30**	**0.36**	**1.80**
Bcl11b	0.74	0.33	1.06	0.88	**0.54**	**0.29**	**0.97**	**0.13**	**1.79**
Man1c1	8.48	8.16	14.05	15.66	**8.32**	**0.23**	**14.86**	**1.14**	**1.79**
Nfatc4	2.09	1.41	3.22	2.99	**1.75**	**0.48**	**3.10**	**0.16**	**1.78**
Dbnl	1.77	1.32	2.27	3.21	**1.54**	**0.32**	**2.74**	**0.66**	**1.78**
Sod3	0.66	0.48	1.38	0.64	**0.57**	**0.13**	**1.01**	**0.52**	**1.77**
Masp1	2.15	2.68	4.78	3.74	**2.41**	**0.37**	**4.26**	**0.74**	**1.77**
Cklf	1.45	3.15	3.48	4.64	**2.30**	**1.21**	**4.06**	**0.82**	**1.77**
Tmem176b	1.18	0.46	1.34	1.53	**0.82**	**0.51**	**1.44**	**0.14**	**1.76**
Sema3f	10.36	7.73	16.13	15.65	**9.05**	**1.86**	**15.89**	**0.34**	**1.76**
Tmem164	4.13	3.18	6.78	5.99	**3.65**	**0.67**	**6.39**	**0.56**	**1.75**
Myo9b	3.47	3.37	7.53	4.42	**3.42**	**0.07**	**5.97**	**2.20**	**1.75**
Galnt11	5.01	6.76	10.56	9.99	**5.88**	**1.24**	**10.28**	**0.41**	**1.75**
Irs3	1.50	3.23	3.78	4.46	**2.36**	**1.22**	**4.12**	**0.48**	**1.74**
Prkaa2	3.94	1.99	6.44	3.87	**2.97**	**1.38**	**5.16**	**1.82**	**1.74**
Arhgap17	0.76	1.67	1.22	3.00	**1.22**	**0.64**	**2.11**	**1.26**	**1.74**

Rgs2	8.70	7.22	15.73	11.85	**7.96**	**1.05**	**13.79**	**2.74**	**1.73**
Amer1	3.25	1.81	5.64	3.11	**2.53**	**1.02**	**4.37**	**1.79**	**1.73**
Lingo1	3.10	1.45	4.59	3.21	**2.27**	**1.16**	**3.90**	**0.97**	**1.72**
Srpr	44.68	48.89	80.55	80.09	**46.78**	**2.97**	**80.32**	**0.33**	**1.72**
Rmdn2	0.92	1.62	2.02	2.33	**1.27**	**0.49**	**2.17**	**0.22**	**1.71**
Tacc2	1.09	3.78	3.40	4.90	**2.43**	**1.90**	**4.15**	**1.06**	**1.71**
Gsta1	1.07	2.72	3.74	2.71	**1.89**	**1.17**	**3.23**	**0.72**	**1.70**
Rdh13	14.41	13.24	8.14	8.45	**13.82**	**0.83**	**8.29**	**0.22**	**0.60**
Thumpd3	4.12	4.39	1.70	3.39	**4.25**	**0.18**	**2.55**	**1.19**	**0.60**
Bcmo1	1.39	2.50	0.89	1.44	**1.95**	**0.79**	**1.16**	**0.39**	**0.60**
P2ry2	9.80	10.15	5.57	6.32	**9.97**	**0.25**	**5.94**	**0.53**	**0.60**
Crb3	5.20	6.28	2.61	4.21	**5.74**	**0.76**	**3.41**	**1.13**	**0.59**
Timm9	1.67	0.90	0.90	0.62	**1.28**	**0.54**	**0.76**	**0.19**	**0.59**
Atl1	27.10	27.32	17.22	15.08	**27.21**	**0.15**	**16.15**	**1.52**	**0.59**
S100a3	10.44	6.60	5.58	4.53	**8.52**	**2.71**	**5.05**	**0.75**	**0.59**
Gpd1	16.23	16.10	10.23	8.93	**16.16**	**0.09**	**9.58**	**0.92**	**0.59**
Mok	2.56	4.77	1.83	2.51	**3.66**	**1.56**	**2.17**	**0.48**	**0.59**
Mtl5	3.27	3.44	2.24	1.73	**3.35**	**0.12**	**1.98**	**0.36**	**0.59**
Actl6b	5.22	2.74	2.74	1.97	**3.98**	**1.75**	**2.35**	**0.54**	**0.59**
Card6	6.25	4.52	3.05	3.29	**5.39**	**1.22**	**3.17**	**0.17**	**0.59**
Nfe2	0.96	1.19	0.45	0.81	**1.08**	**0.17**	**0.63**	**0.26**	**0.59**
LOC688765	2.76	3.01	1.60	1.79	**2.88**	**0.18**	**1.69**	**0.13**	**0.59**
Spop	30.14	27.76	17.43	16.57	**28.95**	**1.68**	**17.00**	**0.61**	**0.59**
Map4k1	4.71	3.17	2.26	2.36	**3.94**	**1.09**	**2.31**	**0.08**	**0.59**
Park7	0.56	1.32	0.33	0.77	**0.94**	**0.54**	**0.55**	**0.31**	**0.58**
Svop	10.56	9.40	6.67	4.95	**9.98**	**0.82**	**5.81**	**1.22**	**0.58**
Tspyl4	7.63	3.74	3.86	2.74	**5.68**	**2.75**	**3.30**	**0.79**	**0.58**
Slc17a9	5.65	6.23	3.85	3.05	**5.94**	**0.41**	**3.45**	**0.57**	**0.58**
Csnk2b	6.43	5.32	2.06	4.76	**5.87**	**0.78**	**3.41**	**1.91**	**0.58**
Atp6v1c2	1.19	2.39	1.01	1.06	**1.79**	**0.85**	**1.04**	**0.04**	**0.58**
Napb	2.09	1.76	0.99	1.23	**1.92**	**0.24**	**1.11**	**0.18**	**0.58**
Rab33a	15.62	19.48	8.46	11.77	**17.55**	**2.72**	**10.11**	**2.35**	**0.58**
38231	6.39	6.28	3.14	4.16	**6.33**	**0.07**	**3.65**	**0.72**	**0.58**
Mapk9	2.28	2.58	1.16	1.64	**2.43**	**0.22**	**1.40**	**0.34**	**0.57**
Znrd1	1.86	5.29	2.95	1.15	**3.58**	**2.43**	**2.05**	**1.27**	**0.57**
Ttc22	5.40	4.67	3.33	2.36	**5.04**	**0.52**	**2.84**	**0.68**	**0.56**
LOC686120	3.66	4.87	2.09	2.72	**4.26**	**0.85**	**2.41**	**0.44**	**0.56**
LOC100360244	2.08	1.82	0.94	1.26	**1.95**	**0.18**	**1.10**	**0.22**	**0.56**
Wdr55	14.85	18.17	8.40	10.18	**16.51**	**2.34**	**9.29**	**1.25**	**0.56**
Lck	2.20	3.00	1.23	1.68	**2.60**	**0.57**	**1.46**	**0.32**	**0.56**
Kank2	25.04	21.28	12.77	13.16	**23.16**	**2.66**	**12.97**	**0.28**	**0.56**
Vpreb3	3.52	3.70	1.41	2.63	**3.61**	**0.13**	**2.02**	**0.86**	**0.56**
Plxnd1	2.78	0.78	1.21	0.77	**1.78**	**1.41**	**0.99**	**0.32**	**0.56**
Zfp951	0.98	1.26	0.58	0.67	**1.12**	**0.20**	**0.62**	**0.06**	**0.56**
Car11	10.11	8.90	4.59	5.94	**9.50**	**0.85**	**5.27**	**0.95**	**0.55**
Cacna1b	6.50	5.18	3.65	2.82	**5.84**	**0.94**	**3.24**	**0.58**	**0.55**
Med23	15.27	16.10	8.34	9.01	**15.69**	**0.59**	**8.68**	**0.48**	**0.55**
Lrcol1	1.43	0.45	0.50	0.54	**0.94**	**0.69**	**0.52**	**0.03**	**0.55**
Stx1a	10.87	11.61	5.94	6.45	**11.24**	**0.52**	**6.20**	**0.36**	**0.55**
Lppr5	5.25	1.42	2.63	1.04	**3.34**	**2.71**	**1.83**	**1.13**	**0.55**
Slc22a5	9.42	5.42	3.91	4.25	**7.42**	**2.83**	**4.08**	**0.24**	**0.55**
Ces1a	3.56	1.74	1.62	1.28	**2.65**	**1.28**	**1.45**	**0.23**	**0.55**
Lin28a	2.10	1.70	0.87	1.21	**1.90**	**0.28**	**1.04**	**0.24**	**0.55**
Rcl1	24.51	28.41	14.36	14.47	**26.46**	**2.76**	**14.41**	**0.07**	**0.54**
Ceacam9	1.36	0.87	0.57	0.64	**1.11**	**0.34**	**0.61**	**0.04**	**0.54**
Rbpjl	1.82	2.71	0.89	1.56	**2.26**	**0.63**	**1.23**	**0.47**	**0.54**
Fjx1	15.37	12.89	8.71	6.60	**14.13**	**1.75**	**7.65**	**1.49**	**0.54**
Zfp180	2.24	3.13	2.88	0.02	**2.68**	**0.63**	**1.45**	**2.02**	**0.54**
Cdh15	1.19	1.10	0.56	0.67	**1.14**	**0.06**	**0.62**	**0.08**	**0.54**
Mfsd2a	3.46	4.14	2.32	1.78	**3.80**	**0.48**	**2.05**	**0.38**	**0.54**

Strn4	8.94	6.78	3.93	4.55	**7.86**	**1.52**	**4.24**	**0.44**	**0.54**
Cpne7	8.71	8.12	4.10	4.90	**8.41**	**0.42**	**4.50**	**0.57**	**0.53**
Gdap1l1	60.04	57.53	29.70	33.17	**58.79**	**1.78**	**31.43**	**2.45**	**0.53**
Ntrk1	22.51	22.37	12.79	11.20	**22.44**	**0.10**	**11.99**	**1.12**	**0.53**
Kcnc1	5.99	2.62	3.01	1.55	**4.31**	**2.38**	**2.28**	**1.04**	**0.53**
Pgm2l1	16.47	12.38	6.48	8.79	**14.43**	**2.89**	**7.64**	**1.64**	**0.53**
Vps72	7.78	8.04	4.52	3.78	**7.91**	**0.18**	**4.15**	**0.52**	**0.53**
Cdkn1c	1.79	1.53	0.86	0.88	**1.66**	**0.19**	**0.87**	**0.01**	**0.52**
Ppp1r3c	1.84	1.16	0.82	0.74	**1.50**	**0.48**	**0.78**	**0.05**	**0.52**
Ppp1r3c	1.84	1.16	0.82	0.74	**1.50**	**0.48**	**0.78**	**0.05**	**0.52**
Gk	2.32	2.90	1.44	1.27	**2.61**	**0.41**	**1.35**	**0.12**	**0.52**
Camk4	0.86	1.30	0.65	0.47	**1.08**	**0.31**	**0.56**	**0.13**	**0.52**
Fblim1	1.41	0.82	0.70	0.45	**1.11**	**0.41**	**0.58**	**0.17**	**0.52**
Unc5cl	1.37	1.44	0.31	1.14	**1.40**	**0.05**	**0.73**	**0.59**	**0.52**
Gpr150	2.19	1.40	0.99	0.86	**1.80**	**0.56**	**0.93**	**0.09**	**0.52**
Nnat	1.71	0.45	1.11	0.00	**1.08**	**0.89**	**0.55**	**0.78**	**0.51**
Npas1	1.62	1.85	0.96	0.82	**1.73**	**0.17**	**0.89**	**0.10**	**0.51**
Dmd	8.04	5.01	4.14	2.57	**6.53**	**2.14**	**3.35**	**1.12**	**0.51**
Dchs1	5.86	4.03	2.95	2.05	**4.94**	**1.29**	**2.50**	**0.63**	**0.51**
Patz1	3.92	6.86	1.13	4.30	**5.39**	**2.08**	**2.71**	**2.25**	**0.50**
RGD1565498	2.58	3.09	1.70	1.14	**2.84**	**0.36**	**1.42**	**0.40**	**0.50**
Serpinf1	1.76	0.49	0.52	0.60	**1.12**	**0.89**	**0.56**	**0.06**	**0.50**
Snap25	2.04	0.43	0.00	1.22	**1.24**	**1.14**	**0.61**	**0.86**	**0.49**
Igsf5	2.37	2.18	1.24	1.00	**2.27**	**0.13**	**1.12**	**0.17**	**0.49**
Jakmip1	6.62	5.99	3.55	2.67	**6.30**	**0.45**	**3.11**	**0.63**	**0.49**
Trpm4	4.45	3.83	2.02	2.06	**4.14**	**0.44**	**2.04**	**0.02**	**0.49**
Dmtn	8.39	6.96	3.87	3.66	**7.68**	**1.01**	**3.76**	**0.15**	**0.49**
Rapgef5	4.57	2.45	1.68	1.76	**3.51**	**1.50**	**1.72**	**0.05**	**0.49**
Sp110	14.95	17.61	7.58	8.35	**16.28**	**1.88**	**7.96**	**0.55**	**0.49**
Adarb1	2.26	1.22	0.54	1.16	**1.74**	**0.73**	**0.85**	**0.44**	**0.49**
Prss53	3.52	2.35	1.20	1.67	**2.94**	**0.83**	**1.43**	**0.34**	**0.49**
Bcan	2.29	1.76	1.13	0.85	**2.03**	**0.37**	**0.99**	**0.20**	**0.49**
Flot2	1.53	3.21	0.79	1.50	**2.37**	**1.19**	**1.15**	**0.50**	**0.48**
Fkbp11	12.75	9.59	5.39	5.40	**11.17**	**2.23**	**5.39**	**0.00**	**0.48**
Omp	1.53	1.28	0.39	0.95	**1.40**	**0.17**	**0.67**	**0.39**	**0.48**
Fn3k	9.63	11.50	5.75	4.25	**10.56**	**1.32**	**5.00**	**1.06**	**0.47**
Sbsn	2.07	2.16	0.66	1.34	**2.11**	**0.06**	**1.00**	**0.48**	**0.47**
Gpnmb	2.37	5.96	1.45	2.48	**4.17**	**2.53**	**1.97**	**0.73**	**0.47**
Galnt9	0.38	4.44	0.32	1.95	**2.41**	**2.87**	**1.14**	**1.15**	**0.47**
Mat1a	1.16	1.85	0.74	0.66	**1.50**	**0.48**	**0.70**	**0.06**	**0.47**
Npw	13.54	13.76	5.81	6.90	**13.65**	**0.16**	**6.35**	**0.77**	**0.47**
Spp2	3.76	0.94	1.25	0.91	**2.35**	**1.99**	**1.08**	**0.24**	**0.46**
Rem2	8.58	6.09	3.76	2.95	**7.34**	**1.76**	**3.35**	**0.57**	**0.46**
Necab3	2.74	2.79	1.29	1.23	**2.77**	**0.04**	**1.26**	**0.04**	**0.46**
Tmem179	16.88	14.65	8.39	5.89	**15.77**	**1.58**	**7.14**	**1.77**	**0.45**
Smad2	4.03	1.77	1.87	0.74	**2.90**	**1.60**	**1.31**	**0.80**	**0.45**
Map7	3.22	2.43	1.34	1.22	**2.83**	**0.56**	**1.28**	**0.09**	**0.45**
Sytl5	3.75	3.63	2.34	0.98	**3.69**	**0.09**	**1.66**	**0.96**	**0.45**
Tmem106a	2.43	1.68	0.97	0.87	**2.05**	**0.53**	**0.92**	**0.07**	**0.45**
Slc4a11	1.57	3.64	1.10	1.23	**2.60**	**1.47**	**1.16**	**0.10**	**0.45**
Nnmt	8.25	9.79	3.75	4.29	**9.02**	**1.09**	**4.02**	**0.38**	**0.45**
Lrtm2	2.94	1.28	0.87	0.99	**2.11**	**1.18**	**0.93**	**0.09**	**0.44**
Plekhd1	4.06	4.05	1.76	1.78	**4.06**	**0.01**	**1.77**	**0.02**	**0.44**
Gipr	2.94	4.21	1.39	1.72	**3.57**	**0.90**	**1.56**	**0.23**	**0.44**
Dll3	2.95	1.69	1.31	0.69	**2.32**	**0.89**	**1.00**	**0.44**	**0.43**
RGD1310110	1.34	1.00	0.44	0.56	**1.17**	**0.24**	**0.50**	**0.08**	**0.43**
Rassf5	1.55	1.43	0.63	0.65	**1.49**	**0.09**	**0.64**	**0.01**	**0.43**
Grin1	9.43	6.29	2.17	4.48	**7.86**	**2.22**	**3.32**	**1.63**	**0.42**
Ccdc116	1.36	2.08	0.47	0.98	**1.72**	**0.51**	**0.73**	**0.37**	**0.42**
Krt23	0.65	2.05	0.51	0.62	**1.35**	**0.98**	**0.57**	**0.07**	**0.42**

Sh3bgr	2.13	1.44	0.84	0.65	**1.79**	**0.49**	**0.75**	**0.13**	**0.42**
Grin1	13.77	15.10	7.45	4.61	**14.43**	**0.94**	**6.03**	**2.01**	**0.42**
Astn1	3.26	1.06	1.22	0.57	**2.16**	**1.55**	**0.90**	**0.46**	**0.42**
Syt3	8.61	7.52	3.31	3.29	**8.07**	**0.77**	**3.30**	**0.01**	**0.41**
Slc22a4	2.07	1.42	0.80	0.62	**1.75**	**0.46**	**0.71**	**0.13**	**0.41**
Bdkrb2	2.44	1.36	0.75	0.79	**1.90**	**0.77**	**0.77**	**0.03**	**0.41**
Cldn9	3.27	2.01	0.99	1.15	**2.64**	**0.89**	**1.07**	**0.11**	**0.41**
Ajuba	7.24	7.24	3.09	2.77	**7.24**	**0.00**	**2.93**	**0.23**	**0.40**
Dclk1	5.87	2.06	2.05	1.15	**3.96**	**2.69**	**1.60**	**0.64**	**0.40**
Slc43a1	10.00	7.75	3.45	3.42	**8.87**	**1.59**	**3.43**	**0.02**	**0.39**
Pde2a	3.50	1.81	0.81	1.22	**2.65**	**1.19**	**1.02**	**0.29**	**0.38**
Parp14	1.88	1.70	0.85	0.52	**1.79**	**0.12**	**0.69**	**0.23**	**0.38**
Hmx3	4.41	1.54	1.25	1.02	**2.97**	**2.03**	**1.14**	**0.16**	**0.38**
Cacng2	5.18	1.69	1.70	0.91	**3.43**	**2.47**	**1.31**	**0.56**	**0.38**
Mybpc3	0.13	3.75	0.19	1.27	**1.94**	**2.55**	**0.73**	**0.76**	**0.38**
Fbll1	9.94	7.09	3.62	2.79	**8.51**	**2.02**	**3.21**	**0.59**	**0.38**
Per2	8.08	8.27	3.53	2.42	**8.17**	**0.13**	**2.97**	**0.79**	**0.36**
Fam21c	8.90	8.96	2.18	4.31	**8.93**	**0.04**	**3.24**	**1.51**	**0.36**
Krt76	2.66	1.24	0.90	0.50	**1.95**	**1.00**	**0.70**	**0.28**	**0.36**
Scn9a	1.99	1.08	0.71	0.40	**1.53**	**0.64**	**0.55**	**0.22**	**0.36**
Batf3	0.84	2.99	0.69	0.66	**1.92**	**1.52**	**0.68**	**0.02**	**0.35**
Slc18a1	3.45	0.30	0.96	0.36	**1.88**	**2.22**	**0.66**	**0.43**	**0.35**
Fxyd5	18.21	18.68	6.52	6.11	**18.45**	**0.34**	**6.31**	**0.29**	**0.34**
Ccnb1ip1	25.49	28.39	8.94	9.35	**26.94**	**2.05**	**9.14**	**0.29**	**0.34**
Cyp27b1	1.81	2.01	0.61	0.61	**1.91**	**0.14**	**0.61**	**0.00**	**0.32**
Sigirr	3.01	3.23	0.96	1.01	**3.12**	**0.15**	**0.99**	**0.03**	**0.32**
Pde2a	2.47	1.08	0.80	0.32	**1.78**	**0.98**	**0.56**	**0.34**	**0.32**
Pcdha13	3.01	3.05	1.05	0.74	**3.03**	**0.03**	**0.89**	**0.22**	**0.30**
Tcam1	5.51	7.58	1.67	1.66	**6.55**	**1.47**	**1.66**	**0.01**	**0.25**
Ubqln2	3.35	3.09	0.80	0.81	**3.22**	**0.18**	**0.81**	**0.01**	**0.25**
Tbx4	3.12	1.28	0.56	0.48	**2.20**	**1.30**	**0.52**	**0.05**	**0.24**
Acsl4	7.38	5.71	1.21	1.81	**6.55**	**1.18**	**1.51**	**0.42**	**0.23**
Pdlim3	1.43	3.31	0.60	0.45	**2.37**	**1.33**	**0.53**	**0.11**	**0.22**
Ppic	10.23	10.74	1.90	2.38	**10.48**	**0.36**	**2.14**	**0.34**	**0.20**
Stk32a	6.65	5.06	0.78	1.30	**5.86**	**1.12**	**1.04**	**0.37**	**0.18**
Mei1	9.36	5.67	0.72	0.59	**7.52**	**2.61**	**0.66**	**0.10**	**0.09**

Annex 4.- Gene expression changes upon MAX re-expression in MNT-depleted UR61 cells.mRNA levels of the whole transcriptome were determined by RNA-seq. The table includes genes showing differential expression upon MAX expression in MNT depleted UR61 cells. The transcriptomes of UR61-MT-MAX sh-MNT and UR61-MT-Hebo sh-MNT, both treated with 100 M Zn^{2+} for 24 h, were compared. Data are mean of two independent experiments with RPKM values ≥ 0.5 and S.D. ≤ 3. The RPKMs of each experiment ("Exp.") are indicated. The fold-change thresholds between both conditions were set as ≥ 1.7 and < 0.6. The mean of the expression data and S.D. of the fold-changes are highlighted in green at the top of the table.

	RPKM				RPKM				Fold Change
	UR61Hebo sh-MNT		UR61MAX sh-MNT		UR61Hebo sh-MNT		UR61MAX sh-MNT		sh-MNT
GENE	Exp.1	Exp.2	Exp.1	Exp.2	mean	S.D.	media	S.D.	MAX vs Hebo
Col6a2	0.75	0.50	6.21	4.38	**0.62**	**0.18**	**5.29**	**1.29**	**8.47**
Arhgdib	0.19	0.83	2.11	3.66	**0.51**	**0.45**	**2.88**	**1.10**	**5.69**
Max	4.27	6.05	26.94	27.46	**5.16**	**1.26**	**27.20**	**0.37**	**5.27**
Patz1	0.01	3.22	7.47	8.05	**1.62**	**2.27**	**7.76**	**0.41**	**4.80**
Car9	1.41	0.93	5.59	2.69	**1.17**	**0.34**	**4.14**	**2.05**	**3.54**
Fam98c	1.87	0.00	2.53	3.92	**0.94**	**1.32**	**3.23**	**0.98**	**3.44**
S100a5	2.43	1.21	6.56	4.68	**1.82**	**0.86**	**5.62**	**1.33**	**3.09**
Wif1	2.00	1.43	5.29	4.84	**1.71**	**0.40**	**5.06**	**0.32**	**2.95**
Synpo	1.53	1.01	3.84	3.50	**1.27**	**0.37**	**3.67**	**0.24**	**2.89**
Car7	2.96	1.22	4.43	7.27	**2.09**	**1.23**	**5.85**	**2.01**	**2.80**
Esd	2.04	0.00	2.58	3.08	**1.02**	**1.44**	**2.83**	**0.36**	**2.78**
Fgfr1	3.19	3.41	9.69	8.47	**3.30**	**0.15**	**9.08**	**0.87**	**2.75**
Kifc3	1.00	2.60	4.74	5.16	**1.80**	**1.13**	**4.95**	**0.29**	**2.75**
Spsb1	0.47	0.53	1.17	1.55	**0.50**	**0.04**	**1.36**	**0.27**	**2.72**
Marcks	0.90	1.31	2.53	3.34	**1.11**	**0.29**	**2.93**	**0.57**	**2.65**
LOC689574	0.72	0.75	1.40	2.47	**0.74**	**0.02**	**1.94**	**0.76**	**2.64**
Cyp26b1	1.29	0.26	2.51	1.58	**0.78**	**0.72**	**2.04**	**0.66**	**2.63**
Rest	0.74	1.09	2.47	2.33	**0.91**	**0.25**	**2.40**	**0.09**	**2.63**
St6galnac3	0.86	1.14	2.54	2.57	**1.00**	**0.20**	**2.55**	**0.02**	**2.56**
RT1-Db1	0.89	1.20	2.48	2.78	**1.05**	**0.22**	**2.63**	**0.21**	**2.51**
Tmem80	0.81	0.34	1.82	1.05	**0.58**	**0.34**	**1.43**	**0.54**	**2.49**
Hoxb8	1.87	1.40	3.40	4.66	**1.64**	**0.33**	**4.03**	**0.90**	**2.46**
Samd14	2.23	1.16	5.46	2.83	**1.70**	**0.76**	**4.14**	**1.86**	**2.44**
Ces1d	1.52	0.27	2.20	2.12	**0.90**	**0.88**	**2.16**	**0.06**	**2.41**
Slc5a5	4.04	2.92	8.44	8.21	**3.48**	**0.79**	**8.32**	**0.16**	**2.39**
Krt80	0.71	0.66	2.67	0.60	**0.69**	**0.04**	**1.64**	**1.46**	**2.38**
Cmah	0.63	0.88	2.21	1.37	**0.75**	**0.18**	**1.79**	**0.60**	**2.37**
Gpr56	7.04	7.11	16.09	17.38	**7.08**	**0.05**	**16.74**	**0.91**	**2.36**
Snai2	2.26	3.88	6.30	7.77	**3.07**	**1.14**	**7.03**	**1.04**	**2.29**
Fzd1	1.33	1.30	2.88	2.98	**1.31**	**0.02**	**2.93**	**0.07**	**2.23**
Nlgn3	0.37	0.64	0.92	1.31	**0.50**	**0.19**	**1.11**	**0.27**	**2.21**
Flrt1	0.86	0.46	1.68	1.24	**0.66**	**0.28**	**1.46**	**0.31**	**2.21**
Vasn	3.39	2.22	7.42	4.83	**2.81**	**0.83**	**6.12**	**1.84**	**2.18**
Smad3	1.26	1.41	3.25	2.55	**1.33**	**0.11**	**2.90**	**0.50**	**2.17**
Gata4	1.47	2.17	2.50	5.38	**1.82**	**0.49**	**3.94**	**2.03**	**2.17**
Stap2	2.49	2.40	5.65	4.89	**2.44**	**0.06**	**5.27**	**0.54**	**2.15**
Sipa1l2	2.99	3.68	6.28	7.88	**3.33**	**0.49**	**7.08**	**1.13**	**2.12**
Pde10a	0.66	0.40	1.32	0.93	**0.53**	**0.19**	**1.12**	**0.28**	**2.11**
Rgs2	5.54	5.19	11.84	10.74	**5.37**	**0.24**	**11.29**	**0.78**	**2.10**
Sh3tc1	4.43	5.84	11.17	10.41	**5.14**	**0.99**	**10.79**	**0.54**	**2.10**
Pard6g	0.62	1.10	2.07	1.53	**0.86**	**0.34**	**1.80**	**0.38**	**2.09**
Mycn	1.63	0.60	2.73	1.94	**1.11**	**0.73**	**2.33**	**0.56**	**2.09**
Plec	1.17	0.25	1.83	1.12	**0.71**	**0.65**	**1.48**	**0.50**	**2.08**
Hist1h2ak	0.66	1.43	0.96	3.36	**1.04**	**0.54**	**2.16**	**1.70**	**2.07**

RGD1562018	1.56	1.36	3.27	2.77	**1.46**	**0.14**	**3.02**	**0.35**	**2.07**
Hcn4	6.82	3.23	10.00	10.77	**5.03**	**2.54**	**10.39**	**0.54**	**2.07**
Patz1	7.04	3.65	12.41	9.57	**5.35**	**2.40**	**10.99**	**2.01**	**2.06**
Popdc2	1.08	0.43	2.36	0.72	**0.76**	**0.46**	**1.54**	**1.16**	**2.03**
Casp6	0.64	0.52	1.11	1.25	**0.58**	**0.08**	**1.18**	**0.10**	**2.02**
Sema3f	8.28	6.26	15.81	13.45	**7.27**	**1.43**	**14.63**	**1.67**	**2.01**
Ier5l	5.32	1.27	5.89	7.29	**3.29**	**2.86**	**6.59**	**0.99**	**2.00**
Slc4a7	0.06	1.41	1.33	1.59	**0.73**	**0.96**	**1.46**	**0.19**	**1.99**
Podxl	1.02	0.61	1.51	1.70	**0.81**	**0.29**	**1.61**	**0.14**	**1.98**
Hint3	0.55	1.44	1.41	2.51	**0.99**	**0.63**	**1.96**	**0.78**	**1.97**
Cep63	1.00	0.37	0.78	1.91	**0.69**	**0.44**	**1.34**	**0.80**	**1.96**
Ext1	9.26	9.57	19.04	17.68	**9.41**	**0.22**	**18.36**	**0.96**	**1.95**
Sema6d	3.77	3.29	6.80	6.95	**3.53**	**0.34**	**6.87**	**0.10**	**1.95**
Mtus2	1.45	2.31	4.10	3.21	**1.88**	**0.61**	**3.65**	**0.63**	**1.94**
Ptpn13	2.49	3.62	5.47	6.36	**3.05**	**0.80**	**5.91**	**0.63**	**1.94**
Usp4	1.40	0.96	2.11	2.46	**1.18**	**0.31**	**2.28**	**0.25**	**1.93**
Fcgrt	7.68	7.84	16.80	13.21	**7.76**	**0.12**	**15.00**	**2.54**	**1.93**
Enpep	1.10	0.66	1.95	1.43	**0.88**	**0.31**	**1.69**	**0.37**	**1.93**
Smim1	5.83	3.80	9.53	8.97	**4.81**	**1.44**	**9.25**	**0.40**	**1.92**
Acacb	0.95	0.86	1.81	1.68	**0.91**	**0.06**	**1.75**	**0.09**	**1.92**
Kcnrg	0.90	0.56	1.05	1.75	**0.73**	**0.24**	**1.40**	**0.50**	**1.92**
Dmrtc1a	1.16	2.06	2.55	3.61	**1.61**	**0.63**	**3.08**	**0.75**	**1.91**
Pdlim4	3.92	3.71	7.90	6.65	**3.81**	**0.15**	**7.27**	**0.88**	**1.91**
Erg	1.03	0.90	2.19	1.47	**0.96**	**0.09**	**1.83**	**0.51**	**1.90**
Iffo2	1.45	1.34	2.83	2.46	**1.40**	**0.08**	**2.64**	**0.26**	**1.89**
Pard3b	0.71	0.55	1.45	0.94	**0.63**	**0.11**	**1.19**	**0.36**	**1.89**
Efna4	3.79	5.57	8.78	8.89	**4.68**	**1.26**	**8.83**	**0.08**	**1.89**
Sod3	0.78	0.41	1.59	0.65	**0.59**	**0.26**	**1.12**	**0.66**	**1.89**
Alk	1.21	0.74	2.33	1.34	**0.97**	**0.33**	**1.84**	**0.70**	**1.89**
Cd46	0.48	0.52	1.04	0.85	**0.50**	**0.03**	**0.95**	**0.13**	**1.88**
Lbh	2.19	1.92	4.17	3.54	**2.05**	**0.19**	**3.85**	**0.44**	**1.88**
Fgfrl1	1.01	1.33	2.15	2.24	**1.17**	**0.23**	**2.19**	**0.06**	**1.88**
Rhbdl3	2.24	1.94	4.23	3.61	**2.09**	**0.21**	**3.92**	**0.44**	**1.87**
Syt13	0.68	0.79	1.54	1.23	**0.74**	**0.08**	**1.39**	**0.22**	**1.87**
Hrh3	2.01	0.55	2.49	2.32	**1.28**	**1.03**	**2.40**	**0.12**	**1.87**
Cast	3.88	3.33	7.39	6.08	**3.60**	**0.38**	**6.74**	**0.92**	**1.87**
Prr24	3.53	1.42	5.23	4.01	**2.48**	**1.49**	**4.62**	**0.86**	**1.86**
Smtnl2	1.68	1.52	3.10	2.85	**1.60**	**0.11**	**2.97**	**0.17**	**1.86**
Zfp384	3.71	0.65	5.49	2.60	**2.18**	**2.17**	**4.05**	**2.04**	**1.86**
Cmtm3	2.73	2.40	4.90	4.59	**2.57**	**0.24**	**4.74**	**0.22**	**1.85**
Man1c1	8.38	6.81	12.33	15.72	**7.60**	**1.11**	**14.02**	**2.39**	**1.85**
Xrcc4	1.75	1.66	3.29	3.00	**1.71**	**0.07**	**3.14**	**0.21**	**1.84**
Vof16	1.18	1.20	2.20	2.18	**1.19**	**0.02**	**2.19**	**0.02**	**1.84**
Amer1	2.60	1.54	4.51	3.11	**2.07**	**0.75**	**3.81**	**0.99**	**1.84**
Fcgr2a	3.48	3.96	7.45	6.21	**3.72**	**0.34**	**6.83**	**0.88**	**1.83**
Cebpd	5.54	2.89	7.70	7.74	**4.21**	**1.87**	**7.72**	**0.02**	**1.83**
Nkd1	1.65	1.00	2.63	2.21	**1.33**	**0.46**	**2.42**	**0.30**	**1.83**
Morn2	0.01	2.82	2.20	2.95	**1.42**	**1.98**	**2.58**	**0.53**	**1.82**
Nhs	0.71	0.82	1.26	1.53	**0.77**	**0.07**	**1.39**	**0.19**	**1.82**
Aplf	0.85	1.08	1.74	1.78	**0.97**	**0.16**	**1.76**	**0.03**	**1.82**
Cast	13.60	12.67	25.21	22.43	**13.14**	**0.66**	**23.82**	**1.96**	**1.81**
Mbp	1.14	1.15	2.72	1.44	**1.15**	**0.01**	**2.08**	**0.91**	**1.81**
Gnpnat1	1.02	0.69	1.82	1.25	**0.86**	**0.23**	**1.54**	**0.40**	**1.80**
Cryz	6.16	6.40	11.60	10.85	**6.28**	**0.17**	**11.23**	**0.53**	**1.79**
Camta1	2.22	1.91	3.50	3.88	**2.06**	**0.22**	**3.69**	**0.27**	**1.79**
Gpld1	1.87	2.50	3.85	3.95	**2.18**	**0.45**	**3.90**	**0.07**	**1.79**
Elmod3	1.37	0.98	2.37	1.81	**1.17**	**0.27**	**2.09**	**0.40**	**1.79**
Nnat	5.00	1.80	7.72	4.36	**3.40**	**2.26**	**6.04**	**2.38**	**1.78**
St3gal1	2.09	3.19	3.06	6.31	**2.64**	**0.78**	**4.68**	**2.30**	**1.77**
Plec	1.28	0.54	2.25	0.98	**0.91**	**0.52**	**1.61**	**0.90**	**1.77**

Bdh2	1.25	4.68	4.54	5.96	**2.97**	**2.43**	**5.25**	**1.00**	**1.77**
Gpr61	0.65	0.36	1.21	0.57	**0.50**	**0.21**	**0.89**	**0.45**	**1.77**
Nfatc4	2.17	1.28	3.47	2.58	**1.72**	**0.63**	**3.02**	**0.63**	**1.76**
Pik3r1	7.01	6.44	12.13	11.45	**6.73**	**0.40**	**11.79**	**0.48**	**1.75**
Radil	6.20	6.24	11.53	10.21	**6.22**	**0.03**	**10.87**	**0.93**	**1.75**
Satb1	5.51	6.60	9.82	11.30	**6.05**	**0.77**	**10.56**	**1.05**	**1.74**
RGD1309821	2.32	2.74	4.40	4.42	**2.53**	**0.30**	**4.41**	**0.01**	**1.74**
Hrk	1.70	1.36	2.64	2.68	**1.53**	**0.23**	**2.66**	**0.03**	**1.74**
Pbx4	1.01	1.03	1.59	1.95	**1.02**	**0.01**	**1.77**	**0.26**	**1.74**
Notch2	1.40	0.95	2.42	1.65	**1.17**	**0.32**	**2.03**	**0.55**	**1.73**
Lingo1	2.12	1.94	3.97	3.06	**2.03**	**0.13**	**3.51**	**0.65**	**1.73**
Bcl2l11	5.68	1.85	6.21	6.74	**3.76**	**2.71**	**6.48**	**0.38**	**1.72**
Fhdc1	3.38	3.24	5.18	6.20	**3.31**	**0.09**	**5.69**	**0.72**	**1.72**
Dusp10	0.90	1.93	2.32	2.50	**1.41**	**0.73**	**2.41**	**0.13**	**1.70**
LOC100910802	1.07	0.58	1.42	1.40	**0.83**	**0.35**	**1.41**	**0.02**	**1.70**
Sh3bp5	10.85	9.51	18.69	15.95	**10.18**	**0.95**	**17.32**	**1.94**	**1.70**
Crebzf	3.30	1.63	1.89	1.07	**2.47**	**1.18**	**1.48**	**0.58**	**0.60**
Cdcp1	9.08	7.54	5.25	4.68	**8.31**	**1.09**	**4.97**	**0.41**	**0.60**
Maob	1.16	2.13	0.84	1.12	**1.64**	**0.68**	**0.98**	**0.20**	**0.60**
Svop	8.43	6.41	5.38	3.46	**7.42**	**1.43**	**4.42**	**1.35**	**0.60**
Hmgn3	3.27	6.96	2.63	3.46	**5.12**	**2.61**	**3.04**	**0.58**	**0.59**
Rad9b	0.92	0.92	0.59	0.50	**0.92**	**0.01**	**0.55**	**0.06**	**0.59**
Rbpjl	1.91	3.06	1.36	1.58	**2.48**	**0.81**	**1.47**	**0.15**	**0.59**
Gpr1	2.37	1.68	1.75	0.64	**2.03**	**0.49**	**1.20**	**0.78**	**0.59**
Bcmo1	2.33	4.40	1.82	2.13	**3.36**	**1.46**	**1.97**	**0.22**	**0.59**
Tubb2b	14.60	16.84	7.88	10.54	**15.72**	**1.59**	**9.21**	**1.88**	**0.59**
Mreg	15.03	16.43	8.55	9.86	**15.73**	**0.99**	**9.21**	**0.92**	**0.59**
Camk4	1.93	1.28	1.34	0.53	**1.60**	**0.46**	**0.93**	**0.58**	**0.58**
Magix	1.07	1.11	0.74	0.53	**1.09**	**0.03**	**0.64**	**0.14**	**0.58**
RT1-N2	0.78	2.65	1.26	0.73	**1.72**	**1.33**	**1.00**	**0.37**	**0.58**
Med23	11.84	11.64	6.69	6.93	**11.74**	**0.14**	**6.81**	**0.17**	**0.58**
Gipr	5.81	7.50	3.63	4.07	**6.66**	**1.19**	**3.85**	**0.31**	**0.58**
Spink8	2.86	0.91	1.68	0.46	**1.88**	**1.38**	**1.07**	**0.87**	**0.57**
Hpdl	5.54	6.90	2.93	4.13	**6.22**	**0.96**	**3.53**	**0.84**	**0.57**
Trim2	2.70	1.66	1.51	0.96	**2.18**	**0.74**	**1.23**	**0.39**	**0.57**
Dmtn	6.80	5.17	3.76	2.96	**5.99**	**1.15**	**3.36**	**0.57**	**0.56**
Crip1	3.46	7.70	2.80	3.44	**5.58**	**2.99**	**3.12**	**0.46**	**0.56**
Rcl1	22.18	23.85	12.77	12.91	**23.01**	**1.18**	**12.84**	**0.10**	**0.56**
Clip4	2.54	2.85	1.49	1.51	**2.69**	**0.21**	**1.50**	**0.01**	**0.56**
Dmd	7.24	6.04	4.85	2.55	**6.64**	**0.85**	**3.70**	**1.63**	**0.56**
Ptgr2	18.24	14.02	10.44	7.45	**16.13**	**2.99**	**8.94**	**2.11**	**0.55**
Ddr1	31.52	31.40	16.08	18.67	**31.46**	**0.08**	**17.38**	**1.84**	**0.55**
Kank2	18.61	14.69	9.02	9.37	**16.65**	**2.77**	**9.19**	**0.25**	**0.55**
Hs3st3b1	6.12	2.64	3.23	1.60	**4.38**	**2.47**	**2.42**	**1.15**	**0.55**
Mst4	2.61	1.57	1.21	1.09	**2.09**	**0.73**	**1.15**	**0.09**	**0.55**
Cenpl	3.38	2.07	0.80	2.19	**2.73**	**0.93**	**1.50**	**0.99**	**0.55**
Thoc7	4.30	3.66	2.02	2.32	**3.98**	**0.45**	**2.17**	**0.22**	**0.55**
Necab3	3.18	3.06	1.67	1.73	**3.12**	**0.08**	**1.70**	**0.05**	**0.54**
LOC102723236	8.09	12.27	4.66	6.43	**10.18**	**2.95**	**5.54**	**1.25**	**0.54**
Fn3k	16.92	15.02	9.38	7.99	**15.97**	**1.34**	**8.69**	**0.98**	**0.54**
Plekhd1	3.09	3.20	1.61	1.80	**3.14**	**0.08**	**1.71**	**0.14**	**0.54**
Tnfaip8l2	0.97	1.87	0.65	0.89	**1.42**	**0.63**	**0.77**	**0.17**	**0.54**
Cspg5	3.11	1.92	1.62	1.10	**2.51**	**0.84**	**1.36**	**0.36**	**0.54**
Dchs1	5.63	4.27	3.41	1.94	**4.95**	**0.96**	**2.67**	**1.03**	**0.54**
Jakmip1	5.62	4.78	3.03	2.58	**5.20**	**0.60**	**2.81**	**0.32**	**0.54**
Gstm6	3.35	2.65	1.81	1.42	**3.00**	**0.49**	**1.62**	**0.27**	**0.54**
Napb	2.03	1.79	0.80	1.25	**1.91**	**0.17**	**1.02**	**0.32**	**0.54**
LOC307727	2.09	1.08	0.85	0.84	**1.58**	**0.72**	**0.85**	**0.01**	**0.53**
Trpm4	5.43	4.39	2.89	2.34	**4.91**	**0.74**	**2.61**	**0.39**	**0.53**
RGD1305645	5.52	4.33	3.49	1.75	**4.93**	**0.85**	**2.62**	**1.24**	**0.53**

Mok	2.55	3.84	1.62	1.78	**3.20**	**0.91**	**1.70**	**0.11**	**0.53**
Actn2	1.35	2.08	0.90	0.93	**1.72**	**0.52**	**0.91**	**0.02**	**0.53**
Mtl5	3.25	3.31	1.82	1.66	**3.28**	**0.05**	**1.74**	**0.11**	**0.53**
Gk	2.69	3.14	1.58	1.51	**2.91**	**0.32**	**1.54**	**0.05**	**0.53**
Pacrg	5.25	1.93	2.85	0.95	**3.59**	**2.34**	**1.90**	**1.35**	**0.53**
Pde2a	1.61	1.14	0.69	0.74	**1.37**	**0.34**	**0.71**	**0.04**	**0.52**
RGD1565498	2.62	4.42	2.03	1.61	**3.52**	**1.28**	**1.82**	**0.29**	**0.52**
Hmx3	3.82	1.30	1.69	0.93	**2.56**	**1.78**	**1.31**	**0.53**	**0.51**
Bcan	3.40	1.91	1.81	0.90	**2.65**	**1.05**	**1.35**	**0.64**	**0.51**
Npas1	2.13	1.83	1.12	0.87	**1.98**	**0.21**	**1.00**	**0.18**	**0.50**
Hs3st3a1	2.38	1.45	1.13	0.80	**1.92**	**0.66**	**0.96**	**0.23**	**0.50**
Nlrp10	0.40	2.46	0.42	1.02	**1.43**	**1.45**	**0.72**	**0.42**	**0.50**
Smndc1	1.35	2.11	0.36	1.38	**1.73**	**0.54**	**0.87**	**0.72**	**0.50**
Mfsd2a	2.53	2.93	1.24	1.50	**2.73**	**0.28**	**1.37**	**0.18**	**0.50**
Rsad2	2.14	0.70	1.00	0.43	**1.42**	**1.02**	**0.71**	**0.40**	**0.50**
Tomt	1.45	1.17	0.63	0.68	**1.31**	**0.20**	**0.65**	**0.04**	**0.50**
Rnh1	5.66	6.61	3.59	2.50	**6.14**	**0.67**	**3.05**	**0.77**	**0.50**
Prss53	4.04	2.41	1.55	1.62	**3.22**	**1.15**	**1.59**	**0.05**	**0.49**
Sbsn	3.40	1.91	1.37	1.25	**2.66**	**1.05**	**1.31**	**0.08**	**0.49**
Sp110	16.83	19.51	9.31	8.48	**18.17**	**1.89**	**8.90**	**0.59**	**0.49**
Atp2a2	5.70	5.63	4.03	1.45	**5.66**	**0.05**	**2.74**	**1.82**	**0.48**
LOC100359977	1.60	1.77	0.85	0.78	**1.68**	**0.12**	**0.81**	**0.05**	**0.48**
Npw	12.00	12.57	5.93	5.86	**12.28**	**0.40**	**5.90**	**0.06**	**0.48**
Zfp951	0.92	1.39	0.49	0.62	**1.16**	**0.34**	**0.55**	**0.09**	**0.48**
Phlda2	1.42	2.62	0.66	1.26	**2.02**	**0.85**	**0.96**	**0.42**	**0.48**
Ccdc116	1.01	1.61	0.48	0.76	**1.31**	**0.43**	**0.62**	**0.20**	**0.47**
Bles03	4.00	2.78	1.51	1.70	**3.39**	**0.86**	**1.61**	**0.14**	**0.47**
Smim17	0.87	1.86	0.78	0.51	**1.36**	**0.70**	**0.64**	**0.19**	**0.47**
Bicd1	7.04	6.10	3.46	2.75	**6.57**	**0.67**	**3.10**	**0.50**	**0.47**
Ppp1r3c	2.13	1.05	0.99	0.50	**1.59**	**0.77**	**0.75**	**0.35**	**0.47**
Ppp1r3c	2.13	1.05	0.99	0.50	**1.59**	**0.77**	**0.75**	**0.35**	**0.47**
Acot7	5.23	2.73	2.70	1.05	**3.98**	**1.77**	**1.87**	**1.17**	**0.47**
Lat2	1.69	1.10	0.83	0.47	**1.39**	**0.42**	**0.65**	**0.26**	**0.47**
Scn9a	1.78	1.18	0.93	0.46	**1.48**	**0.42**	**0.69**	**0.33**	**0.47**
Atp6v1c2	1.25	2.07	0.93	0.62	**1.66**	**0.58**	**0.78**	**0.21**	**0.47**
P2ry2	9.68	8.65	3.93	4.58	**9.17**	**0.73**	**4.26**	**0.46**	**0.46**
Egfl8	4.97	2.78	2.81	0.77	**3.88**	**1.55**	**1.79**	**1.44**	**0.46**
Cdkn1c	3.65	4.34	2.09	1.59	**4.00**	**0.48**	**1.84**	**0.36**	**0.46**
Tmem179	16.34	13.51	7.97	5.76	**14.93**	**2.00**	**6.86**	**1.57**	**0.46**
Slc43a1	7.91	8.00	3.69	3.58	**7.95**	**0.06**	**3.63**	**0.08**	**0.46**
Syt3	9.85	7.46	4.35	3.52	**8.65**	**1.69**	**3.93**	**0.59**	**0.45**
Slc4a11	2.22	4.38	1.39	1.60	**3.30**	**1.53**	**1.50**	**0.15**	**0.45**
Pelo	9.96	6.74	4.24	3.30	**8.35**	**2.27**	**3.77**	**0.67**	**0.45**
Angptl4	1.36	2.39	0.74	0.95	**1.87**	**0.73**	**0.85**	**0.15**	**0.45**
Dctd	0.97	1.41	0.37	0.68	**1.19**	**0.31**	**0.53**	**0.22**	**0.44**
Pde2a	4.83	2.60	2.07	1.20	**3.72**	**1.58**	**1.64**	**0.62**	**0.44**
Sh3bgr	2.02	1.15	0.64	0.74	**1.59**	**0.62**	**0.69**	**0.07**	**0.44**
Fam83f	0.99	1.35	0.44	0.57	**1.17**	**0.25**	**0.51**	**0.09**	**0.43**
Ajuba	5.74	5.94	2.87	2.18	**5.84**	**0.14**	**2.53**	**0.49**	**0.43**
Rassf5	1.30	1.40	0.61	0.55	**1.35**	**0.07**	**0.58**	**0.04**	**0.43**
Fbll1	9.73	6.53	4.07	2.95	**8.13**	**2.26**	**3.51**	**0.79**	**0.43**
Cxcl9	2.35	2.83	1.13	1.10	**2.59**	**0.34**	**1.11**	**0.02**	**0.43**
Ttc22	4.80	3.34	2.10	1.36	**4.07**	**1.03**	**1.73**	**0.52**	**0.43**
Nnmt	5.32	7.32	1.76	3.61	**6.32**	**1.42**	**2.68**	**1.31**	**0.42**
Bcan	1.71	1.36	0.68	0.61	**1.53**	**0.25**	**0.64**	**0.05**	**0.42**
Dll3	2.89	1.15	1.06	0.63	**2.02**	**1.23**	**0.84**	**0.31**	**0.42**
Astn1	2.65	0.86	0.98	0.48	**1.76**	**1.27**	**0.73**	**0.35**	**0.41**
Fam21c	7.17	8.18	2.44	3.91	**7.67**	**0.71**	**3.17**	**1.04**	**0.41**
Cyp27b1	1.88	2.37	0.76	0.99	**2.13**	**0.35**	**0.88**	**0.17**	**0.41**
Slc22a4	1.79	1.22	0.61	0.62	**1.51**	**0.41**	**0.62**	**0.00**	**0.41**

Il18	4.38	1.38	1.20	1.14	**2.88**	**2.12**	**1.17**	**0.04**	**0.41**
Shank2	2.05	0.65	0.67	0.39	**1.35**	**0.99**	**0.53**	**0.20**	**0.39**
Krt23	2.12	4.54	1.49	1.13	**3.33**	**1.72**	**1.31**	**0.25**	**0.39**
Pcdha13	3.72	4.00	1.85	1.10	**3.86**	**0.20**	**1.47**	**0.53**	**0.38**
Thumpd3	1.16	1.61	0.00	1.05	**1.39**	**0.32**	**0.53**	**0.74**	**0.38**
Sigirr	3.88	3.69	1.63	1.23	**3.78**	**0.13**	**1.43**	**0.29**	**0.38**
Sftpd	1.93	4.83	1.15	1.34	**3.38**	**2.05**	**1.25**	**0.14**	**0.37**
Tnnt2	2.16	3.86	0.68	1.54	**3.01**	**1.20**	**1.11**	**0.60**	**0.37**
Mat1a	1.35	1.61	0.60	0.47	**1.48**	**0.19**	**0.54**	**0.09**	**0.36**
Mapkapk3	13.13	15.90	5.25	4.91	**14.51**	**1.96**	**5.08**	**0.25**	**0.35**
Tmem59l	1.98	1.19	0.70	0.38	**1.59**	**0.55**	**0.54**	**0.23**	**0.34**
Sytl5	4.36	4.43	1.95	0.93	**4.39**	**0.05**	**1.44**	**0.72**	**0.33**
Ccnb1ip1	29.65	32.67	11.04	9.23	**31.16**	**2.14**	**10.14**	**1.28**	**0.33**
Mybpc3	0.13	2.98	0.08	0.92	**1.55**	**2.02**	**0.50**	**0.60**	**0.32**
Grin1	9.74	10.46	2.42	4.05	**10.10**	**0.51**	**3.24**	**1.15**	**0.32**
Acsl4	6.15	5.70	1.61	2.17	**5.93**	**0.32**	**1.89**	**0.39**	**0.32**
Fxyd5	20.61	17.14	6.60	5.41	**18.87**	**2.45**	**6.01**	**0.85**	**0.32**
39326	4.72	3.36	2.44	0.00	**4.04**	**0.96**	**1.22**	**1.72**	**0.30**
Ndrg1	2.79	5.96	1.27	1.35	**4.37**	**2.24**	**1.31**	**0.05**	**0.30**
Patz1	3.87	6.10	0.24	2.71	**4.99**	**1.57**	**1.48**	**1.75**	**0.30**
Akr1b8	5.88	9.45	2.33	2.12	**7.66**	**2.53**	**2.23**	**0.15**	**0.29**
Pdp1	6.18	3.66	0.50	2.34	**4.92**	**1.78**	**1.42**	**1.31**	**0.29**
Patz1	6.96	3.46	0.99	2.02	**5.21**	**2.48**	**1.50**	**0.73**	**0.29**
Stk32a	6.87	7.30	1.11	2.57	**7.09**	**0.31**	**1.84**	**1.03**	**0.26**
Krt76	3.10	0.89	0.84	0.17	**1.99**	**1.56**	**0.50**	**0.47**	**0.25**
Hopx	5.53	1.63	1.34	0.41	**3.58**	**2.75**	**0.87**	**0.66**	**0.24**
Pcp4	3.14	1.25	0.57	0.44	**2.20**	**1.34**	**0.51**	**0.09**	**0.23**
Gpr22	3.31	1.86	0.80	0.37	**2.59**	**1.02**	**0.58**	**0.31**	**0.23**
Ppic	9.54	10.83	1.88	2.36	**10.19**	**0.91**	**2.12**	**0.34**	**0.21**
Tcam1	4.47414	6.36472	1.00553	1.23229	**5.42**	**1.34**	**1.12**	**0.16**	**0.21**
Mei1	6.36245	3.50605	0.463467	0.541864	**4.93**	**2.02**	**0.50**	**0.06**	**0.10**

Annex 5.- Validated genes by RT-qPCR. A summary of the genes selected from the RNA-seq data that were validated by RT-qPCR. The general functions, peaks found in ENCODE data project for MYC, MAX and MXI1, the presence of canonical and non-canonical E-boxes in the adjacent regions from TSS and the position where they are located are indicated. Upregulated genes are in red letters and downregulated genes in green.

GENE	FUNCTION	peaks ChIP-seq ENCODE project	E-boxes - 1000 bp TSS		E-boxes + 1000 bp TSS	
		MYC/MAX/MXI1	sequence	position	sequence	position
ENG	pro-angiogenic	YES	**CACGTG**	- 934 bp	**CACGTG**	+ 406 bp
NDRG4	required for cell cycle progression	NO	**CACGCG** **CACGCG**	- 93 bp - 9 bp	**CACGCG**	+ 53 bp
RET	kinase receptor, signaling inducer	NO	**CACGCG**	- 167 bp	None	
TXNRD3	ROS sensor	YES (first exon)	**CATGTG** **CACATG** **CATGCG**	- 997 bp - 853 bp - 43 bp	**CACGCG**	+ 422 bp
CDKN1C	G1 cyclin / ckd inhibitor	YES (first and second exon)	**CACATG**	- 772 bp	**CACGAG**	+ 390 bp
CDC6	DNA replication & chekpoint controls	YES	None		None	
POLE2	DNA repair and chromosome replication	YES (first exon)	**CACATG**	- 344 bp	**CACGCG** **CACGAG** **CATGCG** **CACATG**	+ 93 bp + 444 bp + 725 bp + 772 bp
ORC1	DNA replication initiation	YES	**CATGCG**	- 62 bp	**CACATG**	+ 908 bp
BRCA2	DNA repair	YES	**CACGTG**	- 20 bp	**CACGCG**	+ 666 bp
TRIP13	DNA repair	YES	**CACGTG**	- 422 bp	**CACGTG**	+ 208 bp
NEIL3	DNA repair	YES (first exon)	**CACGCG** **CATGCG**	- 131 bp - 64 bp	**CACATG**	+ 565 bp
EXO1	DNA repair	YES (promoter and first exon)	None		**CACATG** **CATGCG**	+ 107 bp + 109 bp
FANCD2	DNA repair	YES	None		**CACGTG**	+ 328 bp
E2F7	cell cycle	YES	**CATGTG**	- 545 bp	None	
PARPBP	DNA repair	YES	**CATGTG** **CACATG**	- 872 bp - 685 bp	**CACGTG**	+ 961 bp
CHEK1	DNA repair	YES (first exon)	**CACGTG**	- 594 bp	**CACGAG**	+ 347 bp

Publications

OPEN ACCESS Freely available online

PLoS one

p21 as a Transcriptional Co-Repressor of S-Phase and Mitotic Control Genes

Nuria Ferrándiz[1¤], Juan M. Caraballo[1], Lucía García-Gutierrez[1], Vikram Devgan[2], Manuel Rodriguez-Paredes[3], M. Carmen Lafita[1], Gabriel Bretones[1], Andrea Quintanilla[1], M. Jose Muñoz-Alonso[1,4], Rosa Blanco[1], Jose C. Reyes[3], Neus Agell[5], M. Dolores Delgado[1], G. Paolo Dotto[2,6], Javier León[1]*

1 Departamento de Biología Molecular, Instituto de Biomedicina y Biotecnología de Cantabria (IBBTEC), Universidad de Cantabria–CSIC–SODERCAN, Santander, Spain, **2** Cutaneous Biology Research Center, Massachusetts General Hospital, Charlestown, Massachussetts, United States of America, **3** Centro Andaluz de Biología Molecular y Medicina Regenerativa (CABIMER), CSIC, Américo Vespucio s/n, Sevilla, Spain, **4** Instituto de Investigaciones Biomédicas Alberto Sols, CSIC, Madrid, Spain, **5** Departament de Biologia Cellular, Immunologia i Neurociències, Institut d'Investigacions Biomediques August Pi i Sunyer (IDIBAPS), Universitat de Barcelona, Barcelona, Spain, **6** Department of Biochemistry, University of Lausanne, Epalinges, Switzerland

Abstract

It has been previously described that p21 functions not only as a CDK inhibitor but also as a transcriptional co-repressor in some systems. To investigate the roles of p21 in transcriptional control, we studied the gene expression changes in two human cell systems. Using a human leukemia cell line (K562) with inducible p21 expression and human primary keratinocytes with adenoviral-mediated p21 expression, we carried out microarray-based gene expression profiling. We found that p21 rapidly and strongly repressed the mRNA levels of a number of genes involved in cell cycle and mitosis. One of the most strongly down-regulated genes was *CCNE2* (cyclin E2 gene). Mutational analysis in K562 cells showed that the N-terminal region of p21 is required for repression of gene expression of *CCNE2* and other genes. Chromatin immunoprecipitation assays indicated that p21 was bound to human *CCNE2* and other p21-repressed genes gene in the vicinity of the transcription start site. Moreover, p21 repressed human CCNE2 promoter-luciferase constructs in K562 cells. Bioinformatic analysis revealed that the CDE motif is present in most of the promoters of the p21-regulated genes. Altogether, the results suggest that p21 exerts a repressive effect on a relevant number of genes controlling S phase and mitosis. Thus, p21 activity as inhibitor of cell cycle progression would be mediated not only by the inhibition of CDKs but also by the transcriptional down-regulation of key genes.

Citation: Ferrándiz N, Caraballo JM, García-Gutierrez L, Devgan V, Rodriguez-Paredes M, et al. (2012) p21 as a Transcriptional Co-Repressor of S-Phase and Mitotic Control Genes. PLoS ONE 7(5): e37759. doi:10.1371/journal.pone.0037759

Editor: Anja-Katrin Bielinsky, University of Minnesota, United States of America

Received November 8, 2011; **Accepted** April 23, 2012; **Published** May 25, 2012

Funding: This study was supported by grants SAF08-01581 and ISCIII-RETIC RD06/0020/0017 from the Spanish Ministerio de Ciencia e Innovacion (MICINN) to JL; FIS 08/0829 to MDD; BFU2008-00238 and CSD2006-00049 from MICINN, and P06-CVI-4844 from Junta de Andalucía to JCR. NF was the recipient of a postdoctoral fellowship of the University of Cantabria. The funders had no role in study design, data collection and analysis, decision to publish, or preparation of manuscript.

Competing Interests: The authors have declared that no competing interests exist.

* E-mail: leonj@unican.es

¤ Current address: MRC Clinical Sciences Centre, Imperial College Faculty of Medicine, Hammersmith Hospital Campus, London, United Kingdom

Introduction

$p21^{CIP1}$ (p21 herein after) is a member of the Cip/Kip family of inhibitors of cell cycle progression (also including $p27^{KIP1}$ and $p57^{KIP2}$). The first discovered p21 function and so far its best studied biochemical activity was the inhibition of cyclin-dependent kinases [1,2,3,4]. CDKs are protein complexes, composed of a regulatory cyclin and a catalytic CDK subunit, which orchestrate cell cycle transitions. Enforced p21 expression results in cell cycle arrest, which frequently takes place at the G2/M transition and accompanied by polyploidy [5,6,7,8]. p21 is also a p53 target gene that plays a relevant role in p53-induced cell cycle arrest [9,10,11].

However, other studies have shown that p21 has activities in addition to cell cycle arrest. Thus, p21 acts as an inhibitor of apoptosis induced by DNA-damaging agents [12,13,14] and as inducer of senescence [15,16,17] or differentiation (reviewed in [18]). Finally, p21 has been implicated in the control of transcription, through mechanisms that may be coupled to its CDK inhibition activity but also by direct association and modulation of transcription factors. In this way, it has been demonstrated the interaction between p21 and several transcription factors such as CBP, C/EBPα, E2Fs, Myc, Nrf2, STAT3, and others (reviewed in [19,20,21]). p21 has been found to repress several genes through the interaction with the E2F transcription factor [22] or by other mechanisms [15,23,24]. It has also been described as co-activator of the expression of other genes [25,26,27,28]. Nonetheless, there is little information on the biological significance of p21-dependent regulation of gene expression and to what extent it is linked to effects on the cell cycle. It has been shown that CDK2 is not an essential target for p21 in cell cycle inhibition and tumor suppression [29], given further relevance to the gene regulation effects of p21.

To address the relevance of p21-mediated gene regulation we have carried out large-scale expression profiling in two different human systems (keratinocytes and myeloid leukemia cells) upon ectopic expression of p21. p21 provokes a rapid and potent down-regulation of genes involved in the execution and control of mitosis in both models. Mutational analysis revealed that the N-terminal

region of p21 is required for its transcriptional effects in leukemia cell. *CCNE2* (cyclin E2) is one of the most potently down-regulated genes and p21 was found to bind and repress the human CCNE2 promoter.

Methods

Cell culture, transfection, viral infection

Primary human keratinocytes wereprepared from discarded human tissue, mostly from reduction abdominoplasties, with Institutional Review Board approval (MGH#2000-P-002418/3) and were grown as described [30]. K562 are human chronic myeloid leukemia cells, and were purchased from ATCC. Kp21-4 cells are K562 carrying a Zn^{2+} -inducible p21 gene; Kp27-5 cells are K562 carrying a Zn^{2+} -inducible p27 gene [31]. K562 and derivatives were grown in RPMI with 8% fetal calf serum. Adenovirus infections of keratinocytes were performed for 1 h in serum and epidermal growth factor-free-low calcium medium as previously described [32]. Keratinocytes were then incubated in fully supplemented medium for 24 h prior to collection for RNA analysis. Adenoviruses expressing full-length, N-terminal, C-terminal p21, p16, and p27 have been previously reported [32]. For transient transfections of K562, ten millions of cells were transfected with 12 μg of p21-WT-GFP, p21-CT-GFP and p21-NT-GFP expression vectors, as well as the GFP empty vector [33] using Lipofectamine 2000 (Invitrogene). 12 h after transfection, GFP-expressing cells were harvested by flow cytometry (FACSAria cell sorter, BD Biosciences). For transient transfections of Kp21-4, one million cells were electroporated with 2 μg pLKO-shCDK2 (Open Biosystems) or pLKO.1 using an Amaxa nucleofector (kit V). 24 h after transfection $ZnSO_4$ was added (75 μM), the cells were further incubated for 12 h and harvested.

Flow cytometry

One million cells per sample were fixed with 80% ethanol and stained with propidium iodide as described previously [31]. Cells were analysed by flow cytometry on a FACScant (BD Biosciences). Ten thousand events were gated and analysed using CellQuest software (BD Biosciences).

siRNA transfection

Human primary keratinocytes were transfected with 200 nM siRNAs for *CDKN1A* gene (p21) (Stealth RNAi, Invitrogen) and control siRNAs (Stealth RNAi negative control, Invitrogen) using Lipofectamine 2000 following the manufacturer's recommendations. 48 h after transfections, cells were analyzed by RT-qPCR (reverse transcriptional-quantitative polymerase chain reaction)

mRNA determination

Total RNA was isolated using TriReagent (Molecular Research Center) kit (Qiagen). Reverse transcription (RT) was performed with iScript reverse transcriptase (BioRad). Quantitative PCR (qPCR) was performed with the SYBRGreen PCR kit (BioRad) in a BioRad MyiQ apparatus. Primers sequences and amplicon sizes used in the RT-qPCR assays are shown in Table S1. Data were normalized to ribosomal protein S14 (RPS14) mRNA levels.

Gene expression profiling

Total RNA was prepared using RNeasy kit (Qiagen). Biotinilated cRNA was obtained from total RNA and hybridized to Affymetrix HG-U133A chip in the Genomic Facility of Centro de Investigación del Cancer (Salamanca, Spain). Data analysis and hierarchical tree clusters were generated using the dChip software [34], http://biosun1.harvard.edu/complab/dchip/]. The expression data was filtered so as to include genes with expression changes ≥2.4-fold. The data were obtained in compliance with the MIAME guidelines and are deposited in the ArrayExpress database. The accession numbers are E-MEXP-3431 for the expression data with Kp21-4 and Kp27-5 cells and E-MEXP-3430 for expression data of human keratinocytes. The analysis was performed with data from two independent experiments and RNA preparations of each experimental condition or adenoviral infection. The interaction network for differentially expressed genes was generated with the Ingenuity Pathways Analysis software.

Immunoblotting and cell extract fractionation

Total cell lysates and immunoblots were carried out as described [31]. Blots were developed with secondary antibodies conjugated to IRDye680 or IRDye800 (Li-Cor Biosciences) and visualized in an Odyssey scanner. Antibodies used were anti-p21 (C-19), anti-UBF (F5), anti-CDK2 (M2) and anti-α-tubulin (H-300). All were polyclonal antibodies from Santa Cruz Biotech. The isolation of chromatin fraction was performed essentially as described [35]. Briefly, the cells were lysed for 20 min with agitation at 4°C in CSK buffer (10 mM HEPES pH 7.5, 100 mM NaCl, 300 mM sucrose, 3 mM $MgCl_2$, 0.5% Tritón X-100 and protease inhibitors). After centrifugation the supernatant was collected as cytoplasmic plus nucleoplasmic fraction. The pellet was washed at maximum setting with CSK buffer, resuspended in CSK buffer, sonicated and saved as chromatin fraction.

Chromatin Immunoprecipitation (ChIP) assays

ChIP analysis was carried out as described previously [36]. Briefly, 10 millions of K562, Kp21-4 and Kp27-5 cells were fixed with formaldehyde and lysed in SDS lysis buffer. Cross-linked chromatin was fragmented by sonication to an average size of 400 bp. Chromatin was then immunoprecipitated with anti-p21 (C-19, Santa Cruz Biotechnology), anti-p27 (C-19, Santa Cruz Biotechnology), anti-CDK2 (M2, Santa Cruz Biotechnology), anti-histone H3 (FL-136, Santa Cruz Biotecnology) and anti-acetylated-histone H3 (06-559, Millipore). Antibodies and cell lysates were incubated overnight at 4°C, and then with protein G-coupled magnetic beads (Dynabeads, Invitrogen) for 1 h at 4°C. Controls were performed by incubating parallel samples with non-immune IgG. The protein-DNA cross-links were reversed by 4 h incubation at 65°C, and immunoprecipitated DNA was analyzed by quantitative PCR using a BioRad MyiQ apparatus. The signals were normalized to the inputs and the signals obtained with normal rabbit IgG (Santa Cruz Biotechnology) The primers used for PCR reactions are indicated Table S1.

Luciferase reporter assays

Two million of cells were electroporated with 15 μg of pCyCE1-Luc [37,38] carrying a fragment of the human CCNE1 and CCNE2 promoters, respectively, upstream of the firefly luciferase. These luciferase reporters were co-transfected with pCEFL or pCEFL-p21 [39]. Cells were electroporated with the reporters and expression vectors (15 μg) at 260 v and 975 μFa in a BTX electroporator. 24 h alter transfection the cells were treated with 75 μM $ZnSO_4$ for another 24 h. Luciferase activity was then determined with Lysis Solution 1 (Promega), Luciferase Substrate (Promega) and a GloMax 20/20 luminometer (Promega), following the manufacturer's instructions. All transfections were normalized by measuring β-galactosidase activity of the samples. Data are the average of at least three independent experiments and error bars indicate standard deviation.

Results

p21 represses mitotic genes in human leukemia cells

In order to find genes regulated by p21 in human primary cells we carried out a gene expression profiling in human myeloid leukemia K562 cells with conditional expression of p21. We previously described a K562 derivative, termed Kp21-4, that carries a zinc-inducible p21 gene [31]. We performed a kinetic study to identify the expression peak of p21 in this system. The immunoblot results showed that treatment of Kp21-4 cells with 75 μM $ZnSO_4$ resulted in induction of p21 that peaked 4–12 h decreasing afterwards (Figure 1A). This transient induction of p21 was accompanied by proliferation arrest and an increase in polyploid cells after 48–72 h [31]. The cell cycle profile did not change over the first 12 h of p21 induction with $ZnSO_4$ but 6–12 h of p21 induction were sufficient to irreversibly trigger proliferation arrest and polyploidy (Figure S1). Therefore, we chose 12 h as the induction time to analyse p21 effects on the transcriptome of these cells, as gene expression changes later on may be indirect due to other phenotypic effects.

We next carried out the gene expression profiling of Kp21-4 cells upon p21 induction by $ZnSO_4$. In order to identify genes specifically modulated by p21 we compared with the cell line Kp27-5, which carries a Zn^{2+}-inducible p27 allele [31]. p27 is a close relative to p21 that also inhibits CDKs and induce cell cycle arrest [40]. Thus, the comparison serves to identify genes specifically regulated by p21 in our analysis. We subtracted the gene expression changes occurring at 72 h in Kp21-4 cells those genes regulated by p27 in the Kp27-5 cells and genes changed by $ZnSO_4$ treatment in parental K562 cells. We found 350 genes whose expression changed ≥2.3 fold in Kp21-4 after 12 h of p21 induction and which were not regulated at this time point in Kp27-5 or K562 cells treated with $ZnSO_4$ (Figure 1B). The list of the genes with their corresponding expression change is shown in the Table S2.

The dataset used for the clustering analysis of Figure 1B was further analyzed with the Ingenuity Pathways software to reveal the network of interactions between differentially regulated genes. The results showed that the two highest-ranked networks were assembled by interactions between genes related to cell cycle control (Figure S2). Gene ontology analysis revealed that cell cycle-related genes accounted for about one fifth of the regulated genes, i.e., 65 genes (Figure 1C). The expression change of these genes is shown as a heat map in Figure 1D, demonstrating that the vast majority of these genes were down-regulated by p21. The former result defined cell cycle and mitosis as the most relevant functional categories of p21-down-regulated genes. We investigated the kinetics of changes in the RNA levels of 19 genes repressed by p21 from those appearing in Figure 1D plus *BIRC5*, *CCNB1* and *CDK2*, because of their involvement in cell cycle. RNA was prepared from Kp21-4 cells and expression was determined by RT-qPCR at different periods of time up to 12 h after $ZnSO_4$ addition, i.e., when p21 expression is maximal and its effect is already irreversible. The results are shown in Fig. 2A and confirmed that most of the down-regulated genes identified by microarray hybridization were down-regulated as soon as 6 h after the addition of the p21 inducer. $ZnSO_4$ did not modify the expression of any of these genes in parental K562 (data not shown). To confirm the repressive effect of p21 we analyzed the level of acetylated-histone H3, a marker of active chromatin [41], in the chromatin region corresponding to the transcriptional start site of several genes. The results showed a dramatic decrease in the fraction of acetylated-histone H3 as soon as 6 h after p21 induction (Fig. 2B). The data also argues that the decrease in mRNA levels is caused by transcriptional switch-off rather than mRNA degradation

The fast kinetics of gene down-regulation caused by p21, before any change in cell cycle profile could be detected, suggested that the repression is a direct consequence of p21 activity, rather than an indirect effect. CDK2 inhibition is the best known biochemical activity of p21, and it also occurs in K562 [31]. Thus, we explored the possibility that the p21-dependent gene expression regulation described above is a consequence of CDK2 inhibition. We conducted two sets of experiments. First, we showed that the depletion of CDK2 in Kp21-4 cells achieved through siRNA did not modify the p21-dependent repression of the assayed genes. This has been demonstrated by transient expression of a short-hairpin CDK2 vector (Fig. 3). Second, we analysed the effects of p27, which also provokes CDK2 inhibition and cell cycle arrest [31], on the expression of genes down-regulated by p21. In contrast to p21, p27 provoked a dramatic G1 arrest already detectable after 6 h of induction in Kp27-5 cells (Figure S1). p27 was induced in Kp27-5 cells for 3–12 h and the expression of 11 genes was assayed by RT-qPCR. The results showed that p27 did not repress cell cycle genes or repressed them with a much slower kinetics than p21 (Figure S3), despite a similar induction level of p21 and p27 in p21-4 and Kp27-5 cells respectively (Figure S1A). Moreover, we performed gene expression profiling in Kp27-5 cells upon 12 h of p27 induction. The results showed that at this induction time p27 elicited weaker effects on gene regulation than p21. After subtraction of p21-regulated genes the analysis revealed that p27 regulated only 180 genes (with an expression change ≥2.3 fold after 12 h of p27 induction) and none of them was annotated as related to cell cycle, according to the Gene Ontology analysis (Figure S4). The comparison to retrieve shared gene expression profiles by p21 and p27 induction revealed 90 common genes that were regulated by both proteins after 12 h of induction. These genes belong to different functional categories, but only 8 genes were related to cell cycle (Figure S4).

The N-terminal region of p21 is sufficient for gene down-regulation

Next, we asked whether the CDK-cyclin binding domain of p21 was involved in the down-regulation of gene expression. We used two p21 deletion constructs carrying the green fluorescent protein. One construct carried the first 91 amino acids, which included the CDK-cyclin binding region and the second construct the C-terminal region, after the codon 91 [33] (Figure 4A). Although the GFP-N-terminal construct lacked the nuclear localization signal in the p21 region, it partly localizes in the cell nuclei, likely due to the GFP domain [33]. We transfected these constructs as well as the full-length p21-GFP construct and selected the GFP-expressing cells by fluorescent-activated cell sorting. We further tested the expression of several genes with rapid (*CCNE2*, *KIF4A*) and slower (*WEE1*) down-regulation kinetics (see Figure 2). The expression of *CCNE2*, *WEE1* and *KIF4A* in GFP-positive cells was determined by RT-qPCR in the transfected cells. The results showed that the N-terminal p21 was sufficient to provoke the gene down-regulation, although it was a less efficient repressor than the full-length p21. In contrast, C-terminal p21 was inactive as repressor of the assayed genes (Figure 4B).

This indicates that the repressive activity of p21 is independent of the protein-protein interaction domain known to reside in the C-terminal region, as PCNA binding [42].

p21 binds to the human CCNE2 promoter

The observation that p21 provokes a rapid mRNA repression of various genes, suggested that p21 might participate in gene

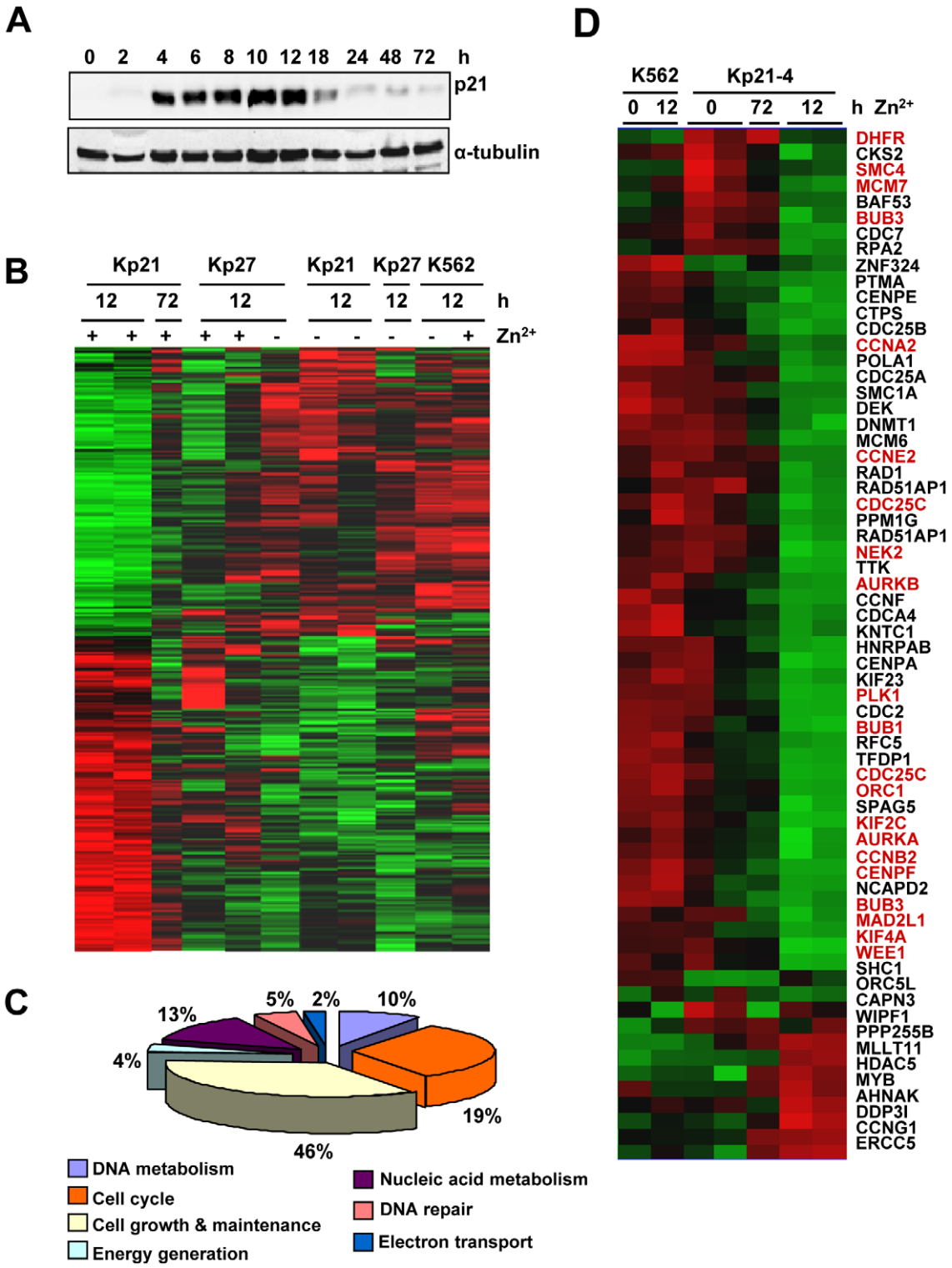

Figure 1. Gene expression changes induced by p21 in K562 cells. A. Expression of p21 in Kp21-4 cells in response to $ZnSO_4$. Cells were treated with 75 μM $ZnSO_4$ for the periods of time indicated. Cell extracts were prepared and the p21 levels analyzed by immunoblot. B. The transcriptome of Kp21-4 cells (Kp21) treated for 12 h with $ZnSO_4$ (to induce p21) were compared to that of cells with induced p27 (Kp27), parental K562 and Kp21-4 treated for 72 h with $ZnSO_4$. The heat map shows the hierarchical clustering with those genes with expression variation ≥2.3-fold between uninduced and p21-induced Kp21-4 cells ($P<0.001$). The heat map shows 350 regulated genes (360 gene probes). C. Distribution of the regulated genes shown in A according with their cell functions. The ontogeny analysis has been carried out with the dChip program. D. Expression changes in 65 genes related to cell cycle and mitosis according to the ontogenic classification. The heat map was obtained as described in B. The genes further validated by RT-qPCR (Figure 2A) are shown in red.
doi:10.1371/journal.pone.0037759.g001

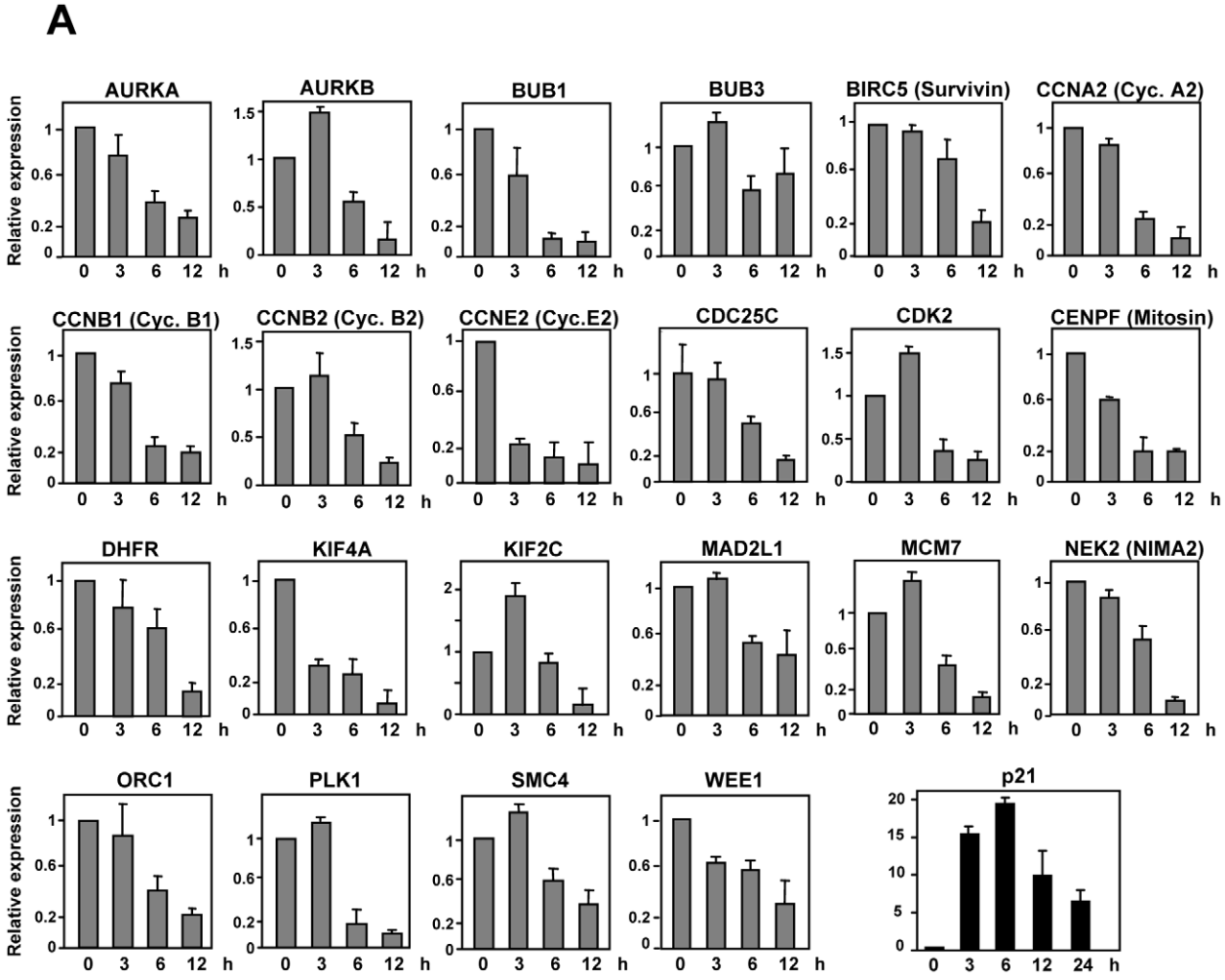

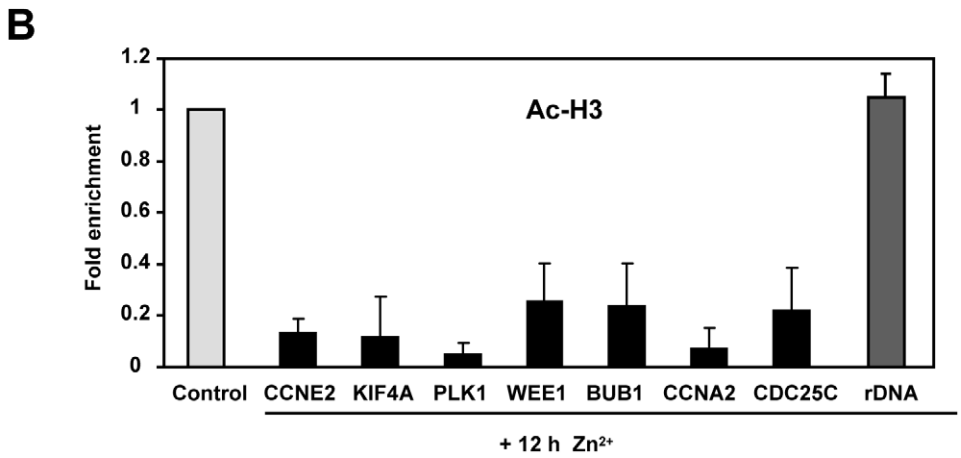

Figure 2. p21-mediated the down-regulation of genes involved in cell cycle. A.The expression of p21 was induced in Kp21-4 cells by 75 μM $ZnSO_4$ and 3, 6 and 12 h later, total RNA was prepared and expression of the indicated genes was determined by RT-qPCR. In some cases an alternative name is given into brackets. Cyc., cyclin. The values are means ±S.E.M. from two independent experiments and two determinations for each RNA. B. Kp21-4 cells were treated for 6 h with 75 μM $ZnSO_4$ to induce p21. Chromatin immunoprecipitation was carried out with anti-histone H3 and anti-acetylated-histone H3 antibodies and (as specificity control) rabbit IgG. The DNA in the immunoprecipitated chromatin was measured by quantitative PCR. The amplicons encompass the transcription start site of the indicated genes. A regulatory sequence of the promoter of rDNA was used as a control. The results are expressed as the ratio of DNA enrichment in chromatin immunoprecipitated with anti-H3 versus acetylated-H3 (''Ac-H3'') and normalized to the values obtained in uninduced cells. The values are the means ±S.E.M of two independent ChIP experiments with two PCR determinations each.

doi:10.1371/journal.pone.0037759.g002

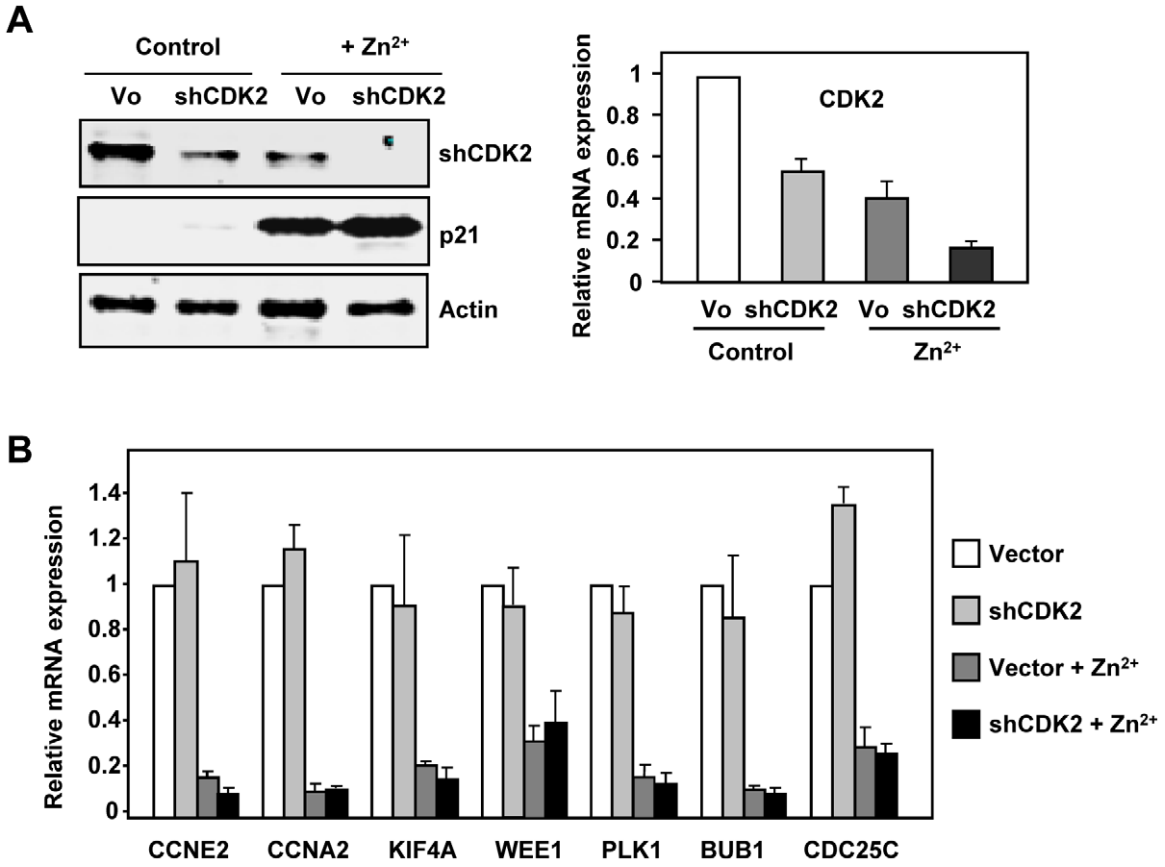

Figure 3. p21-mediated repression of genes is not dependent on CDK2. A. K562 cells were transiently transfected with a short-hairpin CDK2 ("shCDK2") vector and the empty vector (pLKO.1, "Vo"). 24 h after transfection the cells were treated with 75 μM $ZnSO_4$ for 12 h to induce p21 and the silencing of CDK2 was assayed at the protein level by immunoblot (left panel) and at the mRNA level by RT-qPCR (right panel) The expression of p21 and actin was also determined to control the p21 induction by Zn^{2+} and the protein level, respectively. B. The expression of p21 was induced with 75 μM $ZnSO_4$ in K562 transfected with sh-CDK2 and 12 h later, total RNA was prepared and expression of the indicated genes was determined by RT-qPCR. The values are means ±S.E.M. from two independent experiments and two determinations for each RNA.
doi:10.1371/journal.pone.0037759.g003

repression as a transcriptional modulator, a function already reported for p21 (see Introduction). For further analysis, we focused on the *CCNE2* gene because of its pivotal role in S phase entry and because it showed one of the fastest down-regulation kinetics, with a decrease as soon as 6 h after Zn^{2+} addition (Figure 2). We previously reported that most p21 remains nuclear upon induction with Zn^{2+} in Kp21-4 cells [43]. However, in order to act as co-regulator it is required that at least part of the p21 induced by Zn^{2+} in Kp21-4 cells is bound to chromatin. We first carried out a fractionation of Kp21-4 nuclear extracts into chromatin and nucleoplasmic fractions. The results of the immunoblot show a significant amount of p21 bound to the chromatin fraction in Kp21-4 cells induced with $ZnSO_4$ (Figure 5A). This result led us to ask whether p21 could be bound to the promoter of their regulated genes. We performed chromatin immunoprecipitation (ChIP) in Kp21-4 cells with anti-p21 antibody, and asked for p21 binding in the vicinity of the transcription start site (TSS) of human *CCNE2* and other p21-repressed genes. The results showed that p21 was bound to the region encompassing the TSS in Kp21-4 cells upon p21 induction after 12 h of treatment with $ZnSO_4$ (Figure 4B). We also found p21 binding to the promoters of other p21-target genes as *CDK2*, *KIF4A*, *PLK1* and *WEE1* to similar extent than to *CCNE2* promoter (Figure 5B). As additional controls, we performed ChIP experiments in Kp27-5 cells treated with $ZnSO_4$ to induce p27 [31] and in parental K562 also treated with $ZnSO_4$. No enrichment was found in the chromatin precipitated with anti-p21 in both cases. Also, no specific signal was detected with anti-p27 antibody in Kp21-4 cells and in Kp27-5 cells with induced p27 expression (Figure 5B). As the p21 region required for repression includes the cyclin-CDK binding region (Figure 4) we also performed ChIP assays with anti-CDK2 antibody. The results show that in cells overexpressing p21, CDK2 is recruited to the same site of human *CCNE2* that p21 (Figure 4B), which is in concordance with the presence of p21 on that region of the chromatin.

p21 represses CCNE2 promoter activity

The former results show that CCNE2 is rapidly down-regulated by p21 and that p21 is bound to CCNE2 proximal promoter in Kp21-4 cells. To confirm the hypothesis that p21 may act as a transcriptional modulator we carried out luciferase assays with reporters harbouring the human *CCNE2* and (as a control) *CCNE1* promoters. The results demonstrated a modest but significant and reproducible decrease in *CCNE2* promoter upon transfection of a p21 expression vector (Figure 6A). As a second approach, we next used the Kp21-4 cell line and performed the luciferase assays 24 h after the induction of p21 (Figure 6B). Immunoblot analysis revealed the overexpression of p21 in transfected cells (Figure 6A and 6B, lower panels). Taken collectively the results strongly

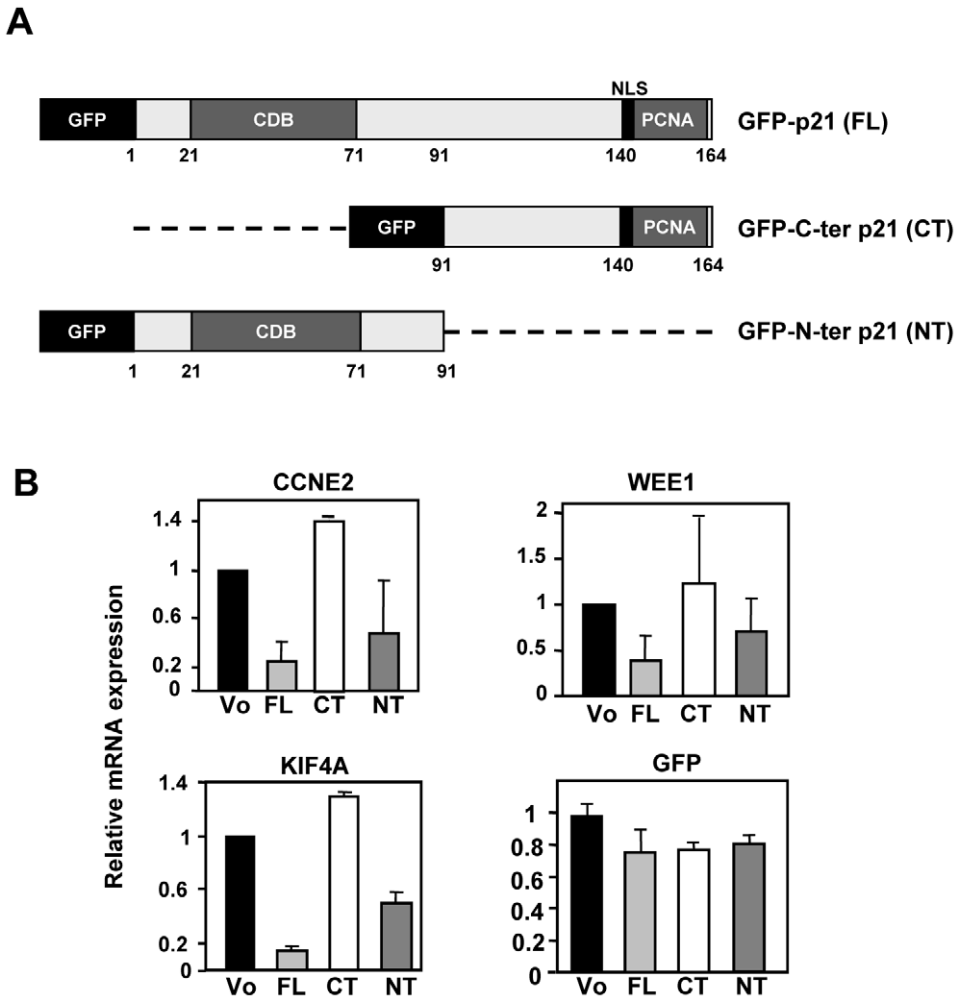

Figure 4. The N-terminal region of p21 is required for its effect as gene repressor. A. Schematic representation of the p21 constructs used. The proteins carry the green fluorescent protein (GFP) in the N-terminal. The position of the CDK binding domain (CDB) and the PCNA binding domain (PCNA) are indicated. B. K562 cells were transfected with expression vectors for the full-length p21 protein (FL), the p21 amino-terminal region (NT) and the p21 carboxy-terminal region (CT). 24 h after transfection the cells were sorted by flow cytometry and the expression of the indicated genes was analysed by RT-qPCR. The values are means ±S.E. from two transfections and two determinations of each mRNA.
doi:10.1371/journal.pone.0037759.g004

suggest a role of p21 in the negative regulation of *CCNE2* and other genes in the K562 system.

p21 represses mitotic genes in human primary keratinocytes

All the previous results have been obtained in a cell line derived from human myeloid leukemia. In order to confirm these results we studied the p21-dependent repression of mitotic genes in a different cellular system. We chose human primary keratinocytes because they are non-tumorigenic, non-immortalized and epithelial cells, in contrast to K562 cells. Human primary keratinocytes were infected with recombinant adenoviruses expressing the full-length p21 protein. A dramatic increase in p21 in infected keratinocytes was demonstrated by RT-qPCR (Figure 7A). As controls, we also infected the keratinocytes with adenovirus carrying the genes for p27, which overexpression was also confirmed by RT-qPCR (Figure 7A). We prepared RNA 24 h after infection and performed large-scale expression assay using the Affymetrix platform. The clustering analysis revealed that p21 provoked the down-regulation of a number genes involved in cell cycle control not shared by cells expressing p27 (Figure 7B). The list of the genes with their corresponding expression change is shown in the Table S3. We next validated by RT-qPCR the p21-mediated repression of several of these genes involved at various checkpoints of cell cycle (*AURKB*, *BIRC5*, *CDC25C*, *CCNE2* and *WEE1*). The results demonstrated the decreased levels of mRNA for all the tested genes, confirming the data of the microarray hybridization (Figure 8A). To fully confirm the effect of p21 as a repressor of these genes in keratinocytes, we silenced p21 through siRNA transfection (Figure 8B). The expression of the five genes was tested in p21-depleted cells and we found that the five genes were up-regulated to various extents (Figure 8C). The results therefore confirm the regulation of the expression of the analyzed genes by p21.

Bioinformatic analysis of p21-targeted genes

As noted in the Introduction, it has been reported that p21 binds to specific DNA sequences of some p21-regulated genes. As p21 lacks any recognizable DNA-binding domain, the interaction must be indirect, i.e., through another transcription factor or co-factor. We previously reported that p21 can bind genes at E2F-

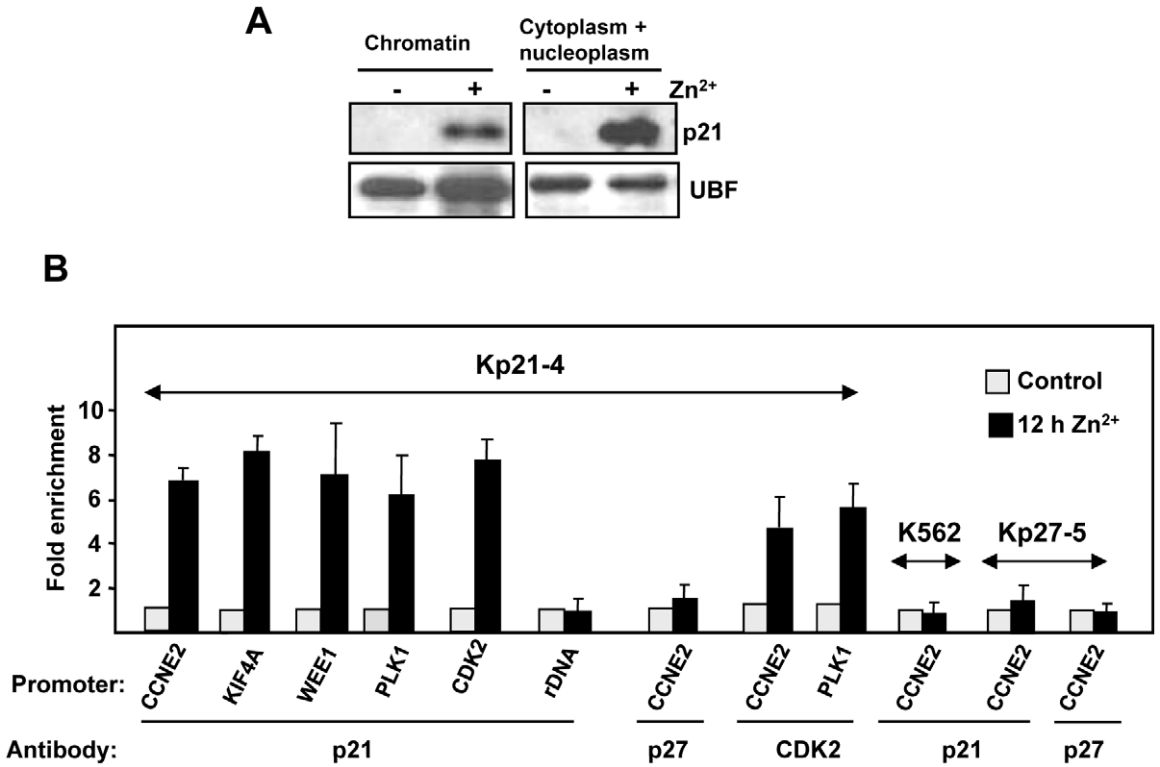

Figure 5. p21 binds to human CCNE2 promoter. A. Kp21-4 cells were treated for 12 h with $ZnSO_4$ and the nuclear extracts were fractionated between insoluble (chromatin) fraction and soluble (nucleoplasmic) fraction. The p21 levels were determined by immunoblot. The transcription factor UBF was used as control of chromatin-bound protein. B. Cells were treated for 12 h $ZnSO_4$ to induce p21 (in Kp21-4 cells), p27 (in Kp27-5 cells), parental K562 cells were also treated with ZnSO4 as negative control. Chromatin immunoprecipitation was performed with anti-p21, anti-p27 and anti-CDK2 antibodies as indicated, and (as specificity control) rabbit IgG. The DNA in the immunoprecipitated chromatin was analysed by quantitative PCR. The amplicons encompass the transcription start site of the indicated genes. rRNA promoter sequences were used negative controls. The results are expressed as enrichment of DNA in chromatin immunoprecipitated with anti-p21 (with respect the signal with anti-rabbit IgG) in cells induced with Zn^{2+}, and normalized to the values obtained in uninduced cells. The values are the means ±S.E.M of three PCR determinations, each from two independent ChIP experiments.
doi:10.1371/journal.pone.0037759.g005

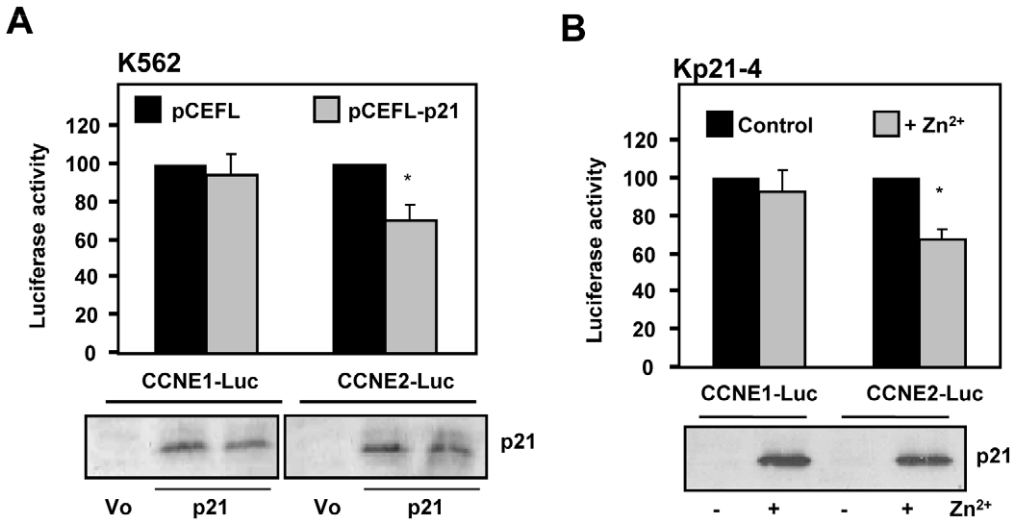

Figure 6. p21 represses the activity of human CCNE2 promoter. A. K562 cells were transfected with luciferase reporters carrying the promoters cyclin E1 and E2 genes (*CCNE1* and *CCNE2*), along with an expression vector for p21 and the corresponding empty vector, and a beta-gal plasmid for transfection efficiency normalization. 24 h after transfection the luciferase activities were determined. The data are normalized to the activity of cells transfected with the empty vector. Lower panel: immunoblot analysis of the transfected cells to assess the expression of p21. B. Kp21-4 cells were transfected with luciferase reporters carrying the promoters cyclin E1 and E2 genes as in (A) and 24 h later the cells were treated with 75 μM $ZnSO_4$ and after 24 h the luciferase activities were determined. The data are normalized to the activity of cells without $ZnSO_4$. Lower panel: immunoblot analysis of the transfected cells to assess the expression of p21.
doi:10.1371/journal.pone.0037759.g006

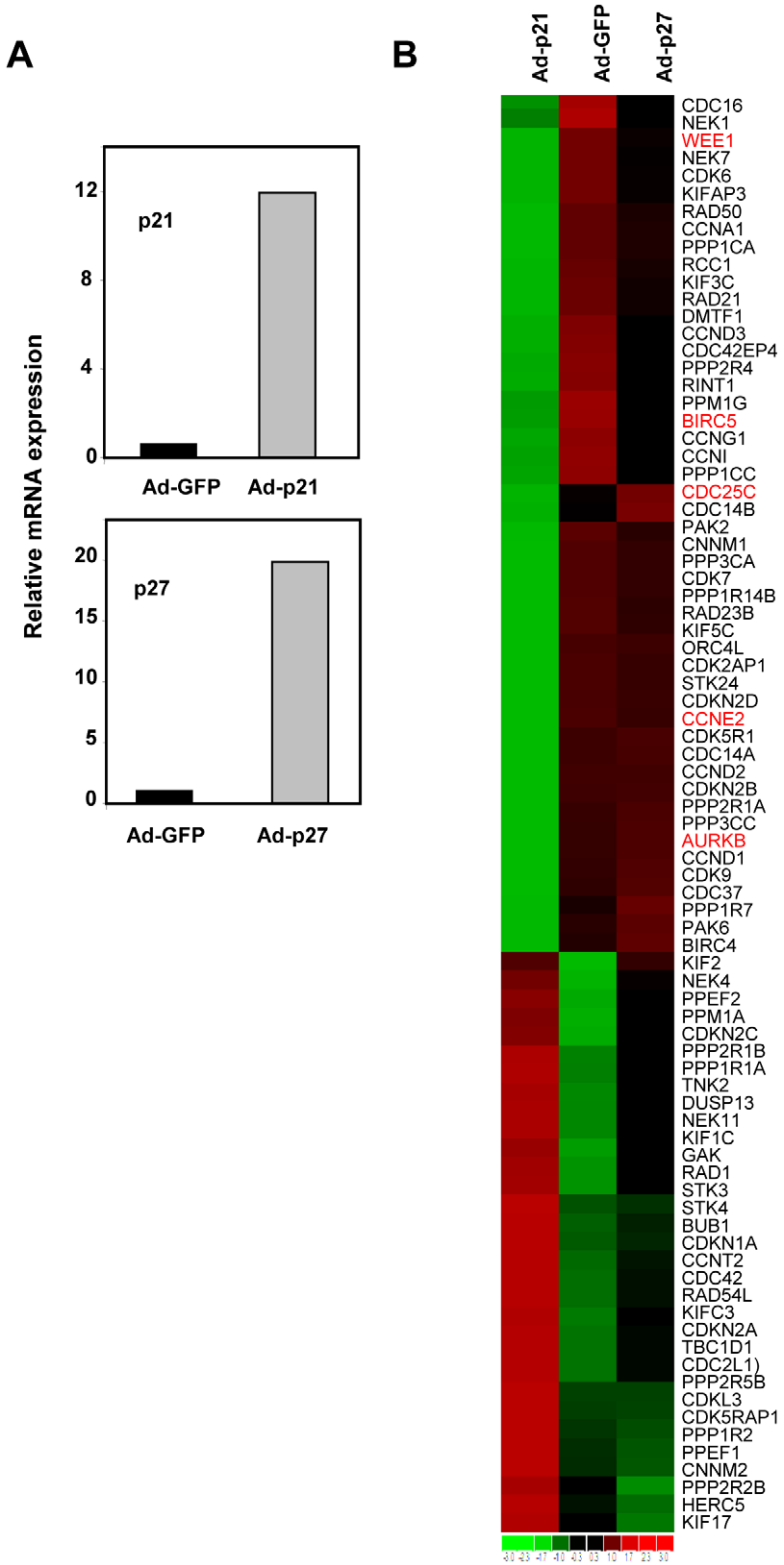

Figure 7. Genes regulated by p21 in human keratinocytes related to cell cycle and cell division. A. Primary human keratinocytes were infected with recombinant adenoviruses expressing p21 (Ad-p21), p27 (Ad-p27). As a control, cells were also infected with adenovirus expressing GFP (Ad-GFP). The mRNA expression of p21 (upper graph) and p27 (lower graph) was determined by RT-qPCR 24 h after infection. Data are represented relative to the expression in Ad-GFP-infected cell. B. Heat-map showing the 82 genes changed by p21 related to cell cycle and cell division with an expression change $>$ 2.3-fold. The names of the regulated genes are indicated at the right. Green indicates genes down-regulated by p21 and red genes up-regulated.
doi:10.1371/journal.pone.0037759.g007

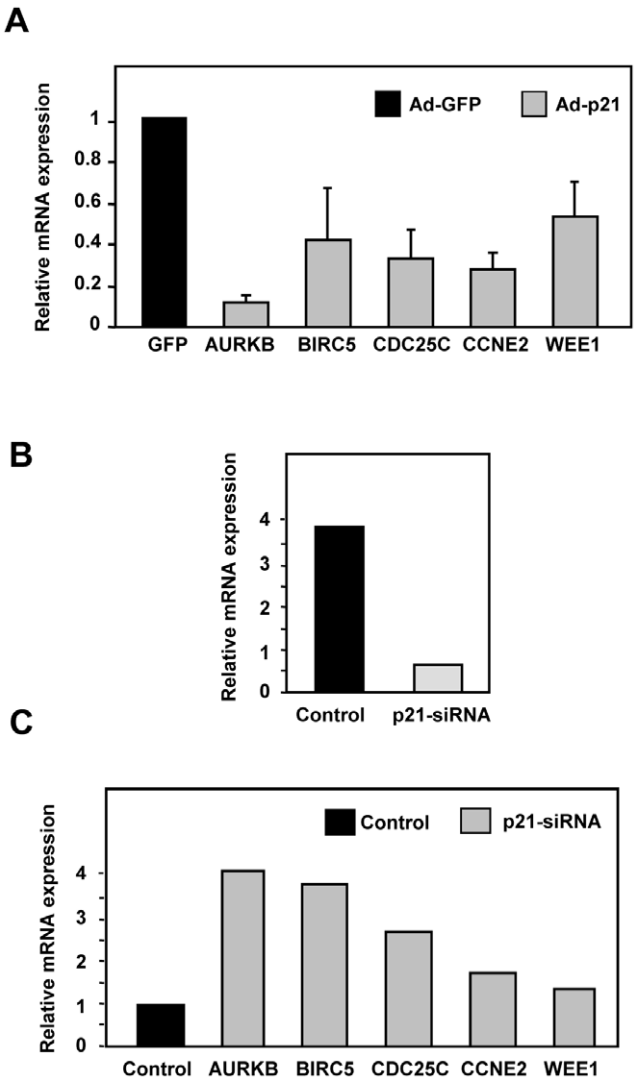

Figure 8. p21-mediated down-regulation of genes involved in mitotic control in human keratinocytes. A. Primary human keratinocytes were infected with adenovirus expressing p21 and ad-GFP as a control. 24 h after infection total RNA was prepared and the mRNA levels of the indicated genes were analysed by RT-qPCR. The values are means ±S.E. from three determinations. B. keratinocytes were transfected with siRNA for p21 and a negative control siRNA. Total RNA was prepared and the mRNA levels of the indicated genes were analysed by RT-qPCR. C. Primary human keratinocytes were transfected with p21 siRNA or control siRNA. 48 h after lipofection total RNA was prepared and the mRNA levels of the indicated genes were analysed by RT-qPCR.
doi:10.1371/journal.pone.0037759.g008

binding elements [23]. Another report showed the binding of p21 to the CDE/CDH element, composed by the the cell cycle-dependent element (CDE) and the cell cycle genes homology region (CHR) [44]. Therefore, we have performed a bioinformatic analysis of the promoters of the 22 genes where p21-mediated down-regulation was validated by RT-qPCR (shown in Figure 2). The results show that a majority of the genes carried several E2F sites in the 5′ regulatory region and/or the first exon (Figure 9) but there were some exceptions (*BIRC5*, *CCNB2*, *DHFR*, *KIF4A*). More interestingly, all genes but one (*BUB1*) contained at least one CDE site in the vicinity of the TSS (Figure 9). In this context it must be noted that human *CCNE2* promoter and first exon are particularly rich in CDE sequences. Thus, p21 may impair transcription of genes in charge of the execution and control of mitosis through the interaction with transcription factors binding to CDE or CDE/CHR motifs.

Discussion

Despite the original description of p21 as a CDK inhibitor, a number of reports have described a role of p21 as transcriptional modulator for different genes such as *WNT* [23], cyclin D1 [27], polo-like kinase 1 (*PLK1*), topoisomerase IIα [44], *CDC25A*, *MYC* [24] and p53 [45]. p21 has also been described as an antagonist of E2F-dependent transcription [22]. Conversely to previous studies, we have analyzed the genome-wide p21-dependent gene regulation in two different human cellular models: a myeloid leukemia cell line (K562) and primary keratinocytes. p21 overexpression was attained through the induction of a conditional transgene by $ZnSO_4$ (in human myeloid cells) or through acute adenoviral infection (in human keratinocytes).

Our results on the gene expression profiling in both cell models showed that p21 provokes a rapid repression of mRNA of genes involved in cell cycle and mitosis control in the two models. Since p21 elicits cell growth arrest this effect could be indirect, i.e., a consequence of the cell cycle arrest. However, in myeloid cells with inducible p21 (Kp21-4 cells), the kinetics of the mRNA down-regulation of most of the analysed genes was almost parallel to the kinetics of the p21 protein up-regulation. This down-regulation of mRNA was also concomitant with the rapid deacetylation of histone H3 at the TSS. The genes repressed by p21 were up-regulated upon p21 silencing, confirming the p21 activity. Moreover, the early p21-induced down-regulation was not reproduced by p27 induction in K562 cells form most genes, despite that p27 also provokes a cell cycle arrest via CDK inhibition. Furthermore, the depletion of CDK2 does not affect the p21-mediated gene repression. Altogether these data argue against the idea that the p21 effects were a direct consequence of the CDK inhibition or of the cell cycle arrest. Thus, it is conceivable that p21 is directly involved in transcriptional repression of a set of genes involved in cell cycle control. Previous unsuccessful attempts to generate a functional p21 fused to the estrogen receptor (so as to get activated by tamoxifen) [46] precluded the analysis of p21 transcriptional effects in the absence of protein synthesis.

It is remarkable the similarity in the short-term transcriptional effects of p21 overexpression observed in two very different cell types (keratinocytes and myeloid cells), despite the different long-term consequence of p21 overexpression in each cell type. p21 inhibits epidermal differentiation in keratinocytes [25,32] whereas it induces polyploidy and megakaryocytic differentiation in K562 [31]. It is of note however, that the transcriptional changes that we have observed occur before any phenotypic change can be detected in either cell line. In Kp21-4 cells, the polyploidy is detectable 3–4 days after induction and at this time point, the expression of CDC25, cyclin A and cyclin E are recovered, likely to allow DNA synthesis for endoreplication [8]. Previous studies in a fibrosarcoma cell line also showed p21 repressed genes involved in mitosis followed by polyploidy three days after p21 induction [7], suggesting that polyploidization may be a common effect of p21 in tumor cells.

We further analysed the regulation of *CCNE2* (cyclin E2), one of the genes undergoing a fastest down-regulation. ChIP assays revealed that p21 binds in the vicinity of the TSS of human cyclin E2 gene (as well as other four genes: *CDK2*, *KIF4A*, *PLK1* and *WEE1*). The results are consistent with previous literature showing

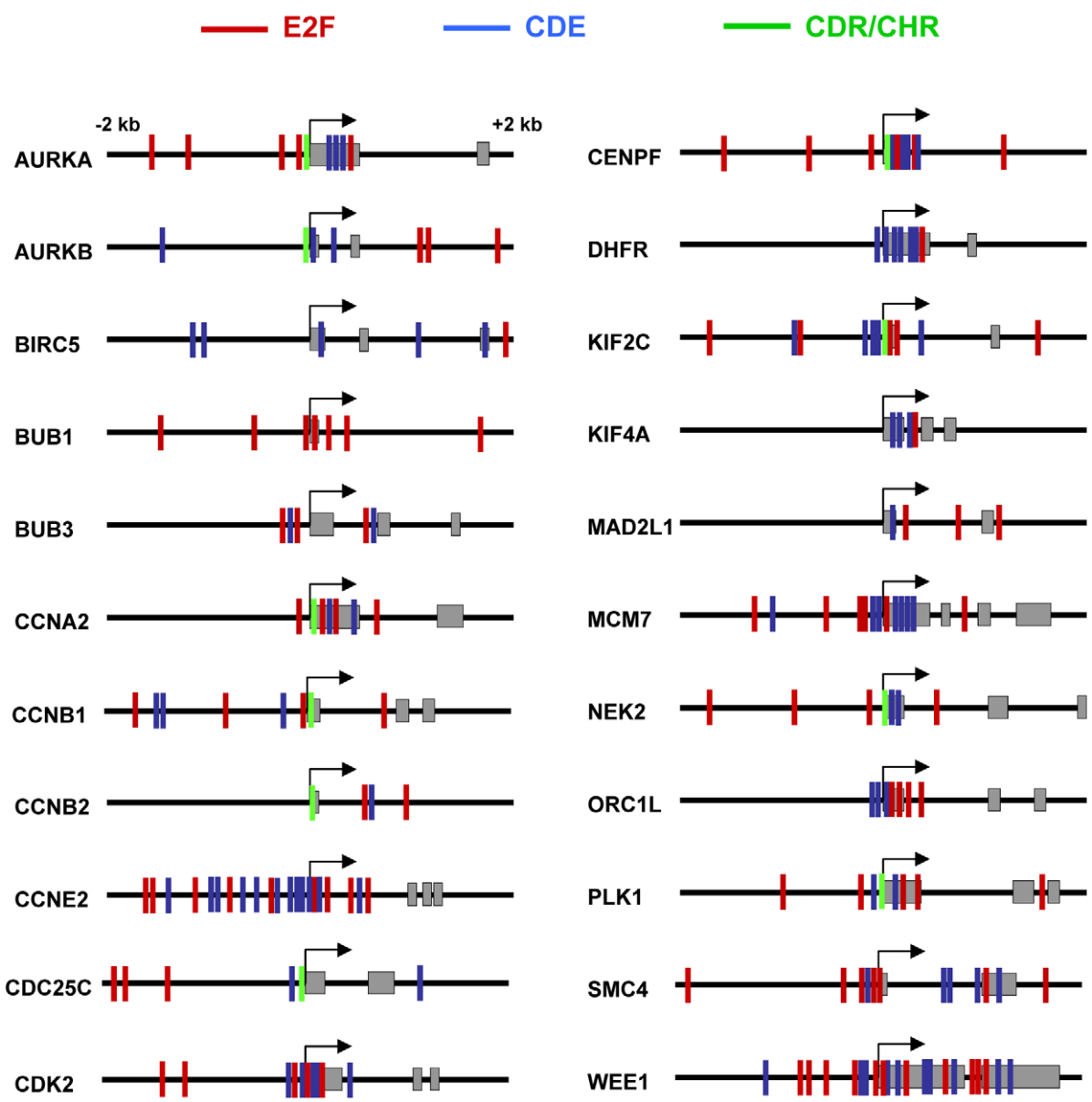

Figure 9. Putative regulatory sites in genes down-regulated by p21. Schematic representation of the E2F (red), CDE (blue) and CDE/CHR (green) sites in the p21-regulated genes analysed in Figure 2. The region analysed encompass 2 kb upstream and downstream the transcription start site (marked by an arrow). Exons are represented as grey boxes. E2F sites: $TTT^{C}/_{G}{}^{C}/_{G}{}^{C}/_{G}{}^{C}/_{G}$. CDE sites: $^{T}/_{G}GGCGG$. CDE/CHR sites: $GCG^{C}/_{G}N_{2-5}\ TT^{A}/_{G}AA$.
doi:10.1371/journal.pone.0037759.g009

chromatin binding of p21 in several models (see Introduction). In contrast, upon induction of p27 for 12 h in Kp27-5 cells, we could not detect significant binding of p27 to CCNE2 promoter.

In full agreement with the results observed at the mRNA level and ChIP assays, luciferase reporter experiments showed that p21 repressed the human *CCNE2* promoter. The mutational analysis revealed that CCNE2 gene repression depends on the N-terminal region of p21, i.e., the region involved in the binding to cyclin-CDK complexes. The C-terminal domain of p21 is not required, but seems to contribute for full activity of p21 as repressor. It is noteworthy that p21 does not repress CCNE1 promoter (if it does) as efficiently as CCNE2, arguing for a differential role of both cyclins.

Taken together the data argue for a role of p21 as co-repressor of gene transcription for genes related to cell cycle. As p21 lacks any recognizable DNA-binding domain, the interaction must be indirect, i.e., through another transcription factor or co-factor. It has been reported that p21 binds to specific DNA sequences of some genes. For instance, we have previously shown that this is the case for *WNT4* repression, which depends on the interaction with E2F1 [23]. Also, it has been reported that p21 repress the mitotic control gene PLK1 through binding to the CDE/CHR element [44]. The CDE/CHR elements control the transcription of genes with maximum expression in G2 phase and in mitosis and are repressed in G0 and G1 phases, although the transcription factor(s) responsible are still unidentified [47]. It has been recently reported that p27 binds to some promoters through E2F4 sites in mouse fibroblasts [48]. Our analysis showed that many of the p21-downregulated genes contained one or several E2F binding sites, but at least four genes did not (*BIRC5*, *CCNB2*, *DHFR*, *KIF4A*),

despite that a relaxed consensus sequence as E2F's binding site was used for the analysis, which includes E2F4 sites (Figure 9). Our analysis does not give information regarding the specific E2F family member involved, so the differential binding of E2F factors on the different genes is an open possibility. More interestingly, we found that all genes but one (*BUB1*) contained at least one CDE site in the vicinity of the TSS. In this context it must be noted that human CCNE2 promoter and first exon are particularly rich in CDE sequences. Thus, p21 may impair transcription of genes in charge of the execution and control of mitosis through the interaction with transcription factors binding to CDE or CDE/CHR motifs.

Altogether, our results indicate that p21 is a multifunctional protein with the capacity to act through at least two mechanisms to control cell cycle: directly inhibiting CDKs and indirectly regulating genes involved in cell cycle control. The relative importance of each mechanism await further investigation, but it is of note that p21 is able to arrest the cell cycle in CDK2-deficient cells [29], arguing for the importance of transcriptional repression in the p21 functions in cell biology. Additional studies are required to dissect out the mechanisms involved in the transcriptional repression mediated by p21.

Supporting Information

Figure S1 Cell cycle alterations mediated by p21 and p27 in K562 cells. A. Immunoblots showing the induction of p21 in Kp21-4 cells and p27 in Kp7-5 cells after 6 and 12 h of treatment with 75 μM $ZnSO_4$. B. Absence of cell cycle profile alteration after short induction times of p21. Cell cycle profile of Kp21-4 and Kp27-5 cells upon induction of p21 and p27 with 75 μM $ZnSO_4$ for 6 and 12 h. The cell cycle profile was determined by flow cytometry of propidium iodide-stained cells. C. p21 induces an irreversible accumulation of G2 and polyploid cells whereas p27 induces a reversible accumulation in G1. Kp21-4 and Kp27-5 were treated with ZnSO4 for 12 h. The cells were then washed to remove the inducers, further incubated for 84 h and the cell cycle profile was determined by flow cytometry (4 days after the induction). The fraction of cells in G1, G2 or polyploidy cells (>G2) is indicated in each case.
(TIF)

Figure S2 Interaction networks of genes regulated by p21 in K562 cells. A knowledge-based database (Ingenuity Pathways Analysis) was seeded with the genes regulated by p21 at 12 h of induction (Table S2). The two networks with the highest score are shown. The program processed 279 genes (137 up-regulated, 142 down-regulated). The ontogeny category of the networks is as indicated at the bottom. Genes in red were up-regulated and those in green were down-regulated. The meanings of node shape and lines are indicated at the bottom.
(TIF)

Figure S3 Comparison of the gene regulation mediated by p21 and p27 in K562 cells. p21 was induced in Kp21-4 cells and p27 was induced in Kp27-5 cells by 75 μM $ZnSO_4$. After 3, 6 and 12 h of induction, total RNA was prepared and expression of the indicated genes was determined by RT-qPCR. The data for Kp21-4 cells are the same than in Figure 2. The values are means ±S.E.M. from two independent experiments and two determinations for each RNA
(TIF)

Figure S4 A. Gene expression regulation mediated by 12 h induction of p27 in K562 cells. The transcriptome of Kp27-5 cells (Kp27) treated for 12 h with $ZnSO_4$ (to induce p27) were compared to that of cells with induced p21 (Kp21) and parental K562 treated for 12 h with $ZnSO_4$. The heat map shows the hierarchical clustering with those genes with expression variation ≥2.3-fold between uninduced and p27-induced Kp27-5 cells after subtraction of the gene expression changes due to p21 in Kp21 cells($P<0.001$). The heatmap shows 179 genes. B. Common genes regulated by both p21 and p27 in K562 cells. Kp21-4 and Kp27-5 cells were treated for 12 h with 75 μM $ZnSO_4$ to induce p21 and p27 respectively. The heat map shows the hierarchical clustering with those genes with expression variation ≥2.3-fold between uninduced cells and Zn^{2+} –treated cells which are regulated in both cell lines($P<0.001$). The heat map shows 90 genes. The genes related to cell cycle according with Gene Ontology are shown in red.
(TIF)

Table S1 Primers used in PCR reactions in this work. The forward primer is in the first line. All correspond to human genes except GFP (Green Fluorescent Protein from *Aequorea victoria*, encoded in the plasmid pEGFP-C1). An alternative common name of the gene is included for some genes.
(DOC)

Table S2 Genes regulated by p21 in K562 cells. The table list the genes showing an expression change in Kp21-4 cells treated with $ZnSO_4$ (p21 inducer) for 12 h, after subtracting those genes changed by $ZnSO_4$ in parental K562 cells (i.e., changed by $ZnSO_4$) and in Kp27-5 cells (i.e., induced by p27). The 253 genes are included in the heat map of Fig. 1B. The table includes genes with ID and with a fold change ≥$\log_2$1.2 (≥2.3-fold) and with a signal difference ≥50 between both experimental conditions (as defined by dChip program and with Affymetrix U133 biochip data). Values are mean of fold changes (expressed as $\log_2$) of two independent experiments ($P<0.001$). For those genes represented by two or three Affymetrix probes, the fold change is the mean between the values of the probes. A negative fold change indicates down-regulation upon p21 induction.
(DOC)

Table S3 Genes regulated by p21 in primary keratinocytes. The table list the genes showing an expression change in human primary keratinocytes infected with adenovirus-p21 as described in Methods. RNA was analysed 24 h after infection. The 75 genes are included in the heat map of Fig. 7. The table includes genes with a fold change ≥$\log_2$1.2 (≥2.3-fold) and with a signal difference ≥50 between both experimental conditions (as defined by dChip program and with Affymetrix U133 biochip data). Values are mean of fold changes (expressed as $\log_2$) of two independent experiments ($p<0.001$). For those genes represented by two or three Affymetrix probes, the fold change is the mean between the values of the probes. A negative fold change indicates down-regulation upon p21 induction.
(DOC)

Acknowledgments

We thank Pilar Frade and Maria Aramburu for technical assistance. We are also grateful to Alberto Gandarillas and Ana Zubiaga for helpful comments on the manuscript.

Author Contributions

Conceived and designed the experiments: NF PD JL. Performed the experiments: NF JMC LGG VD MRP GB AQ MJMA MCL RB JCR. Analyzed the data: NF NA MDD GPD JL. Contributed reagents/materials/analysis tools: VD MDD. Wrote the paper: NF JL.

References

1. Harper JW, Adami GR, Wei N, Keyomarsi K, Elledge SJ (1993) The p21 Cdk-interacting protein Cip1 is a potent inhibitor of G1 cyclin-dependent kinases. Cell 75: 805–816.
2. Gu Y, Turck CW, Morgan DO (1993) Inhibition of CDK2 activity in vivo by an associated 20K regulatory subunit. Nature 366: 707–710.
3. Dulic V, Kaufmann WK, Wilson SJ, Tlsty TD, Lees E, et al. (1994) p53-dependent inhibition of cyclin-dependent kinase activities in human fibroblasts during radiation-induced G1 arrest. Cell 76: 1013–1023.
4. Serrano M, Hannon GJ, Beach D (1993) A new regulatory motif in cell-cycle control causing specific inhibition of cyclin D/CDK4. Nature 366: 704–707.
5. Bates S, Ryan KM, Phillips AC, Vousden KH (1998) Cell cycle arrest and DNA endoreduplication following p21Waf1/Cip1 expression. Oncogene 17: 1691–1703.
6. Niculescu AB, 3rd, Chen X, Smeets M, Hengst L, Prives C, et al. (1998) Effects of p21(Cip1/Waf1) at both the G1/S and the G2/M cell cycle transitions: pRb is a critical determinant in blocking DNA replication and in preventing endoreduplication. Mol Cell Biol 18: 629–643.
7. Chang BD, Broude EV, Fang J, Kalinichenko TV, Abdryashitov R, et al. (2000) p21Waf1/Cip1/Sdi1-induced growth arrest is associated with depletion of mitosis-control proteins and leads to abnormal mitosis and endoreduplication in recovering cells. Oncogene 19: 2165–2170.
8. Munoz-Alonso MJ, Ceballos L, Bretones G, Frade P, Leon J, et al. (2011) MYC accelerates p21(CIP) -induced megakaryocytic differentiation involving early mitosis arrest in leukemia cells. J Cell Physiol 227: 2069–2078.
9. Brugarolas J, Chandrasekaran C, Gordon JI, Beach D, Jacks T, et al. (1995) Radiation-induced cell cycle arrest compromised by p21 deficiency. Nature 377: 552–557.
10. Deng C, Zhang P, Harper JW, Elledge SJ, Leder P (1995) Mice lacking p21CIP1/WAF1 undergo normal development, but are defective in G1 checkpoint control. Cell 82: 675–684.
11. Efeyan A, Collado M, Velasco-Miguel S, Serrano M (2007) Genetic dissection of the role of p21Cip1/Waf1 in p53-mediated tumour suppression. Oncogene 26: 1645–1649.
12. Weiss RH (2003) p21Waf1/Cip1 as a therapeutic target in breast and other cancers. Cancer Cell 4: 425–429.
13. Janicke RU, Sohn D, Essmann F, Schulze-Osthoff K (2007) The multiple battles fought by anti-apoptotic p21. Cell Cycle 6: 407–413.
14. Gartel AL, Tyner AL (2002) The role of the cyclin-dependent kinase inhibitor p21 in apoptosis. Mol Cancer Ther 1: 639–649.
15. Chang BD, Watanabe K, Broude EV, Fang J, Poole JC, et al. (2000) Effects of p21Waf1/Cip1/Sdi1 on cellular gene expression: implications for carcinogenesis, senescence, and age-related diseases. Proc Natl Acad Sci U S A 97: 4291–4296.
16. Pantoja C, Serrano M (1999) Murine fibroblasts lacking p21 undergo senescence and are resistant to transformation by oncogenic Ras. Oncogene 18: 4974–4982.
17. Iglesias-Ara A, Zenarruzabeitia O, Fernandez-Rueda J, Sanchez-Tillo E, Field SJ, et al. (2010) Accelerated DNA replication in E2F1- and E2F2-deficient macrophages leads to induction of the DNA damage response and p21(CIP1)-dependent senescence. Oncogene 29: 5579–5590.
18. Munoz-Alonso M, Leon J (2003) G1 phase control and cell differentiation. In: Boonstra J, ed. G1 phase progression. New York: Landes Bioscience. pp 1–29.
19. Dotto GP (2000) p21(WAF1/Cip1): more than a break to the cell cycle? Biochim Biophys Acta 1471: M43–56.
20. Perkins ND (2002) Not just a CDK inhibitor: regulation of transcription by p21(WAF1/CIP1/SDI1). Cell Cycle 1: 39–41.
21. Chen W, Sun Z, Wang XJ, Jiang T, Huang Z, et al. (2009) Direct interaction between Nrf2 and p21(Cip1/WAF1) upregulates the Nrf2-mediated antioxidant response. Mol Cell 34: 663–673.
22. Delavaine L, La Thangue NB (1999) Control of E2F activity by p21Waf1/Cip1. Oncogene 18: 5381–5392.
23. Devgan V, Mammucari C, Millar SE, Brisken C, Dotto GP (2005) p21WAF1/Cip1 is a negative transcriptional regulator of Wnt4 expression downstream of Notch1 activation. Genes Dev 19: 1485–1495.
24. Vigneron A, Cherier J, Barre B, Gamelin E, Coqueret O (2006) The cell cycle inhibitor p21waf1 binds to the myc and cdc25A promoters upon DNA damage and induces transcriptional repression. J Biol Chem 281: 34742–34750.
25. Devgan V, Nguyen BC, Oh H, Dotto GP (2006) p21WAF1/Cip1 suppresses keratinocyte differentiation independently of the cell cycle through transcriptional up-regulation of the IGF-I gene. J Biol Chem 281: 30463–30470.
26. Poole JC, Thain A, Perkins ND, Roninson IB (2004) Induction of transcription by p21Waf1/Cip1/Sdi1: role of NFkappaB and effect of non-steroidal anti-inflammatory drugs. Cell Cycle 3: 931–940.
27. Fritah A, Saucier C, Mester J, Redeuilh G, Sabbah M (2005) p21WAF1/CIP1 selectively controls the transcriptional activity of estrogen receptor alpha. Mol Cell Biol 25: 2419–2430.
28. Snowden AW, Anderson LA, Webster GA, Perkins ND (2000) A novel transcriptional repression domain mediates p21(WAF1/CIP1) induction of p300 transactivation. Mol Cell Biol 20: 2676–2686.
29. Martin A, Odajima J, Hunt SL, Dubus P, Ortega S, et al. (2005) Cdk2 is dispensable for cell cycle inhibition and tumor suppression mediated by p27(Kip1) and p21(Cip1). Cancer Cell 7: 591–598.
30. Nguyen BC, Lefort K, Mandinova A, Antonini D, Devgan V, et al. (2006) Cross-regulation between Notch and p63 in keratinocyte commitment to differentiation. Genes Dev 20: 1028–1042.
31. Munoz-Alonso MJ, Acosta JC, Richard C, Delgado MD, Sedivy J, et al. (2005) p21Cip1 and p27Kip1 induce distinct cell cycle effects and differentiation programs in myeloid leukemia cells. J Biol Chem 280: 18120–18129.
32. Di Cunto F, Topley G, Calautti E, Hsiao J, Ong L, et al. (1998) Inhibitory function of p21Cip1/WAF1 in differentiation of primary mouse keratinocytes independent of cell cycle control. Science 280: 1069–1072.
33. Rodriguez-Vilarrupla A, Diaz C, Canela N, Rahn HP, Bachs O, et al. (2002) Identification of the nuclear localization signal of p21(cip1) and consequences of its mutation on cell proliferation. FEBS Lett 531: 319–323.
34. Li C, Wong WH (2001) Model-based analysis of oligonucleotide arrays: expression index computation and outlier detection. Proc Natl Acad Sci U S A 98: 31–36.
35. van Betteraey-Nikoleit M, Eisele KH, Stabenow D, Probst H (2003) Analyzing changes of chromatin-bound replication proteins occurring in response to and after release from a hypoxic block of replicon initiation in T24 cells. Eur J Biochem 270: 3880–3890.
36. Vaque JP, Fernandez-Garcia B, Garcia-Sanz P, Ferrandiz N, Bretones G, et al. (2008) c-Myc inhibits Ras-mediated differentiation of pheochromocytoma cells by blocking c-Jun up-regulation. Mol Cancer Res 6: 325–339.
37. Ohtani K, DeGregori J, Nevins JR (1995) Regulation of the cyclin E gene by transcription factor E2F1. Proc Natl Acad Sci U S A 92: 12146–12150.
38. Rodriguez-Paredes M, Ceballos-Chavez M, Esteller M, Garcia-Dominguez M, Reyes JC (2009) The chromatin remodeling factor CHD8 interacts with elongating RNA polymerase II and controls expression of the cyclin E2 gene. Nucleic Acids Res 37: 2449–2460.
39. Delgado MD, Vaque JP, Arozarena I, Lopez-Ilasaca MA, Martinez C, et al. (2000) H-, K- and N-Ras inhibit myeloid leukemia cell proliferation by a p21WAF1-dependent mechanism. Oncogene 19: 783–790.
40. Besson A, Dowdy SF, Roberts JM (2008) CDK inhibitors: cell cycle regulators and beyond. Dev Cell 14: 159–169.
41. Li B, Carey M, Workman JL (2007) The role of chromatin during transcription. Cell 128: 707–719.
42. Luo Y, Hurwitz J, Massague J (1995) Cell-cycle inhibition by independent CDK and PCNA binding domains in p21Cip1. Nature 375: 159–161.
43. Ferrandiz N, Caraballo JM, Albajar M, Gomez-Casares MT, Lopez-Jorge CE, et al. (2010) p21(Cip1) confers resistance to imatinib in human chronic myeloid leukemia cells. Cancer Lett 292: 133–139.
44. Zhu H, Chang BD, Uchiumi T, Roninson IB (2002) Identification of promoter elements responsible for transcriptional inhibition of polo-like kinase 1 and topoisomerase IIalpha genes by p21(WAF1/CIP1/SDI1). Cell Cycle 1: 59–66.
45. Lohr K, Moritz C, Contente A, Dobbelstein M (2003) p21/CDKN1A mediates negative regulation of transcription by p53. J Biol Chem 278: 32507–32516.
46. Maclaren A, Clark W, Black EJ, Gregory D, Fujii H, et al. (2003) v-Jun stimulates both cdk2 kinase activity and G1/S progression via transcriptional repression of p21 CIP1. Oncogene 22: 2383–2395.
47. Muller GA, Engeland K (2009) The central role of CDE/CHR promoter elements in the regulation of cell cycle-dependent gene transcription. Febs J 277: 877–893.
48. Pippa R, Espinosa L, Gundem G, Garcia-Escudero R, Dominguez A, et al. (2012) p27(Kip1) represses transcription by direct interaction with p130/E2F4 at the promoters of target genes. Oncogene In press.

Garcia-Sanz P., Quintanilla A, Lafita MC., Moreno-Bueno G., García-Gutierrez L., Tabor V., Varela I., Shiio Y., Larsson LG., Portillo F., Leon J. (2014) *Sin3b interacts with Myc and decreases Myc levels.*

J Biol Chem. 2014 Aug 8; 289(32):22221-36.

doi: 10.1074/jbc.M113.538744.